GL01176

7/E

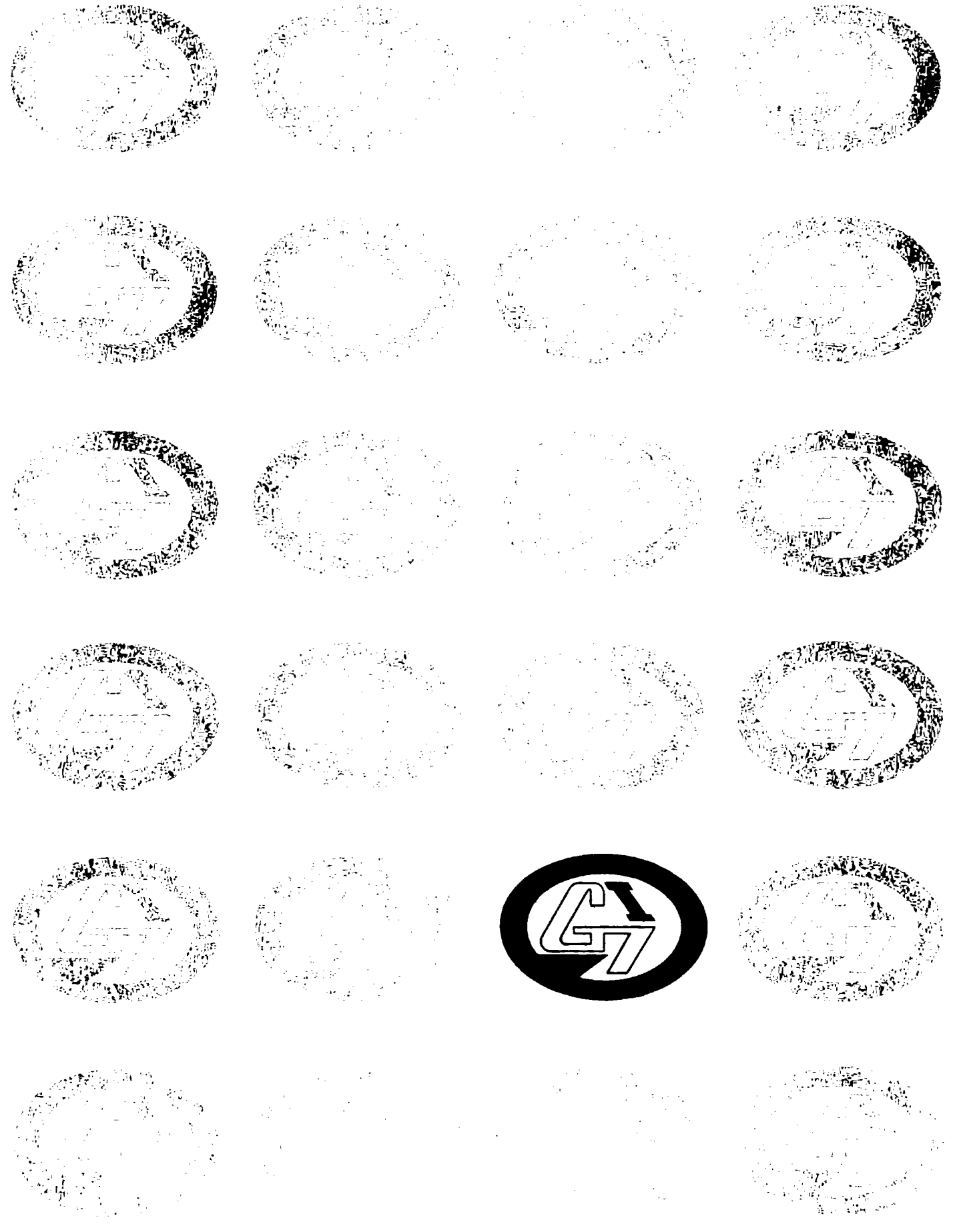

Proposal EY-R-08-007

Geothermal Reservoir Assessment Case Study

to

ENERGY RESEARCH AND DEVELOPMENT ADMINISTRATION

Nevada Operations Office
P.O. Box 14100
Las Vegas
Nevada 89114

from

GROUP SEVEN, INC.
1301 Arapahoe Street
Golden
Colorado 80401

5/27/77

RESTRICTIONS

Data contained in Figures 2 and 4 and all of Appendix I shall not be used, except for evaluation purposes, provided that if a contract is awarded to this proposer as a result of or in connection with the submission of this proposal, the government shall have the right to use or disclose any data to the extent provided in the contract. This restriction does not limit the government's right to use or disclose any technical data obtained from another source without restriction.

CONTENTS

APPENDICES

FIGURES

Response to request for proposal number EY-R-08-007, geothermal reservoir assessment case study, published by the United States Energy Research and Development Administration, Nevada Operations Office, P.O. Box 14100, Las Vegas, Nevada 89114.

A. Proposers Name and Address:

Group Seven, Inc.
1301 Arapahoe Street
Golden, Colorado 80401

B. Technical Proposal:

1. Investigation Site. It is here proposed that surface and subsurface geophysical investigations be undertaken in and around the areas known as Roosevelt Hot Springs KGRA (known geothermal resource area), Cove Fort-Sulphurdale KGRA, and Thermo Hot Springs KGRA, in the state of Utah. The limits of the area within which the geophysical studies are to be carried out and the locations of the KGRA's are shown on Figure 1.

A map of the current ownership of surface and subsurface rights in the Milford area is shown in Figure 2.

The Roosevelt Hot Springs, Cove Fort-Sulphurdale, and Thermo Hot Springs KGRA's lie along the boundary between the Colorado Plateau geological province to the east and the Basin and Range geological province to the west (Figure 3). In the vicinity of these three KGRA's, the transition zone between the Basin and Range province and the Colorado Plateau province is about 100 kilometers

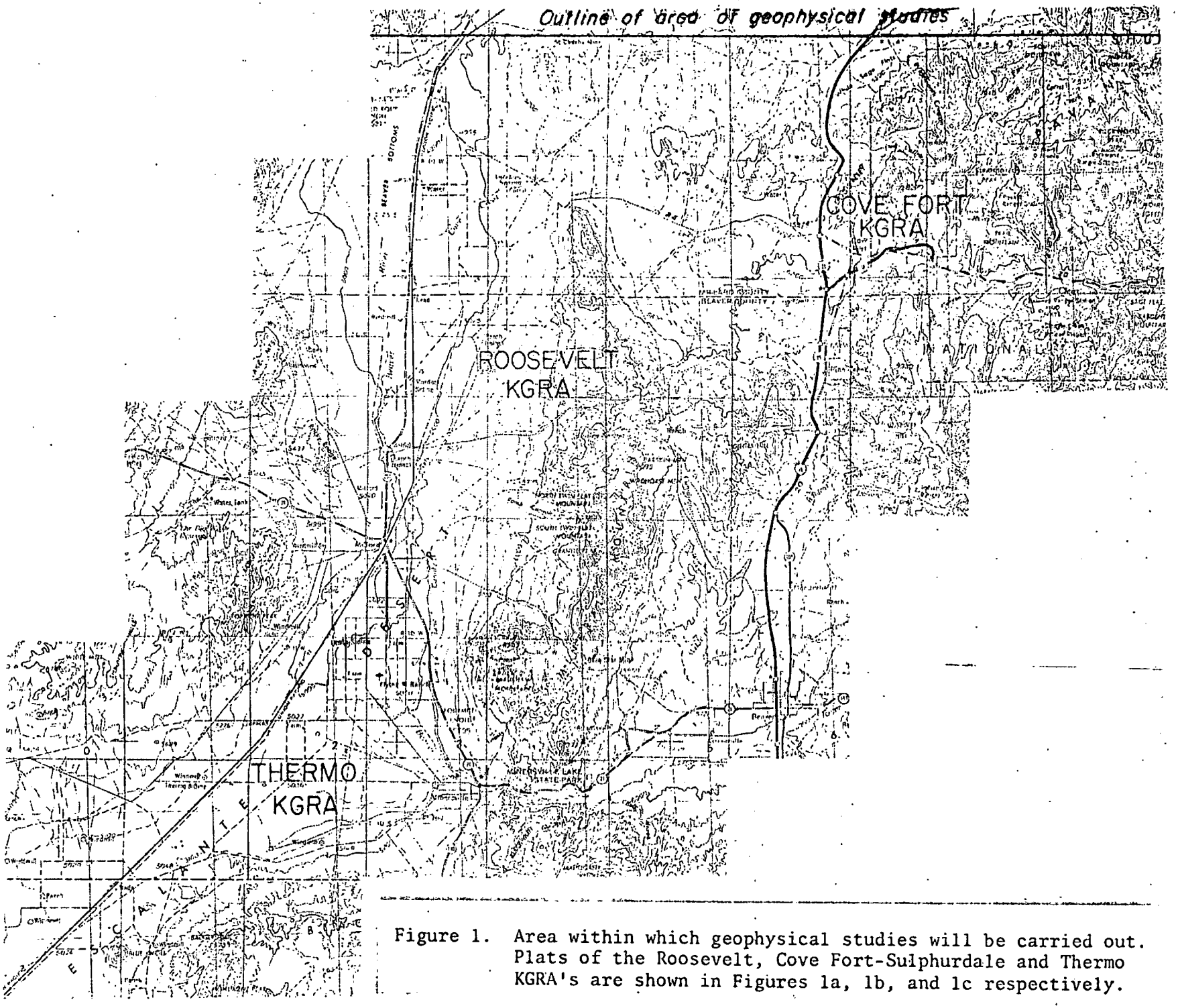

Figure 1. Area within which geophysical studies will be carried out. Plats of the Roosevelt, Cove Fort-Sulphurdale and Thermo KGRA's are shown in Figures 1a, 1b, and 1c respectively.

ROOSEVELT HOT SPRINGS AREA

T. 26 S., R. 9 W., T. 27 S., R. 9 W., S.L.M., Utah

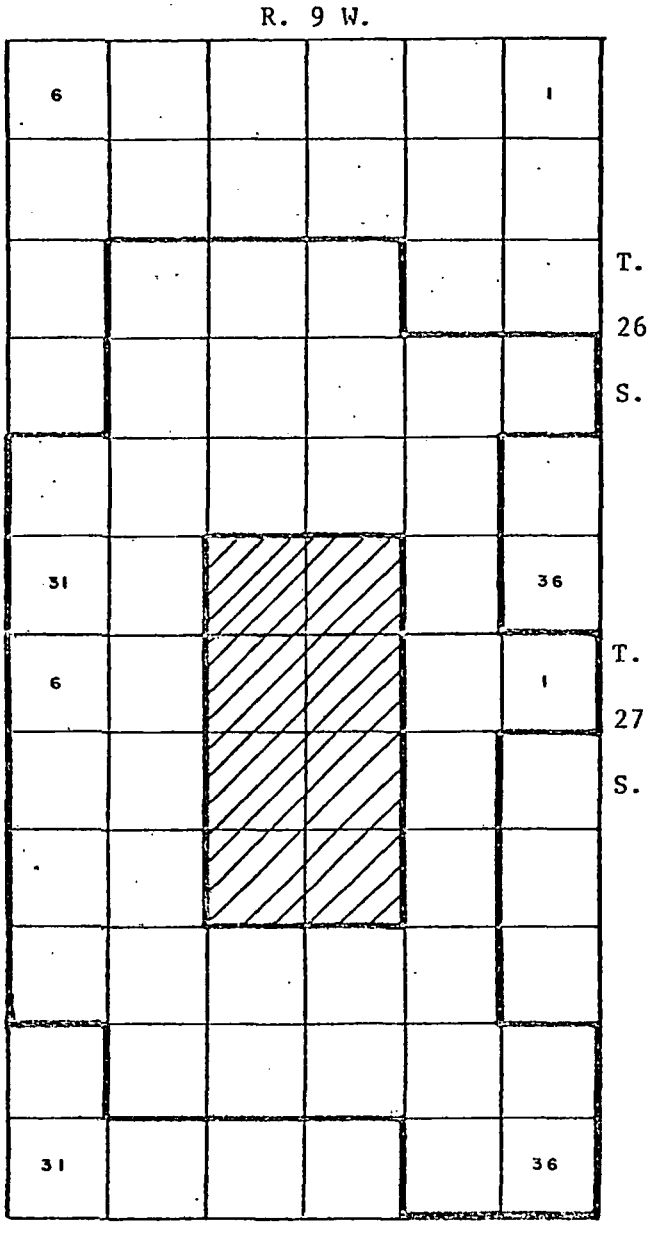

Pursuant to the authority vested in the Secretary of the Interior by Sec. 21 (a) of the Geothermal Steam Act of 1970 (84 Stat. 1566, 1572; 30 U.S.C. 1020), and delegations of authority in 220 Departmental Manual 4.1 H, Geological Survey Manual 220.2.3, and Conservation Division Supplement (Geological Survey Manual) 220.2.1 G, the described lands delineated hereon are hereby redefined known geothermal resources areas, revision effective February 1, 1974.

Total Previously Defined	5,201
Total Additional	24,590
Total in Field	29,791

Conservation Manager, Central Region
U.S. Geological Survey

Date

Figure 1a. Plat of Roosevelt Hot Springs KGRA.

Cove Fort-Sulphurdale Known Geothermal Resources Area
Beaver and Millard Counties, Utah
Tps. 24-26 S., Rs. 6-7 W., S.L.M., Utah

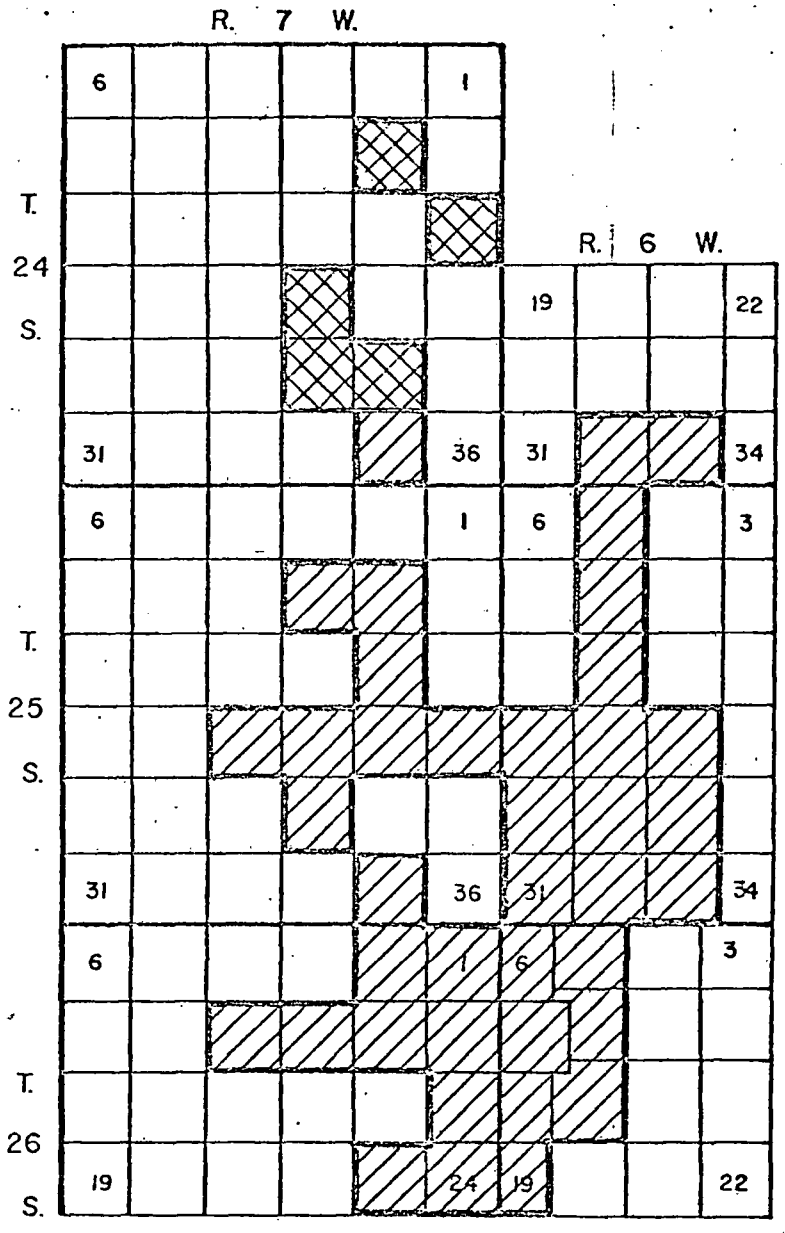

Pursuant to the authority vested in the Secretary of the Interior by Sec. 21 (a) of the Geothermal Steam Act of 1970 (84 Stat. 1566, 1572; 30 U.S.C. 1020), and delegations of authority in 220 Departmental Manual 4.1 H, Geological Survey Manual 220.2.3, the Conservation Division Supplement (Geological Survey Manual) 220.2.1 G, the described lands delineated hereon are hereby redefined known geothermal resources areas, revision effective September 1, 1976.

Total Previously Defined	24,374 acres
Total Additional	3,200
Total in Field	28,074 acres more or less

Conservation Manager, Central Region
U. S. Geological Survey

Date

Figure 1b. Plat of Cove Fort-Sulphurdale KGRA.

Thermo Hot Springs Geothermal Resources Area
Beaver and Iron Counties, Utah
Salt Lake Meridian
T. 29 S., R. 13 W., T. 30 S., Rs. 11-13 W., T. 31 S., R. 12 W.

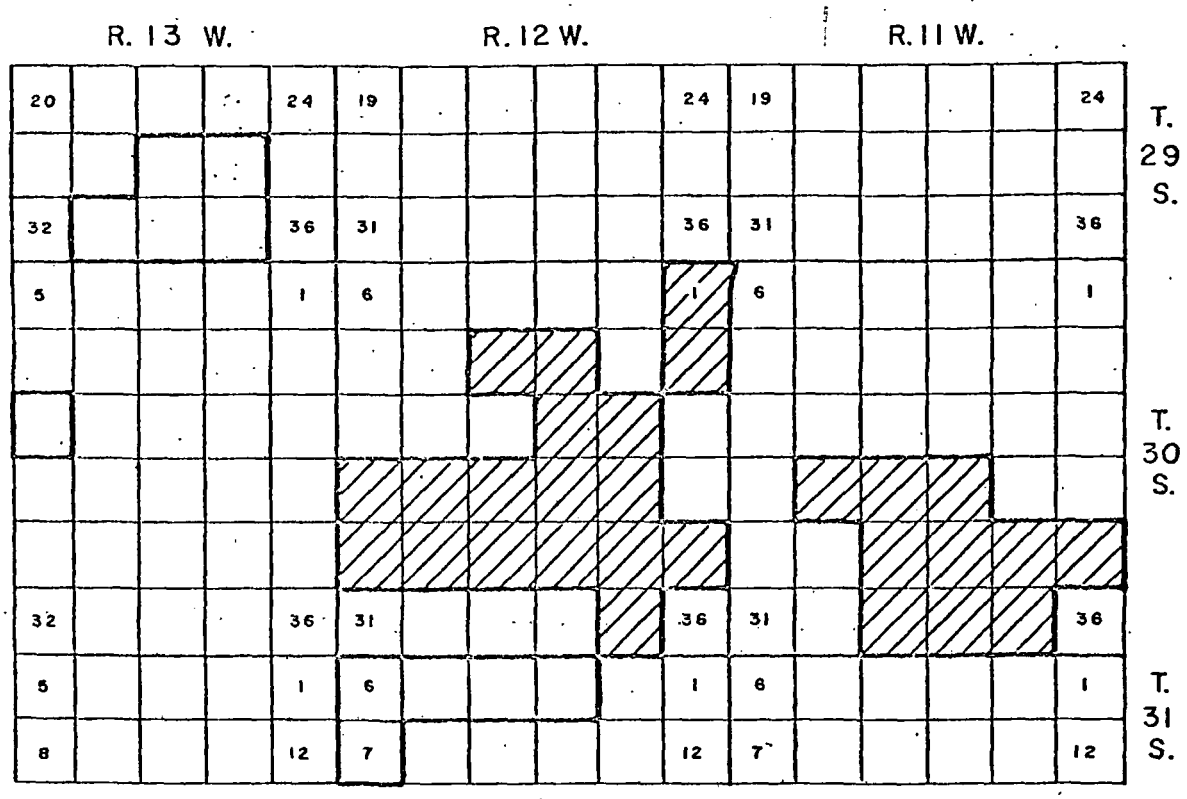

Pursuant to the authority vested in the Secretary of the Interior by Sec. 21 (a) of the Geothermal Steam Act of 1970 (84 Stat. 1566, 1572; 30 U.S.C. 1020), and delegations of authority in 220 Departmental Manual 4.1 H, Geological Survey Manual 220.2.3, the Conservation Division Supplement (Geological Survey Manual) 220.2.1 G, the described lands delineated hereon are hereby redefined known geothermal resources areas, revision effective February 1, 1974.

Total Previously Defined	17,922 acres
Total Additional	8,097 acres
Total in Field	26,019 acres

Conservation Manager, Central Region
U.S. Geological Survey

Date

Figure 1c. Plat of Thermo Hot Springs KGRA.

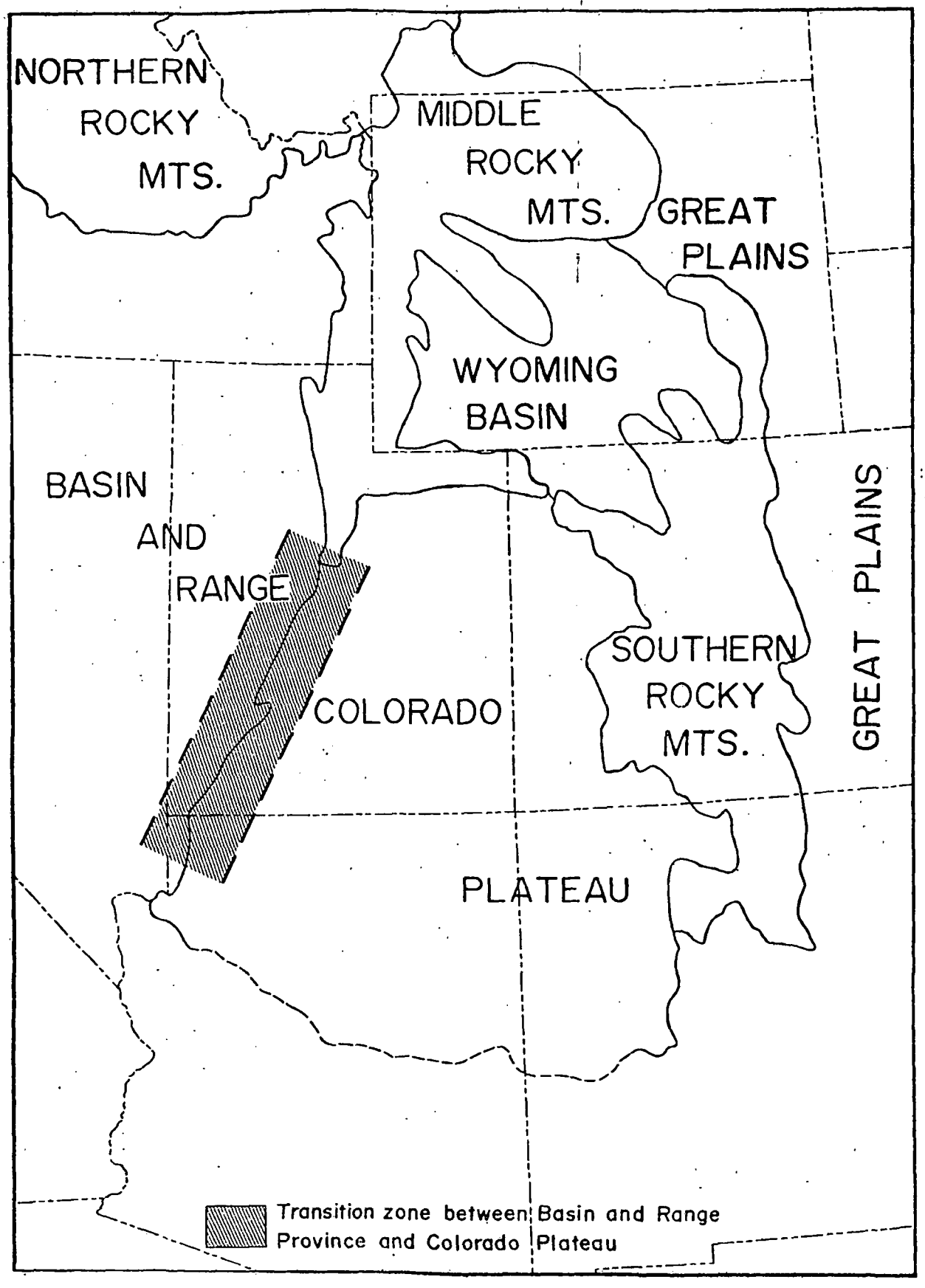

Figure 3. Setting of Transition Zone between Basin and Range Province and Colorado Plateau.

wide, extending from the Sevier Fault, within the Colorado Plateau province, to the western boundary of the Escalante Valley. Because of the occurrence of hot springs and other data indicating high heat flow along this transition zone, exploration for geothermal reservoirs has been intense in recent years. The geology of the area is highly complex, with rocks being a complicated mixture of Tertiary extrusive igneous facies mixed with volcano-clastic sediments, which in turn have been repeatedly intruded by quartz-monzonite, mainly in the form of laccoliths. Quaternary basalts occur both within the transition zone and on the Colorado Plateau itself, indicating that the transition zone may still be the location of tectonic activity. These Quaternary basalts indicate that the mantle has been involved in the tectonics, providing a source for high heat flow in the area. The geology is described in more detail in Appendix I.

During the past 18 months, several successful geothermal test wells have been drilled in and near the Roosevelt Hot Springs KGRA. Companies involved in this exploration include Phillips Petroleum Company, Natomas Oil Company, and AMAX, Inc. From the information available at this time, these wells produce a mixture of steam and water at temperatures above 500°F. Flow rates for several of the test wells have been in the vicinity of a million pounds of fluid per hour. Because of the high temperatures and the high production rates, it appears that the Roosevelt KGRA represents a major geothermal field. As yet, the extent of the field has not been fully defined either by geological and geophysical investigations

or by drilling. While extensive geophysical and geological studies have been carried out both by the companies involved in the exploration and by the University of Utah under contract to the U.S. Geological Survey and the Energy Research and Development Administration, these studies have been fragmented and so far have not provided a complete picture of the subsurface structure. It is proposed here to supplement the existing geophysical and geological data in the public domain by additional surveys as will be described in the subsequent part of this proposal.

Program Data Offered:

GROUP SEVEN, INC. proposes to carry out additional geochemical surveys, electrical resistivity surveys, electromagnetic surveys, evaluation of existing and new gravity data, and subsurface investigations of physical properties of the reservoir using moderate depth drill holes drilled as part of this program.

The geochemical study will consist of detailed measurements of mercury content in soil. The principal source of mercury in soil is igneous rock from which the mercury has been leached by water and transported to the surface. High temperatures accelerate this process, and anomalous concentrations of mercury have been found in regions of thermal activity. Often this mercury is concentrated in the soil over fracture zones where vertical permability is good. Inasmuch as the geothermal wells drilled at the Roosevelt Hot Springs KGRA appear to produce from fracture zones, the use of mercury soil analyses should be effective in locating these zones.

It is planned that soil mercury determinations be made at approximately 2,000 locations over the survey area defined in Figure 2. Approximately one-half of these measurements will be done on a random basis over an equal density sampling grid of the area. The other half of the measurements would be made on a close sampling grid at near locations where high mercury contents in the soil had been discovered during the first half of the survey.

At the present time, extensive electrical resistivity data are available from work done by the University of Utah. Almost all of these resistivity data have been obtained with the dipole-dipole technique, which is an effective means for measuring resistivity at very shallow depths. However, it lacks the resolution to detect conducting zones at depth such as may be associated with a fracture controlled geothermal reservoir. We propose here to carry out a resistivity survey using the rotating dipole method developed by GROUP SEVEN, INC. The method is described in detail in Appendix II. It offers the possibility of recognizing the existence of conductive zones in the subsurface with a higher degree of certainty than the dipole-dipole method. An example of the results obtained with the rotating dipole method in a part of the Roosevelt KGRA is shown in Figure 4. Coverage of the rest of the area proposed here, as shown in Figure 2, will require two months of crew effort. Over this interval, 8 to 10 source locations will be occupied. One hundred to one hundred fifty resistivity stations will be recorded from each of these sources.

It is becoming clear that areas of low resistivity are not uniquely related to the presence of geothermal fluids in regions with as complicated a geological structure as the Utah Thermal Belt. Geothermal reservoirs do have the characteristic that in many cases the rock at great depths beneath the reservoir has an unusually low resistivity. At the present time, the principal method for searching for these deep zones of electrical conductivity is the magnetotelluric method. The magnetotelluric method provides poor results in areas with complex surface structure such as exists in the Utah Thermal Belt. GROUP SEVEN, INC. has developed and is using a controlled source time-domain electromagnetic sounding method to obtain information on resistivities at depths ranging from 2 to 5 kilometers. It is proposed here that a time-domain electromagnetic survey be carried out over the proposed area to define the boundaries of the conductive zone which probably exists in the upper crust. The time-domain electromagnetic method is described in detail in Appendix III. We propose doing 350 soundings within the proposed survey area, an effort which will require two crew months of time.

We propose to reinterpret the existing gravity data covering the area of the Utah Thermal Belt, as outlined in Figure 2. Based on the electrical surveys described in the preceeding paragraph, the configuration of the surficial basins can be determined. Combining these data with interpretations of existing gravity data can provide a highly reliable description of the subsurface structure in the survey area. The effort required for this part of the study will be one month of office work.

It is proposed that six wells be drilled to intermediate depth to test the significance of the features found in the various surface geophysical tests. These wells will be drilled to a depth of approximately 1,000 feet at locations which appear to be of particular interest on the basis of the results of the surface surveys. Downhole measurements will include temperature surveys, electric logs, neutron logs, density logs, geochemical tests of fluids produced, and cuttings logs.

Environmental Evaluation:

Performance of surface geophysical surveys as outlined above normally are considered to have no environmental impact. Drilling of intermediate-depth test holes will require at least the preparation of an impact assessment, and possibly an evaluation, depending on locations selected.

Schedule:

GROUP SEVEN, INC. is prepared to undertake the geophysical surveys listed above within three months of the initiation of a contract with the Energy Research and Development Administration. Field work will be completed within six months following that time. Progress reports can be prepared on a bi-weekly or monthly basis. Final reports on the results of the geophysical investigations will be submitted to ERDA within three months following the completion of field work. Locations for the intermediate depth test holes will be made at that time, and drilling would take place during

the following twelve months. Final reports on the program as a whole would be submitted within three months after the completion of drilling.

Cost:

In place of GSA optional form 60, contract pricing proposal, the following cost proposal is submitted:

Cost Proposal:

Part 1 - Surface Geophysics	
1. 4 crew months electrical @ $35,000.00	$140,000
2 man months geochemical sampling @ $4,500.00	9,000
6 man months scientific and professional @ $2,000.00	12,000
12 man months technical and support @ $825.00	10,000
Overhead @ 65% of scientific, professional, technical, and support salaries	14,300
Computer costs	10,000
Report preparation, printing costs	2,000
	197,300
Part 2 - Drilling Subcontract	
Estimated @ $35/ft., 6,000 ft. for 6 holes	210,000*
+ 2% management fee	4,200
Part 3 - Borehole Surveys	
Estimated at $10,000/1,000 ft. well	60,000*
+ 2% management fee	1,200
Total	$472,700

(*) Estimates only. Contracts are to be let to subcontractors according to ERDA requirements, with a 2% management fee.

1. Costs for field surveys are based on a unit of one crew month. This cost includes all salaries for field personnel, field expenses and travel, use of equipment, and all direct costs related with field operations. Both the resistivity survey and the electromagnetic survey require the same field equipment and crew members. The unit cost per month of field operations is $35,000.00.

2. Drilling will be done by subcontract with a competent and reputable drilling concern. Until the holes are located, the probable cost of drilling cannot be estimated accurately. The cost will be in the vicinity of $35.00 per foot for normal drilling operations, for a total of 6,000 feet of drilling, a cost of $210,000 is anticipated. Specific cost proposals will be submitted to ERDA at the time sites are selected and a drilling contractor has been obtained. GROUP SEVEN, INC. will charge a 2% management fee for supervision of the drilling contract.

3. Logging of the bore holes will be subcontracted to a reputable and reliable well logging company. Each well will require mobilization charge for the logging crew from the nearest office of the company selected. No exact cost can be estimated until drill hole sites have been selected and a logging service company has been picked.

It is anticipated the cost will be approximately $10,000 per well, or a total of $60,000. A cost proposal will be submitted to ERDA at the time logging is to be subcontracted. GROUP SEVEN, INC. will charge a 2% fee for management of the services.

4. Overall supervision of the program, reduction of data, and preparation of reports will be done at the Golden office of GROUP SEVEN, INC. A total amount of effort involved here is considered to be six man months of scientific and professional effort, and twelve man months of clerical, secretarial, drafting and computer technician time. Only on this time will an overhead rate be specified. GROUP SEVEN, INC. will charge an overhead rate of 65% of direct salaries.

A summary of the costs to the government is:

1.	Services offered by GROUP SEVEN, INC.	$197,300
2.	Drilling subcontract	214,200
3.	Geophysical well logging subcontract	61,200
	Total	$472,700

Business and Management:

GROUP SEVEN, INC. was organized in 1969 by G. V. Keller, Norman Harthill, J. I. Pritchard, and J.J. Jacobson as a Colorado corporation to provide geophysical services in the form of high quality electrical resistivity surveys. Between 1969 and 1973, GROUP SEVEN, INC. carried out contract surveys for the United Nations, U.S. Bureau of Reclamation, U.S. Navy Office of Petroleum Reserves,

the Agency for International Development, Union Oil Company, Chevron Oil Company, Gulf Oil Company, Getty Oil Company, Amoco Oil Company, Marathon Oil Company and Phillips Petroleum Company. Most of the contract activities were in exploration for geothermal reservoirs.

In 1973, GROUP SEVEN, INC. (Colorado) was sold to Geothermal Kinetics, Inc. of Phoenix, Arizona. The company was reorganized as GROUP SEVEN, INC. (Nevada) and has operated solely for the benefit of Geothermal Kinetics, Inc. since that time. From 1973 to the present, GROUP SEVEN, INC. has maintained from 1 to 3 field crews in continuous operation in electrical surveys, and has expanded the scope of operations to include gravity surveys, and their interpretation and, geochemical surveys.

GROUP SEVEN, INC. has maintained a leadership position in developing new and high capability electrical exploration techniques. Primary among these has been the development of the rotating dipole method for direct current surveys and the time-domain electromagnetic method for deep penetration surveys. GROUP SEVEN, INC. was the first commercial concern to make use of the highly sensitive Josephson Junction magnetometer for field surveys. At present, the company carries out rotating dipole resistivity surveys, dipole-dipole surveys, Schlumberger sounding surveys, time-domain electromagnetic surveys, and magnetotelluric surveys. The choice of technique is based upon a decision as to the most effective means for solving specific exploration problems.

GROUP SEVEN, INC. is managed by Dr. Norman Harthill, who is Executive Vice President. Names and resumes of the principal project personnel are appended.

ERDA may contact Mr. Michael O'Donnell of Geothermal Kinetics, Inc., 301 W. Indian School Road, Phoenix, Arizona 85013, to discuss this proposal or with previous clients of the company. Among the previous clients are Dr. C. W. Berge of Phillips Petroleum Company, Mr. Glen Campbell of Gulf Minerals, Dr. Dan Kim of Amoco Production and Dr. Carel Otte of Union Oil. In addition, Mr. William Ruckelshaus, Senior Vice President of Weyerhauser, Inc. and Dr. John Sawhill, President of New York University are conversant with our work.

The document titled "General Contract Provisions" is acceptable as a basis for contract negotiations.

Financial Statement:

GROUP SEVEN, INC. is a wholly-owned subsidiary of Geothermal Kinetics, Inc. GROUP SEVEN, INC. does not now nor never has had any long-term indebtedness, and operates on a current cash flow basis. All specialized equipment to be used in these surveys is owned by GROUP SEVEN, INC. Non-specialized equipment, such as vehicles, are leased. Bank references are Valley National Bank, Phoenix, Arizona and First National Bank, Golden, Colorado. The most recent balance sheet for the parent corporation, GKI, is attached.

RESUME

GEORGE V. KELLER

George V. Keller was born in New Kensington, Pennsylvania on December 16, 1927. He attended public schools there, and later, the Pennsylvania State University. At Penn State, he majored in Geophysics and Mathematics, receiving the B.Sc. degree in 1949, the M.Sc. degree in 1951, and the Ph.D. degree in 1953.

From 1952 to 1964, Dr. Keller was employed by the U. S. Geological Survey as a geophysicist. His duties there included establishing a physical properties laboratory, development of borehole logging methods for mineral prospecting, development of methods for detecting nuclear detonations, operation of an exploration program from a drifting ice station in the Arctic Ocean during the IGY, and development of crustal-scale electrical surveys.

During the Academic year 1959-1960, Dr. Keller taught at the Colorado School of Mines. He joined the faculty at CSM on a permanent basis in 1964, teaching courses in information theory and electrical prospecting. He is now Head, Department of Geophysics.

While at CSM, Dr. Keller has been engaged in both research and consulting in addition to teaching. He has received research support from ten governmental agencies over the years for studies related to electrical properties of rocks and electrical exploration. He also has served as consultant to these government agencies, as well as to about a dozen major companies in resource development.

Dr. Keller spent the academic year 1968-1969 on leave from CSM, working for the Department of Scientific and Industrial Research, working on the development of prospecting methods for use in the search for geothermal energy. On his return from New Zealand, he formed Group Seven, Inc., along with several of his former students. Group Seven, Inc. offered exploration services, mainly electrical, and soon became heavily engaged in geothermal exploration. In 1973, Group Seven was sold to Geothermal Kinetics, Inc., of Phoenix, but Dr. Keller still serves as President of the Company, and as consultant.

Dr. Keller is the coauthor or author of about 90 articles that have appeared in the technical literature, two books, and eight book-length translations of Russian technical material.

RESUME

NORMAN HARTHILL

Personal

Birthdate:	June 19, 1937
Birth Place:	Glasgow, Scotland
Nationality:	British; permanent resident of United States, citizenship applied for.
Marital Status:	Unmarried

Education

High School:	Hillhead High School, Glasgow, Scotland 1949-1955 Graduated with University entrance qualifications in English, French, Mathematics, Physics and Chemistry
University:	Glasgow University 1955-56 Civil Engineering, including 6 months practical experience on a hydroelectric project
B.Sc.	University College of Wales, Aberystwyth, Cards 1959-63 Graduated with honors, 1963 Major: Geology Minors: Physics, Mathematics
M.Sc.	Colorado School of Mines, Golden, Colorado 80401 1964-69 Geophysics; June, 1967 Thesis title: The audio magnetotelluric method of measuring earth resistivity.
D.Sc.	Geophysics; June 1969 Thesis title: Deep electromagnetic probing: geological considerations.
Academic Interests:	Electrical structure of the earth, thermal structure of the earth, structural geology

Professional Experience

1969 - Present	Group Seven, Inc. founder member with Prof. G. V. Keller. Present Position--Executive Vice President and General Manager. Duties: To delineate exploration strategy and tactics, interpretation of the results of electrical, electromagnetic and geophysical well logging surveys. The unification of results of all geophysical surveys with geology and geochemistry to provide a comprehensive interpretation. Report preparation.

1974 Consultant to the Federal Electricity Commission of Mexico on geothermal exploration and evaluation of reserves.

1972 January - May
National Autonomous University of Mexico (visiting professor).
Duties: To teach a course in electromagnetic theory; geothermal research.

1967 (Summer) Kennecott Copper Corporation. Field evaluation of an audio frequency magnetotelluric system.

1965-69 Research assistant to Prof. G. V. Keller in the development of natural field and controlled source electromagnetic sounding systems.

1963-64 Seismograph Service Ltd. Assistant computer, reflection seismograph crew, Muscat and Oman.

Publications

Time-domain electromagnetic sounding, 1976: I.E.E.E. Trans., Geoscience Electronics, v. GE-14, n. 4, p. 256-260.

The dipole mapping method, 1975: Geophysics, v. 40, n. 3, p. 451-472. (with G. V. Keller, R. Furgerson, C. Y. Lee and J. J. Jacobson)

The CSM test area for electrical prospecting, 1968, Geophysics, v. 33, n. 4, p. 675-679.

Scholarships: Society of Exploration Geophysicists
Scholarship holder 1964-67

Professional Societies: Society of Exploration Geophysicists
American Geophysical Union

Military Service

1957-59 Royal Artillery; tank, Lance Bombardier.

Languages: French, Speech: fluent.
Reading: fluent.
Writing: with some difficulty.

Spanish, Same.

PROFESSIONAL RESUME

John M. Jordan

PERSONAL DATA

Name:	John (Jack) M. Jordan
Address:	14543 W. 3rd Avenue Golden, CO 80401
Phone:	303-278-3073
Marital Status:	Single
Birthdate:	January 20, 1944

EDUCATIONAL BACKGROUND

September, 1961- June, 1965	Illinois Benedictine College, Lisle, Ill. B.S. Physics
September, 1969- May, 1972 and January, 1974- May, 1974	Colorado School of Mines, Golden, CO Master of Science, Geophysical Engineering (includes 24 hours undergraduate Geology) Thesis Title: Geothermal Investigations in the San Luis Valley, South-Central Colorado.

MILITARY HISTORY

August, 1965- April, 1969	Served in U.S. Army. Entered as Private; received Honorable Discharge as First Lieutenant. Training includes language courses in Czech and Laotian (Thai), Field Artillery Commander-basic course; Military Advisor-special warfare school; and Military Intelligence-officer's basic course. Assignments included Assistant U.S. Army attache-Laos.

PROFESSIONAL EXPERIENCE

Summer, 1970	Geophysicist with Standard Oil of Calif., at Bakersfield. Carried out ground magnetic survey in Nevada. Reduced and contoured data, and modeled (2-D) gravity and magnetic profiles to estimate the extent of buried volcanic flows.

Summer, 1971	Office of Naval Research, deep crustal studies project consisting of electric field (dipole receiver) and electromagnetic field (loop receiver) measurements in western Nevada and eastern Oregon using the Los Angeles-Bonneville Dam (Columbia River) HVDC power line as a source.
May, 1972-October, 1973	Senior Geophysicist and Resistivity Party Chief for Group Seven, Inc.; made detailed resistivity measurements over 15 geothermal prospects in six western states. Measurements included dipole-dipole resistivity, dipole mapping, Schlumberger dc soundings, and time-domain electromagnetic (TDEM) soundings. Responsible for data acquisition, quality control, permitting, data reduction and initial interpretation, and equipment and vehicle maintenance.
June, 1974-April, 1975	Geophysicist, Gulf Research and Development, Harmarville, PA. Involved in processing marine and land seismic data. Assigned to minerals research group, planned and carried out detailed seismic survey with Gulf equipment in Tennessee to detect sphalerite deposits in limestone and then processed and interpreted data.
May, 1975-Present	Senior Geophysicist and Manager of field operations. Responsible for data acquisition and processing, as well as equipment design and development.

RESUME

FREDERICK E. BERKMAN

Personal

Birthdate:	July 22, 1943
Birthplace:	McKeesport, Pennsylvania
Marital Status:	Married, two children

Education

High School:	Beaver Area High School, Beaver, Pennsylvania, 1957-61.
University:	Colorado School of Mines, 1961-66. Professional engineer, geophysical engineering (Gp.E.) 1968-77. Colorado School of Mines, full and part time study towards advanced degrees in geophysics. Thesis under preparation. Thesis Title: A Magnetic Model of the Long Valley Caldera, California.

Professional Experience

1976-Present	Senior Geophysicist, Group Seven, Inc. Gravity and magnetic interpretation.
1975-76	Geologic assistant, U.S.G.S., Lakewood, California.
1968-69	Instructor in mechanics and descriptive geometry, Colorado School of Mines.
1967	Chief, gravity crew, Phelps Dodge Corporation, Douglas, Arizona

Miscellaneous

Languages:	Spanish, read and speak.
Aviation:	Commercial multi-engine pilots license.

RESUME

TAHSIN TASCI

Personal

Name:	M. Tahsin Tasci
Age:	26
Birth date:	January 16, 1950
Birth place:	Mersin, Turkey
Nationality:	Turkish; permanent resident: United States
Marital Status:	Single
Health:	Excellent, no physical defects

Education

High School: Tevfik Sirri Gür Lisesi, Mersin, Turkey.
1961-1967
Graduated with honors (highest grades) 1967.
Received the Turkish Science Foundation Scholarship for two years (1966, 1967) and was awarded a college scholarship for four years.

Passed the comprehensive exams to qualify for the 8-year Turkish Petroleum Corporation scholarship to study abroad (U.S.A.), 1967. University entrance examinations results were in the top 10%, 1967.

University: Michigan State University, East Lansing, Michigan.
1968
Completed the Intensive Course in English.

B. Sc. Colorado School of Mines, Golden, Colorado 80401.
1968-1972

Major: Geophysics
Minor: Mathematics

M. Sc. Colorado School of Mines, Golden, Colorado 80401.
1972-1975

Geophysics: March, 1975
Thesis Title: Exploration for a Geothermal System in the Lualualei Valley, Oahu, Hawaii.
The areas of interest: Geophysical methods used in geothermal exploration.

Professional Experience: Worked two years with Group Seven, Inc. as a party chief doing geothermal exploration. The methods used were Time Domain Electromagnetic Soundings, Rotating Dipole Mapping, Self Potential Surveys, Schlumberger Soundings, Magnetotelluric Measurements, and Temperature Measurements.

Present Position: Senior Geophysicist supervising field operations, data reduction and interpretation.

1975 Annual Report

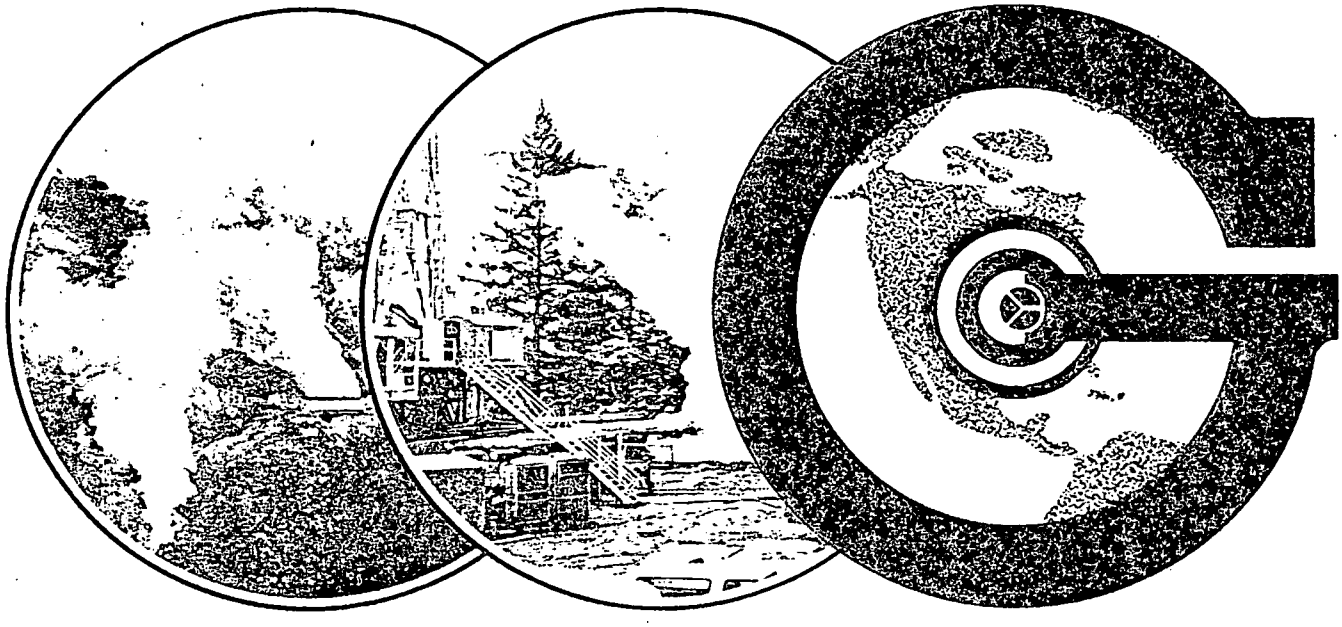

GEOTHERMAL KINETICS INC.

GEOTHERMAL KINETICS INC.

301 West Indian School Road, Phoenix, Arizona 85013 Telephone (602) 248-0202

William D. Ruckelshaus
Chairman of the Board

Paul W. Eggers
President

Mike O'Donnell
Executive Vice President
and General Manager

Ward H. Austin Jr.
Vice President
Exploration

Dent N. Hand
Secretary/Treasurer

BOARD OF DIRECTORS

Paul W. Eggers
Dallas, Texas

Murray Fasken
Midland, Texas

Robert E. Fasken
Toronto, Canada

Seymour Halpern
Jamaica, New York

Dent N. Hand
Phoenix, Arizona

Mike O'Donnell
Phoenix, Arizona

William D. Ruckelshaus
Washington, D.C.

John C. Sawhill
New York, N.Y.

George Smith
Toronto, Canada

Robert M. Smith
Toronto, Canada

LAND DEPARTMENT

2920 H Street • Bakersfield, California 93301
Tel. (805) 327-7774

Joe Covello
Land Manager

SUBSIDIARIES

GROUP SEVEN INC.

Golden, Colorado

Dr. George V. Keller
President

Dr. Norman Harthill
Executive Vice President

John M. Jordan
Field Supervisor

Dr. Hans Leitinger
Party Chief

M. Tahsin Tasci
Party Chief

Steve Williams
Party Chief

GEO DRILLING INC.

Phoenix, Arizona

Bert McComack
General Manager

General Counsel	Bank	Auditors	Transfer Agent
Snell & Wilmer	**Valley National Bank**	**Peat, Marwick, Mitchell & Co.**	**Valley National Bank**
Suite 3100 Valley Center	Indian-Central Office	100 West Clarendon	Corporate Trust Division
Phoenix, Arizona 85073	Phoenix, Arizona 85013	Phoenix, Arizona 85013	Phoenix, Arizona 85073

President's Report to Shareholders

Perhaps the most significant news this year is that a major hurdle has been cleared in your company's plans for development of GKI's 408-acre leasehold in the Geysers Field in California, the location of our Rorabaugh No. 1 steam well.

Operations have been suspended there because Union Oil Company contested ownership of the geothermal resources. Basically, our rights are based on our lease with the owner of the mineral rights to the property. Union Oil claimed the geothermal rights belonged to the owner of the surface and groundwater rights. On June 1, 1976 the Superior Court in Sonoma County ruled that GKI is the owner of the contested geothermal resources and is entitled to the possession and control of all geothermal steam power in and under the 408-acre Rorabaugh lease. The court rendered a landmark decision on geothermal resources, in essence ruling that geothermal steam is a mineral resource and not a water resource. Union Oil Company will have sixty days after the judgement is entered in which to file Notice of Appeal.

Virtually all of your company's exploration and drilling activities during the past year were joint operations with McCulloch Oil Corporation, pursuant to agreements reached in 1974. With funds from McCulloch Oil, GKI obtained additional leasehold acreage in Utah, in the Geysers area, and in the Imperial Valley in Southern California.

The first well on the Francisco Prospect in the Geysers area has been completed as a commercial producer with a bottom hole pressure of approximately 110,000 pounds, and we currently are drilling a well on the Utah property. Both of these prospects appear to have great potential for geothermal production. We also conducted geothermal research in other parts of the western United States, including Oregon and Montana.

Your management also has been very active in efforts to obtain legislation granting intangible drilling expense deduc-

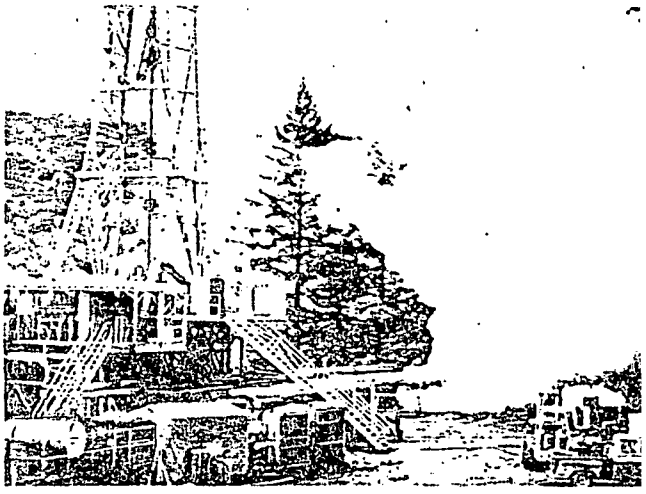

Above: GKI's Rorabaugh No. 1 geothermal well in the Geysers Field in California. Below: Dr. Norman Harthill, executive vice-president of GKI's Group Seven Inc. subsidiary, is a pioneering authority on geophysical exploration.

tions and depletion allowances on geothermal production. The Superior Court ruling on the Rorabaugh property could be extremely helpful in supporting our position with the Internal Revenue Service because the court specifically held that a geothermal resource is not water, but a mineral resource.

Sen. Paul Fannin of Arizona has introduced federal legislation providing for the deduction of intangible drilling expenses and a 22% business deduction against gross income. This has been made part of a tax bill which has passed the Senate Finance Committee and we are hopeful the legislation will pass the full Senate and the House. In support of the legislation, we have met with various senators, members of the Finance Committee, and members of the Joint Conference Committee.

On another front, GKI board chairman William D. Ruckelshaus and his legal firm represented GKI in support of a guaranteed loan program, through which funds could be made available for drilling and development of geothermal properties. In addition, I testified as president of GKI before the House Science Committee, recommending regulations covering the guaranteed loan program. The final regulations, as adopted, show evidence that our recommendations have been incorporated, and we are working with Energy Research and Development Act administrators to obtain guaranty loan money during the coming year.

Our Group Seven Inc. subsidiary continues to make significant strides in developing advanced technology for geophysical exploration, for which Dr. George V. Keller, president, and Dr. Norman Harthill, executive vice president, are to be commended. Ward H. Austin Jr., GKI's vice president for exploration, also deserves commendation for continuing excellence in advancing the technology in geological research. We believe we are in the forefront in the industry in geological and geophysical sciences.

In closing my comments on a truly satisfying year of progress for Geothermal Kinetics Inc., I also would like to express appreciation to GKI's executive vice president and general manager, Mike O'Donnell, and to our secretary/treasurer, Dent N. Hand, for their dedication to our company's interests; both work long hours with a lean staff to help GKI maintain its position of leadership in the industry.

Paul W. Eggers

Phoenix, Arizona
June 1, 1976

Paul W. Eggers
President

Above: An aerial photo showing geothermal development north of GKI's Utah leaseholds.

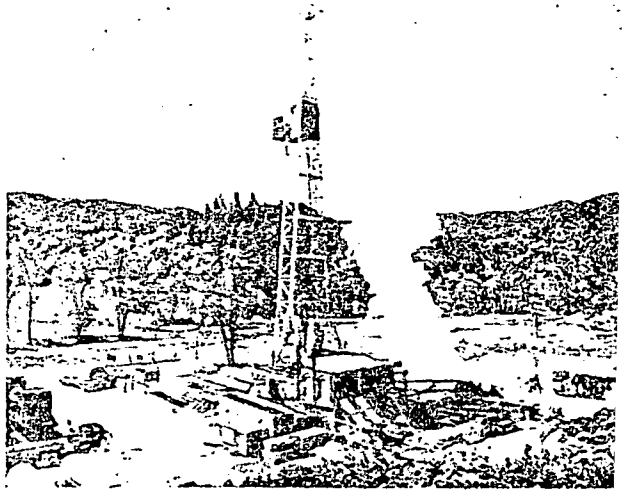

Above: GKI's first completed geothermal well in the promising Francisco Prospect. Below: Sid Ali Nadir Omari analyzes data with Group Seven Inc.'s computer in Golden.

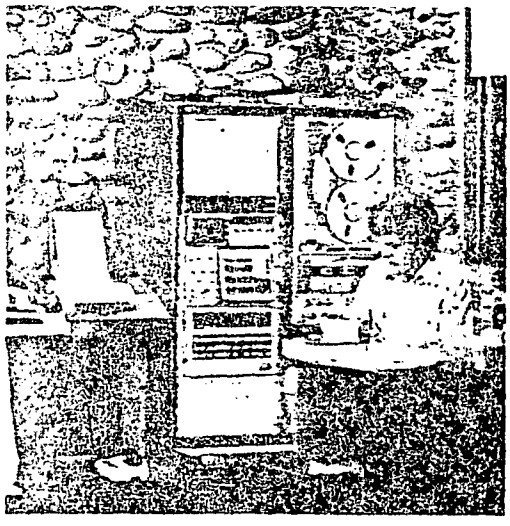

Geothermal Kinetics Inc. and Subsidiaries

(Companies in the Development Stage)

Consolidated Financial Statements, December 31, 1975

(With Accountants' Report Thereon)

Report of Independent Accountants

The Board of Directors
Geothermal Kinetics Inc.:

We have examined the consolidated statements of assets and unrecovered costs, liabilities, and common stock and additional paid-in capital of Geothermal Kinetics Inc. and subsidiaries (companies in the development stage) as of December 31, 1975 and the related consolidated statements of cash receipts and disbursements for the year ended December 31, 1975 and the period from June 29, 1971 (inception) to December 31, 1975. Our examination was made in accordance with generally accepted auditing standards, and accordingly included such tests of the accounting records and such other auditing procedures as we considered necessary in the circumstances.

The Company and its subsidiaries are in the development stage and realization of unrecovered costs is dependent upon future profitable operations (Note 1 to Consolidated Financial Statements). Also, the payment of current liabilities as they become due is dependent upon the Company and its subsidiaries' ability to generate sufficient funds from future profitable operations and/or obtain additional capital contributions or financing. We do not express an opinion on the Company and subsidiaries' ability to attain profitable operations or to obtain additional capital contributions or financing.

The Company is currently involved in a legal action described in Note 12. The final outcome of this suit is not presently determinable and no recognition has been given in the financial statements to the effect, if any, of such litigation.

In our opinion, subject to the effect, if any, on the financial statements of the ultimate resolution of the matters discussed in the preceding paragraphs, the consolidated statements of assets and unrecovered costs, liabilities, and common stock and additional paid-in capital at December 31, 1975 present fairly the information stated therein on the basis described in Note 1 to consolidated financial statements and the consolidated statements of cash receipts and disbursments presents fairly the cash transactions of the Company and its subsidiaries for the year ended December 31, 1975 and the period from June 29, 1971 (inception) to December 31, 1975.

Phoenix, Arizona
March 24, 1976
Except for the second paragraph of Note 12, which is as of June 1, 1976.

Peat, Marwick, Mitchell & Co.

Consolidated Statement of Assets and Unrecovered Costs, December 31, 1975

Cash		$ 171,314
Drilling Revenues Receivable		32,222
Prepaid Expenses		24,874
Total Current Assets		228,410
Notes Receivable from Officers, Including Accrued Interest of $23,429 (Note 2)		156,602
Furniture and Equipment (Note 3)	$ 850,607	
Less Accumulated Depreciation	380,148	
Net Furniture and Equipment		470,459
Other Assets, At Cost		9,750
Unrecovered Costs (Notes 4 and 5):		
Development of Wells	1,954,661	
Undeveloped Geothermal Leaseholds	1,450,175	
Promotional and Exploration Costs	2,874,645	
	6,279,481	
Less Receipts Applied as Reduction of Costs	2,253,633	
Net Unrecovered Costs		4,025,848
Total Assets and Unrecovered Costs		$ 4,891,069

SEE ACCOMPANYING NOTES TO CONSOLIDATED FINANCIAL STATEMENTS

Consolidated Statement of Liabilities, December 31, 1975

Accounts Payable and Accrued Expenses (Current)	$ 142,737
Advance from Parent (Note 8)	1,048,000
Total Liabilities	$ 1,190,737

Consolidated Statement of Common Stock and Additional Paid-in Capital (Notes 6 and 8), December 31, 1975

Common Stock of 1¢ Par Value. Authorized 5,000,000 Shares; Issued 3,536,850 Shares	$ 35,369
Additional Paid-in Capital	3,664,963
Total Common Stock and Additional Paid-in Capital	$ 3,700,332
Commitments and Contingencies (Notes 4, 11 and 12)	

Consolidated Statements of Cash Receipts and Disbursements, Year Ended December 31, 1975 and the Period from June 29, 1971 (Inception) to December 31, 1975

	Year Ended December 31, 1975		Inception to December 31, 1975	
Receipts:				
Sales of Common Stock		$ -		$ 3,186,782
Loans from Bank		-		144,500
Advances from Parent		-		1,298,000
Drilling Income		212,692		923,015
"Bottom Hole" Contribution		-		135,000
Reimbursements from Co-venturers		15,041		73,800
Receipts from McCulloch Oil Corporation (Note 5)		1,609,819		1,788,091
Research Income		-		220,000
Acquisition of 100% of Group Seven, Inc. (Note 7):				
Cash in Bank		-	$ 2,269	
Collection of Accounts Receivable Existing at Date of Acquisition		-	32,350	34,619
Sale of Equipment		1,800		49,803
Interest		8,500		29,564
Other		-		4,135
		1,847,852		7,887,309
Noncash Items -- Decrease (Increase) in Receivables and Prepaid Expenses		111,627		(80,525)
Total Receipts		1,959,479		7,806,784
Disbursements:				
Purchase of Equipment		41,669		361,628
Repayment of Loans and Contracts Payable		-		157,458
Deferred Costs:				
Development of Wells	$ 216,483		$ 2,924,725	
Undeveloped Geothermal Leaseholds	547,139		1,455,457	
Promotional and Exploration Costs	1,174,271	1,937,893	2,829,685	7,209,867
Repayment of Advances from Parent		-		250,000
Loans to Officers		-		133,173
Payment of Group Seven, Inc. Liabilities Existing at Date of Acquisition		-		2,267
Other		9,750		47,447
		1,989,312		8,161,840
Noncash Items:				
Depreciation		(138,536)		(383,633)
Increase in Accounts Payable and Accrued Expenses		(13,542)		(142,737)
Total Disbursements		1,837,234		7,635,470
Net Increase in Cash		122,245		171,314
Cash Balance at Beginning of Period		49,069		-
Cash Balance at End of Period		$ 171,314		$ 171,314

SEE ACCOMPANYING NOTES TO CONSOLIDATED FINANCIAL STATEMENTS

Geothermal Kinetics Inc. and Subsidiaries

(Companies in the Development Stage)

Notes to Consolidated Financial Statements, December 31, 1975

(1) BASIS OF PRESENTATION AND SUMMARY OF SIGNIFICANT ACCOUNTING POLICIES

(a) Basis of Presentation

The Company is in the development stage. Its primary activity is geothermal resource exploration and development, particularly with respect to geothermal steam for sale to electric utility companies for the generation of electricity. Management, at this time, cannot estimate at what date operating revenue may be realized. Accordingly, all costs, whether related to productive or nonproductive prospects, (including pre-operating, exploration and development, and geothermal lease acquisition costs) have been deferred, net of certain pre-operating revenues.

The amounts shown in the accompanying consolidated financial statements arise from transactions effected in cash, stock issued for the fair value of goods and services received, or by incurring obligations payable in cash, determined on the accrual basis. The accompanying consolidated financial statements do not purport to present financial position or results of operations in accordance with generally accepted accounting principles.

In June, 1975 the Financial Accounting Standards Board issued Statement of Financial Accounting Standards No. 7, "Accounting and Reporting by Development Stage Enterprises". This statement requires that essentially the same accounting and reporting standards applicable to established operating enterprises shall apply to companies in the development stage, with special accounting practices and reporting formats precluded. Implementation is required for fiscal years ending on or after January 1, 1976. It is anticipated that application of this statement will have a significant effect upon the financial statements; however, the extent of the effect has not yet been determined.

(b) Principles of Consolidation

The consolidated financial statements include the accounts of the Company and its two wholly-owned subsidiaries. All significant intercompany balances and transactions have been eliminated in consolidation.

Certain geothermal prospects are subject to joint venture agreements or other agreements where the ownership interest of the Company is less than 100%. The costs of the Company's proportionate interest in these prospects are included in the financial statements on the same basis as described in (a) above.

(c) Depreciation

Depreciation of equipment and furniture and fixtures is provided over the estimated useful lives of the respective assets on the straight-line basis.

(d) Income Taxes

The Company and its subsidiaries file consolidated income tax returns. Intangible exploratory and development costs are deducted as incurred for Federal and state income tax purposes. Investment tax credits will be recorded as a reduction of the provision for Federal income taxes in the year benefited.

(2) NOTES RECEIVABLE FROM OFFICERS

Loans are evidenced by 6½% interest-bearing demand notes and, except for one $8,000 note, are secured by shares or interest in shares of United Siscoe Mines Limited common stock having a market value at December 31, 1975 of approximately $115,000. Both officers are full-time employees of the Company and management does not intend to demand payment in the near future.

(3) FURNITURE AND EQUIPMENT

A summary of cost of furniture and equipment by category at December 31, 1975 follows:

Drilling Equipment and Tools	$ 680,514
Research Equipment	148,005
Automotive Equipment	13,634
Office Furniture and Fixtures	8,454
	$ 850,607

(4) UNRECOVERED COSTS

A summary of unrecovered costs by category and type of expenditure at December 31, 1975 follows:

	Development Of Wells	Undeveloped Geothermal Leaseholds	Promotional And Exploration Costs	Total Unrecovered Costs
General and Administrative	$ 51,956	$ -	$ 1,931,466	$ 1,983,422
Leasehold Acquisition Costs	-	1,216,964	-	1,216,964
Delay Rentals	-	233,211	-	233,211
Intangible Drilling Costs	1,499,113	-	-	1,499,113
Well Equipment	226,730	-	-	226,730
Exploration Costs	-	-	737,152	737,152
Depreciation	176,862	-	206,027	382,889
	$ 1,954,661	$ 1,450,175	$ 2,874,645	6,279,481
Less Receipts Applied as Reduction of Costs:				
Reimbursements from Co-venturers				58,759
Research Income				220,000
Receipts from McCulloch Oil Corporation (Note 5)				1,788,091
"Bottom Hole" Contribution				135,000
Other				51,783
				2,253,633
Net Unrecovered Costs				$ 4,025,848

The Company and its subsidiaries have received drilling revenues amounting to $923,015, of which $578,255 has been from ventures in which the Company has been a participant. All of these revenues have been applied as a direct reduction of the intangible drilling costs reflected above. The Company also received research income of $175,000 from a venture in which it was a participating member, which is included in research income and offset against unrecovered costs.

At December 31, 1975, the Company had under geothermal lease approximately 149,000 acres, of which approximately 4,300 acres have been contributed to joint ventures and approximately 123,000 acres are subject to joint development or joint venture agreements. The remaining terms of such leaseholds range from one to ten years. Annual lease payments approximate $311,000. The leases provide for royalty payments to the lessors of 10% to 18¼% of gross receipts received from the sale of steam, if and when steam is sold commercially.

(5) JOINT VENTURES AND OTHER AGREEMENTS

The Company has been a party to three joint venture agreements for the purpose of developing geothermal resources. Additionally, the Company has entered into agreements with McCulloch Oil Corporation for the development of certain prospects of mutual interest.

(a) Utah Steam Venture

In December 1974 the Company entered into a joint venture agreement for the exploration and development of certain geothermal prospects. Assets, income, profits, costs and expenses are shared equally except for the costs of drilling certain test wells, on which the Company is responsible for costs in excess of $500,000 for each well. At December 31, 1975 leaseholds approximating 4,300 acres along with all scientific data accumulated thereon had been contributed by the Company to the venture. The Company's unrecovered costs associated therewith are included in the consolidated statement of assets and unrecovered costs and approximate the following:

Promotional and Exploration	$ 300,000
Undeveloped Geothermal Leaseholds	200,000
Development of Wells	475,000
	$ 975,000

Subsequent to December 31, 1975 a joint venture agreement was entered into between Utah Steam Venture (of which the Company is a participant) and McCulloch Oil Corporation for the development of certain geothermal prospects. These prospects are owned by the Company but are subject to the Utah Steam Venture agreement. McCulloch is obligated to pay certain costs of drilling two test wells. The Utah Steam Venture has the option to participate in subsequent development, revenues and costs in various proportions.

(b) Montana Venture

In August, 1974 the Company entered into a joint venture agreement for the purposes of carrying out an exploration program in Montana and adjacent states, with the goal of locating drillable prospects and the ultimate development of geothermal steam. Assets, income, profits, costs and expenses are shared equally except for certain initial exploration, lease acquisition and development costs, which are shared in various proportions. At December 31, 1975 there were no unrecovered costs included in the consolidated statement of assets and unrecovered costs associated with prospects subject to the terms of this agreement.

(c) Casa Grande Venture

In March, 1974 the Company entered into a joint venture agreement (Casa Grande Venture) for the

exploration and development of geothermal steam resources. The Venture was terminated in January, 1975 and all leaseholds conveyed to the Company.

(d) McCulloch Oil Corporation

In December, 1974 the Company entered into an agreement with McCulloch Oil Corporation for the exploration and development of geothermal resources. This agreement and subsequent amendments and modifications thereto provide for development of certain prospects of mutual interest. McCulloch is obligated to pay certain costs and to drill or cause to be drilled test wells, in consideration for which McCulloch receives an interest in the prospects. The amount of interest received by McCulloch in each prospect will vary dependent upon elections by Geothermal Kinetics to either retain a 30% carried interest or a 50% participating interest on all development subsequent to the initial test well, except for two prospects on which it can retain either a 30% carried interest or a 10% overriding royalty interest in the proceeds from the sale of steam.

Through December 31, 1975 the Company has received a total of $1,788,091 from McCulloch in accordance with the terms of the aforementioned agreements, $1,060,204 of which was expended to acquire leaseholds and to perform certain exploration work on prospects of mutual interest. As of December 31, 1975 McCulloch had not yet earned a working interest in any prospect presently owned by the Company and the total $1,788,091 has been offset against unrecovered costs.

The agreements also provide that McCulloch shall receive a credit equal to certain amounts not expended by the Company on prospects of mutual interest. This credit is to be used by McCulloch to acquire interest in certain other prospects owned by the Company to be mutually agreed upon at a future time. At December 31, 1975 this credit amounted to $244,216.

(6) COMMON STOCK AND ADDITIONAL PAID-IN CAPITAL

Common stock transactions from June 29, 1971 (inception) to December 31, 1975 are summarized as follows:

	Common Stock	Additional Paid-In Capital (a)	Total Stockholders' Equity
Shares Issued for Cash:			
Other Than Exercise of Options	$ 14,533	$ 1,209,849	$ 1,224,382
Upon Exercise of Options by United Siscoe Mines Limited	7,520	1,954,880	1,962,400
Shares Issued in Consideration for Various Assets and Leaseholds	12,636	488,714	501,550
Shares Issued in Acquisition of Group Seven, Inc. (Note 7)	480	11,520	12,000
Balances at December 31, 1975	$ 35,369	$ 3,664,963	$ 3,700,332

(a) Commissions totaling $109,657 were paid on the sale of common stock in accordance with an agreement granting options to United Siscoe Mines Limited. The commissions were netted against additional paid-in capital.

At December 31, 1975 approximately 62% of the outstanding common stock was owned by United Siscoe Mines Limited (a Canadian corporation) and its partly-owned subsidiary. Officers and directors of the Company owned approximately 9% of the outstanding shares at that date.

(7) BUSINESS COMBINATION

The company formed a subsidiary, Group Seven Inc. (a Nevada corporation), during 1973. Through Group Seven Inc. (a Nevada corporation), the Company effected a business combination with Group Seven, Inc. (a Colorado corporation) and acquired its net assets in exchange for 48,000 shares of the Company's common stock, effective July 31, 1973.

The acquired company, Group Seven, Inc. (a Colorado corporation), accounted for its transactions on a modified cash basis. At the date of acquisition adjustments were made to reflect the assets, liabilities and retained earnings of the acquired company on a basis consistent with that of Geothermal Kinetics Inc. These adjustments increased assets approximately $51,000 while increasing liabilities and retained earnings $37,000 and $14,000 respectively. The assets and liabilities were recorded on the basis of historical cost and are summarized after adjustments, as follows:

Assets:		**Liabilities, All Current**	$ 51,000
Cash and Other Assets	$ 3,000	**Stockholders'Equity:**	
Accounts Receivable	47,000	Common Stock	12,000
Equipment, Net	45,000	Retained Earnings	32,000
	$ 95,000		$ 95,000

The retained earnings of Group Seven, Inc. prior to acquisition by the Company and subsequent to elimination of intercompany profits, are not material to the consolidated financial statements and have been credited to unrecovered costs -- promotional and exploration expenses.

Group Seven Inc. specializes in the exploration of geothermal resources.

(8) STOCK OPTIONS

During 1975 the Company extended the expiration date on options held by the President and a member

of the Board of Directors to purchase 40,000 shares of common stock at $2.70 per share from July 5, 1976 to December 31, 1979 and granted additional options to purchase 75,000 shares at $2.85 per share to the Chairman of the Board of Directors and the President.

Options outstanding and exercisable at December 31, 1975 are as follows:

	Number of Shares	Exercise Price	Options Expire
United Siscoe Mines Limited	1,098,000	$ 3.50	December 31, 1979
United Siscoe Mines Limited	200,000	10.00	June 30, 1976
Officers and Directors:			
Chairman of the Board of Directors	50,000	2.85	December 31, 1979
Member of the Board of Directors	15,000	2.70	December 31, 1979
President	50,000	2.70-2.85	December 31, 1979
	1,413,000		

Subsequent to December 31, 1975, United Siscoe Mines Limited gave notice of intent to exercise options to purchase 310,000 shares of common stock at $3.50 per share, to be paid for by converting the balance of its advance to the Company ($1,048,000) plus $37,000 cash.

(9) INCOME TAXES

At December 31, 1975 the Company and its subsidiaries had tax net operating loss carry-forwards approximating the amounts tabulated below:

Year of Expiration	Amount
1976	$ 158,000
1977	946,000
1978	673,000
1979	629,000
1980	665,000

The amount previously estimated for the net operating loss expiring in 1979 ($960,000) has been revised, based upon determinations made when the 1974 income tax returns were filed during 1975.

Investment tax credit carry-forwards are not material.

(10) TRANSACTIONS WITH OFFICERS AND/OR SHAREHOLDERS AND OTHER RELATED PARTIES

The President, who also is a minority stockholder, is a partner in a law firm retained by the Company as legal counsel. Payments to this firm for legal services approximated $51,000 in 1975, $65,000 in 1974 and $37,000 for the 17 months ended December 31, 1973.

On September 2, 1975 the Company entered into a three-year agreement to retain the services of a law firm in which the Chairman of the Board of Directors is a partner. The agreement provides for a monthly retainer fee of $3,750. In 1975 this firm was paid approximately $19,000 for legal services.

(11) COMMITMENTS

The Company and its subsidiaries occupy offices and hold certain property under lease arrangements, all of which are classified as operating leases. A summary of noncancellable long-term lease commitments follows:

Year Ending December 31,	Equipment	Real Property	Total Commitment
1976	$ 22,754	$ 3,600	$ 26,354
1977	11,920	3,300	15,220
1978	2,878	-	2,878

The Company has the following minimum annual commitments in connection with certain employment agreements with officers and directors and the retainer agreement described in Note 10.

Year Ending December 31,	Employment Agreements	Retainer Agreement	Total Commitment
1976	$ 80,000	$ 45,000	$ 125,000
1977	42,500	45,000	87,500
1978	3,333	30,000	33,333

(12) LITIGATION

The Company is plaintiff in a suit to quiet title on certain geothermal resources contained within a parcel of land in Sonoma County, California. The Company is claiming a leasehold interest in such resources as a sublessee from the owner of the mineral estate. The defendants claim a similar interest in the same resources as sublessees from the surface owners of the property. The complaint was filed in November, 1973 and the defendants filed a cross-complaint for actual damages in the amount of at least $5,000 and exemplary damages in the amount of $100,000. The Company filed a cross-complaint seeking an equitable adjustment of the rights of the parties if it should be found to have been a trespasser. The cross-complaints were severed from the quiet title action by court order in January 1976. The trial on the quiet title action ended on March 1, 1976 and the matter was submitted to the court for a decision.

On June 1, 1976, the Superior Court in Sonoma County, California rendered an opinion which vested full title to these geothermal resources in the Company, and dismissed the claims of Union Oil Company as to any right of ownership to these resources. The court has directed a judgement to be entered in accordance with this opinion. Union Oil Company has 60 days from the date this judgement is entered on the docket in which to appeal this decision.

7/E

APPENDIX I

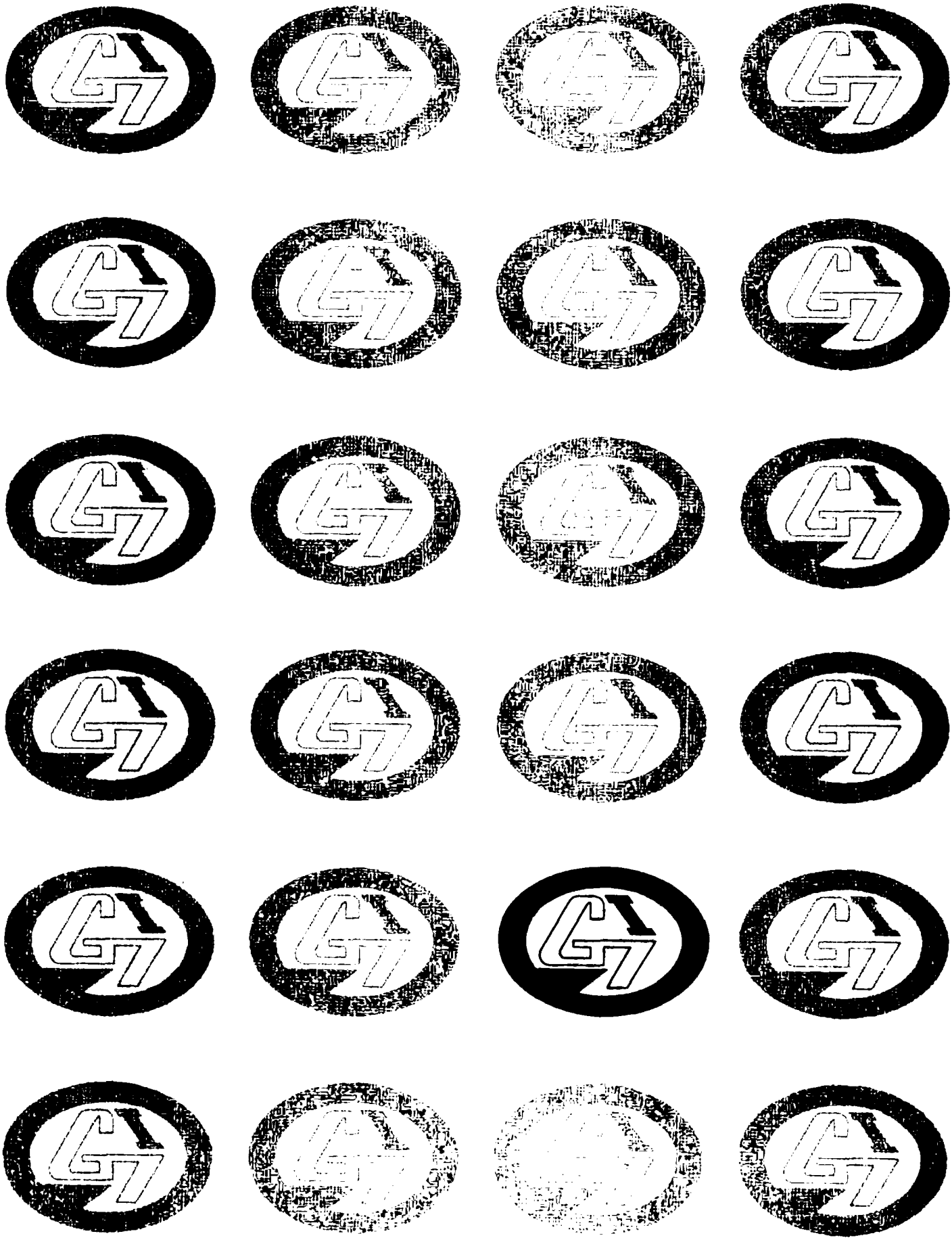

APPENDIX I

PROPOSAL EY-R-08-007

to

ENERGY RESEARCH AND DEVELOPMENT ADMINISTRATION

from

GROUP SEVEN, INC.

1301 Arapahoe Street

Golden, Colorado 80401

A SURVEY

OF THE

GEOTHERMAL POTENTIAL

OF THE

ESCALANTE DESERT

UTAH

Prepared for:
GEOTHERMAL KINETICS, INC.
301 West Indian School Road
Phoenix
Arizona 85013

Prepared by:
GROUP SEVEN, INC.
1301 Arapahoe Street
Golden
Colorado 80401

9 February 1977

TABLE OF CONTENTS

Section 1

LITERATURE SEARCH--GEOLOGY

In this section, a brief description of the geology of southwestern Utah will be given in order to provide a framework for more detailed geological and geophysical investigations. The geologic history of the Great Basin of the western United States has been studied by many workers. It is proposed here to give a brief summary of this history mainly following the work of Burchfiel and Davis (1972) who have synthesized the work of prevous authors. The geology of the area is complex involving sediments from Precambrian to Recent together with some 40 million years of intense igneous activity (Figure 1-1).

The late Precambrian and Paleozoic geosyncline occupied the greater part of what is now the Great Basin. The western limits of the Basin are somewhat obscure but the eastern margin occupies essentially the position of the Wasatch-Hurricane fault zone which is the western physiographic boundary of the Colorado Plateau (Figure 1-2). Typical eugeosynclinal and miogeosynclinal rocks were deposited, the miogeosyncline occupying the eastern part of the Basin. In the middle and late Paleozoic, thrusting to the east took place. A major change in tectonic patterns occurred during the late Paleozoic or the early Mesozoic which resulted in a marginal arc complex cross-cutting the Paleozoic geosynclinal and structural trends. The western edge of the Mesozoic continent was approximately that of the present continent while the eastern margin of

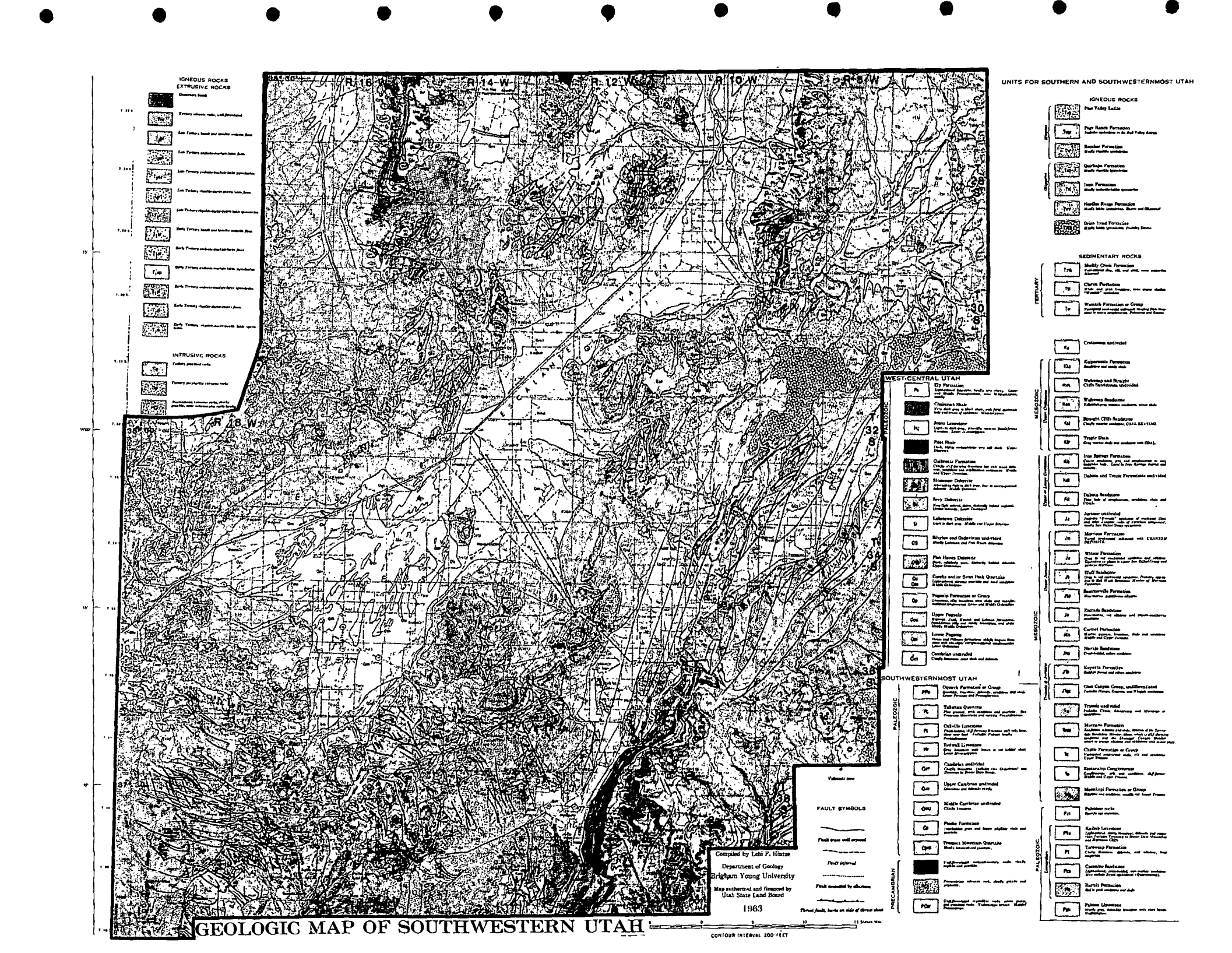
R. 18 W.
R. 16 W.
R. 14 W.
R. 12 W.
R. 10 W.
R. 8 W.
IGNEOUS ROCKS
EXTRUSIVE ROCKS
INTRUSIVE ROCKS
FAULT SYMBOLS
Compiled by Lehi F. Hintze
Department of Geology
Brigham Young University
Map authorized and financed by
Utah State Land Board
1963
GEOLOGIC MAP OF SOUTHWESTERN UTAH
CONTOUR INTERVAL 200 FEET
UNITS FOR SOUTHERN AND SOUTHWESTERNMOST UTAH
IGNEOUS ROCKS
SEDIMENTARY ROCKS
WEST-CENTRAL UTAH
SOUTHWESTERNMOST UTAH
CENOZOIC
MESOZOIC
PALEOZOIC
PRECAMBRIAN

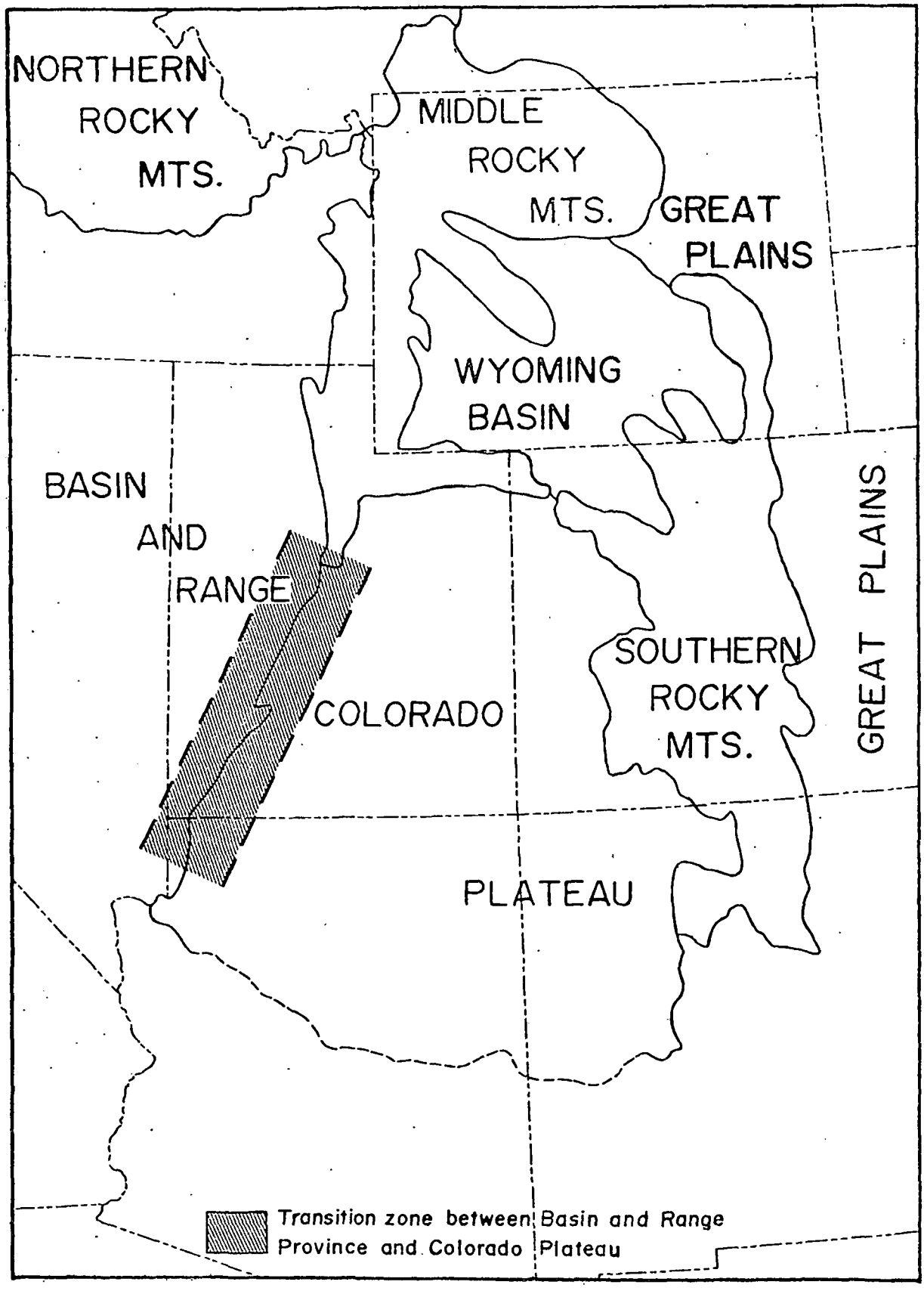

Figure 1-2. Setting of Transition Zone between Basin and Range Province and Colorado Plateau.

the Mesozoic geosyncline followed that of the Paleozoic geosyncline. In the late Jurassic, the Sevier Arch appeared and affected sedimentation in central and southern Utah (Harris, 1959). The culmination of this orogenic feature was thrusting to the east which caused Paleozoic miogeosynclinal rocks to be deposited on top of continental rocks of Cretaceous age. The Sevier orogeny has been described and analyzed by workers such as Armstrong (1968) and Miller (1966).

In southwestern Utah, the Tertiary opened with a brief period of continental deposition (Claron formation). This quiescent period was immediately followed by the initiation of a long period of extensive igneous activity. The geochronology of the Tertiary igneous activity has been described by Armstrong (1970). Starting approximately 33 million years ago, a period of extrusive silicic volcanism accompanied by silicic intrusion began in the eastern Basin and Range Province. The activity was continuous until perhaps 15 million years ago, although the activity changed in intensity during this period (Figure 1-3). There was a lull between 15 and 11 million years ago which was followed by a period of acid intrusion followed by a period of silicic volcanism until about 2 million years ago. The latest igneous activity has been the extrusion of basaltic lavas in the Quaternary. This igneous activity occurred in the Transition Zone between the Colorado Plateau to the east and the Basin Range Province to the west (Figures 1-1 & 1-2). Essentially, the eastern boundary of the Tertiary igneous activity

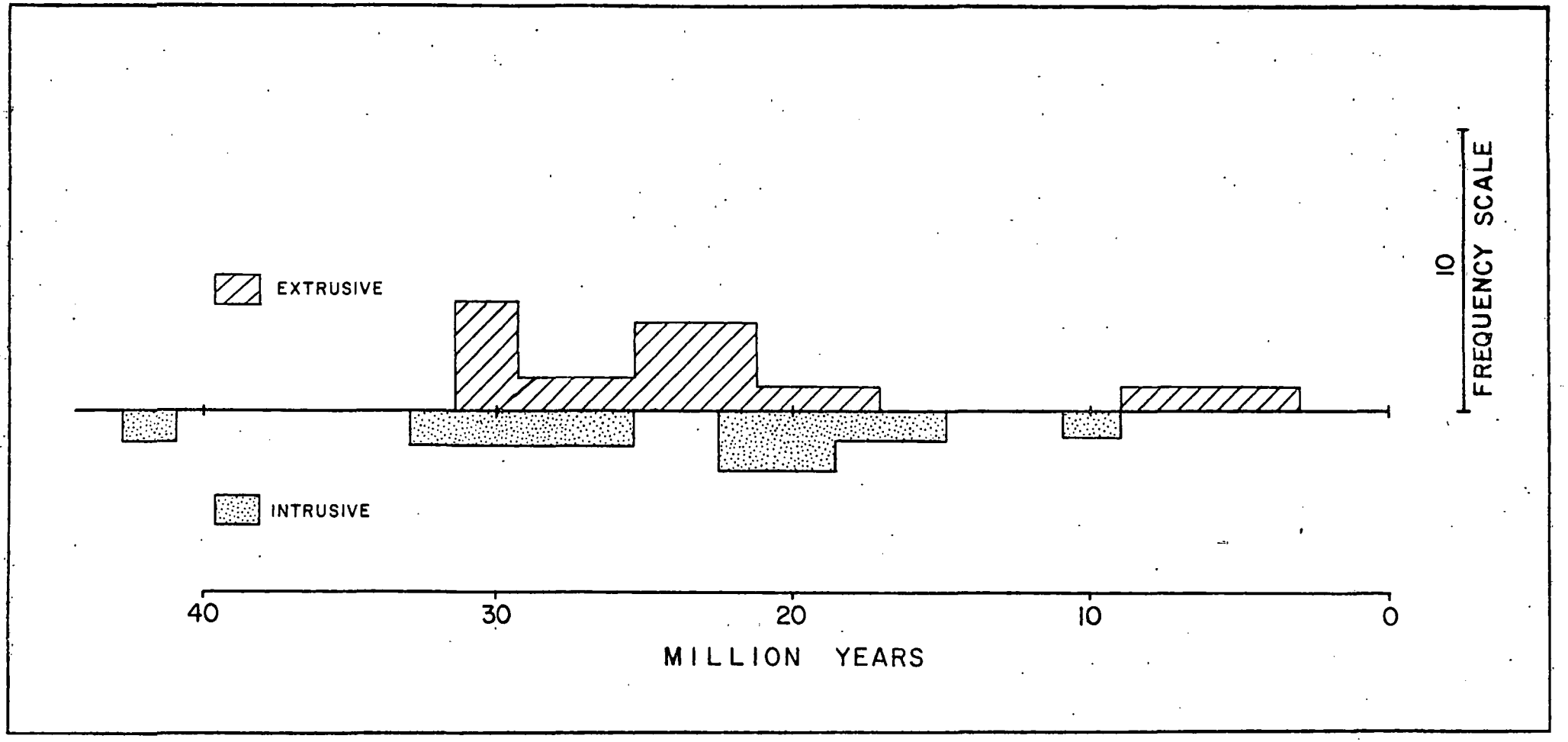

Figure 1-3. Geochronology of igneous rocks in southwestern Utah (after Armstrong, 1970).

is the eastern boundary of the Paleozoic and Mesozoic geosynclines. From this evidence, it would thus appear that the eastern boundary of the geosynclines has, throughout geologic history, marked a profound change in the earth's crust and mantle. This zone of change became most active in the early Tertiary. That it has continued to be active, is evident from the intense igneous activity which has taken place up to the present.

In southwestern Utah, the Transition Zone between the Basin Ranges and the Colorado Plateau is about 100 kilometers wide (Figure 1-2), it extends from the Sevier fault, within the Colorado Plateau, to the western boundary of the Escalante Valley (Figure 1). The search for geothermal reservoirs has been concentrated in that area of the Transition Zone west of the Hurricane-Wasatch fault. The geology in this area is a highly complicated mixture of Tertiary extrusive igneous rocks mixed with volcano-clastic sediments which has been repeatedly intruded by quartz-monzonite, mainly in the form of laccoliths. This complex overlies and is intruded into Mesozoic formations which outcrop in limited areas (Figure 1). The initial work in deciphering this volcanic stratigraphy was carried out by Macken (1960) and continued by Anderson (1971) and Anderson et al. (1975). This work has shown that there is a pile of intermediate lava flows and volcanic breccia with attendant clastic deposits covered over by Quaternary lake and stream deposits. Of great interest is what lies underneath the Tertiary volcanics in the Transition Zone. It has been

reported by Miller (1966) that the Blue Mountain thrust lies on top of an autochthon similar to the Colorado Plateau section. This fact leads to the question, is the Plateau section contained within the Transition Zone, and do the thrust plates, which carried Paleozoic limestones over the Cretaceous sediments, extend into the Transition Zone? Hamilton and Meyers (1966) and Atwater (1970) have theorized that the western part of the continent has been translated to the northwest causing crustal stretching in the Great Basin. The eastern boundary of this movement is the Wasatch-Hurricane Front. If such movement took place, then it is probable that the rocks of the eastern Great Basin were stretched and broken in a manner similar to those of the Basin Ranges and do exist, perhaps discontinuously, beneath the Transition Zone.

In the western part of the Transition Zone lie the youngest sedimentary rocks, mainly Quaternary lake beds, which indicates that the greatest subsidence has taken place along the Basin-Range-Transition Zone boundary. The Quaternary basalts which occur both within the Transition Zone and on the Plateau itself would indicate that the Transition Zone between the Basin Ranges and the Colorado Plateau is still a focus of tectonic activity. That basalts are present indicates that faults have tapped the mantle. These Quaternary basalts have been down-faulted into Mesozoic sediments (Figure 1) confirming that tensional forces are still operating along the western edge of the Colorado Plateau.

These phenomena indicate the Transition Zone has the prerequisites for the development of geothermal reservoirs. These prerequisites are:

1. Mantle intrusion into the crust.
2. A great thickness of porous rocks to provide an insulating blanket so that high temperature gradients may be developed.
3. Sufficient volume of rocks to entrap large bodies of hot water.

REFERENCES

Anderson, J. J., 1971, Geology of the southwestern High Plateaus of Utah--Bear Valley formation, an Oligocene-Miocene volcanic arenite: Geol. Soc. America Bull., v. 82, p. 1179-1205.

Anderson, J. J., Rowley, P. D., Fleck, R. J., and Nairn, A.E.M., 1975, Cenozoic geology of southwestern High Plateaus of Utah: Geol. Soc. America Spec. Paper 160, 88 p.

Armstrong, R. L., 1968, Sevier orogenic belt in Nevada and Utah: Geol. Soc. Amer. Bull., v. 79, p. 429-458.

Armstrong, R. L., 1970, Geochronology of Tertiary igneous rocks, eastern Basin and Range Province, western Utah, eastern Nevada, and vicinity, U.S.A.: Geochim. Cosmochim. Acta, v. 34, p. 203-232.

Atwater, T., 1970, Implications of plate tectonics for the Cenozoic evolution of western North America: Geol. Soc. America Bull., v. 81, p. 3513.

Burchfiel, B. C. and Davis, G. A., 1972, Structural framework and evolution of the southern part of the cordilleran orogen, western United States: Am. Jour. Sci., v. 272, p. 97-118.

Hamilton, W., and Myers, W. B., 1966, Cenozoic tectonics of the western United States: Reviews of Geophys., v. 4, n. 4, p. 509-550.

Mackin, J. H., 1960, Structural significance of Tertiary volcanic rocks in southwestern Utah: Amer. Jour. Sci., v. 258, p. 81-131.

Miller, G. M., 1966, Structure and stratigraphy of southern part of the Wah Wah mountains, southwest Utah: Amer. Assoc. Petrol. Geol. Bull., v. 50, n. 5, p. 858-900.

Section 2

LITERATURE SEARCH--GEOPHYSICS

The Transition Zone (Figure 2-1) between the Basin Ranges and the Colorado Plateau in western Utah has been studied using a variety of geophysical methods. The results indicate that a lateral discontinuity in the crust and upper mantle exists under the Wasatch-Hurricane fault zone. The salient features of the geophysics of the crust and upper mantle are detailed below.

Southwestern Utah is part of the Intermountain Seismic Belt described by Smith and Sbar (1974), earthquakes are numerous and swarm activity took place north of Cedar City in 1971. These latter events indicated normal faulting along a north-northeast trending fault plane. Smith and Sbar indicate that few earthquakes have taken place below 25 km during the time period analyzed (1961-70). Several seismic refraction studies by Prodehl (1970), Braile et al. (1974) and Keller et al. (1975) show that there is a marked thickening of the crust from 30 km under the Basin Ranges to 43 km under the Colorado Plateau. These studies indicate that the 43 km crustal thickness is reached about 50 km east of the physiographic boundary of the Colorado Plateau. Braile et al. (1974) and Keller et al. (1975) further state that their data indicate that a protrusion of mantle rock into the crust exists within the Transition Zone between the two provinces.

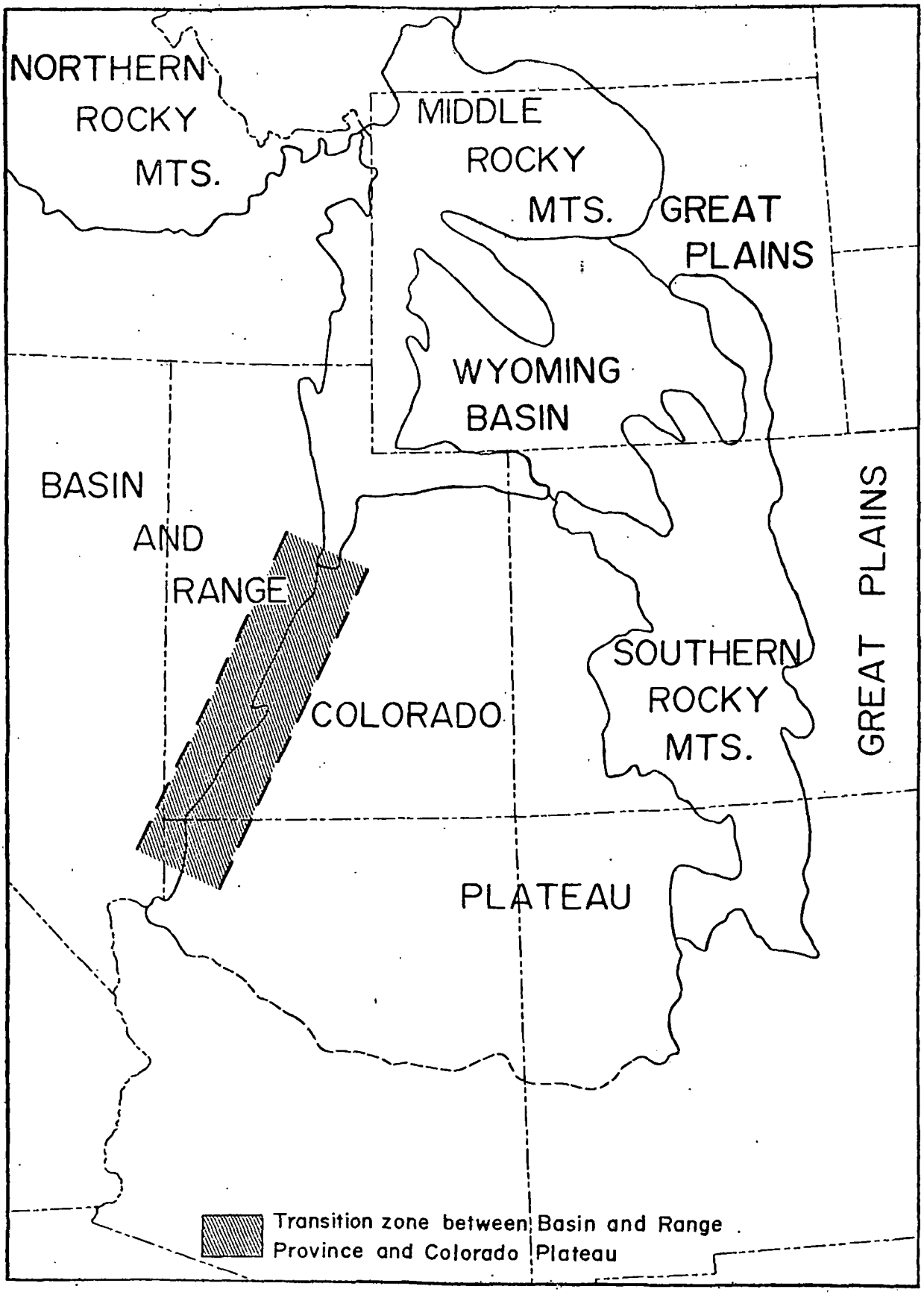

Figure 2-1. Setting of Transition Zone between Basin and Range Province and Colorado Plateau.

An examination of the simple Bouguer gravity map of Utah shows that there is a strong gravity gradient from high over the Basin Ranges to low over the Colorado Plateau. In part, this gradient may be due to topographic relief but, alternatively, it is probably due to the shallower crust under the Basin Ranges. Cook and Hardman (1967), in their gravity survey of Hurricane fault area, Utah, show that the northeast-southwest tectonic trends of the Wasatch Front extend to the western side of the Escalante Valley i.e. to the western margin of the Transition Zone.

The aeromagnetics of the region have been discussed by Shuey et al. (1973). One of the major features of their map is a linear magnetic low running along the Wasatch Front immediately east of the physiographic boundary. The authors propose that the magnetic low marks the western edge of the Curie isotherm downwarp under the Colorado Plateau. They also believe the magnetic highs to the west of the low are due to igneous intrusions.

The deep electrical structure of western North America has been analyzed using geomagnetic variations by Gough and his associates at the University of Alberta (see, for example, Porath and Gough, 1971; Reitzel et al., 1970). The latest map published by the University of Alberta group (Gough, 1975), part of which is shown in Figure 2-2, shows the electrical conductivity of the upper mantle under western North America. Under the Wasatch Front, and coincident with the Intermountain Seismic Belt and the linear magnetic low of Shuey et al., lies an elongate zone of high electri-

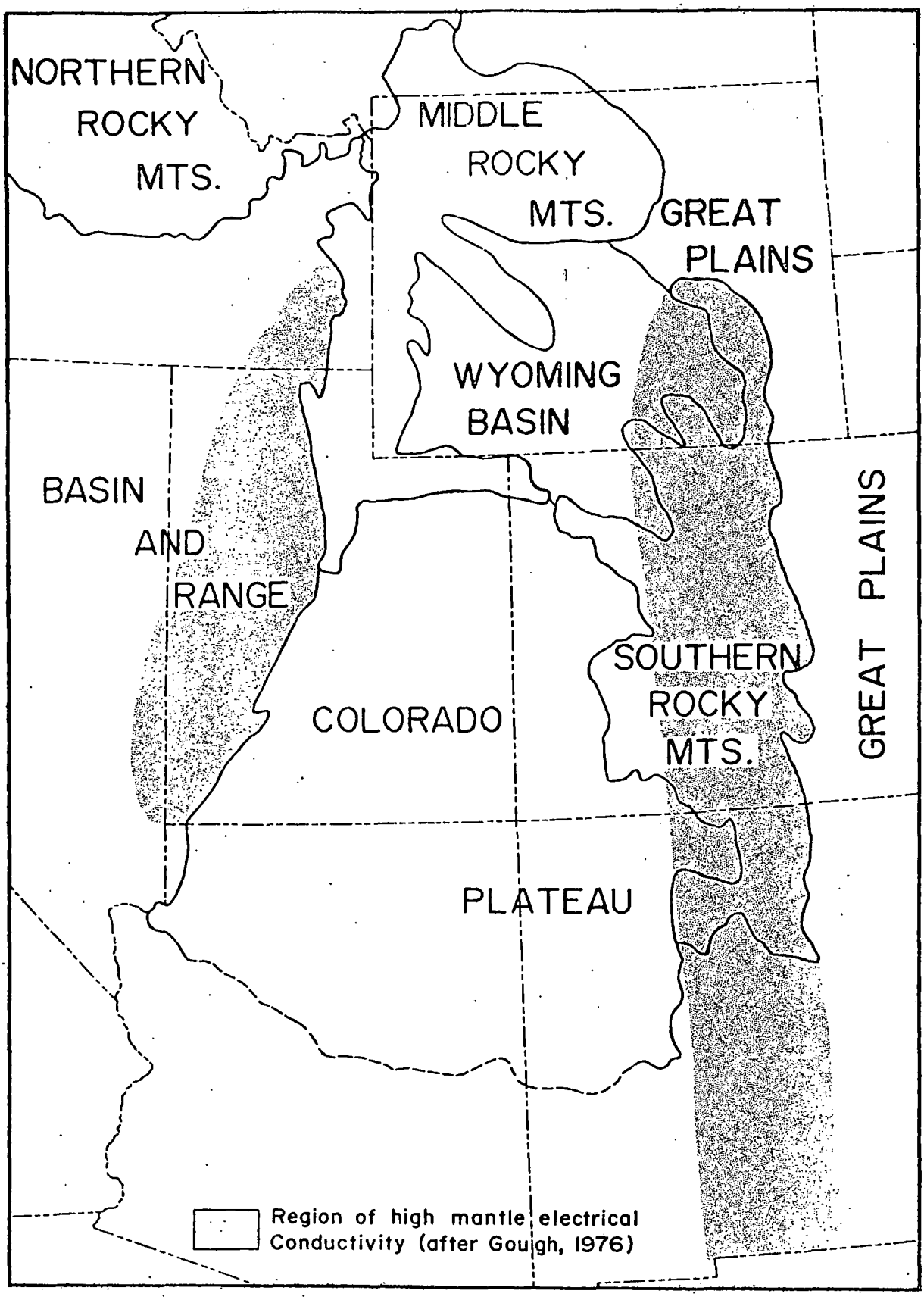

Figure 2-2. Region of high mantle electrical conductivity (after Gough, 1976).

cal conductivity. This zone, and its companion zone under the Rio Grande Trench, have the highest electrical conductivities in western North America; the conductive layer is believed to be on the order of 100 km thick. Porath (1971), from similar data, has shown that a protrusion of high conductivity rock with an amplitude of 70 km reaches to within 120 km of the earth's surface under the Wasatch Front. The profile for which this interpretation is valid lies about the latitude of Milford, Utah.

Apart from these rather generalized studies, which reveal a lateral mantle discontinuity which is indicated by the surface geology, little detailed work is available in the literature. The University of Utah has carried out detailed, shallow penetration electrical resistivity studies along with gravity and magnetics in the area of Roosevelt Hot Springs. None of these studies have shed any light on the origin of the heat source of the geothermal reservoir at Roosevelt. Below are the results of a series of electrical geophysical investigations of the Escalante desert region, which endeavored to locate geothermal reservoirs.

REFERENCES

Braile, L. W., Smith, R. B., Keller, G. R., Welch, R. M., Meyer, R. P., 1974, Crustal structure across the Wasatch Front from detailed seismic refraction studies: Jour. Geophys. Res., v. 79, p. 2669-2677.

Cook, K. L., and Hardman, E., 1967, Regional gravity survey of the Hurricane fault area and Iron Springs district, Utah: Geol. Soc. Amer. Bull., v. 78, p. 1063-1076.

Gough, D. I., 1975, Electrical conductivity in the upper mantle and recent tectonics of western North America: Inst. Earth and Planetary Phys., Ann. Rep. 1975, Univ. Alberta.

Keller, G. R., Smith, R. B., Braile, L. W., 1975, Crustal structure along the Great Basin-Colorado Plateau transition from seismic refraction studies: Jour. Geophys. Research, v. 80, n. 8, p. 1093-1098.

Porath, H., and Gough, D. I., 1971, Mantle conductive structures in the western United States from magnetometer array studies: Geophys. Jour. Roy.Astr. Soc., v. 22, p. 261-275.

Prodehl, C., 1970, Seismic refraction study of crustal structure in the western United States: Geol. Soc. Amer. Bull., v. 81, p. 2629-2646.

Reitzel, T. S., Gough, D. I., Porath, H., Anderson, C. W., III, 1970, Geomagnetic Deep Sounding in the western United States: Geophys. Jour. Roy. Astr. Soc., v. 19, p. 213-235.

Shuey, R. T., Schellinger, D. K., Johnson, E. G., Alley, L. B., 1973, Aeromagnetics and the transition between the Colorado Plateau and Basin Range provinces: Geology, v. 1, p. 107-110.

Smith, R. B. and Sbar, M. L., 1974, Contemporary tectonics and seismicity of the western United States with emphasis on the Intermountain Seismic Belt: Geol. Soc. Amer. Bull., v. 85, p. 1205-1218.

Section 3

GEOCHEMISTRY

Water from Shallow Wells

The Escalante Desert has no natural thermal phenomena, the closest hot spring is at Thermo, some 15 miles to the northeast. A hot spring was reported at Newcastle in the late nineteenth century, but the site is now covered by a reservoir. Chemical sampling of waters was thus restricted to the available water wells in the valley. The wells and springs sampled are listed in Table 3-I, where it can be seen that the majority of wells are cold. However, the relatively high silica content, the high chloride content and the low Na/K ratios suggest that part of the water might be thermal in origin. It is felt that the chloride content of the cold water might be the most significant parameter. An isochloride map is shown in Figure 3-1. Although the wells sampled are scattered, the variation in chloride content indicates a significant change in water chemistry occur in the Escalante Desert. There are two areas of high chloride concentration one which stretches from the center of T34S, R16W, to the southwest into T35S, R16W. The other is in the north half of T35S, R15W (Figure 3-1).

It was also found that certain wells contained water which was principally carbonate in nature, these wells can be divided into two groups. The grouping may be seen in Figure 3-2. One set of carbonate waters lies to the north of a line running approximately from the northeast corner of T34S, R15W to the southeast corner of

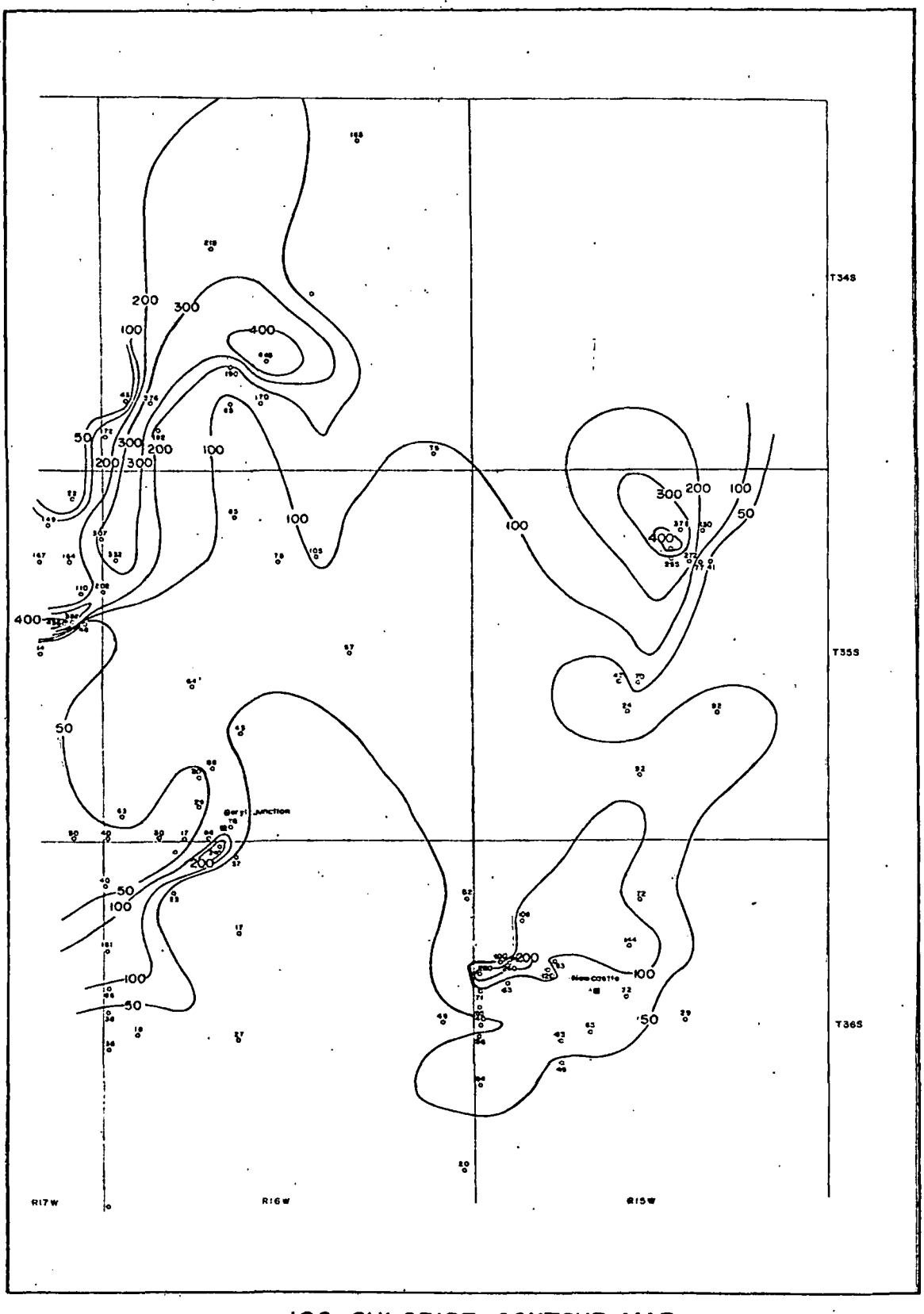

Figure 3-1. Map of chloride values of water from shallow wells and springs in the Escalante Desert region, Utah.

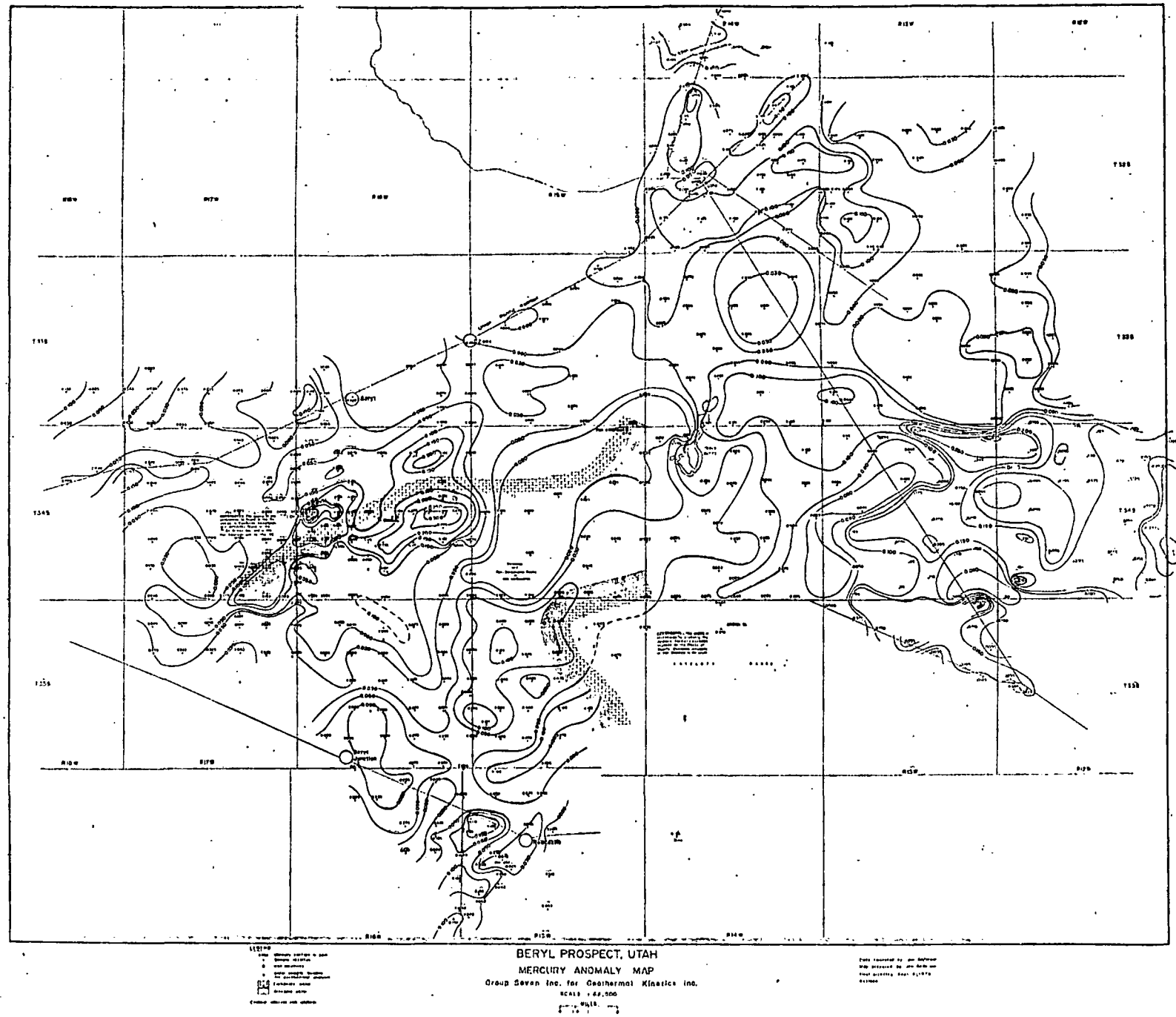

Figure 3-2. Soil mercury content in the Escalante Desert region, Utah.

T34S, R17W. The other grouping is that of three wells in the northeast corner of T35S, R15W.

Mercury Soil Survey

The second geochemical method which was employed in the Escalante Desert region was a survey of the mercury content of soil. The principal source of mercury is igneous rock from which it is leached by water and transported to the surface. The application of heat intensifies this process and it is well known that anomalous concentrations of mercury are found in the regions of thermal phenomena (Dall'Anglio, 1966, White, 1967).

Five hundred thirty-eight soil samples were collected in the Escalante Desert region and analyzed for their mercury content. The locations of the samples are shown in Figure 3-2. A histogram was prepared of the mercury concentration in parts per billion and is shown in Figure 3-3; the data are plotted on a semi-logarithmic basis because of the wide range of values of mercury concentration. The most significant feature of the histogram is a peak between the concentrations of 75 and 80 ppb. Subsidiary peaks occur between 45 and 50 ppb, 25 and 30 ppb and 15 and 20 ppb. The majority of concentrations are less than 70 ppb and the average background appears to lie between 25 and 60 ppb. So that any concentrations greater than 60 ppb are anomalous. Apart from the peak between 75 and 80 ppb, there are no significant departures from a downward trending curve as concentrations increase. However,

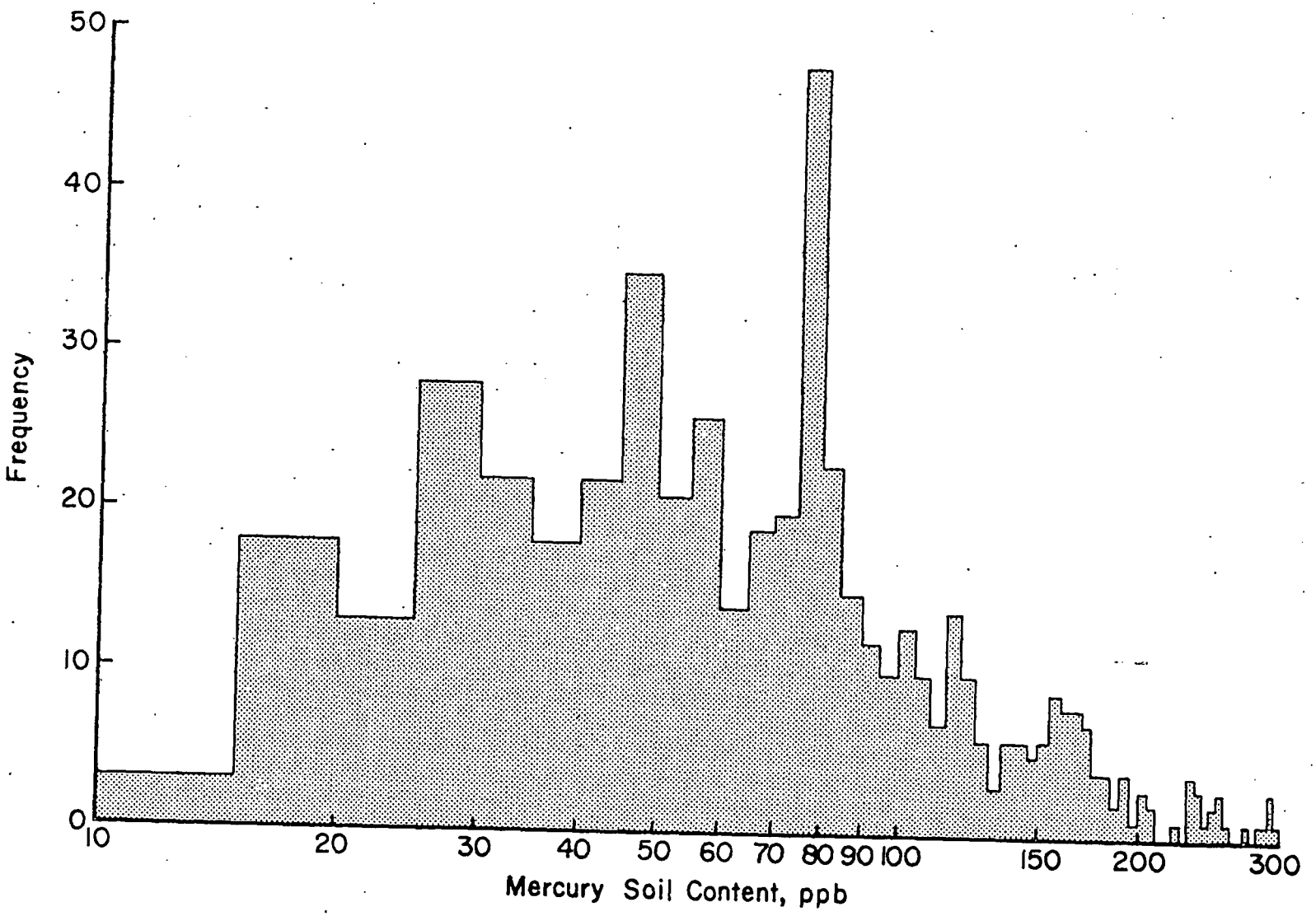

Figure 3-3. Histogram of mercury soil content from Escalante Desert region, Utah.

there are a significant number of anomalous values within the area sampled which indicates that a process other than straight-forward leaching and transport by water is operating. In the literature, such a phenomenon has been attributed only to increased subsurface temperature.

The highest concentrations of mercury in the Escalante Desert occur in T34S, R16W, where there are several samples which contained over 300 ppb. The region of these high concentrations is elongated east-west and lies on the boundary between waters which are principally of silicic type and those which are principally of a carbonate type. In the southern part of the Escalante Desert, the concentration reaches over 100 ppb in several places but no where does it approach the high concentrations to the north. To the northeast, in the Lund area mercury concentrations reach levels greater than 150 ppb. These anomalies represent increases of mercury concentration by a factor of between 3 and 6 times background which indicates that some process which causes increased mobility of the mercury has taken place and has concentrated mercury in the upper soil layer at two distinct areas within the Escalante Desert which are described above.

Water From Deep Wells

In the Escalante region, deep wells have been drilled at Roosevelt hot springs northeast of Milford, and in the Escalante Desert, #1 State was drilled in S22, T34S, R16W and #1 DeArman

drilled in S18, T34S, R16W. An oil test (State of Utah "B" #1) was drilled by the Pan American Oil Company west of Table Butte in S6, T34S, R14W. The chemical analysis of the water encountered in the Pan American well is not available at present. At Roosevelt, the wells produce sodium chloride water at temperatures in excess of 500°F. The #1 State well has Na-HCO_3 water which is similar to the non-thermal ground water of the area. The slight increase in sulphate (SO_4), sodium (Na), potassium (K) and silica (SiO_2) when compared to cold ground water is probably due to mixing, at some moderate depth, of cold surface waters and hot waters from depth. The #1 DeArman well produces sodium chloride (NaCl) water at a measured surface temperature of 208°F. Production was at a rate of 1,600 bbl per hour from a depth of 8,000 feet.

Several shallow warm wells were drilled near Newcastle in T36S, R15W Sections 16 and 17, the deepest to 500 feet. The temperatures of the shallower wells (less than 200 feet) are on the order of 92 to 96°F. However, the water produced from the 500 foot well has a temperature of 204°F at the surface and it is reported that 250°F were measured at a depth of 500 feet. Sodium sulphate ($NaSO_4$) is abundant in the water produced by the Newcastle warm wells. The water appears to be a mixture of thermal water with non-thermal water which has dissolved the sulphate ion from sulphate rich volcanic rock.

The trilinear plots shown in Figures 3-4 and 3-5 show the differences between chemical constituents of the analyzed waters.

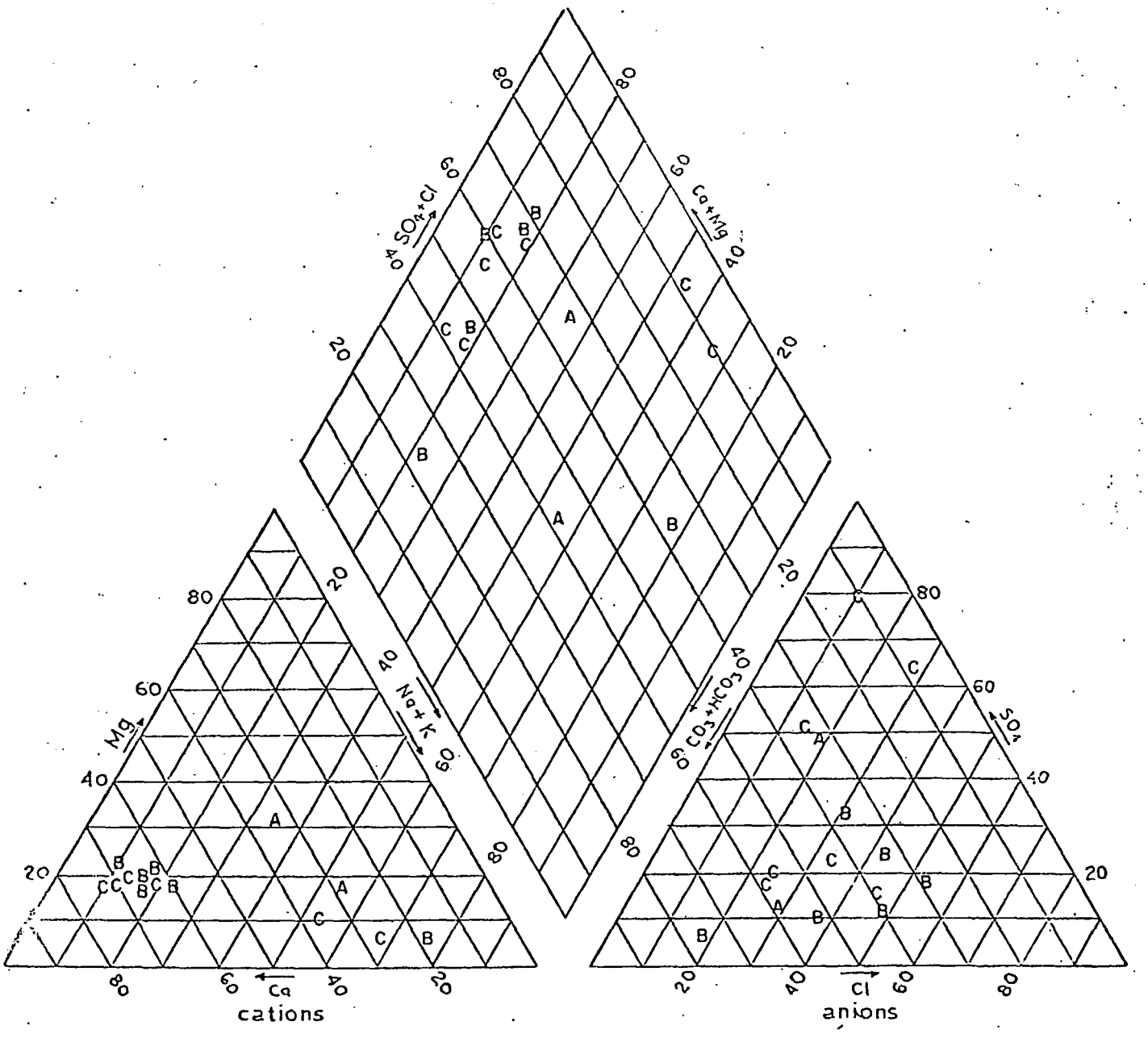

A Lund Area

B Beryl Area

C Newcastle Area

Figure 3-4. Percentage chemical composition of non-thermal (<20°C) ground water in southwestern Utah.

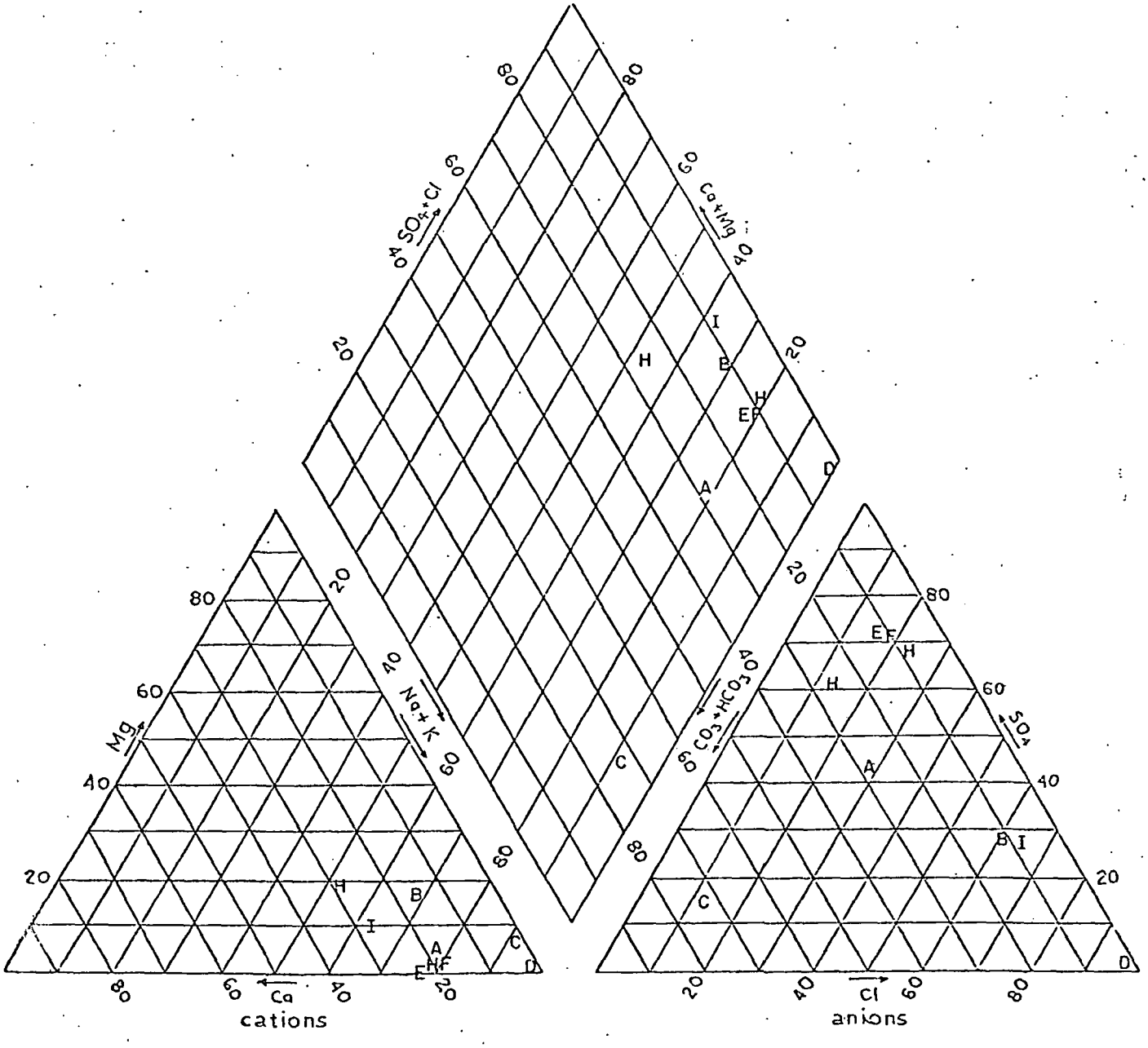

A	Thermo	G	Newcastle Warm Well 2
B	De Arman	H	Radium Warm Sp. (Minersville)
C	State	I	Meadow Hot Sp.
D	Roosevelt		
E	Newcastle Hot Well		
F	Newcastle Warm Well		

Figure 3-5. Percentage chemical composition of thermal (>30°C) ground water in southwestern Utah.

Basically, the plots show that the Roosevelt water is unmixed thermal water and that the other waters contain geothermal constituents. By using the mixing criteria developed by Fournier and Truesdell (1974), it can be seen that the #1 State has about 80% non-thermal water contained in it. The #1 DeArman has about 20% non-thermal water, and the deep Newcastle well has about 50% mixing of cold water.

An analysis of the geochemical thermometers SiO_2, Na/K and Na/K/Ca applied to the produced water from the wells in the Escalante desert gives the following results for temperatures at depth:

#1 State	450 - 470°F
#1 DeArman	430 - 450°F
Newcastle deep well	425°F

All of the geochemical evidence presented above indicates that none of the waters produced from depth in the Escalante desert is a pure thermal water similar to that at Roosevelt. However, the evidence shows that a geothermal reservoir must exist in the Escalante Valley in order that the water produced from both deep and shallow wells should have the chemical composition which it does.

REFERENCES

Dall'Anglio, Mario, Roit, R., and Tonani, F., 1966, Prospezione geochimica del mercurio; Industria Mineraria, v. 17, N. 9, p. 391-398.

Fournier, R. O., and Truesdell, A., 1974, Geochemical indicators of subsurface temperature--Part 2, estimation of temperature and fraction of hot water mixed with cold water: Jour. Research U. S. Geol. Survey, v. 2, n. 3, p. 263-270.

White, D. E., 1967, Mercury and base-metal deposits with associated thermal and mineral waters, in Barnes, H. L., Editor, Geochemistry of Hydrothermal Ore Deposits: New York, Holt, Rinehart, and Winston, Inc., p. 575-631.

Section 4

GRAVITY

The Simple Bouguer anomaly map of southwestern Utah is shown in Figure 4-1. On this map, four major areas can be distinguished. On the east is the Colorado Plateau where contours are regular and gravity gradients are very small. In the northwest part of the area is the Basin and Range Province whose north-south structures are well delineated by the gravity contours. In the southern part of the map, the gravity contours run west-northwest east-southeast and show a strong gradient southward from the Colorado Plateau to the Basin and Range. The fourth major area shown on the map is the Transition Zone between the Basin Ranges and the Colorado Plateau. North of Adamsville this transition is shown to be a simple gravity gradient which extends from the northeast-southwest trending boundary of the Colorado Plateau into the north-south features of the Basin Ranges. However, south of Adamsville the gravity gradient between the two provinces becomes much less pronounced. There is still a noticeable gradient from the Colorado Plateau to the west, but the north-south Basin Range structures do not commence immediately west of the Plateau boundary, instead they commence west of the Escalante Desert and the Escalante Valley. In this zone, which is about 50 miles across, the major feature is a high caused by the laccolithic intrusions of Iron Mountain and Granite Mountain. If this feature is removed, there remains a quasi-circular gravity low encompassing the Escalante Desert. This feature is also at the point where the

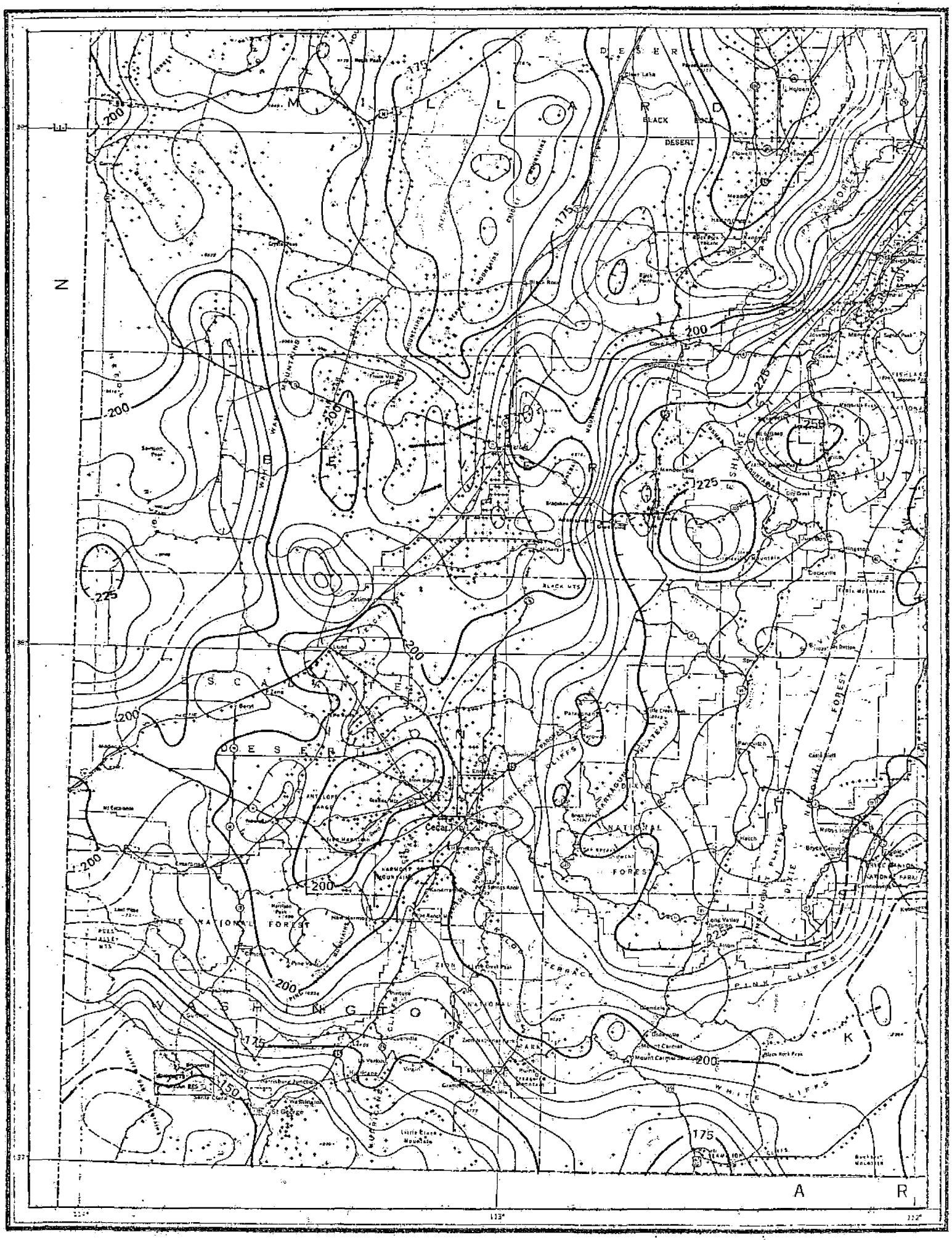

Figure 4-1. Simple Bouguer anomaly map of southwestern Utah (from Cook, Montgomery, Smith and Gray, 1975).

Wasatch-Hurricane trend meets the west-northwest east-southeast trending Texas lineament. Because of its anomalous position and anomalous gravity, the Escalante region became the focus of further exploration which is detailed below.

The detailed gravity maps of the Escalante Desert are shown in the Figures 4-2 (Beryl area) and 4-3 (Lund area). The data displayed on these maps was gathered by GROUP SEVEN, INC. and reduced to give complete Bouguer anomalies. In Figure 2, the most prominent features are a series of three gravity lows trending northwest to southeast across the central part of the map. In the southwest corner of the map is a gravity high which outlines an area of Tertiary volcanics shown on the geologic map of southwestern Utah (Figure 1-1, Section 1). In the southeast corner of the map is another gravity high which outlines the Antelope Hills, a Tertiary volcanic pile, possibly underlain by a quartz-monzonite intrusion. In the north central part of the map there is a large high which cuts across the boundary between the Basin-Range structures and the Transition Zone. In the northeast corner of the map are two grabens, both are long and linear, and are separated by a well-defined horst. This horst was named the Table Butte Horst by Cook and Hardman (1967). The graben to the north was named the Lund graben, that to the east, the Avon graben by the same authors. The gravity coverage to the northeast is contained in Figure 4-3, in this figure, the main features are the Avon and Lund grabens. The Lund graben is clearly fault-bounded to the northwest and less distinctly so to the south.

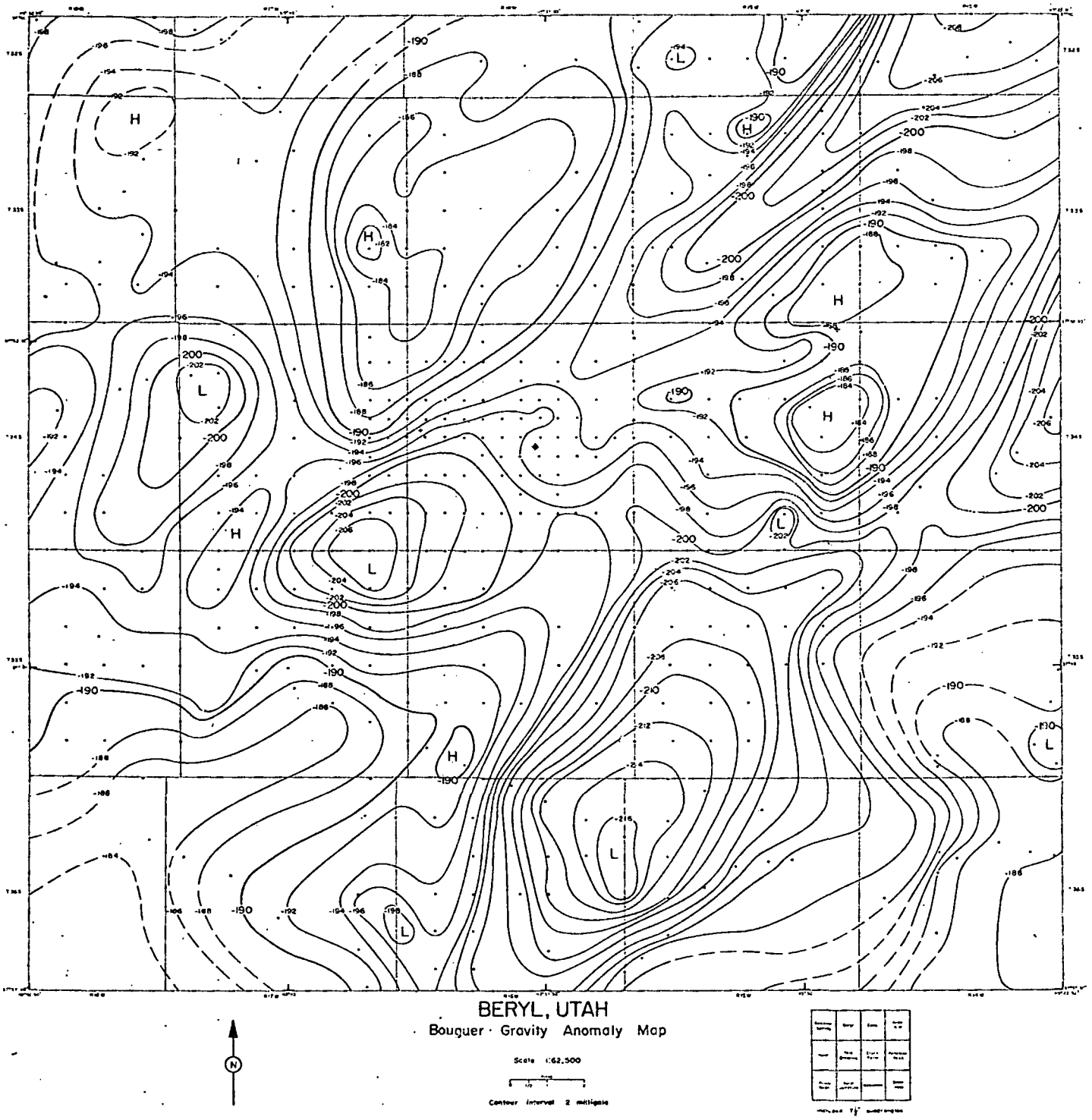

Figure 4-2. Complete Bouguer anomaly map of Beryl area, Escalante Desert, Utah.

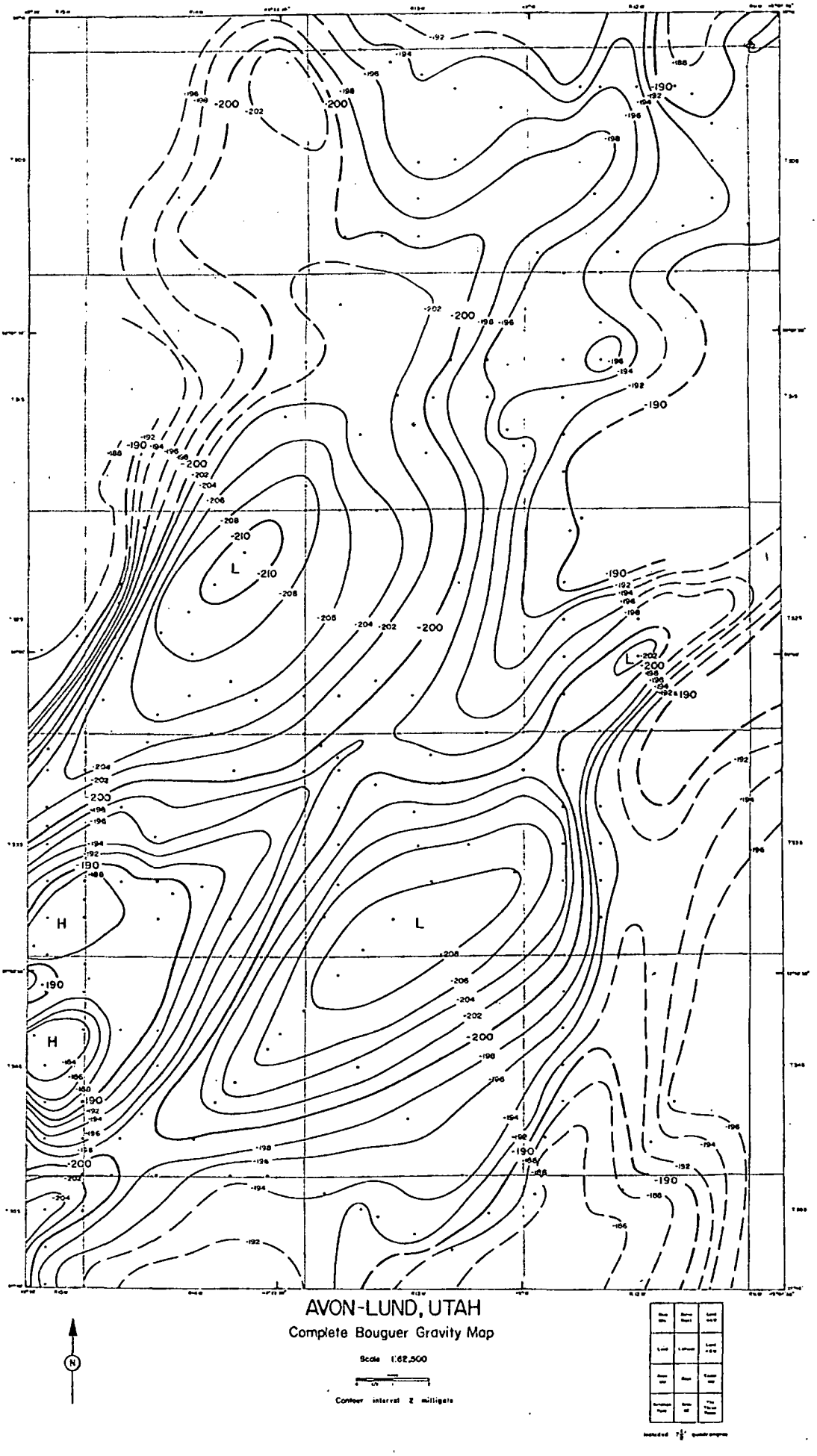

Figure 4-3. Complete Bouguer anomaly map of Avon-Lund area, Escalante Desert, Utah.

On the east, faulting is much less pronounced. The Avon graben is less elongate than the Lund graben and is fault-bounded on the east and on the northwest, the gradients to the south and to the north are much less conspicuous. The axes of the grabens trend northeast-southwest parallel to the Wasatch Front to the east.

These gravity data indicate that tectonic complexity increases to the southwest from the Lund-Avon area. The boundary between the two areas is rather diffuse, but trends north-northwest from the northern end of the Antelope Hills. The multiple, well-delineated gravity lows and the steep gradients associated with them argue for the presence of considerable block faulting within the desert margin. The block faulting may be complicated by the presence of dissected thrust sheets which are remanents of the Sevier Orogeny (Armstrong, 1968).

REFERENCES

Armstrong, R. L., 1968, Sevier orogenic belt in Nevada and Utah: Geol. Soc. Amer. Bull., v. 79, p. 429-58.

Cook, K. L., and Hardman, E., 1967, Regional gravity survey of the Hurricane fault area and Iron Springs district, Utah: Geol. Soc. Amer. Bull., v. 78, p. 1063-1076.

Section 5

MAGNETICS

The source of the magnetic data for the Escalante desert region is the aeromagnetic map of parts of Richfield and Cedar City quadrangles published by the U.S.G.S. at a scale of 1:250,000 (Figure 5-1). The principle feature of high magnetic intensity is a linear belt which runs in a curving path from northeast to west across the northern part of the map. In the northeast, the belt of magnetic highs trends almost due north-south and attains the maximum intensities shown on the map. This area of high intensity coincides with the Mineral Mountains east of Milford. At the south end of the Mineral Mountains, the trend of high magnetization turns due west and crosses the Escalante Valley, then turns west-southwest and runs along the southeast border of the Basin-Range Province. This latter high region is probably due to topography in part and also to the presence of the basaltic flows which occur on the northwestern margin of the Escalante desert. The east-west portion of the high intensity feature which crosses the Escalante Valley lies north of the intrusive and extrusive volcanic centers of the Black Mountain area and appears to be caused by deep sources in the basement. Two other regions of high intensity, lying west of Cedar City, correspond exactly with the mineralized quartz-monzonite intrusions which contain commercial quantities of various iron ores. In the southern part of the aeromagnetic map, where the geological

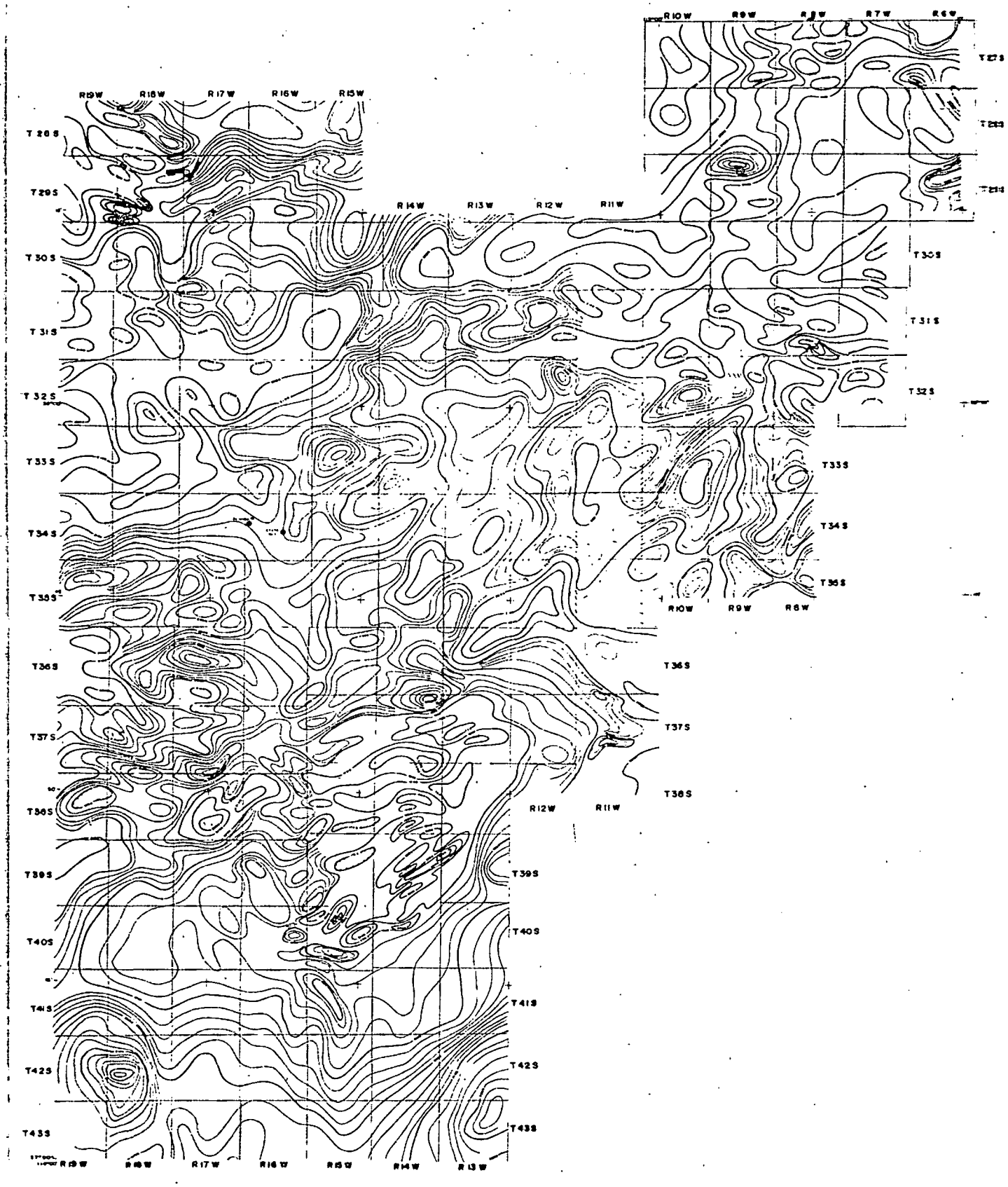

Figure 5-1. Aeromagnetic map of Escalante Desert region, Utah.

map of Utah shows the exposures of many Tertiary igneous intrusive rocks including the Pine Valley Laccolith, there is a large magnetic low. In the Escalante desert itself, the magnetic intensities lie between 2,000 and 2,100 gammas, which are higher than the intensities over the volcanic rocks exposed to the east and south. One possible interpretation is that the volcanic rocks exposed along the east margin of the Escalante desert are thicker beneath the Quaternary lake sediments comprising the shallow fill in the central valleys. Large changes in the magnitude of total magnetization and in the direction of remanent magnetization have been measured from samples of the Tertiary volcanic units (Anderson et al., 1975). These measurements complicate straight-forward thickness interpretations. In addition, well developed fault systems have severely altered the depositional shape of most of the volcanics units. Other down-dropped areas, such as the valleys north of Milford and north of Beaver, show the same magnetic intensity as does the Escalante desert.

The aeromagnetics of this part of the southwest Utah correlate well with the known geological features. It will be possible to use this data in conjunction with gravity and other geophysical data to aid in making an accurate geological interpretation of this complex tectonically active region.

Section 6

DIPOLE MAPPING

GROUP SEVEN, INC. carried out a geophysical survey of the Escalante desert region of Utah in order to delineate possible geothermal reservoirs. The area covered lies between the southern edge of T35S and the northern edge of T32S, on the west the boundary is the western edge of R18W and to the east the eastern edge of R13W. The total area covered is 1,400 square kilometers (540 square miles). The area is shown in Figure 6-1. The physical characteristic of a geothermal reservoir which is often most diagnostic is its electrical resistivity, if no other parameter is involved, the resistivity in a geothermal reservoir must be 5-to-7-fold lower than that in the surrounding rocks (Figure 6-2). This contrast can be even greater if the geothermal waters are more saline than the surrounding waters or if the porosity is higher in the reservoir than outside of it.

The dipole and rotating dipole methods were selected for use on a semi-reconnaissance basis. Since its development in 1968 in New Zealand, the dipole mapping method (Risk, 1970, Keller, et al., 1975), has been the most widely applied method of electrical geophysics in geothermal exploration. The basis of the method is that a grounded cable, several kilometers long, is energized with a periodic asymmetric square wave of electric current. Electric fields generated by the current are measured at many points around

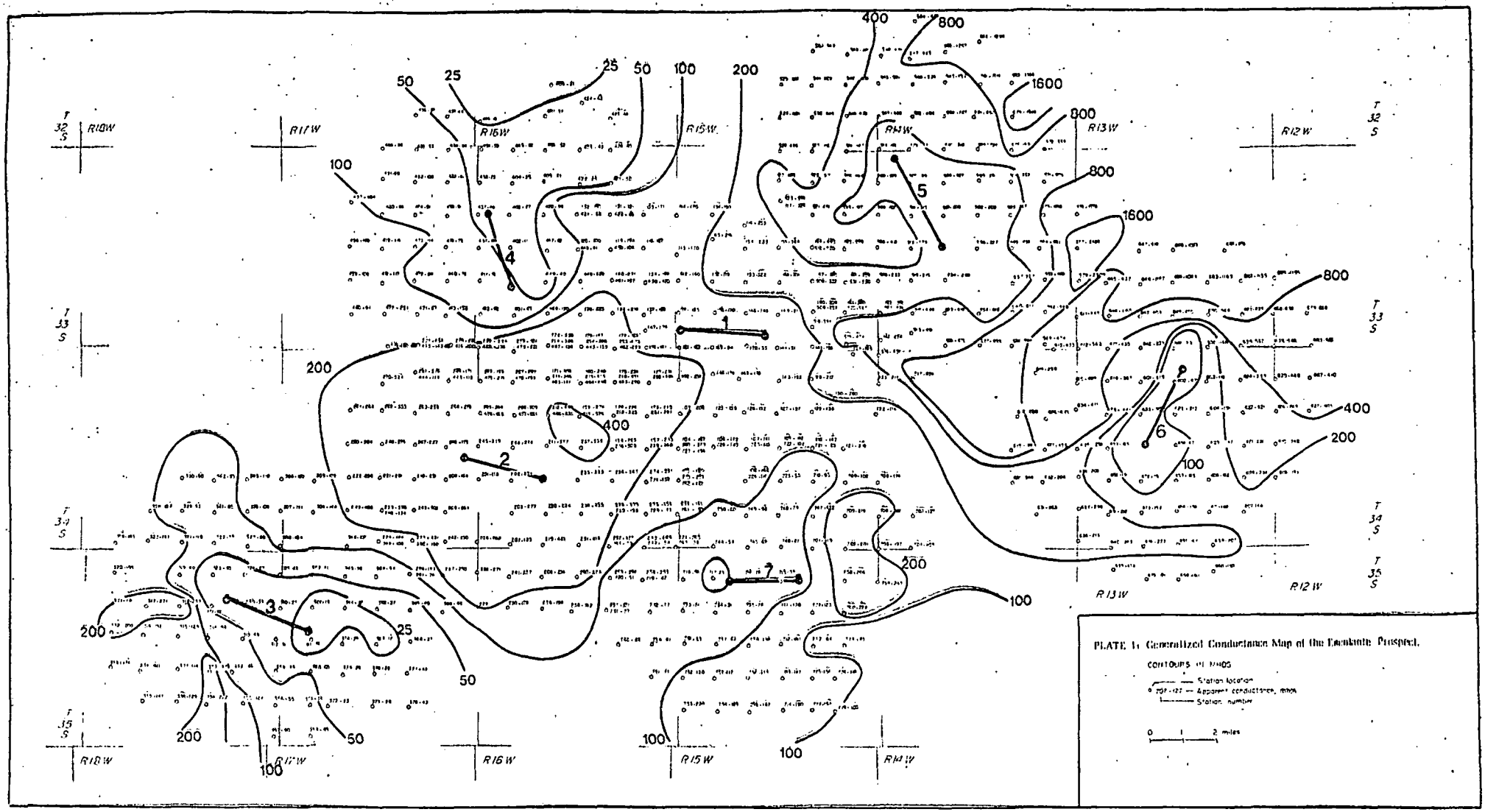

Figure 6-1. Generalized conductance map of the Escalante Desert. Contours in mhos.

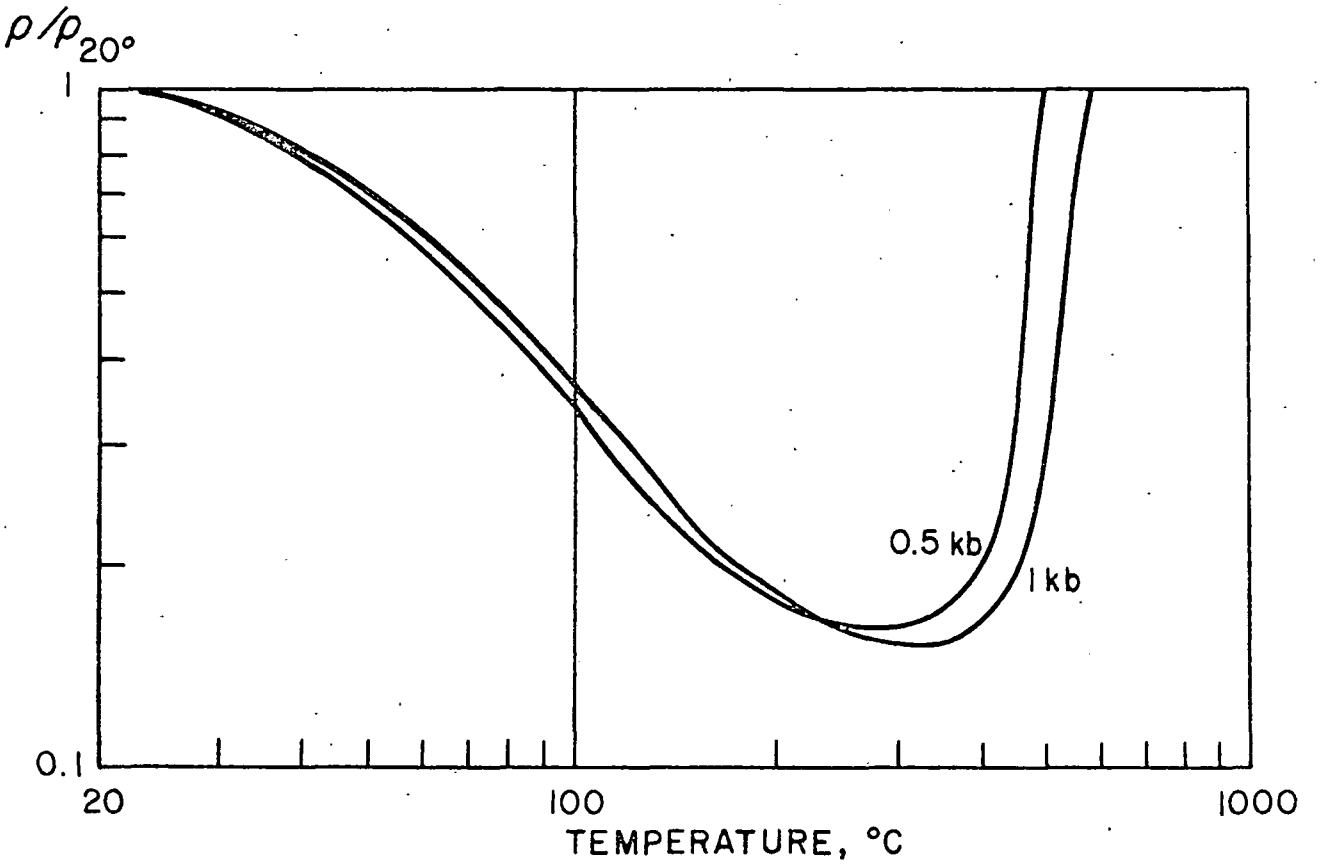

Figure 6-2. Variation in resistivity of a dilute solution of sodium chloride as a function of temperature and pressure.

the source using orthogonal electric dipoles; penetration into the earth increases with offset distance from the transmitting electrodes. The period of the square wave is chosen to be sufficiently long so that skin depth problems are not serious; periods of 30 seconds and/or 60 seconds were used. A resistivity is calculated for each measurement location using the magnitude of the total electric field measured at that location; an isoresistivity map is then drawn. The chief advantage of the dipole method is that large areas of country can be surveyed in a relatively short time. The chief disadvantage is that frequently interpretation of the results is ambiguous. To overcome the ambiguity, several sources located around a prospect can be used to illuminate the prospect area, but this process becomes tedious and expensive. To obviate this disadvantage of the single dipole method, the quadripole or rotating dipole method was developed. In this method, two roughly orthogonal sources are used. Current is transmitted sequentially from each source and is measured using orthogonal receiving dipoles as in the dipole mapping method. The transmitted currents can be manipulated mathematically so that they appear to give rise to electric field vectors which rotate through 360^{o} at the receiver station. Thus, if a resistivity is calculated as the electric field vector rotates, an ellipse of resistivity is generated at each measurement site. Having an embarrassment of data, a choice must be made as to which data are most significant. Theoretical studies indicate that the mean of the maximum and

minimum resistivities (ρ max + ρ min)/2 and the ellipticity (ρ max/ρ min)$^{\frac{1}{2}}$ are most diagnostic. The former parameter gives resistivities which are relatively undistorted near-lateral resistivity boundaries, while the latter delineates lateral boundaries. By using the rotating dipole mapping method, many of the disadvantages of the dipole mapping method can be overcome while retaining its simplicity. Full details of both methods can be found in Appendix I.

The original survey of the Escalante desert was carried out using the single-dipole mapping method as the rotating dipole method had not then been developed. However, a good idea of how the resistivity of the rocks of the Escalante Valley varies can be gained from this survey. The data on Figure 6-1 are presented as conductances. The conductance of a layer of rock is the thickness of the layer divided by its resistivity. The calculation of conductance and the reasons for its use to describe variation in electrical properties of rocks is given in Appendix I. Inasmuch as the resistivity appears in the denominator of the conductance term, geothermal reservoirs will appear as regions of high conductance.

As shown on Figure 6-1, seven sources were used to cover the Escalante desert. The region of highest conductance is in the northeast corner of the map to the northeast of Source 5, where there is an area of conductance greater than 800 mhos with a maximum of 1,646 mhos. Southwest of Source 5 is a 200 mho contour

which appears to delimit the large area of high conductance to the northeast. To the west and southwest of this 200 mho contour, the conductances are generally much lower than conductances to the northeast. Apparently, the 200 and 400 mho contours indicate the presence of a boundary in resistivity which could be caused by either a change in rock type, or a change in water salinity. In the center of the Escalante desert, surrounding Source 2, is a 200 mho contour enclosing a high of 538 mhos. This high is defined not only from Source 2, but also from the surrounding sources. Outside of the high conductance zone, conductances decrease to less than 25 ohm-m. On the basis of the data presented in Figure 6-1, it was felt that two areas merited further work, they were the northeast corner of the prospect where the 800 mho contour opened to the northeast and the center of the valley surrounding Source 2. These prospects are known as the Lund Prospect and the Beryl Prospect respectively.

To further define the resistivity structure of the Lund Prospect, a rotating dipole survey was carried out using four pairs of sources (Figure 6-3). The sources were placed sufficiently close together so that the recording stations overlapped. The data shown in Figure 6-3 are expressed as mean resistivity, in ohm-m, as described above and in Appendix I. The principal feature of the Lund area is a closed 2 ohm-m contour situated immediately north of the town of Lund. This 2 ohm-m contour is enclosed within a 5 ohm-m contour which trends to the southwest and en-

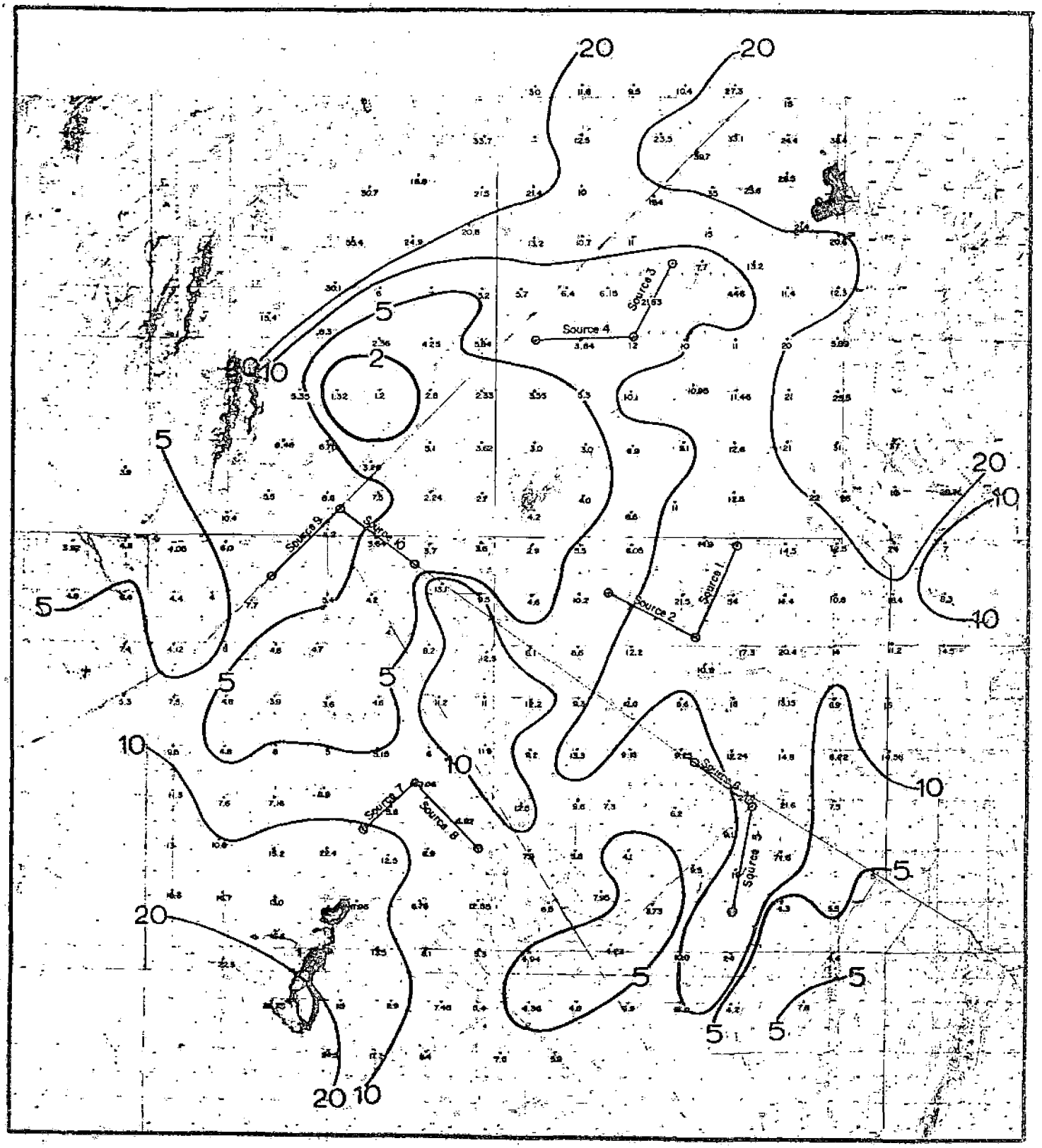

Figure 6-3. Mean of mean resistivity map of Lund Prospect, Escalante Desert. Contours in ohm-meters.

closes some 25 square miles of land. To the north and east, the resistivities rise rapidly as they do to the southwest. Directly to the west of Sources 9 and 10 is an open 5 ohm-m contour which lies partially within the Basin-Range Province. The resistivities also rise to the southeast. Resistivities which are on the order of less than 5 ohm-m are normally indicative of geothermal reservoirs in the absence of saline waters and/or marine shales.

A similar survey to that carried out at Lund was carried out in the Beryl Prospect using one source pair (Figure 6-4). The results showed that around the source pair, particularly to the northeast, is a closed low of less than 10 ohm-m, the lowest resistivity within this low is 6.7 ohm-m. The resistivities rise rapidly to the south indicating that a major boundary lies about 2 miles south of the sources. To the north, the resistivities also rise rapidly. East and west there is no such prominent closure. Although the resistivities within the Beryl anomaly are not ultra-low, such as those within the Lund anomaly, they do represent a considerable contrast with resistivities in the rest of the Escalante Valley and it is thought that the area represents a viable geothermal prospect.

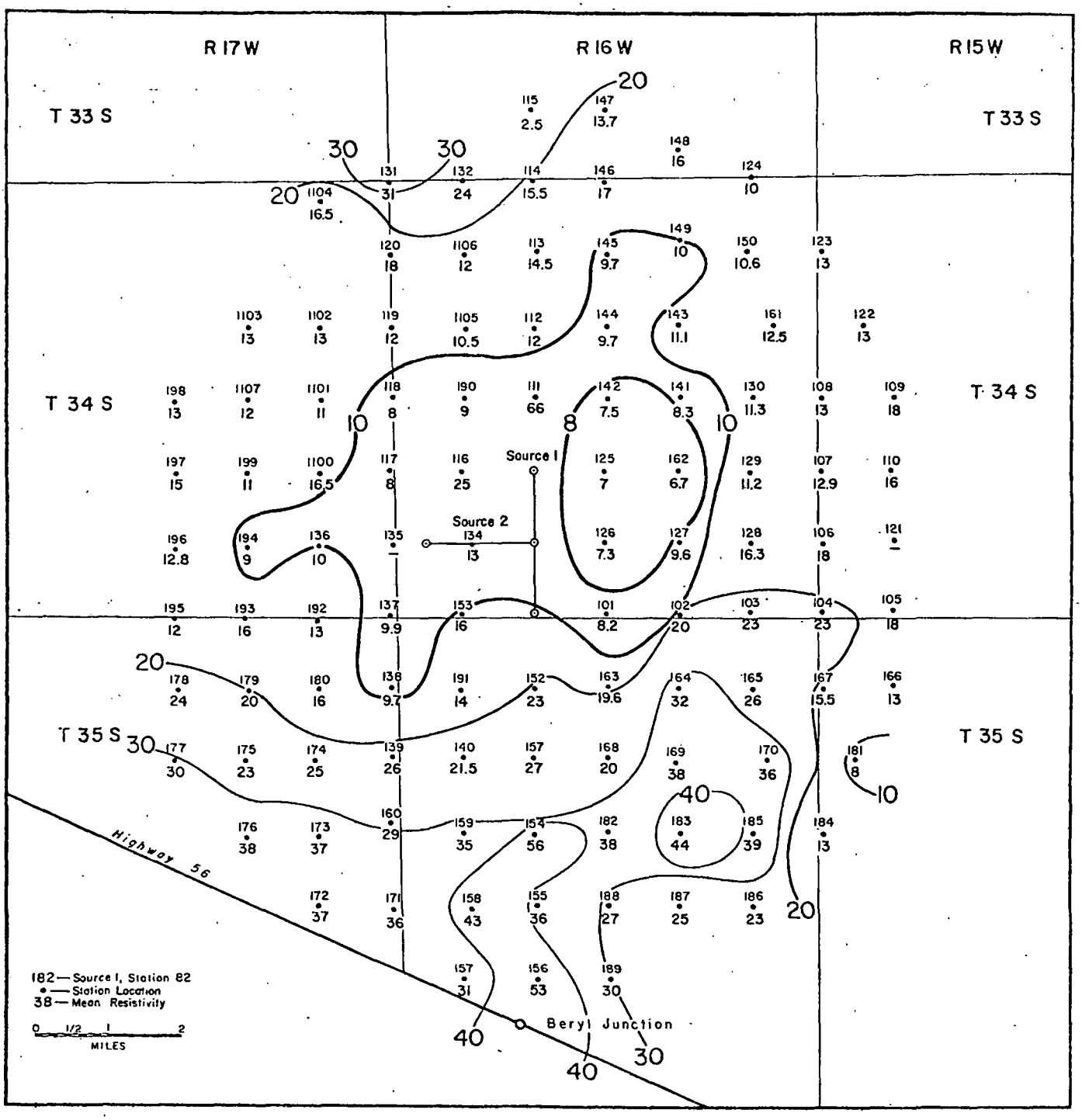

Figure 6-4. Mean resistivity map of the Beryl Prospect. Contours in ohm-meters.

REFERENCES

Keller, G. V., Furgerson, R., Lee, C. Y., Harthill, N., and Jacobson, J. J., 1975, The dipole mapping method: Geophysics, v. 40, n. 3, p. 451-472.

Risk, G. F., MacDonald, W. J. P., and Dawson, G. B., 1970, D. C. resistivity surveys of the Broadlands Geothermal Region, New Zealand: Geothermics, v. 2, pt. 1, p. 287-294.

Section 7

RESISTIVITY SECTIONING

In order to substantiate the presence of low resistivities at depth, a series of four pole-dipole sounding traverses, or resistivity sectionings were made across the area of interest in the Beryl Prospect (Figure 7-1). This method involves laying out 4 miles (6.4 kilometers) of wire as an electrical source and measuring electrical fields in line with the source to a distance of 2 miles, both towards the middle of the source and away from it. When one set of measurements has been taken, one mile of the wire is picked up, added to the other end, two new source electrodes established, and measurements are taken again. The process is repeated until the traverse under investigation has been covered. The field work is quite rapid and in this way qualitative verification of the dipole mapping results can be made. The data are presented in the conventional manner by calculating a resistivity for each measurement and plotting it where a perpendicular dropped from the measurement location intersects a 45^{o} line. Four such traverses were carried out (Figure 7-1) and are presented in Figures 7-2, 7-3, 7-4 and 7-5.

Resistivity section 1 runs east-west for 11 miles through the resistivity anomaly (Figure 7-2). The principal feature of the section is a large zone of low resistivities, less than 7 ohm-m, which occurs for 5 miles in the center of the section. To the west,

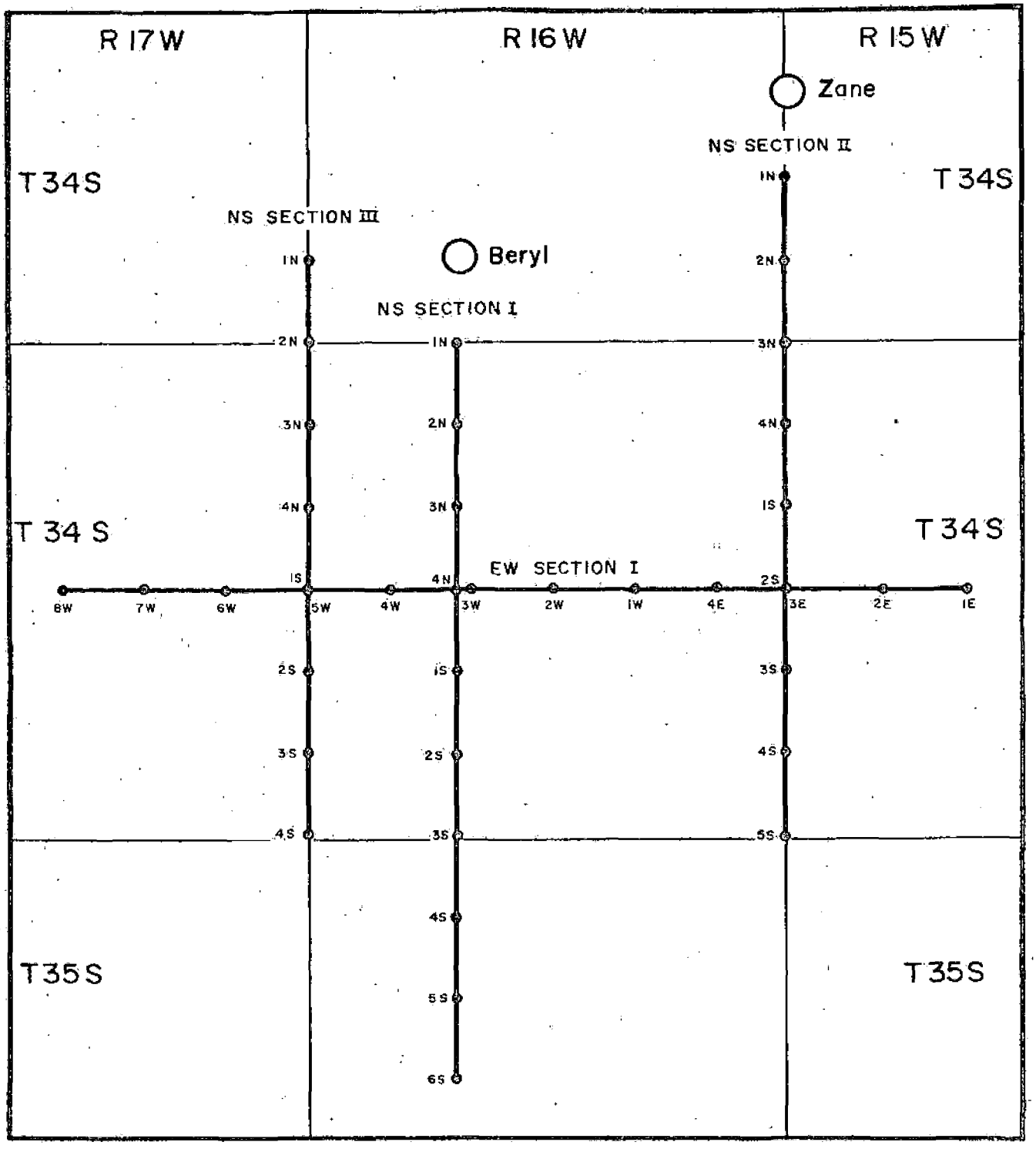

Figure 7-1. Location map of resistivity sectioning traverses, Beryl Prospect.

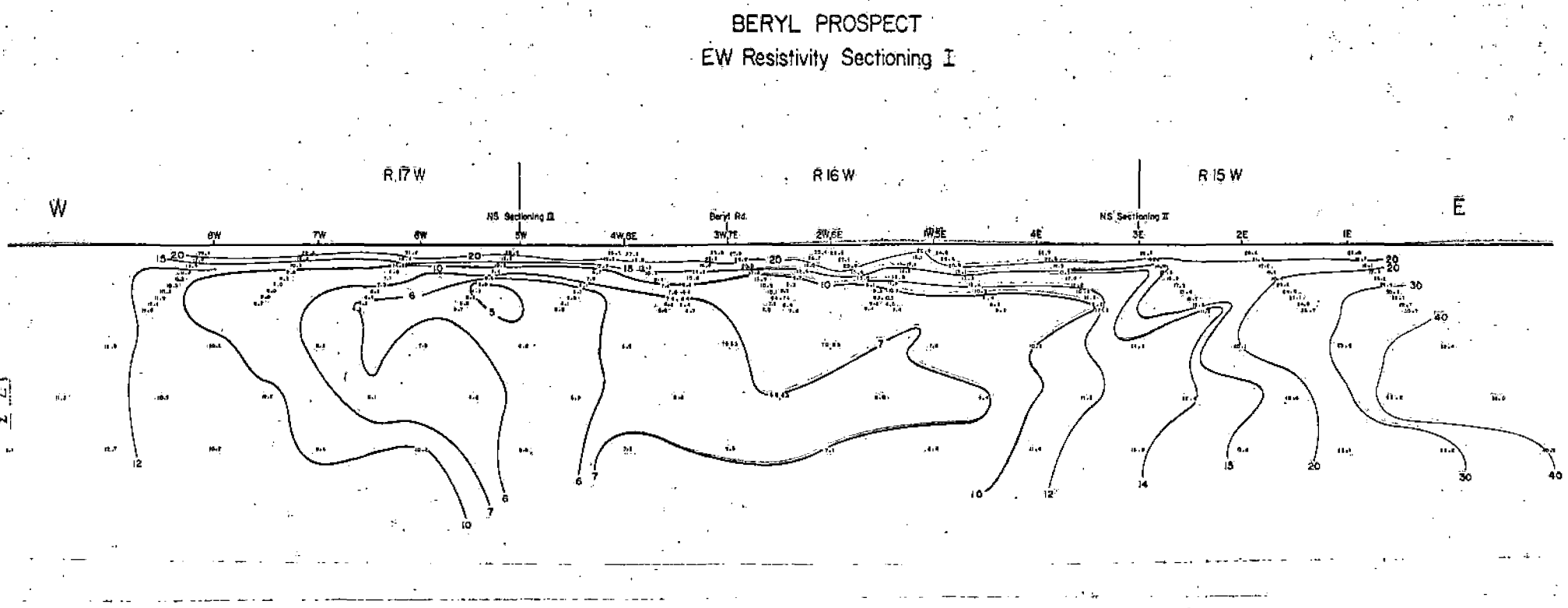

Figure 7-2. E-W resistivity section, contours in ohm-meters.

the resistivities rise slowly to greater than 12 ohm-m. To the east, the resistivities rise rapidly and reach values of over 30 ohm-m. In a vertical direction, the resistivities increase very rapidly to values over 30 ohm-m. The shape of the contours surrounding the central low indicate that the resistivities increase downwards. This resistivity section indicates there are strong lateral changes in electrical resistivity in the subsurface.

North-south resistivity section 1 runs along the Beryl-Beryl Junction Road for 9 miles (Figure 7-3). There are two low resistivity anomalies, one in the northern half of the traverse and the other in the southern half. The northern anomaly has a low resistivity of 4.3 ohm-m. The anomaly is bounded to the north where the resistivities reach 20 ohm-m and also is bounded at depth where the resistivities reach 22.8 ohm-m. The resistivities in the southern anomaly are less than 10 ohm-m, the lowest is 7.3 ohm-m. The resistivities increase rapidly in all directions away from the smaller southern anomaly. The zone of high resistivity between the two resistivity lows must indicate a change of rock type as the increase in resistivity is too great to be explained by a change of water chemistry. The east-west traverse crosses the southern end of the northern anomaly and has similar resistivities at the same depths as in section 4.

North-south section 2 runs north-south for a distance of 8 miles, starting 1 mile south of Zane (Figure 7-4). The principal feature is an area of low resistivity, less than 10 ohm-m, in the

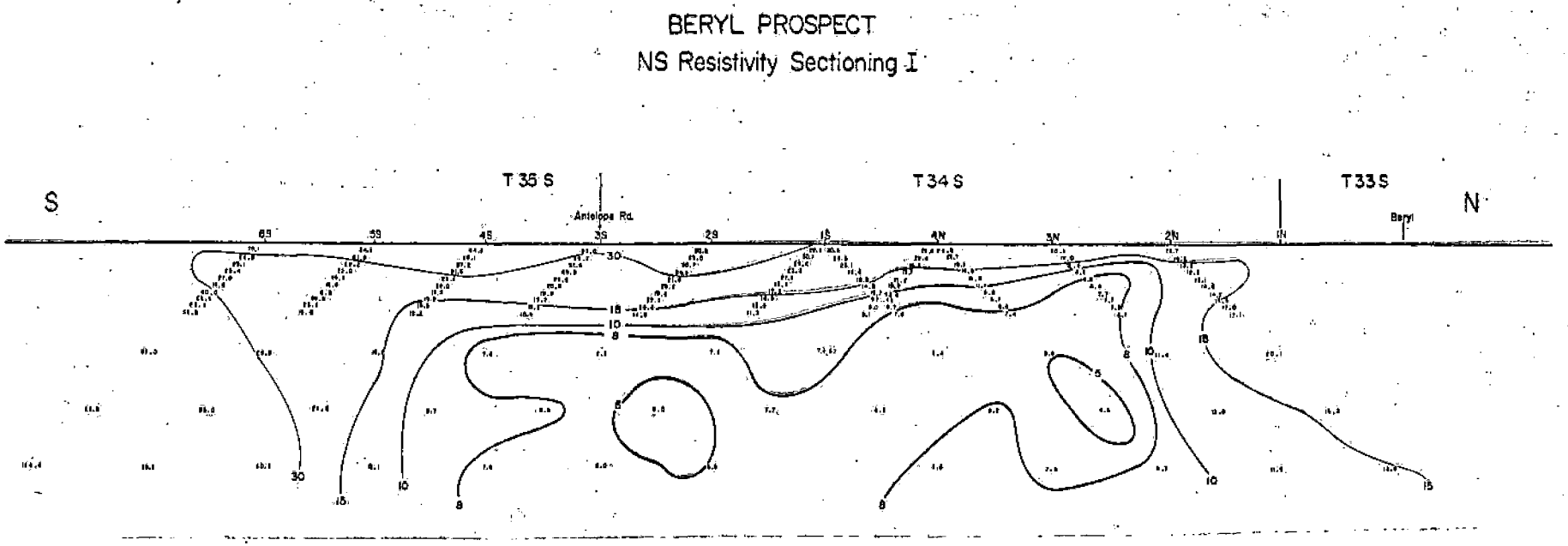

Figure 7-3. N-S resistivity section I, traverse along Beryl Road, contours in ohm-meters.

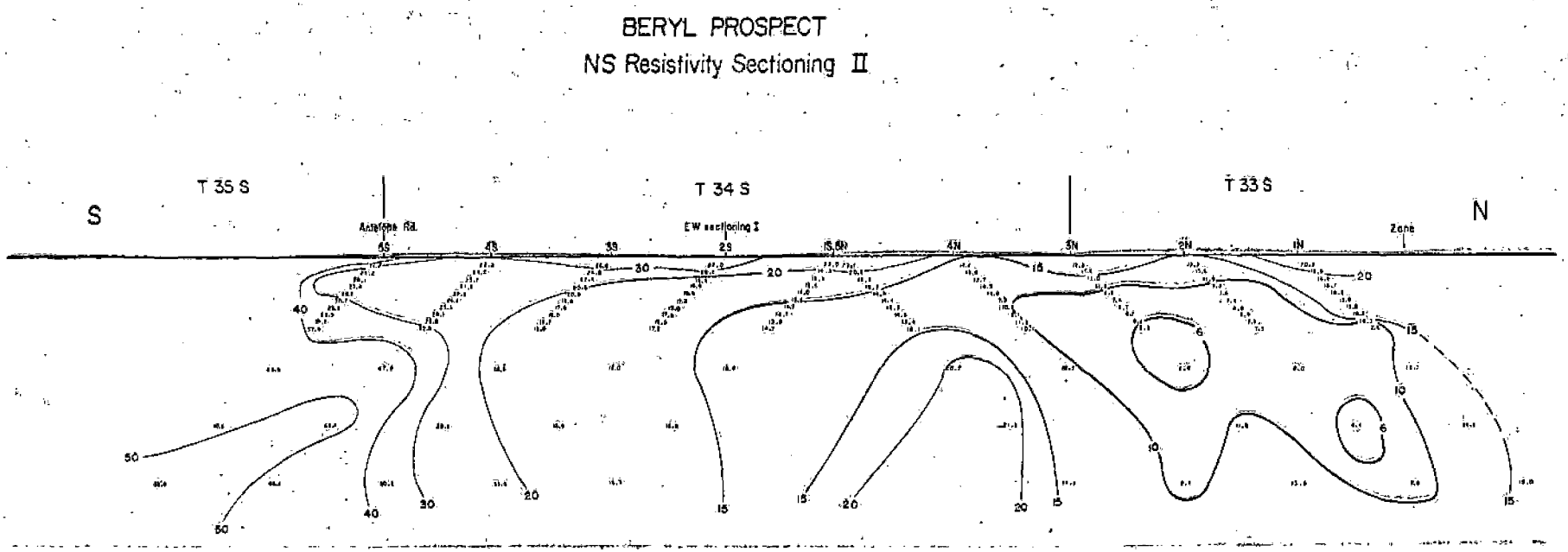

Figure 7-4. N-S resistivity section II, contours in ohm-meters.

northern part of the traverse. The lowest resistivities inside the 10 ohm-m contour are less than 6 ohm-m. The 10 ohm-m contour is bounded vertically as well as horizontally, and the resistivity increases gradually outwards from the anomaly. Only in the southern part of the traverse are high resistivities seen.

North-south resistivity section 3 lies in the western part of the area and extends north-south for a distance of 7 miles (Figure 7-5). The principal feature of the section is a central low resistivity zone bounded by a 10 ohm-m contour. To the south, the anomaly persists to greater depths but is bounded at shallower depths. To the north, the resistivity increases gradually to greater than 30 ohm-m. There is a suggestion that the anomaly is bounded at depth. It is worth noting that the east-west resistivity section crosses resistivity section 3 exactly at the lowest part of the anomaly, and that the resistivities and their depth distributions are identical on both sections.

The principal feature of the four resistivity sections is that there is substantial volumes of very low resistivity rock at depth. The boundaries of the low resistivity areas exhibit rapid lateral changes in resistivity similar to known geothermal reservoirs such as Wairakei or Broadlands. These resistivity sections closely corroborate the findings of the dipole mapping program which showed that substantial volumes of low resistivity rock occurred at depth under the Beryl Prospect.

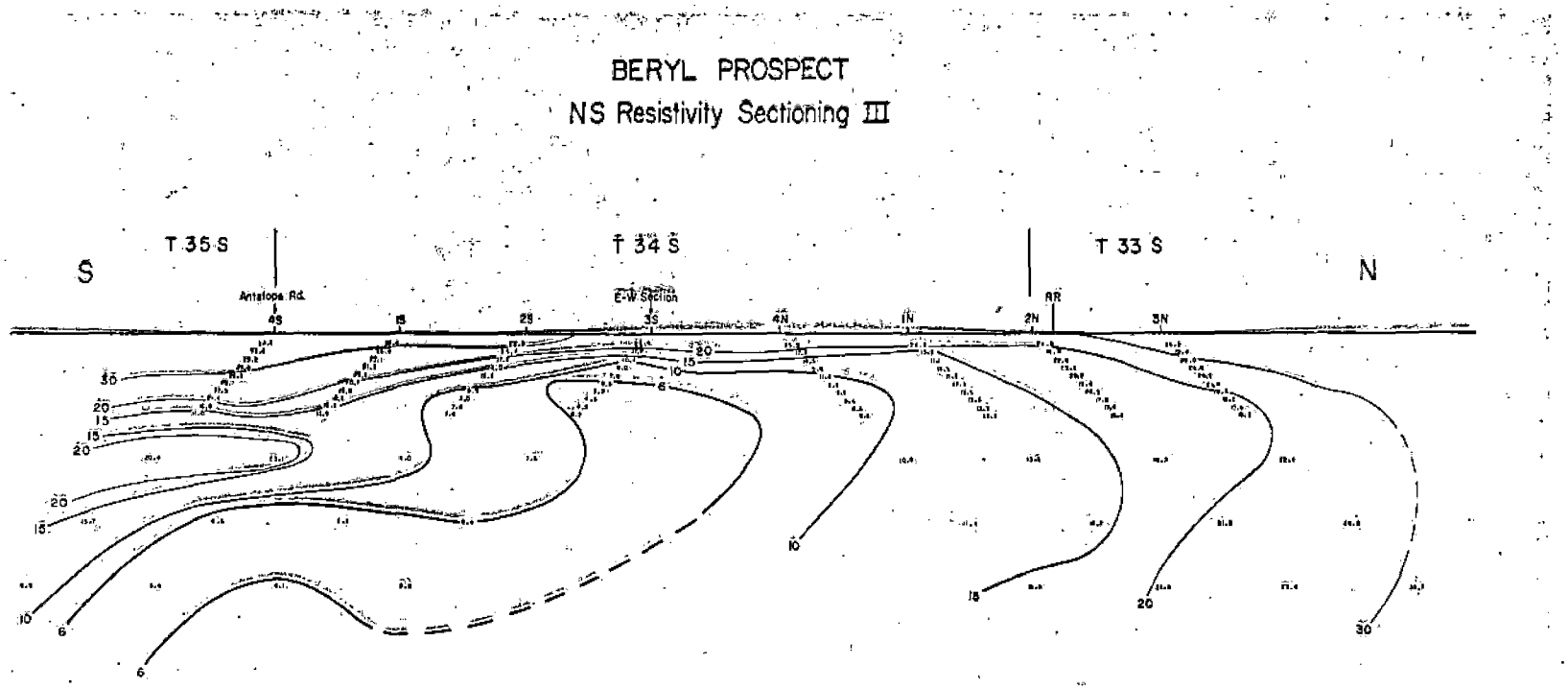

Figure 7-5. N-S resistivity section III, contours in ohm-meters.

Section 8

TIME DOMAIN ELECTROMAGNETIC SOUNDING

The two techniques, dipole mapping and resistivity sectioning, whose results have already been discussed, give only qualitative indications of how electrical resistivity varies with depth. Such information is necessary to determine the volume of potential reservoirs and drilling depths which will adequately test possible production zones. The Time Domain Electromagnetic (TDEM) sounding technique was employed to provide vertical profiles of resistivity throughout the region of the electrical resistivity anomalies. This technique measures the time rate of decay of the vertical component of the magnetic field generated by a square wave of current injected into the earth by an electric dipole source (Figure 8-1). A description of the technique is given in Appendix II and it has been discussed in the literature by Harthill (1969, 1976), Jacobson (1969) and Keller (1970). Source dipoles 1 mile (1.6 kilometers) long, of #2 A.W.G. wire were used; power was supplied by a 200 kw diesel generator and the resulting current square wave attained 500 amperes peak to peak. The transmitted signal was measured by two, single vertical axis cryogenic magnetometers employing Josephson junctions in a liquid-helium filled dewar. These instruments have effective areas of up to 234 and 2,100 square kilometers respectively; attenuation and filtering is selectable. Cryogenic magnetometers have significant advantages over the induction loops used during the development of the TDEM

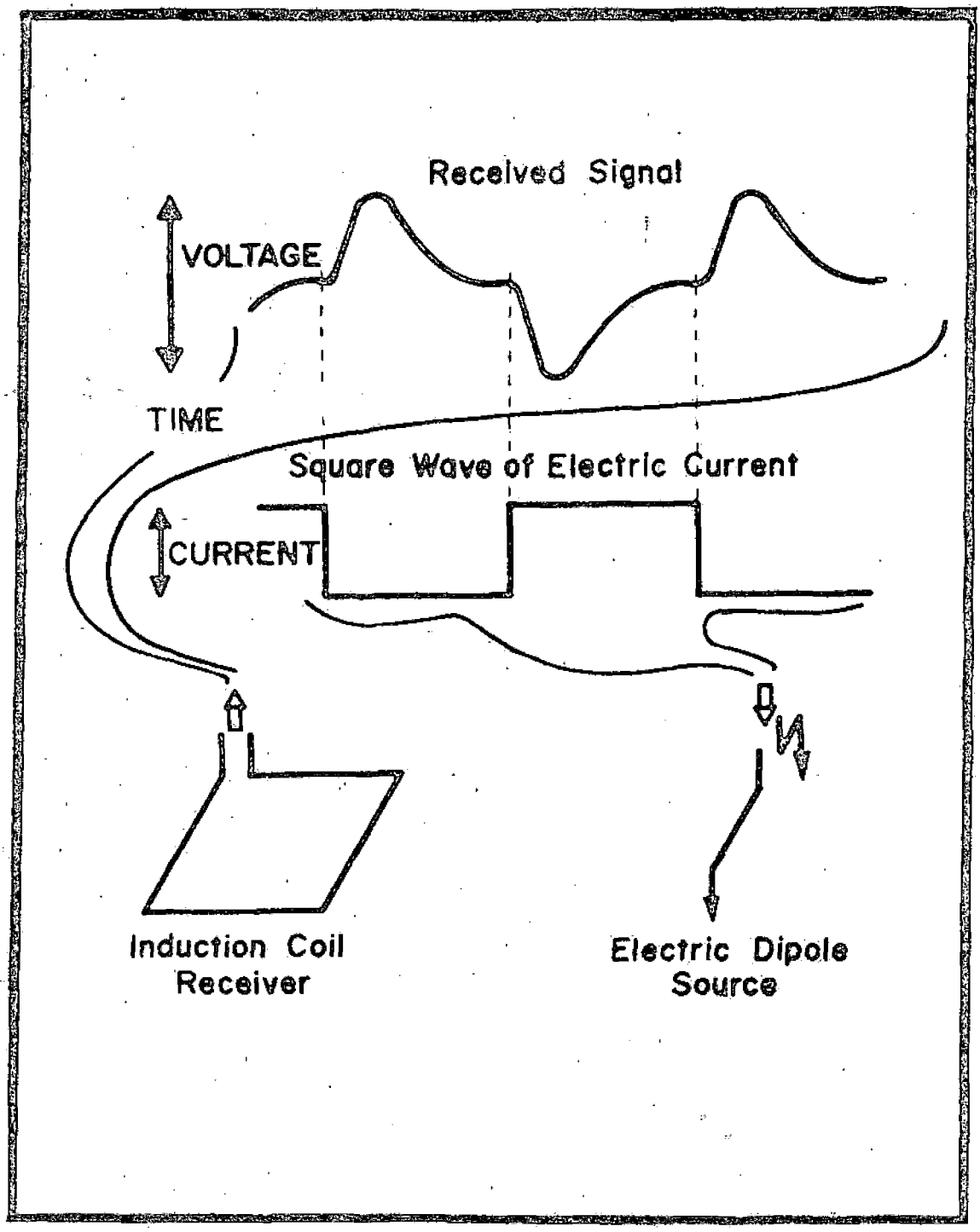

Figure 8-1. Time Domain Electromagnetic Sounding: Equipment Schematic.

method, the two major advantages are: rapid set-up time and greatly increased effective loop areas. A typical received signal is shown in Figure 8-2.

The TDEM sources were located so that adequate penetration could be attained in the zone of interest. The effective penetration of an electromagnetic wave is basically controlled by skin depth. The offset distance is also related to penetration in that as the distance between the source and the measuring point is increased, high frequencies are attenuated and lower frequencies predominate in the received signal. It is possible to distinguish horizontal boundaries to depths between 1/3 and 1/2 of the offset distance. Offset distances in the 10 kilometer range were attained in the survey of the Escalante desert.

The voltage measured at the receiver is:

$$v(t) = \frac{3ALI\cos\Theta}{2\pi R^4} \rho a \qquad (1)$$

where

- $v(t)$ = Voltage at any given time after the initiation of the transient
- A = Effective area of the receiver
- L = Source length
- I = Current in source
- ρa = Apparent resistivity
- Θ = Angle between vector from source center to receiver and perpendicular bisector of source
- R = Distance between source center and receiver

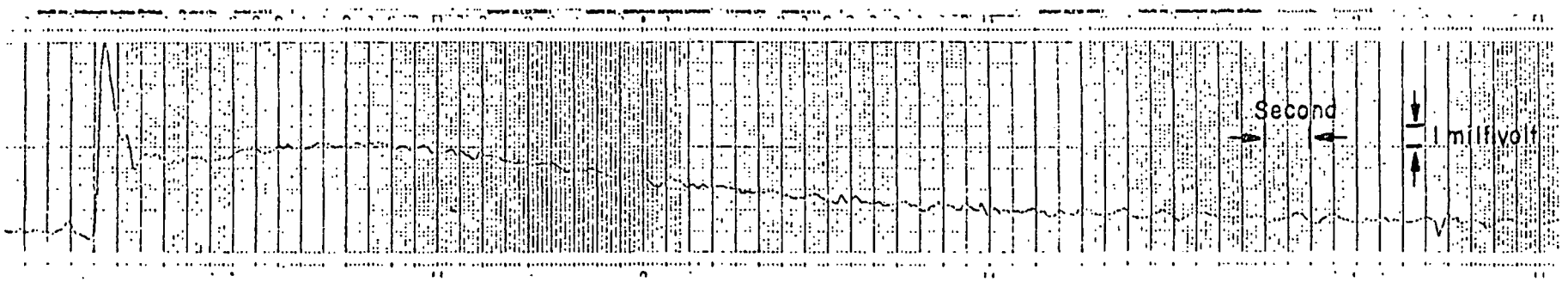

Figure 8-2. Facsimile of raw TDEM transient 3217. Horizontal scale is time, vertical scale is voltage (60% reduction from original).

Equation 1 shows that signal strength is azimuthally dependent, and decreases as the angle θ increases. Thus, from any one source, measurements are taken only between two vectors which extend from each source electrode at an angle of about 30° from a perpendicular to the source. One of the advantages of the TDEM sounding method is that the response from the earth which the receiver senses apparently comes from a limited volume of the earth directly beneath the receiver. This property became evident from the results of surveys in areas where structures and lateral resistivity changes are well known. The interpretation of TDEM soundings is treated at length in Appendix II and will not be described here. The soundings described below were interpreted using a technique in which the variation of voltage with time was inverted to give the variation of resistivity with depth.

In the Lund area, 130 soundings were made from five different sources, giving an average density of greater than 4 per square mile. In the interpretation process a layered earth model is created by using a sensitivity index to determine the goodness of fit. In certain models, either the thickness or the resistivity of the layers, or both parameters, may be varied within wide limits without affecting the fit of the model curve to the field curve. If a small change in either of the layer parameters causes a large error of fit, then these parameters must be very close to the true parameters of the real geoelectric layer. The output of the inversion technique is shown in Figure 8-3.

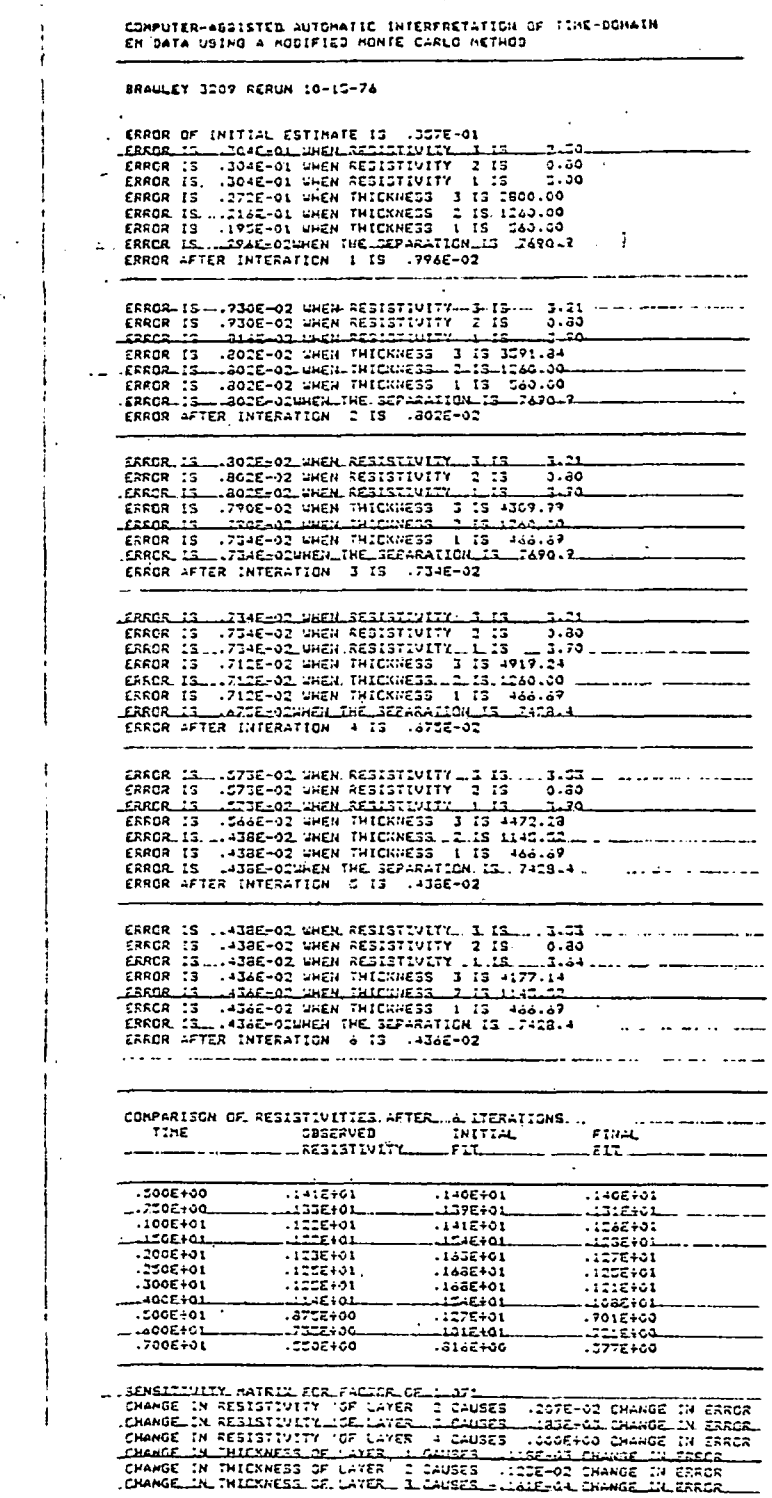

```
COMPUTER-ASSISTED AUTOMATIC INTERPRETATION OF TIME-DOMAIN
EM DATA USING A MODIFIED MONTE CARLO METHOD

BRAWLEY 3209 RERUN 10-15-76

ERROR OF INITIAL ESTIMATE IS  .357E-01
ERROR IS  .304E-01 WHEN RESISTIVITY  3 IS     3.50
ERROR IS  .304E-01 WHEN RESISTIVITY  2 IS     0.80
ERROR IS  .304E-01 WHEN RESISTIVITY  1 IS     3.00
ERROR IS  .277E-01 WHEN THICKNESS  3 IS 3800.00
ERROR IS  .216E-01 WHEN THICKNESS  2 IS 1260.00
ERROR IS  .195E-01 WHEN THICKNESS  1 IS  560.00
ERROR IS  .194E-02WHEN THE SEPARATION IS 7490.2
ERROR AFTER INTERATION  1 IS  .798E-02

ERROR IS  .930E-02 WHEN RESISTIVITY  3 IS     3.21
ERROR IS  .930E-02 WHEN RESISTIVITY  2 IS     0.80
ERROR IS  .814E-02 WHEN RESISTIVITY  1 IS     3.70
ERROR IS  .802E-02 WHEN THICKNESS  3 IS 3891.84
ERROR IS  .802E-02 WHEN THICKNESS  2 IS 1260.00
ERROR IS  .802E-02 WHEN THICKNESS  1 IS  560.00
ERROR IS  .802E-02WHEN THE SEPARATION IS 7690.2
ERROR AFTER INTERATION  2 IS  .802E-02

ERROR IS  .802E-02 WHEN RESISTIVITY  3 IS     3.21
ERROR IS  .802E-02 WHEN RESISTIVITY  2 IS     0.80
ERROR IS  .802E-02 WHEN RESISTIVITY  1 IS     3.70
ERROR IS  .790E-02 WHEN THICKNESS  3 IS 4309.79
ERROR IS  .790E-02 WHEN THICKNESS  2 IS 1260.00
ERROR IS  .734E-02 WHEN THICKNESS  1 IS  466.69
ERROR IS  .734E-02WHEN THE SEPARATION IS 7690.2
ERROR AFTER INTERATION  3 IS  .734E-02

ERROR IS  .734E-02 WHEN RESISTIVITY  3 IS     3.21
ERROR IS  .734E-02 WHEN RESISTIVITY  2 IS     0.80
ERROR IS  .734E-02 WHEN RESISTIVITY  1 IS     3.70
ERROR IS  .712E-02 WHEN THICKNESS  3 IS 4919.24
ERROR IS  .712E-02 WHEN THICKNESS  2 IS 1260.00
ERROR IS  .712E-02 WHEN THICKNESS  1 IS  466.69
ERROR IS  .427E-02WHEN THE SEPARATION IS 7428.4
ERROR AFTER INTERATION  4 IS  .673E-02

ERROR IS  .673E-02 WHEN RESISTIVITY  3 IS     3.03
ERROR IS  .673E-02 WHEN RESISTIVITY  2 IS     0.80
ERROR IS  .673E-02 WHEN RESISTIVITY  1 IS     3.70
ERROR IS  .666E-02 WHEN THICKNESS  3 IS 4472.28
ERROR IS  .438E-02 WHEN THICKNESS  2 IS 1140.02
ERROR IS  .438E-02 WHEN THICKNESS  1 IS  466.69
ERROR IS  .438E-02WHEN THE SEPARATION IS 7428.4
ERROR AFTER INTERATION  5 IS  .438E-02

ERROR IS  .438E-02 WHEN RESISTIVITY  3 IS     3.03
ERROR IS  .438E-02 WHEN RESISTIVITY  2 IS     0.80
ERROR IS  .438E-02 WHEN RESISTIVITY  1 IS     3.64
ERROR IS  .436E-02 WHEN THICKNESS  3 IS 4177.14
ERROR IS  .436E-02 WHEN THICKNESS  2 IS 1147.32
ERROR IS  .436E-02 WHEN THICKNESS  1 IS  466.69
ERROR IS  .436E-02WHEN THE SEPARATION IS 7428.4
ERROR AFTER INTERATION  6 IS  .436E-02

COMPARISON OF RESISTIVITIES AFTER  6 ITERATIONS.
   TIME          OBSERVED          INITIAL          FINAL
                 RESISTIVITY       FIT              FIT

 .500E+00        .141E+01         .140E+01         .140E+01
 .750E+00        .133E+01         .139E+01         .131E+01
 .100E+01        .122E+01         .141E+01         .126E+01
 .150E+01        .122E+01         .134E+01         .123E+01
 .200E+01        .123E+01         .163E+01         .127E+01
 .250E+01        .122E+01         .168E+01         .125E+01
 .300E+01        .122E+01         .168E+01         .121E+01
 .400E+01        .114E+01         .174E+01         .108E+01
 .500E+01        .877E+00         .127E+01         .901E+00
 .600E+01        .752E+00         .101E+01         .771E+00
 .700E+01        .650E+00         .816E+00         .677E+00

SENSITIVITY MATRIX FOR FACTOR OF  1.37
CHANGE IN RESISTIVITY OF LAYER  3 CAUSES  .207E-02 CHANGE IN ERROR
CHANGE IN RESISTIVITY OF LAYER  2 CAUSES  .183E-03 CHANGE IN ERROR
CHANGE IN RESISTIVITY OF LAYER  1 CAUSES  .000E+00 CHANGE IN ERROR
CHANGE IN THICKNESS OF LAYER  3 CAUSES  .135E-03 CHANGE IN ERROR
CHANGE IN THICKNESS OF LAYER  2 CAUSES  .122E-02 CHANGE IN ERROR
CHANGE IN THICKNESS OF LAYER  1 CAUSES  .181E-04 CHANGE IN ERROR
```

Figure 8-3. Computer output of computer interpretation of TDEM sounding 3209.

In the Lund area, the geoelectric section is best modeled by three layers. The surface layer has a maximum thickness of 400 meters and has a highly variable resistivity which reflects the heterogeneity of the near subsurface. The parameters of this layer are not particularly sensitive to change. The second layer thickness ranges between 1 and 2 kilometers, however the changes from point to point are not radical. The resistivities of this second layer range from less than 1 ohm-m to 10 ohm-m, the average being between 3 and 5 ohm-m. The resistivity and thickness of this layer are highly sensitive to change, so that they reflect a true variation in the geology of the Lund basin. The resistivity of the second layer is the parameter which best reflects the lateral changes in the subsurface, and is shown as the contour map of Figure 8-4. The third layer represents the insulating basement, its thickness is taken to be infinite and its resistivity was chosen merely to reflect the insulating properties of the basement.

In Figure 8-4, the most prominent low resistivity feature in the Lund area is linear, up to 4 miles wide and enclosed by the 2 ohm-m contour, which is centered on the town of Lund. South of Lund, the resistivities decrease to less than 0.7 ohm-m, while to the north, the lowest resistivities are 0.8 ohm-m. The 2 ohm-m contour closes to the southwest but is open to the north. The contours of 3 ohm-m and greater which enclose this 2 ohm-m contour are also open to the north and to the southwest. To the west, towards the mountains, the resistivities slowly increase to values between

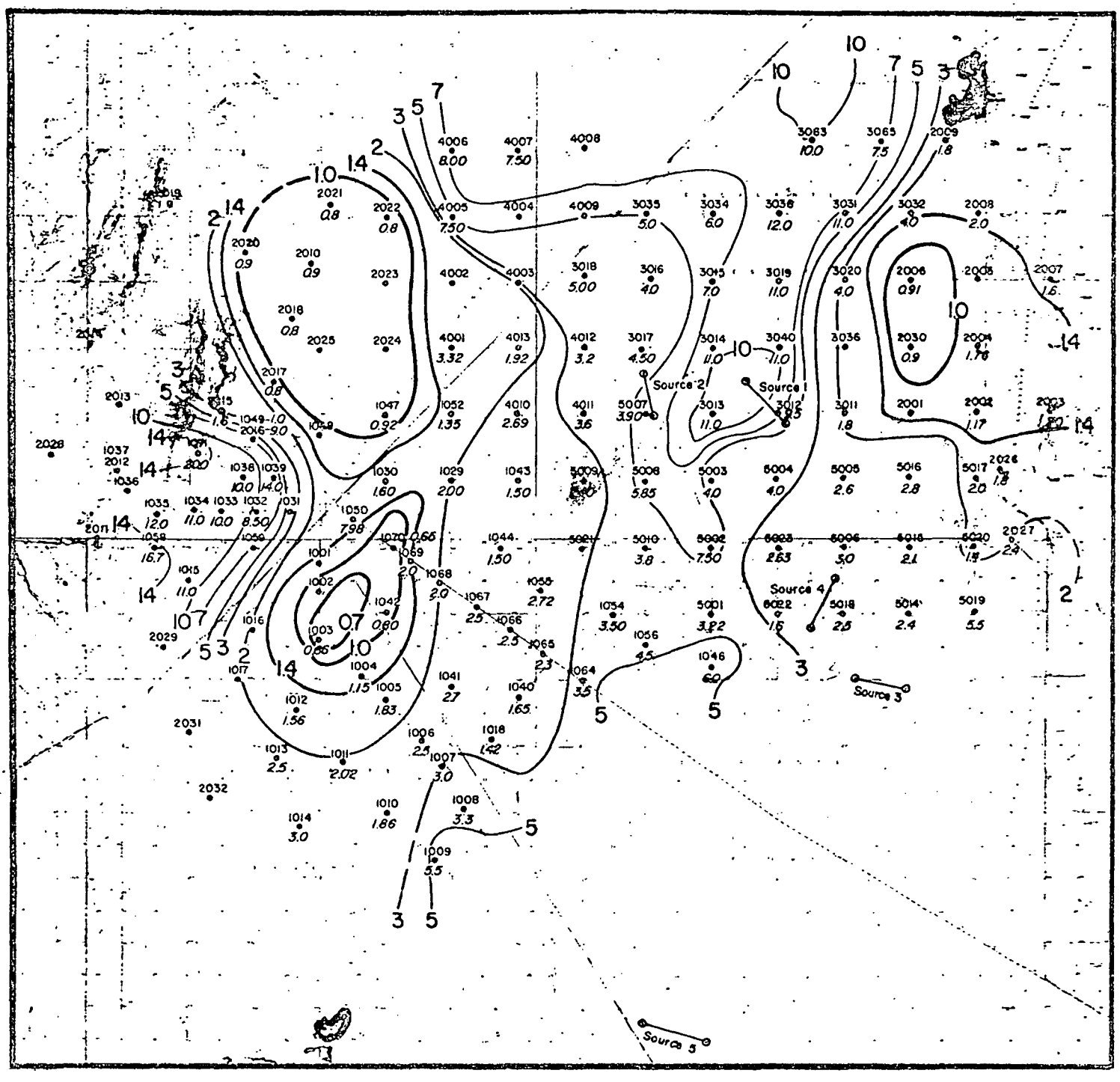

Figure 8-4. Map of second-layer resistivity, Lund Prospect, contours in ohm-meters.

5 and 10 ohm-m. In the eastern part of the area surveyed there is a restricted low enclosed by a 1.4 ohm-m contour, the central part of this low reaches less than 1 ohm-m and covers an area of some 2 square miles. The resistivities increase to the south.

A resistivity-thickness section was prepared using TDEM soundings which were recorded along the highway from Lund southeast to Cedar City (Figure 8-5). The surface layer thickness is highly variable, it changes from 150 meters to slightly greater than 500 meters. The resistivity also varies widely from 20 ohm-m to 92 ohm-m. It is felt that these property changes correspond to changes in deposition. The second layer is subdivided into two sections, to the west of Lund, and to the east. To the west of Lund, resistivities of the second layer based on two soundings are 14 and 20 ohm-m. Immediately east of Lund, the second layer resistivity drops to 1.6 ohm-m and then to 0.8 ohm-m. Further to the east, the resistivity increases to 2 ohm-m and then gradually increases over a distance of two miles to 5 ohm-m and greater. It is interesting to note that the thickness of the second layer does not vary widely across this section. The thickest section and the highest resistivities occur in the eastern part of the traverse. The third layer resistivities are relatively meaningless.

The second layer, east of Lund, is made up of porous rock possibly containing saline water. The increase in resistivity to the east could be caused by either a decrease in the possible salinity or by a decrease in porosity. However, in the wells

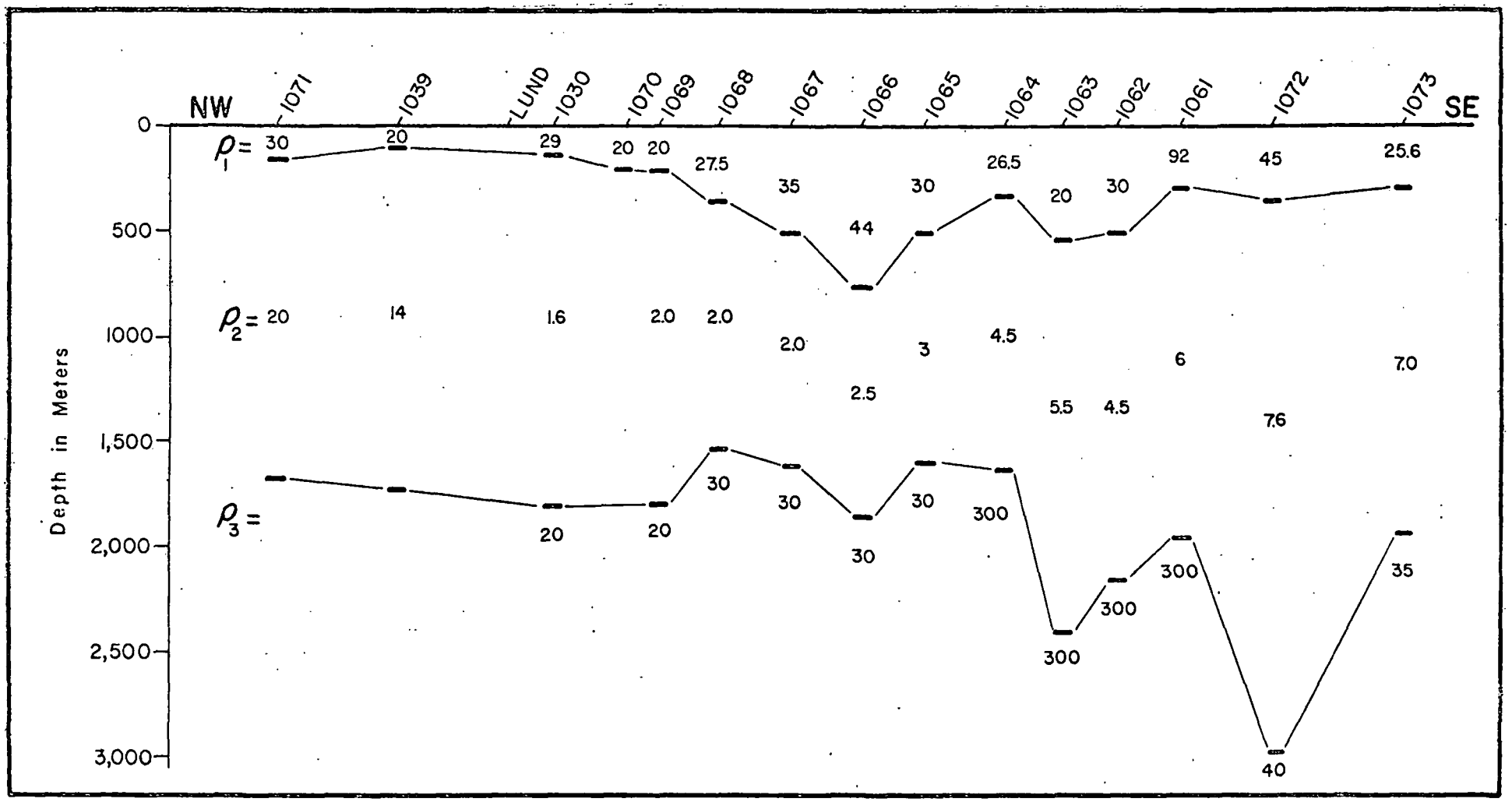

Figure 8-5. Resistivity section from northwest to southeast through the Lund Prospect based on TDEM sounding results.

drilled to date in the Escalante desert, there is no sign that extensive internal drainage took place to give rise to salty connate waters, nor is there any evidence that marine shale may also exist in the area. The lowest resistivities occur immediately east of a fault which passes northeast to southwest through Lund. The second cause of such a large variation in resistivity of the second layer, is that very hot water could migrate vertically in the fault zone and collect in the porous sediments. There appears to be high heat flow throughout the Transition Zone, thus the eastern part of the section, could be composed of rocks containing warm water, which would also lower the resistivity. Higher temperatures in the center of the cross section would cause the rock resistivity to be lowered still further.

A similar, but more widespread, TDEM sounding survey was carried out over the Beryl prospect. This set of soundings has proved to be more difficult to interpret in the geologic sense than soundings in the Lund area. A comparison of the gravity data from each area shows that, tectonically, the Beryl prospect is much more complicated than the Lund prospect. The interpretation process is continuing in the light of new information from surface and well cuttings and from geophysical well logs in the two wells drilled to date.

REFERENCES

Harthill, N., 1976, Time-domain electromagnetic sounding: I.E.E.E. Trans., Geoscience Electronics, v. GE-14, n. 4, p. 256-260.

Harthill, N., 1969, Deep electromagnetic sounding: geological considerations: D.Sc. Thesis, Colorado School of Mines.

Jacobson, J. J., 1969, Deep electromagnetic sounding: technique: D.Sc. Thesis, Colorado School of Mines.

Keller, G. V., 1970, Induction methods in prospecting for hot water: Pisa, First United Nations Symposium on the Development and Use of Geothermal Resources.

Section 9

MAGNETOTELLURICS

The electrical geophysical techniques employed to delineate geothermal reservoirs do not, by their lack of penetration below a depth of several kilometers, provide much information on the sources of heat which gave rise to the geothermal reservoirs. It has been shown, in the section on the regional geophysics of the Wasatch-Hurricane Front, that a protrusion of mantle into the crust had been defined by various techniques. From the major mantle intrusion, smaller intrusions moved into the upper crust generating magma of intermediate composition. This intermediate magma was the source of the extensive extrusive and intrusive igneous activity along the Wasatch-Hurricane Front. These lesser intrusions, together with higher heat flow engendered by the major body of hot rock, must be the sources of the geothermal reservoirs in the Transition Zone between the Basin Ranges and the Colorado Plateau. In order to try to investigate directly the effects of these sources, a series of 64 magnetotelluric soundings were carried out in three traverses across the Transition Zone (Figure 9-1).

The magnetotelluric method is one which utilizes natural electromagnetic fields at very long periods to obtain the vertical distribution of electrical resistivity within the crust and upper mantle. The source of the electromagnetic fields are time-varying electric currents in the ionosphere which induce electric and magnetic fields within the earth. By recording and analyzing the

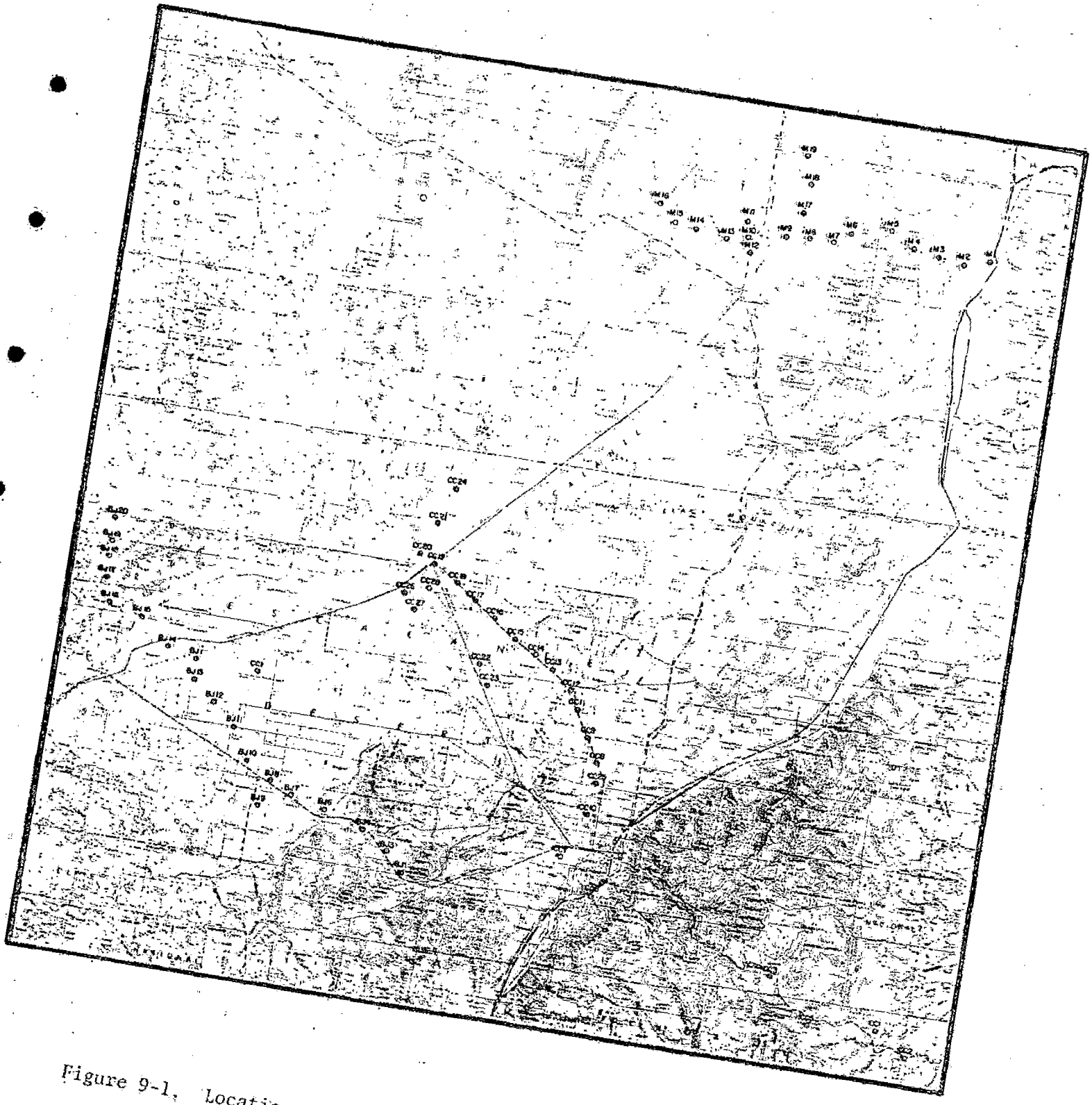

Figure 9-1. Location of magnetotelluric soundings in the Escalante Desert region, Utah.

fields at different frequencies, a sounding curve can be generated which represents the change of resistivity with depth. In the field, two horizontal components of the electric and magnetic fields are measured. The electric field sensors are simply lengths of wire connected between non-polarizing electrodes. The magnetic field sensors are superconducting elements housed in a liquid-helium dewar. The voltages from the electric and magnetic field sensors were recorded using an oscillographic recorder. At each measuring station, the fields were recorded for 100 minutes. Thus, it was possible to determine the amplitudes of frequencies as low as 1000 seconds. The upper limit of the spectrum recorded is a period of 10 seconds. Processing of the data is underway and preliminary interpretations indicate that the results will be very useful in determining the electrical structure of the lower crust in southwest Utah.

Section 10

DRILLING

Two deep wells were drilled in the Escalante desert by McCulloch Oil-Geothermal Kinetics, Inc. to test the geothermal potential of the Beryl prospect. The first was #1 State drilled in Sec 22, T34S, R16W to a total depth of 4,986 feet (1,520 m). The second was #1 DeArman drilled in Sec 18, T34S, R16W to a total depth of 12,300 feet (Figure 10-1). The locations of both wells were chosen as a result of the geological and geophysical exploration described elsewhere in this report. In the course of drilling the wells, continuous mud logging was carried out and complete suites of geophysical and continuous temperature logs were run. In this section, particular emphasis will be placed on the interpretation of the temperature logs. The stratigraphic section encountered by #1 State is shown in Figure 10-2, as are the continuous temperature logs. From the surface to a depth of 372 feet (113 m) sands, silts and conglomerates are encountered, the rock type then changes to a soft bentonitic lake clay, with some sands, which persists to 1,200 feet (366 m). At 1,200 feet (366 m) the shale changes to volcanics and welded tuffs which persist to a depth of 1,940 feet (591 m). The basement rock, a quartz-monzonite is then encountered and persists, with no mineralogical changes, to a depth of 4,986 feet (1,520 m). The upper part of the quartz-monzonite, between 1,940 feet (591 m) and 3,200 feet (976 m), is highly fractured.

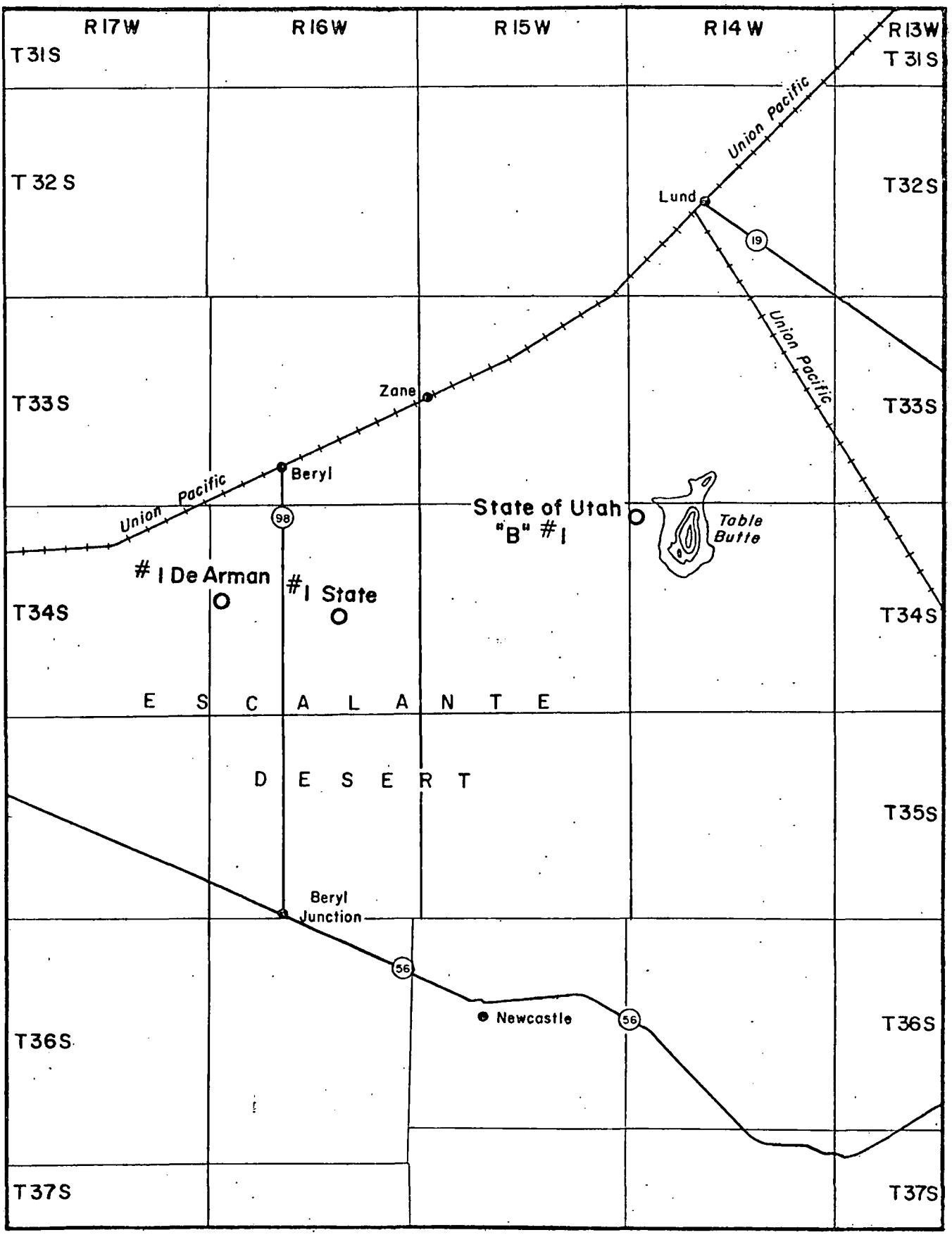

Figure 10-1. Location map of deep wells in the Escalante Desert region, Utah.

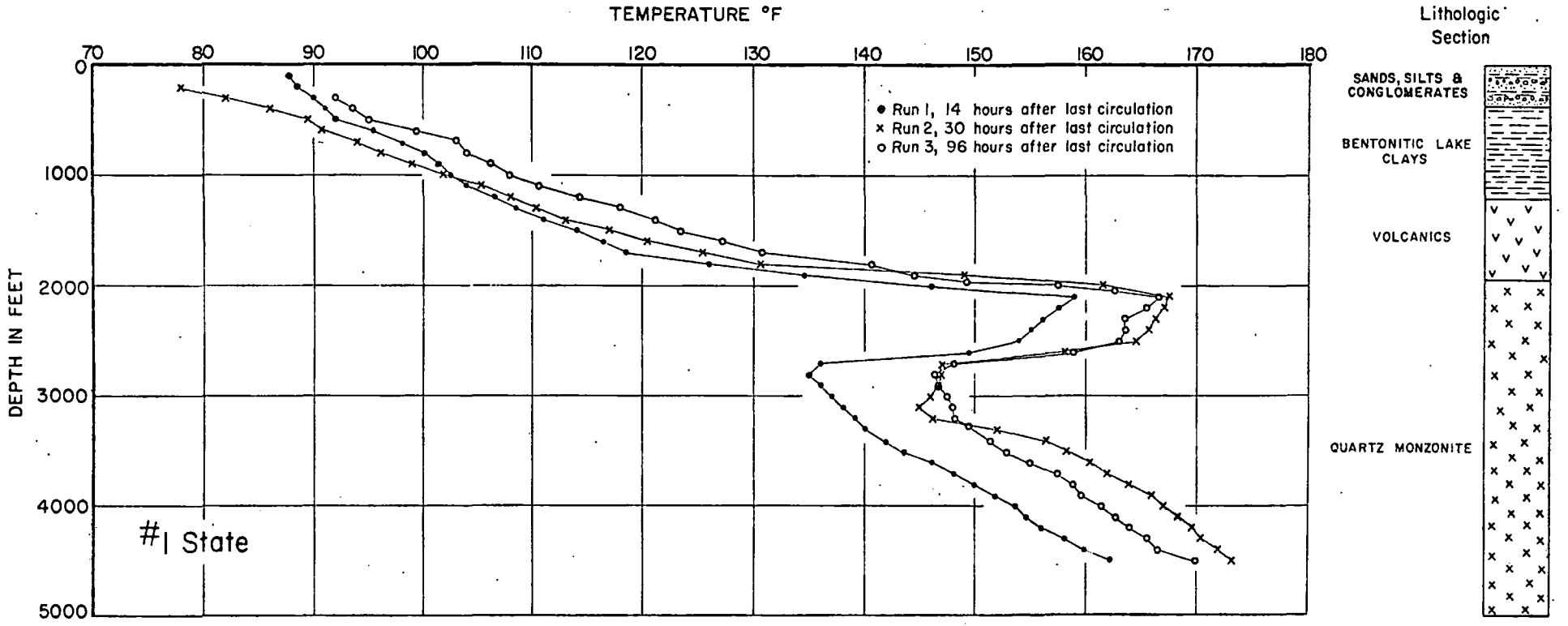

Figure 10-2. Temperature vs. depth for #1 State well with lithologic section.

Large open fractures, one of which caused the drill bit to drop by some 30 feet, were encountered at 4,500 feet (1,390 m).

When the hole had reached a total depth of 4,986 feet (1,520 m), two continuous temperature logs were run by Schlumberger. The first was begun 14 hours after circulation had been stopped, the second was started 30 hours after stopping circulation, giving a time interval of 16 hours between the temperature logs. These logs are shown as runs 1 and 2 in Figure 10-2. Both logs show a linear temperature gradient from a depth of 200 feet (61 m) to a depth of 1,700 feet (518 m), within this zone, the second run has a higher gradient than the first. The crossover point, as the lower part of the hole heats and the upper part cools is at 1,040 feet (317 m); the temperature at this point is 103°F. The temperature gradients within the mud column in this upper section are 2.2°F per 100 feet for run 1 and 2.6°F per 100 feet for run 2. At 1,700 feet (518 m), the temperature begins to rise rapidly and there is a pronounced bulge in both temperature profiles. At a depth of 2,100 feet (640 m), the increase in temperature begins to reverse and decreases sharply at a depth of 2,500 feet (762 m). At 2,700 feet (893 m), the linear increase in temperature is resumed until a depth of 4,986 feet (1,520 m). A third temperature log was run starting 96 hours after circulation was stopped, its character is exactly similar to that of runs 1 and 2 (Figure 10-2). In the lower part of the hole, the temperature gradient is 1.8°F per 100 feet. The temperature difference between the upper and lower parts of the

hole appears to be caused by an inflow of hot water which causes the gradient above to be greater than that in the lower part of the well.

The temperature gradients shown in Figure 10-2 are the gradients in the mud column, not in the rock. It was not possible to run continuous temperature logs until the hole had stabilized, so that true rock temperature remains unknown. However, there are two points in the well where true rock temperature can be established. The first is at the surface, where the average annual temperature of the water in non-thermal water wells is 10°C (50°F) (Mr. Lorin Sperry, State Water Engineer, State of Utah Division of Water Resources, Cedar City, Utah, personal communication). The second true temperature is the crossover point between temperature runs 1 and 2. If a well is allowed to remain undisturbed after drilling is completed, then the temperature in the mud column will change with time; the mud in the lower part of the well will heat, while in the upper part, the mud will cool down. If temperature logs are run at relatively short time intervals, say 12-to-20 hours, it will be seen that the later logs have a higher gradient than the initial logs. The point at which the later log crosses the earlier represents a point of equilibrium where the temperature in the mud column is no longer changing. At the changeover between runs 1 and 2, the temperature is 103°F at a depth of 1,040 feet (317 m). The difference between the temperature at the crossover point and the temperature at the surface is thus 53°F and the

temperature gradient between the two points is 5.3°F per 100 feet. If an average thermal conductivity for shale, 5 X 10^{-3} cal/cm/sec/°C, is attributed to the volcanic and clastic section in the upper part of the well, then the heat flow in the upper part of the hole is 4.83 HFU. If the gradient of 1.8°F per 100 feet is taken as a rough approximation of the true temperature gradient in the quartz-monzonite, then the heat flow which it represents, using a thermal conductivity of 7.5 ca./cm/sec/°C, is 2.46 HFU. Sass, et al. (1971) made heat flow determinations in 7 drill holes located in the Neck of the Desert some 20 miles east of the Beryl Prospect. The wells were drilled above a Tertiary intrusive quartz-monzonite (Mackin, 1960). It is not reported if the wells penetrated the quartz-monzonite. They may have done so, as the thermal conductivities used to determine heat flow lie in the median range for granite (Sass et al., 1971). The temperature gradients recorded ranged from 1.34 to 1.67°F per 100 feet, while the heat flows, calculated from these data, range from 1.99 to 2.36 HFU. These results are very close to that calculated for the lower part of #1 State.

The disparity between the heat flow in the bottom part of the hole and that in the upper means that almost 50% of the heat flow in the upper section of the hole (i.e. shallower than a depth of 1,700 feet (518 m) , is contributed by the flow of hot water in the upper part of the quartz-monzonite. The hot water, flowing in a layer about 600 feet (183 m) thick, effectively doubles the heat flow above 1,700 feet (518 m) indicating that the source must

be relatively close to the site of #1 State. Because of the high ambient heat flow below the hot water zone, it was felt that the source of the hot water encountered in #1 State could be a thick section of clastic rocks. Such a section would have a relatively low thermal conductivity, in which a high temperature gradient could be built up, giving rise to water of a temperature hot enough to sustain commercial production of electricity. With this concept in mind, the #1 DeArman well was sited some 4 miles west of the #1 State.

The section penetrated by the #1 DeArman is shown in Figure 10-3 as are the continuous temperature logs. The surface layers are composed of sandstones, silts and conglomerates to a depth of 400 feet (122 m). This upper layer is followed by bentonitic clay, with some scattered sand lenses, which persists to a depth of 1,557 feet (475 m). From 1,557 feet (475 m) to a depth of 4,622 feet (1,410 m) is a volcanic sequence composed of ignimbrites and tuffs. At 4,622 feet (1,410 m), the volcanics change to dolomite and limestone of the Tertiary Claron formation, which continue to a depth of 5,298 feet (1,615 m). At this point, the lower Claron formation is encountered which consists of red beds, volcanics, red and green shales, limestones and dolomites. These continental deposits persist to a depth of 6,070 feet (1,850 m), when upper Devonian dolomite and limestone are encountered. These Paleozoic carbonates persist to the bottom of the hole which is 12,295 feet (3,750 m).

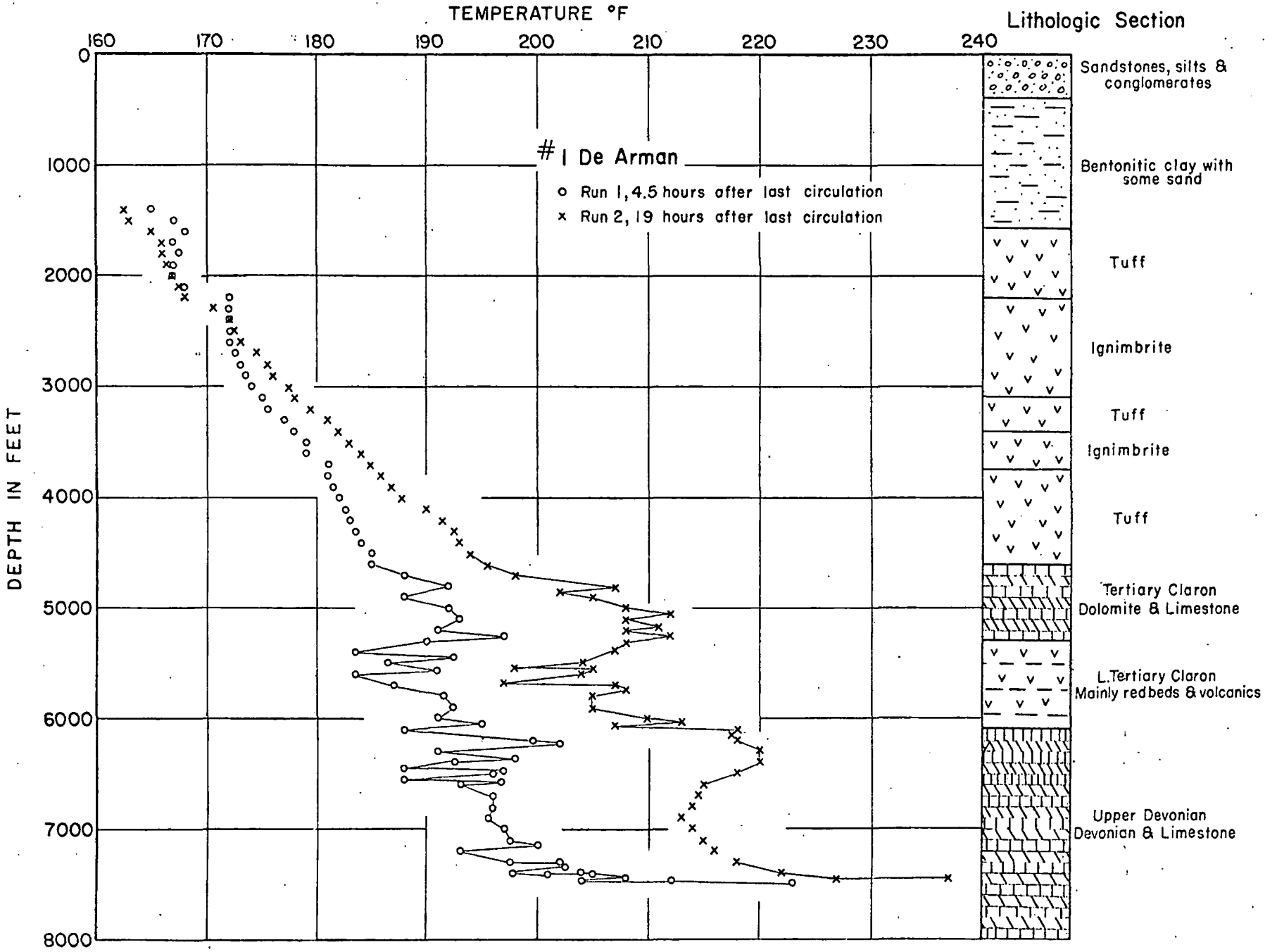

Figure 10-3. Temperature vs. depth, 6/9/76, for #1 DeArman well with lithologic section.

The first set of continuous temperature logs were run when the well had reached a depth of 7,500 feet (2,286 m) (Figure 10-3); two runs were made, separated by a time of 14½ hours. In character they are very similar to the logs run at the #1 State well. In the upper part, they have linear temperature gradients to a depth of 4,600 feet (1,400 m). Below 4,600 feet (1,400 m), the temperature curves make two radical departures towards higher temperatures. The upper departure is coincident with the Claron limestone, the second is coincident with the upper part of the Paleozoic limestones. A third departure may be represented by the bottom 400 feet of the log. Where each of the three increases in temperature occur, the cuttings show that the limestone has been dolomitized. While dolomite occurs in the upper Devonian, no dolomite has been encountered at any outcrop of the Claron formation (Hintze, 1973). It is thus interesting to speculate that dolomitization has occurred through the addition of geothermal water to the formations. The magnesium content of the water produced from the #1 DeArman is three times that of the surface water in the area. The dolomitization would also lead to increased permeability. The zones of higher temperature are undoubtedly due to flow of hot water into the well.

Between the three incursions of hot water lie temperature points which are in line with the linear gradient of the upper part of the hole. The upper of these two zones is coincident with the basal Claron formation which is composed of non-permeable

rocks. In the second non-permeable layer, between 6,900 feet (2,100 m) and 7,300 feet (2,225 m), the cuttings contained a great amount of secondary calcite.

The crossover point between the first and second logs occurs at a temperature of 170°F at a depth of 2,500 feet, again using a surface temperature of 50°F, the change represents a temperature gradient of 4.84°F per 100 feet. Using a thermal conductivity of 5×10^{-3} cal/cm/sec/°C, this gradient represents a heat flow of 4.4 HFU which is almost identical to that measured in the #1 State.

After logging to 7,500 feet (2,286 m), drilling was continued; at 7,730 feet (2,356 m), a cavern was encountered, the bottom of which was at a depth of 7,771 feet (2,370 m). Circulation was lost completely, and after much work and application of lost circulation material, the hole was whip-stocked at 7,105 feet (2,166 m). In the redrilled part of the hole, a similar cavern was encountered between 7,736 feet (2,358 m) to 7,767 feet (2,368 m). Casing was installed through the cavern zone and drilling continued to a total depth of 12,295 feet (3,737 m). Much lost circulation was encountered between 8,000 and 9,000 feet and the hole was drilled using lost circulation material together with much make-up water.

After the hole had reached a total depth, two continuous temperature logs were run on the 15th of July 1976, some 37 days after the first set of well logs (Figure 10-3) were run on the 9th of June, 1976. These latter logs are shown in Figure 10-4. Bear

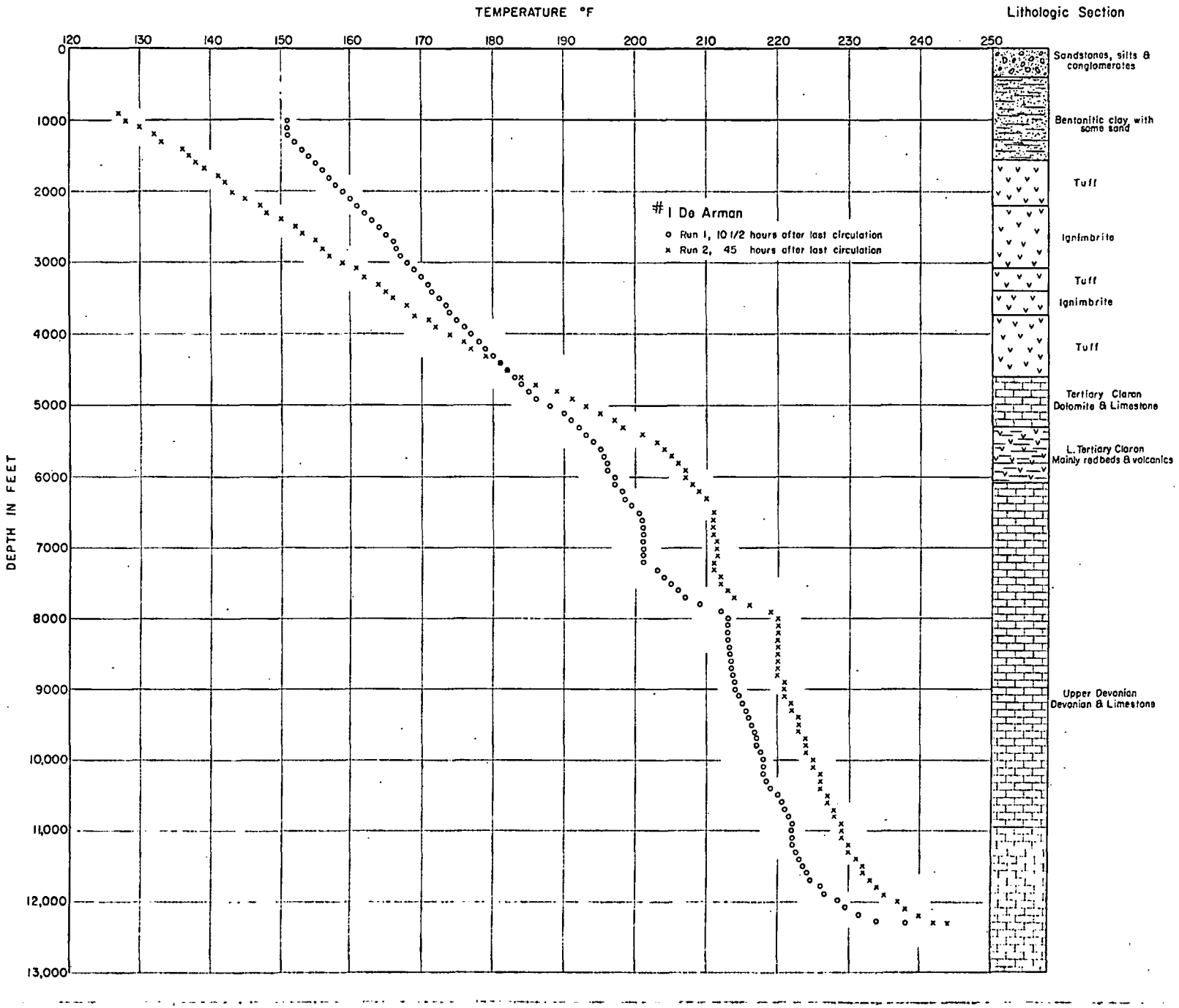

Figure 10-4. Temperature vs. depth, 7/15/76 for #1 DeArman well, with lithologic section.

in mind that, in the interval between the two sets of logging, continuous circulation of mud was kept up while fishing and trying to by-pass the cavern zone. This activity, coupled with extensive addition of make-up water and lost circulation material considerably modified the permeability characteristics of the well.

Both logs are linear to a depth of 5,500 feet, the first having a gradient in the mud column of 0.9°F per 100 feet, the second run some 32 hours later, has a gradient of 1.55°F per 100 feet in the mud. At 5,500 feet (1,677 m), the gradient decreases and becomes zero between 6,400 feet (1,950 m) and 7,500 feet (2,287 m). At this point, the gradient again increases but becomes zero at a depth of 8,000 feet (2,439 m). This condition persists until 9,100 feet (2,770 m), where the gradient increases to 0.4°F per 100 feet. Between 11,200 feet (3,410 m) and total depth, the gradient increases but this is probably due to the comparative lack of disturbance by drilling of the bottom of the hole. It is believed that the sections where the two temperature logs show no gradient are zones of very high permeability which, before drilling, contained hot water but that now with the addition of lost circulation material and much cold water, appear only as zones of constant temperature. The zones of hot water between depths of 4,900 feet (1,493 m) and 6,500 feet (1,981 m) shown on Figure 10-3, are not apparent in Figure 10-4. The highest temperature measured in the hole, was on the last temperature run when 245°F (118°C) was seen at the bottom of the hole.

At the cessation of drilling, the hole was stimulated into producing water by pumping air through the drill pipe at a depth of 800 feet. The well continued to flow and has proved to be able to flow spontaneously after being closed in. After flowing for some time, the temperature of the surface water stabilized at 208°F (98°C).

When the cavern was encountered at a depth of 7,730 feet (2,357 m), a temperature of 285°F had been measured at that depth using maximum reading thermometers. Accordingly, a plug was set at a depth of 8,073 feet (2,460 m), and the zone from 7,760 feet (2,366 m) to 7,790 feet (2,375 m) was perforated. The perforations were successful and the well started to flow of its own accord, again stabilizing at a temperature of 208°F. The maximum flow from the perforated zone was 1,900 bbl per hour. The high temperature of the water, 285°F, was not regained.

The results from the drilling and temperature logging indicate that copious supplies of geothermal water exist at relatively shallow depths in the Escalante desert. The temperature of the produced water is higher than would be generated by the base heat flow in either #1 State or #1 DeArman. Thus, it must have come from a reservoir situated close to the two wells. It must be close and water velocity must be high in order for the temperatures to be as high as they are.

REFERENCES

Hintze, L. F., 1973, Geologic history of Utah: Brigham Young Univ. Geol. Studies, v. 20, part 3.

Mackin, J. H., 1960, Structural significance of Tertiary volcanic rocks in southwestern Utah: Amer. Jour. Sci., v. 258, p. 81-131.

Sass, J. H., Lachenbruch, A. H., Munroe, R. J., Greene, G. W., and Moses, T. H., Jr., 1971, Heat flow in the western United States: Jour. Geophys. Research, v. 76, p. 6376-6413.

Section 11

CONCLUSIONS AND RECOMMENDATIONS

The Transition Zone between the Basin Ranges and the Colorado Plateau is a proven goethermal province. Wells which produce hot water at temperatures greater than 500°F (250°C) have been drilled northeast of Milford at Roosevelt Hot Springs. The production area at Roosevelt lies immediately east of the boundary between the Basin Ranges and the Transition Zone. The regional geology and geophysics indicate that the conditions which have caused the geothermal reservoir at Roosevelt should continue to the northeast and southwest along the strike of the Transition Zone.

At the southwest end of the Transition Zone, in the Beryl Prospect, the two wells which were drilled did not encounter water at temperatures which would lead to commercial production of electricity at present. However, the wells did prove a geothermal reservoir does exist in the Escalante desert. Measured temperatures are greater than one-half of the geochemical temperatures, indicating that the reservoir is in the vicinity of the drill holes. The measured temperatures would be lower if the water had travelled more than a few miles. The heat flow which was measured in the lower parts of the wells is too low to produce the measured water temperatures at the depths where they were encountered. To locate the geothermal reservoir in the Escalante desert, a complete synthesis must be made of the available geologic and geophysical

data. To supplement these data, hydrologic studies should be carried out to determine the regional water gradient. A more extensive program of magnetotelluric sounding would permit better definition of heat sources.

The Lund Prospect has resistivity characteristics similar to geothermal reservoirs such as Wairakei, in that from a central zone of low resistivity, the resistivities increase rapidly outwards. The zone of low resistivity at Lund is also a zone of anomalous water chemistry and an area of high mercury soil content. The position of the Lund anomaly, immediately east of the surface trace of a major thrust fault and straddling the fault, or faults, separating two major tectonic provinces, makes it ideal to be the repository of hot water moving up the faults. However, at Lund there are few natural thermal phenomena. This lack could be due to the permeability barrier of lake clay which is the surface rock in the area. It is strongly felt that the Lund anomaly is a potential geothermal reservoir, but before drilling a deep test, the following should be carried out:

1. Complete satellite photo study (in process). 1" = 1 mile photo
2. Detailed surface geological sectioning, primarily in mountains north and west of Lund. Objective to find the correlatives of possible reservoir formations and/or shale sections.
3. Repeat water geochemical work using improved and faster techniques. Soil mercury survey to be extended.
4. Magnetotellurics to establish heat source.

5. Self Potential survey to establish water flow in sub-surface.

6. Three temperature gradient holes to a depth of 1,500 feet in the following locations:

   a) Core of resistivity anomaly.
   b) Central basin.
   c) Hanging wall of thrust.

7. Additional resistivity maps and refinements.

8. Schlumberger soundings in center of resistivity anomaly.

9. TDEM at ¼ and ½ mile spacing around proposed location of deep test.

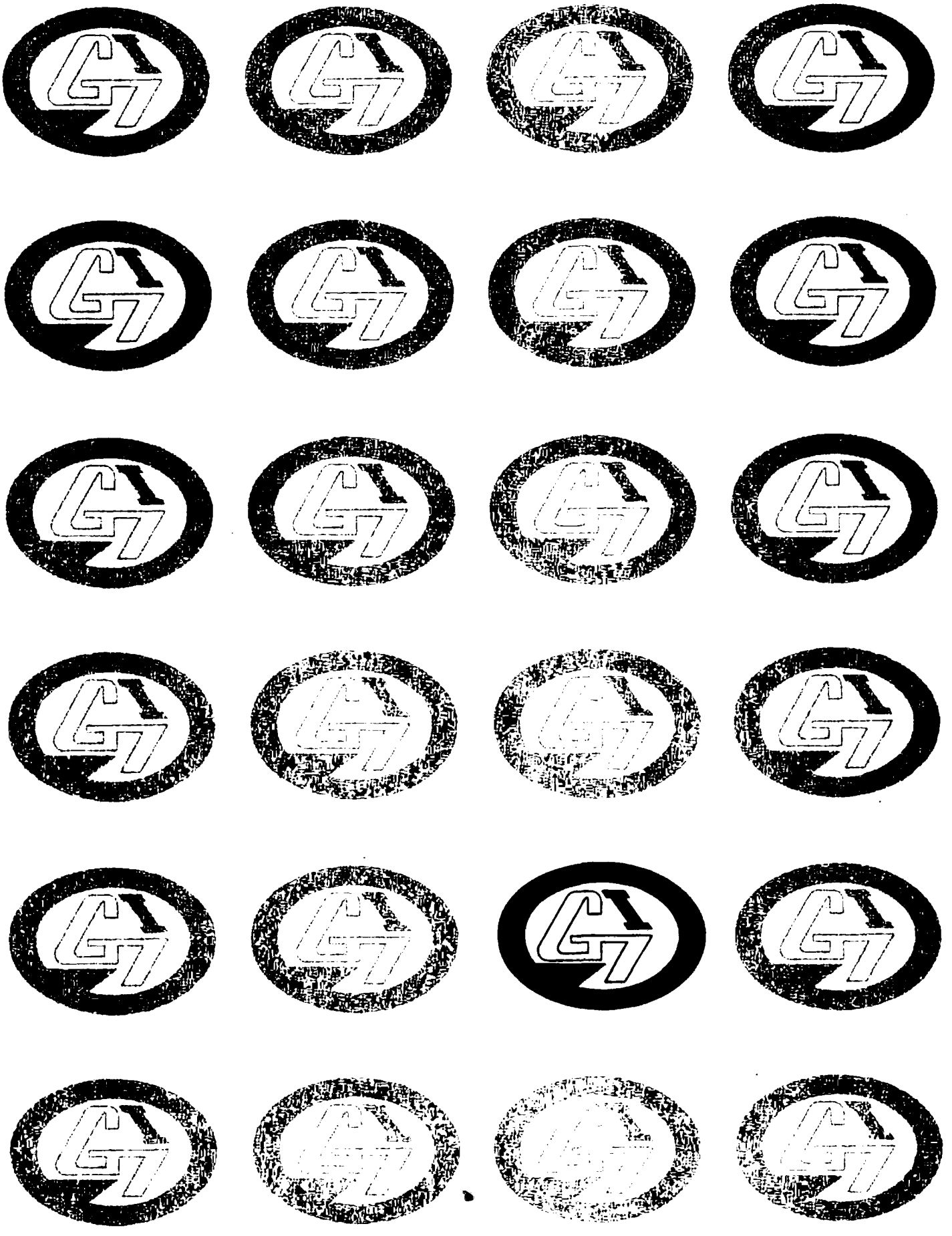

APPENDIX II

PROPOSAL EY-R-08-007

to

ENERGY RESEARCH AND DEVELOPMENT ADMINISTRATION

from

GROUP SEVEN, INC.

1301 Arapahoe Street

Golden, Colorado 80401

DETERMINING THE RESISTIVITY OF A RESISTANT LAYER IN THE CRUST

George V. Keller and Robert B. Furgerson

Colorado School of Mines
Golden, Colorado 80401

DETERMINING THE RESISTIVITY OF A RESISTANT LAYER IN THE CRUST

George V. Keller and Robert B. Furgerson

ABSTRACT

Direct-current resistivity surveys are capable of determining only the resistivity-thickness product for the resistant portion of the earth's crust. In order to estimate the resistivity in this resistant zone, it is necessary to combine the results of direct current soundings with the results of electromagnetic or magneto-telluric soundings, which are capable of determining only the thickness of the resistant zone. Knowing the thickness and the thickness-resistivity product provides an unambiguous value for resistivity, at least in principle. However, distortions of direct-current soundings by lateral changes in resistivity usually limit the determination of the resistivity-thickness product to a minimum possible value, and often this minimum constraint is very loose. In an attempt to improve the reliability with which the resistivity-thickness product can be determined, a rotating dipole survey procedure has been devised and tried in central Wisconsin. The results, when combined with magneto-telluric interpretations in the same areas provided by Prof. Smith and Bostick of the University of Texas, Austin, indicate the maximum resistivity in the crust to be at least several million ohm meters. These results offer the prospect that further improvements in the joint interpretation of direct-current and electromagnetic survey data will permit reasonably accurate determinations of the maximum resistivity in the crust. Such information should have considerable utility in earthquake prediction studies and in exploration for geothermal energy.

INTRODUCTION

The problem of determining the maximum resistivity in the earth's crust has proven to be particularly difficult to solve. Attempts to study the distribution of resistivity values on a crustal scale (Keller, 1971; Brace, 1971) have yielded the information that resistivity exhibits a maximum in the upper or middle part of the earth's crust. Near-surface rocks are rendered relatively conductive by the presence of electrolyte in pore spaces in the rock. Below the zone of maximum resistivity, it has been recognized that rocks become progressively more conductive with increasing depth. It is generally assumed that this increase in conductivity is caused by increasing temperature which liberates ions in the solid phase of a rock, but other phenomena, including increased hydration of the rock or development of electronically conducting minerals, may occur also.

Knowledge of the maximum resistivity in the crust is of growing importance in two applications; in earthquake prediction and in exploration for geothermal resources. Laboratory studies indicate that diagnostic changes in electrical properties take place when a rock is loaded almost to its breaking point. The strongest rocks, which are usually the ones which determine when and where an earthquake occurs, tend to be the rocks with the highest resistivity. Thus, in the use of resistivity surveys for earthquake prediction, it would be highly desirable to be able to determine the resistivity in the resisitant portion of the crust with reasonable accuracy and reliability.

In geothermal exploration, we are concerned with locating areas in which the resistivity of the rock has been lowered from normal values by unusually high temperatures. At very shallow depths, where hot water-laden rocks have extremely low

resistivities, or at very great depths, where rocks at or near the melting point have extremely low resistivities, exploration is relatively straightforward; it is far easier to detect and measure the resistivity of a mass of conductive rock than of a resistive rock. The problem which remains unsolved is that of recognizing the effects of elevated temperature at moderate depths in the resistant part of the crust. Here, we are capable of determining the actual resistivity distribution only within an order of magnitude, at best, so that the effect of elevated temperature usually cannot be recognized.

THE PROBLEM

The nature of the problem can be seen by considering the capabilities of various electrical sounding techniques for resolving a simplified version of the crustal resistivity profile. Consider the simple three-layer profile indicated on Figure 1; here, the crust and upper mantle are represented by three layers, each of which is characterized by a single value of resistivity.

Many investigations of crustal conductivity profiles have been carried out using the magneto-telluric method. The magneto-telluric sounding method has come into use over the past decade with development dating from a paper by Cagniard (1953). Cagniard demonstrated mathematically that if natural electromagnetic noise could be assumed to consist of planar electromagnetic waves propagating vertically into the earth, the conductivity of the earth can be computed with a simple formula from measurements of the electric field and magnetic field intensities. Inasmuch as the distance that an electromagnetic wave can penetrate into a conductor depends upon frequency, soundings are made by measuring the electric and magnetic field intensities at a variety of frequencies.

The depth to which the conductivity profile can be determined with the magneto-telluric method is determined by the frequencies analyzed. For the earth resistivity profile shown in Figure 1, where the resistivity contrasts between layers are assumed to be very large (greater than 100:1), a magneto-telluric curve exhibits ambiguities in interpretability caused by large constrasts in resistivities. When the middle layer in the sequence of three has a much higher resistivity than the outer two, the magneto-telluric sounding curve is

nearly independent of the resistivity of the middle layer, and depends only on the thickness of that layer. The maximum value of apparent resistivity that can be measured in such a three-layer sequence is:

$$\rho_{a,max} = \frac{h_1 + h_2}{2S_1} \qquad \ldots 1$$

where $h_1 + h_2$ is the combined thickness of the top two layers and S_1 is the ratio h_1/ρ_1 for the first layer. The quantity S is termed the conductance of a layer. In areas where the surface-layer conductance is only a few mhos, the maximum apparent resistivity in a crustal-scale survey may be several tens of thousands of ohm-meters. When the conductance is a few thousand mhos, as in a sedimentary basin, the maximum apparent resistivity will be less than 100 ohm-meters. The frequency at which the maximum apparent resistivity is observed is given by

$$\omega_{max} = \frac{1}{\mu\ (h_1 + h_2) S_1} \qquad \ldots 2$$

The frequencies for maximum apparent resistivity in a three-layer H-equivalent section are given graphically in Figure 2.

Thus, it appears that the MT method is effective in detecting the presence and properties of the first and third layers in our hypothetical crustal model, but is quite ineffective in determining the resistivity in the second layer. This same limitation will hold true for all electromagnetic methods in which the effects of eddy currents induced in the earth are measured; in highly resistant zones, only very small induction currents are generated, and these are difficult to detect.

Another approach to determining the crustal resistivity profile, which has been used to a lesser extent than the MT method, is the direct-current resistivity sounding. The direct-current sounding method is the best known and understood of the electrical probing methods, perhaps because it has been in use for many years, or perhaps because it can be treated mathematically at an easier level than the ac probing methods. The essential feature of a direct-current probing method is that the current supplied to the ground has a low enough spectrum of frequencies that the flow of current may be described solely with Laplace's equation, and with no consideration of magnetic effects from the current flow. It is difficult to predict at what frequency these effects become important even when the resistivity distribution in the ground is known, and usually, a frequency far below a reasonable limit is used in dc soundings to assure that there is no error contributed by ac coupling effects.

Many specific field techniques have been used in dc soundings, but for crustal-scale surveys, only two of these have found favor--the Schlumberger technique and dipole technique. The Schlumberger electrode array consists of four colinear electrode contacts (Kunetz, 1966). In making a sounding, the outer two electrodes, which are used to supply current to the ground, are moved progressively away from the center of the spread. The inner two electrodes, at the center of the array, are used to measure the voltage drop developed by the current. In discussing the Schlumberger array, the assumption is made that the separation between the inner measuring electrodes is small compared to the separation between the outer current electrodes. If this assumption is valid, the ratio of voltage drop to electrode separation can be said to be approximately equal to the electric field intensity.

With the dipole array, four electrodes are used also (Al'pin, 1966), but they are not arranged geometrically in the same manner as with the Schlumberger array. Current is supplied to the ground with one pair of electrodes, usually fixed in location, while a component of the electric field is mapped as a function of distance from this current source with a second pair of electrodes. If the separation between the current electrodes is much less than the distance to the location at which the electric field is being detected, then it is possible to characterize the source solely in terms of its dipole moment--current intensity times electrode separation.

Normally, the electric field is mapped away from the dipole source along one of the principal directions. When the component of electric field parallel to the source axis is mapped outwards on the equatorial axis, this sounding is termed an equatorial dipole sounding. For a horizontally layered earth, this procedure produces the same apparent resistivity curve as a function of separation as does the Schlumberger array, though this similarity does not hold for any other earth geometry. When the electric field is measured at locations along the axis of the source, the sounding is termed a polar dipole sounding, and the apparent resistivities behave quite differently from those measured with a Schlumberger or equatorial dipole array. Other locations of the receiving electrodes may be used also and the electric field may even be mapped in detail in the plane about the source dipole (see Al'pin, 1966; Keller and others, 1975).

Both the Schlumberger and dipole arrays have advantages and disadvantages relative to one another when they are used for crustal-scale resistivity soundings, and so the choice of one or the other is not always clearcut. The principal disadvantage of the Schlumberger array is that the span between

current electrodes must be increased to hundreds of kilometers to provide information about the lower crust and upper mantle, even under favorable conditions. When this can be done, considerable information can be obtained on the resistivity profile through the crust, as may be seen in the paper by van Zijl (this volume).

In order to provide a detectable signal at the receiving electrodes at such large spacings, the voltages applied to the current line must be of the order of hundreds to several thousand volts. Extensive precautions must be taken so that such a length of current-carrying wire does not comprise a hazard to life. One satisfactory solution to this problem is the use of out-of-service power lines, which are already protected. In recent years, considerable work has been done during grounding tests of high-voltage direct-current transmission lines. A limitation of such an approach is the fact that soundings must be made at locations where there are available power lines, rather than at locations which may be the most interesting from the geological point of view.

Advocates of the use of dipole arrays for crustal-scale resistivity soundings apparently feel that the operational ease of the method is the chief advantage over the Schlumberger array. With a dipole source length of 1 to 10 kilometers, it is usually possible to make soundings even in densely inhabited areas, with judicious choice of the source location. Very large currents are required to provide measurable signals at the maximum spacings.

In the crustal model (Fig. 1), because the surface layer is much more highly conductive than the crystalline basement, apparent resistivity values observed at relatively short spacings begin rising with a slope of nearly +1. At somewhat larger spacings, the apparent resistivity reaches a maximum and then decreases rapidly at larger spacings. For the

Schlumberger and equatorial dipole arrays, the spacing at which the maximum occurs is (Keller, 1968)

$$a_{max} = \left(\frac{S_1 T_2}{2} \right)^{1/2} \qquad \ldots 3$$

where S_1 is the longitudinal conductance of the surface layers and T_2 is the product $\rho_2 h_2$, termed the transverse resistance of the second layer.

It is readily apparent that the spacing to which one must go to establish the maximum on the apparent resistivity curve for a crustal-scale sounding increases both with the conductance of the surface layers and with the transverse resistance of the crust. The results of such soundings which have been reported in the literature provide values for T_2 ranging from 10^6 to 10^9 ohm-m^2. The conductance of surface rocks may range from a few mhos where the rocks consist only of weathered crystalline basement to some thousands of mhos in deep sedimentary basins. The spacings required to measure maximum apparent resistivity are shown graphically in Figure 3 as a function of S_1 and T_2.

The value of apparent resistivity observed at the maximum depends on S_1 and T_2, and is essentially independent of the resistivity in the second layer. The equation may be rewritten as:

$$\rho_{a,max} = \left(\frac{2T_2}{S_1} \right)^{1/2} \qquad \ldots 4$$

The maximum value for apparent resistivity in a crustal-scale sounding is shown graphically in Figure 4 as a function of S_1 and T_2.

Ideally, for the simplified three-layer model of the crust, it is possible to determine the resistivity of the middle layer by making measurements both with a dc sounding

system, which detects the product $T_2 = \rho_2 h_2$, and an ac sounding system, such as the magneto-telluric method, which detects only h_2. It is to be expected that less than perfect results will be obtained in practice because the earth conductivity profile is not as simple as that shown in Fig. 1, and because lateral changes in the properties of any of the layers, but especially the surface layer, will complicate the patterns of apparent resistivity measured in the field. In order to evaluate the merits of a combined ac-dc sounding program for studying the properties of the resistant part of the crust, the Office of Naval Research sponsored a study in north central Wisconsin, carried out jointly by investigators from the University of Texas (UTA), the University of Wisconsin (UW), and the Colorado School of Mines (CSM). This paper will describe the dc resistivity studies carried out by CSM; the results of other studies are described in companion papers in this volume by Smith and others (UTA) and by Clay and others (UW).

ROTATING DIPOLE METHOD

A serious limitation to the use of dipole surveys for crustal-scale resistivity soundings is the high degree of sensitivity of such arrays to errors caused by lateral changes in resistivity of near-surface rocks. Surface inhomogeneities in resistivity cause effects which are often indistinguishable from the effects of layering at depth, so that simple dipole sounding surveys provide highly ambiguous results. These ambiguities can be minimized by carrying out highly redundant dipole surveys, using a technique which was called the "dipole mapping method" (Keller and others, 1975). A dipole mapping survey is conducted by making measurements of electric field intensity over the entire surface area reached by measurable currents from the source dipole, rather than only along specific traverses. In this way, areas of anomalously high or low surface resistivity can be recognized from the patterns they evoke on a contour map of values of apparent resistivity, and measurements which are relatively little affected by surface effects can be selected for interpretation as resistivity sounding curves. An extensive set of dipole resistivity maps obtained by computer simulation has been prepared to show how dipole resistivity maps reflect surface inhomogeneities of various sorts (Furgerson and Keller, 1974).

Examination of these computer-generated simulations indicates not only the extent of anomalies associated with surface irregularities in resistivity, but also that the extent of an anomaly is strongly dependent on the mutual geometric relationship of the electrode array and the position of the feature with anomalous resistivity. In other words, the effect

of a surface irregularity in resistivity can be maximized or minimized by an appropriate selection of the orientation of the source and receiver dipoles.

One approach to obtaining data to examine the maximum and minimum effects from surface irregularities is to make measurements of electric field from several sources, located so that they lie in various directions from the point where measurements are being made. This type of redundancy is very expensive in terms of field effort, and is ineffective unless the approximate locations of the surface irregularities are known ahead of time so that appropriate source locations can be selected.

An approach to obtaining multiple coverage from dipole sources which appears to be more practical is the use of a single rotating dipole source. Measurements are made at a receiver location as a function of the orientation of the source dipole, as the source dipole is swung through a 360^{o} rotation. As the source rotates, the direction of current flow at the receiver site will rotate through all possible directions, and apparent resistivity values which are maximally and minimally affected by surface irregularities will be measured.

It is not necessary to rotate the dipole source physically; if it were, the complexity of the surveying technique would be too great for the measurement to be feasible. However, the source dipole can be rotated in effect by using only two dipoles at the source, oriented in two directions which, preferably, would be orthogonal to one another. These two source dipoles are then powered simultaneously with current intensities which will provide a resultant dipole moment in the desired direction. Thus, by changing the ratio of cur-

rents to the two source dipoles, the resultant moment can be rotated through a full circle.

A more practical field procedure yet consists of making only two sets of electric field measurements at a receiver site, one for each of the two orientations of source dipole. Then, the two electric field vectors can be added in the proper proportions to find the electric field that would have been measured with any orientation for the source dipole.

Apparent resistivities for a given source location-receiver location combination may be computed in a variety of ways. For example, one might use only the component of the electric field parallel to the source dipole, to compute a so-called parallel-field apparent resistivity, or only the component of the electric field in a direction perpendicular to the axis of the source dipole, or only the component directed radially away from the source dipole (all of these ways of computing apparent resistivity have been described by Al'pin, 1966). Based on experience with the dipole mapping method up to the present time, we have elected to use the "total-field apparent resistivity" method of expressing resistivities measured with the rotating dipole technique. This definition of apparent resistivity is based on the use of the magnitude of the electric field vector at the receiver site, regardless of the direction in which it lies. The expression for computing apparent resistivity using the magnitude of the electric field is:

$$\rho_T = \frac{2\pi R^3}{[(3\cos\theta\sin\theta)^2+(3\sin^2\theta-1)^2]^{1/2}} \frac{E_T}{M} \qquad \ldots 5$$

where R is the distance between source and receiver, θ is the angle between the resultant axis of the dipole source and the radius vector from the source to the receiver, M is the moment

of the source, defined as the product of current and source dipole length, and E_T is the magnitude of the resultant electric field at the receiver site. The geometry described by this equation is shown on Figure 5.

Equation 5 is strictly applicable only if the separation between current electrodes is vanishingly small, as well as the separation between receiver electrodes. This requirement is met within reasonable limits of accuracy when the distance R is more than five times as great as either the length of the source dipole or the receiver dipole. This condition poses no particular limitation in crustal scale surveys, where dipole lengths are rarely greater than 1 to 2 kilometers, while dipole separations up to 100 kilometers may be used.

The layout of two dipole arrays for use in a rotating dipole survey and the way in which rotation is accomplished are indicated in Figure 5. In this illustration, the two sources are taken to have real moments M_1 and M_2, which are the products of current intensity and length for the two sources. Two total-field vectors, ET1 and ET2, are measured as each of the two sources is powered individually. Then, several directions, α, are selected as normals to the direction of a composite source. The moment of one of the sources, say M_2, is scaled by the factor β so that when the scaled moment βM_2 is added to the actual moment, M_1, the components of the two source moments in the normal direction α exactly cancel. The resultant moment is then in the desired direction. The total electric field that would be measured with this combined source is determined by adding ET1 to the scaled electric field βET2. The resistivity is then computed using eq. 5 as though a single-source dipole measurement had actually been made with the combined source.

Rotating dipole survey data may be presented in many formats. For example, the direction α may be selected so that the measurement made at any receiver station is along a principal axis of the combined source; that is, all points on a dipole map can be computed for an exactly equivalent polar or equatorial dipole array. Another approach is to determine the apparent resistivity values for a series of directions covering an angle of 180°, and then select the maximum and minimum values as representing the possible range that can be measured at a given receiving point. We have not yet carried out an extensive enough study to determine the best format for presenting rotating dipole resistivity data, but a few calculations which have been carried out are useful in describing the behavior of such data.

Figures 6 to 13 show some ways of presenting rotating dipole data for computed values of apparent resistivity for a simple model, that of a vertical plane separating two regions with true resistivities that differ by a factor of 10. In one case, the crossed dipole source is located in the more resistive medium (Figures 6 to 9) and in the other case, the crossed dipole source is located in the more conductive medium (Figures 10 to 13). Apparent resistivity values can be presented as though each of the dipole sources in a crossed pair were used to make an independent dipole mapping survey. The four single-source dipole maps are shown in Figures 6, 7, 10, and 11. The major shortcoming of single source dipole coverage is apparent on these four maps; the apparent resistivity values observed close to the boundary on the side toward the source show a complicated pattern. Some values of apparent resistivity are greater than any real resistivity in the model, while others are lower than any real value.

In our experience to date, the simplest contour maps seem to be those in which the average of the maximum and minimum values of apparent resistivity obtained on rotation is plotted (Figures 8 and 12). On these maps, the resistivity measured on the side of the boundary towards the source varies only slightly from the correct value. The values measured on the far side of the boundary are also uniform, but are not equal to the actual resistivity.

Another parameter which can be used to describe the results of a rotating dipole survey is the ellipticity of the pattern of apparent resistivity values obtained on rotation. This is defined as the square root of the ratio of the maximum and minimum values of apparent resistivity for a single receiver station. Contour maps of the values for ellipticity (Figures 9 and 13) show that the maximum ellipticity is measured along the boundary between the two regions with different resistivity, and closely defines the boundary.

FIELD SURVEYS

During the summer seasons of 1973 and 1974, rotating dipole surveys were carried out in north central Wisconsin in the areas outlined on Figure 14. Much of the area where the surveys were carried out is covered by glacial till with an average thickness of 15 meters, but ranging in thickness from 0 to 100 meters. Because of the glacial cover, the geology of the bedrock is poorly known, but the bedrock is believed to be predominantly granitic. According to Weidman (1907), the suboutcrop should be 85% granite and syenite, 5% greenstone, diorite and gabbro, 2% slate and greywacke, 2% quartzite and conglomerate, and 2% gneiss and schist. On the basis of this information, one would expect central Wisconsin to be an area in which high resistivities would be present in the crust.

In the field surveys, source dipoles with a length of approximately 1600 meters were used. Metal culverts were used to obtain relatively low ground contact resistances. At locations where three culverts could be found to form an L-shaped combination of source dipoles, the two sources were set up and energized sequentially. That is, the power source was first connected to one dipole, and electric field observations were made at all the receiver sites where measurements could be made. Then, these stations were reoccupied as the second source was energized.

The primary energy was a gasoline-engine motor-generator set with a capacity of 25 KVA at 235 v 60 Hz. The output of the generator set was stepped up to 1000 volts using a variable transformer, and then rectified and switched to supply alternating DC steps of current to the cables connecting the power

supply to the electrodes. The switching was done in such a way as to form an asymmetric waveform; that is, the length of a current step in one direction was about twice the length in the opposite direction. This made it possible to specify the polarity of the signals recorded at a receiver site. The periodicity of the current transmissions was once per 20 seconds. The amplitude of the current steps ranged from a low of about 10 amperes to a high of about 60 amperes, depending on the contact resistance for a particular source.

At a receiver site, voltages were measured with two orthogonal electrode pairs in order to determine two components of the total electric field vector. The separation between receiver electrodes was 30 meters. The voltage from a pair of receiver electrodes was filtered, amplified, and recorded on an analog recorder.

Three pairs of dipole sources were used to provide coverage over most of the crystalline sub-outcrop area of north-central Wisconsin. Some overlapping coverage was provided between adjacent sources, as may be seen from the location maps showing the position of the individual source dipoles and receiving stations (Figure 15).

The use of a pair of orthogonal dipole sources combined with the detection of both magnitude and direction of the electric field vector at a receiver station provides a highly redundant measurement scheme; that is, more quantities are measured than are needed to compute a single value of apparent resistivity. As a consequence, apparent values of resistivity can be computed in many different ways. Unless the earth is completely uniform, these various computed values are likely to vary widely. The field data obtained from the three pairs of dipole sources used in Wisconsin were reduced using the rotating source concept described at the beginning of this paper. The two observed electric field vectors observed at

each station (one for each direction of the source dipole) were added together in various proportions to provide single resultant vectors pointing in a variety of direction. Apparent resistivity values were computed using the total-field expression (eq. 5) which discards information on the direction of the E-field, and requires knowledge only of the magnitude. The resulting group of apparent resistivity values, one for each direction of a composite E-field vector, when plotted as a function of the direction of the E-field, form an ellipse. These ellipses may then be characterized by a relatively small number of parameters. The ones used here in presenting the data visually are the average resistivity (formed by averaging the maximum and minimum radii of the ellipse of resistivity), the direction of the major diameter of the ellipse, and the ellipticity (defined here as the square root of the ratio of the lengths of the major and minor axes of the ellipse).

Contour maps of the average resistivity obtained on rotation are shown in Figure 16 for each of the three surveys. It should be noted that lateral changes in resistivity dominate the contour patterns. If the area were laterally uniform, with resistivity varying only as a function of depth, apparent resistivities would contour more or less concentrically about the source. Here, no strong concentric pattern is easily recognized, and, in fact, measurements made from Source 1 (Figure 16a) indicate a fault-like boundary between areas of relatively low and relatively high resistivity about 20 km. east of the source location.

Maps giving contours of the value of ellipticity, and the directions of the major axes of the resistivity ellipses, are shown in Figure 17. It can be seen that local areas of high ellipticity are associated with lateral changes in apparent resistivity.

Our major interest is in the information these data can provide us about the resistivity at depth. The data in Figures 16 and 17 merely indicate that considerable caution must be used in attempting to determine resistivities at depth, in view of the strong lateral effects that are present. One approach to extracting information about resistivities at depth is to plot apparent resistivity values as a function of distance from the source, assuming that measurements made at greater distance reflect resistivities at greater depths in the earth. Such plots are shown in Figure 18 for the three dipole surveys carried out in Wisconsin.

Although the data plotted in Figure 18 are widely scattered, there is a pronounced tendency for apparent resistivity to increase with distance, as would be the case if actual resistivity were to increase with depth. A similar plot for synthetic data, obtained by computing apparent resistivities for a grid of observation points for a two layer model in which the substratum is ten times as resistive as the overburden, is shown in Figure 19 for comparison. Some scatter is present in this synthetic plot, but the scatter is far less than that shown by the real data in Figure 18. The scatter is contributed primarily by lateral changes in resistivity.

Interpretation

As a step in interpretation, it is tempting to average these highly redundant data in an effort to mask the scatter and effects of lateral inhomogeneities. Such averaging requires the assumption that effects caused by lateral inhomogeneities will be randomly distributed. In fact, this is not the case; apparent resistivity values will be lowered to a greater extent by a conductive inhomogeneity than they will be raised by a resistive inhomogeneity. As a consequence, any average of a

large number of observations will be consistently lower than the resistivity which would be observed in the absence of the inhomogeneities. If we recognize that this biasing of averages is present, we can still use the averages to characterize the gross behavior of apparent resistivity with distance from the source, as is done in Figure 20. Here, all values of apparent resistivity we measured (each value being the average of the major and minor axes of a resistivity ellipse) were grouped in three classes; values determined at distances of 10 to 20 kilometers, 20 to 40 kilometers, and greater than 40 kilometers. Within each group, the geometric mean distance and the geometric mean resistivity were computed. These values are shown as 3 dots in the upper right corner of Figure 20. The vertical bars shown for the shorter distance are taken from an unpublished report prepared by Ben K. Sternberg of the University of Wisconsin (private communication, February 1975). The bars summarize resistivity surveys done in this area by a number of earlier investigators using the Schlumberger and dipole sounding techniques, with the width of each bar indicating the principal spread of data for eight soundings. Curve "C" was computed by Sternberg for an earth model in which the resistivity becomes infinite at a depth of seven kilometers. This "basement" is overlain by two layers, one extending to 10 meters depth with a resistivity of 250 ohm-meters, and the other extending from there to 7 kilometers depth with a resistivity of 4000 ohm-meters. The fit is good.

If observations could have been carried to greater distances, we would expect to see the data shown in Figure 20 pass through a maximum. The product of apparent resistivity and spacing at that maximum would be very nearly equal to the transverse resistance (the product of resistivity and thickness) for the resistant portion of the crust. Because the data do not appear

to reach a maximum, we can say only that the last point specifies a minimum value for that maximum, which lies between 5 and 6 x 10^9 ohm-m^2.

Magneto-telluric soundings carried out in this same area by Bostick, Smith, and Boehl (this volume) provide an estimate of 15 to 20 kilometers for the thickness of this resistant zone. For this thickness, the resistivity would have to average 250,000 to 400,000 ohm-meters over the entire interval to provide a transverse resistance of 5 to 6 x 10^9 ohm-m^2.

In fact, it is highly unlikely that the resistivity is uniform over such a depth range in the earth. The effects of temperature should cause a gradational decrease in resistivity from its maximum value in the crust as one goes deeper in the crust or mantle. The upper boundary of the conductive regions will be sensed at shallower depths with a dc sounding method than with a magneto-telluric sounding method. Therefore, the straightforward calculation of average resistivity in the resistant part of the crust just done is not a fruitful exercise.

The problem can readily be demonstrated in more analytical terms. Consider an earth model in which the actual resistivity rises to a very large value in the upper part of the crust, and then decreases gradually over a long interval into the mantle. The transverse resistance derived from dc soundings might pertain to only a few kilometers of this zone while the total thickness derived from magnetotelluric data would be much greater, perhaps several hundred kilometers. To investigate this phenomenon, synthetic sounding curves were computed for a number of hypothetical crustal models (the model profiles are shown in Figure 21). These synthetic soundings, both dc and magneto-telluric, were then interpreted by a conventional least-squares inversion technique, with the constraint that the synthetic soundings be matched with a three or four layer earth model.

However, there was no significant difference between the closeness of fit for the three-layer and four-layer models. This is characteristic of true equivalence between interpretations and indicates that for these models, a three-layer interpretation is the best that can be done in practice. There rms error in fit ranged from a low value of about 0.33 percent (Case 4) to a high value of 1.82 percent (Case 5). These errors in fit are less than that which is normally obtainable in fitting real data, which contain some experimental error. Normal errors in fit obtained after least squares inversion are typically 2 to 3 percent for good dc resistivity data, and 3 to 5 percent for good magneto-telluric data.

As had been expected, it was found that the average resistivity for the resistant zone in these three-layer interpreted models, using the combination of dc soundings to find T_2 and magneto-telluric soundings to find h_2, was much than the maximum resistivity in the initial profile. This phenomenon is shown graphically in Figure 22, which shows the relationship between

$$\rho_2 = \frac{T_2 \text{ (dc sounding)}}{h_2 \text{ (MT sounding)}}$$

and the maximum resistivity in the initial profile. The interpretations for each set of models are connected by lines, so that the effect of the one variable parameter in each model can be seen.

In Figure 22, the maximum resistivities interpreted with a three-layer model fall below the actual maximum resistivity by factors ranging from 5 to 100, with the median factor being in the neighborhood of 10. If these results are valid, we can conclude that for the dc and magneto-telluric surveys carried out in Wisconsin, the maximum resistivity in the crust should be 10 times as great as the value derived from a straightforward

combination of the interpretations of the dc and MT surveys. The maximum resistivity in the crust over some short interval of several kilometers is probably 2.5 to 4 million ohm-meters.

REFERENCES

Alpin, L. M., 1966, The theory of dipole sounding; in Dipole methods for measuring earth conductivity: N. Y., Consultants' Bureau, 302 p.

Brace, W. F., 1971, Resistivity of saturated crustal rocks to 40 km. based on laboratory studies: in Heacock, J. G., (Ed), The structure and physical properties of the earth's crust: Am. Geophys. Un: Monograph 14, pp. 243-256.

Cagniard, L., 1953, Basic theory of the magneto-telluric method of geophysical prospecting: Geophysics, v. 18, pp. 605-635.

Furgerson, R. B., and Keller, G. V., 1974, Computed dipole resistivity effects for an earth model with vertical and lateral constrasts in resistivity; Technical Report to Office of Naval Research, 12 March, 194 pp.

Keller, G. V., 1971, Electrical properties of the earth's crust -- a survey of the literature: Colorado School of Mines, ONR contract N00014-70-C-0290.

Keller, G. V., 1968, Electrical prospecting for oil: Colorado School of Mines Quarterly, vol. 63, no. 2.

Keller, G. V., Furgerson, R. B., Lee, C. Y., Harthill, N., and Jacobson, J. J., 1975, The dipole mapping method: Geophysics, in press

Kunetz, Geza, 1966, Principles of direct-current resistivity prospecting: Gebruder Borntraeger, Berlin, 103 pp.

Weidman, S., 1907, The geology of north central Wisconsin: Wisconsin Geol. and Nat. History Survey Bull. 16, Sci. Series 4.

List of Illustrations

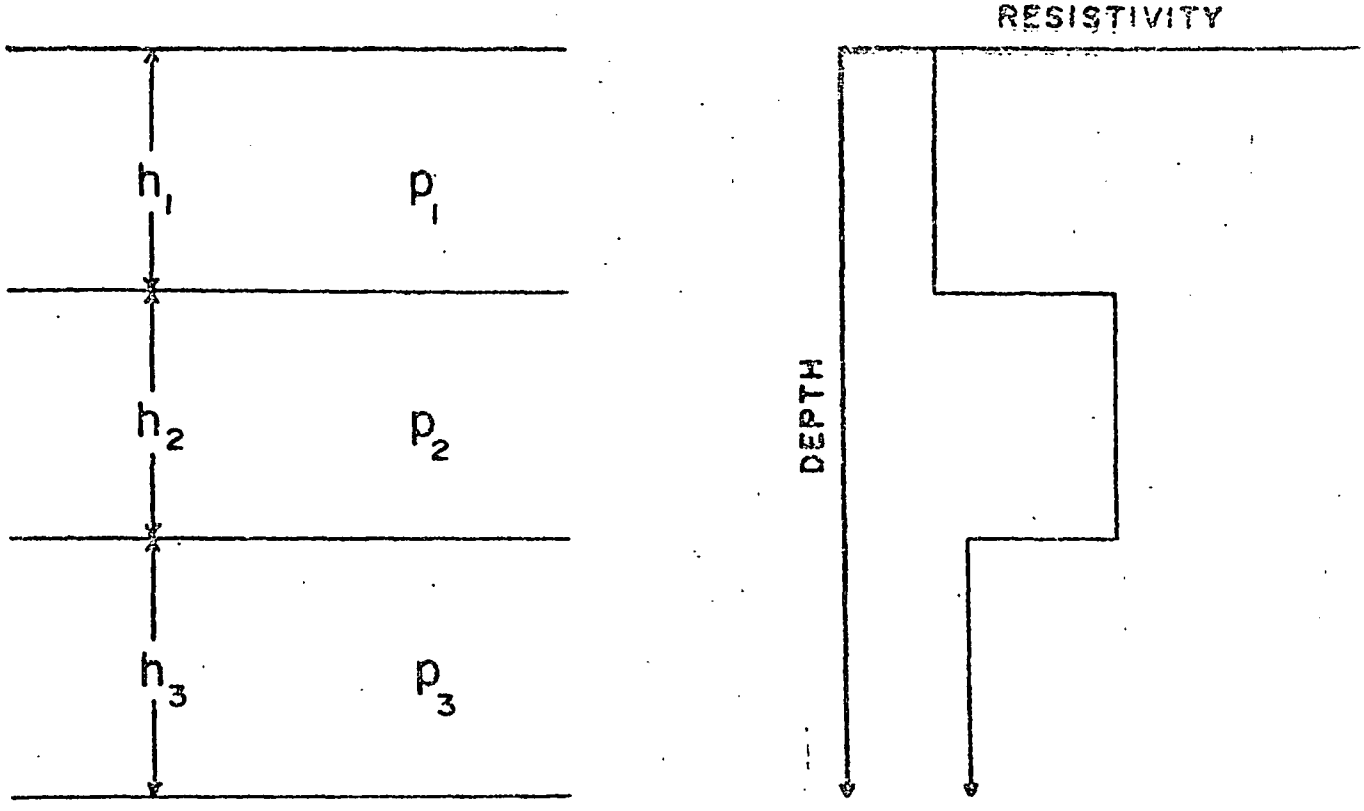

FIGURE 1

SIMPLIFIED CRUSTAL RESISTIVITY PROFILE

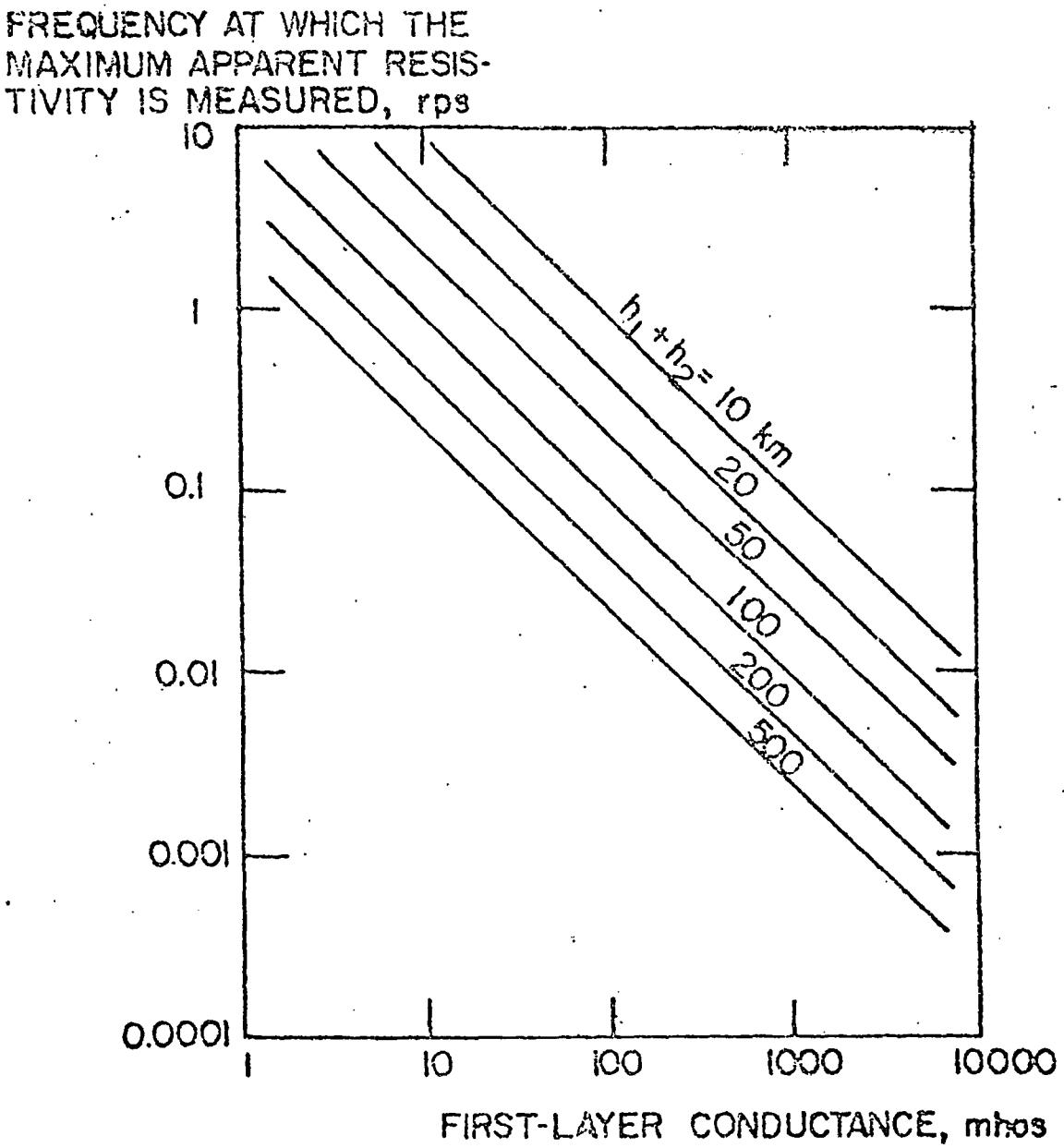
FREQUENCY AT WHICH THE MAXIMUM APPARENT RESISTIVITY IS MEASURED, rps
10
1
0.1
0.01
0.001
0.0001
1
10
100
1000
10000
$h_1 + h_2$ = 10 km
20
50
100
200
500
FIRST-LAYER CONDUCTANCE, mhos

Fig. 2

Fig. 2

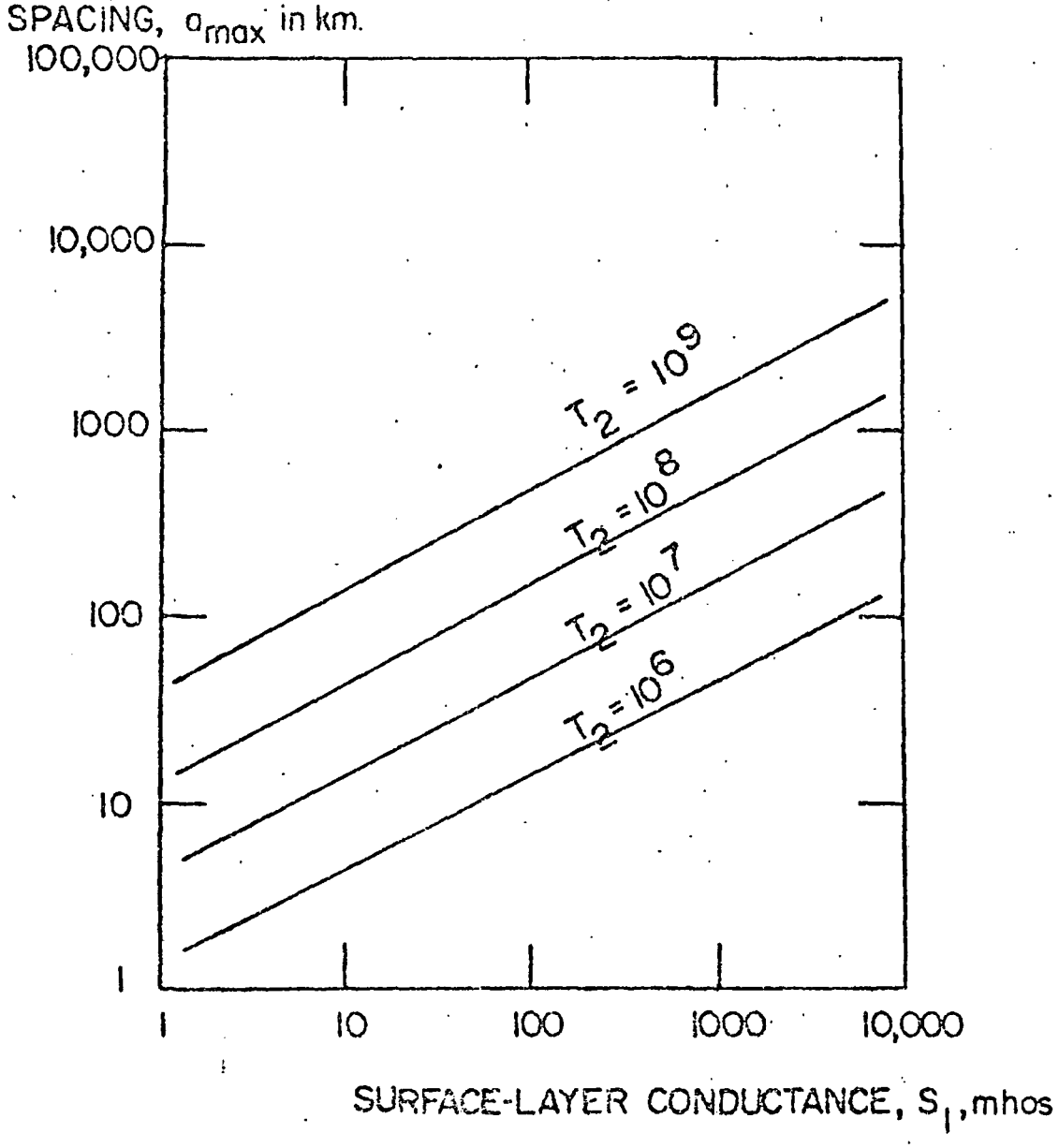
SPACING, a_{max} in km.
100,000
10,000
1000
100
10
1
$T_2 = 10^9$
$T_2 = 10^8$
$T_2 = 10^7$
$T_2 = 10^6$
1
10
100
1000
10,000
SURFACE-LAYER CONDUCTANCE, S_1, mhos

FIGURE 3

59-3

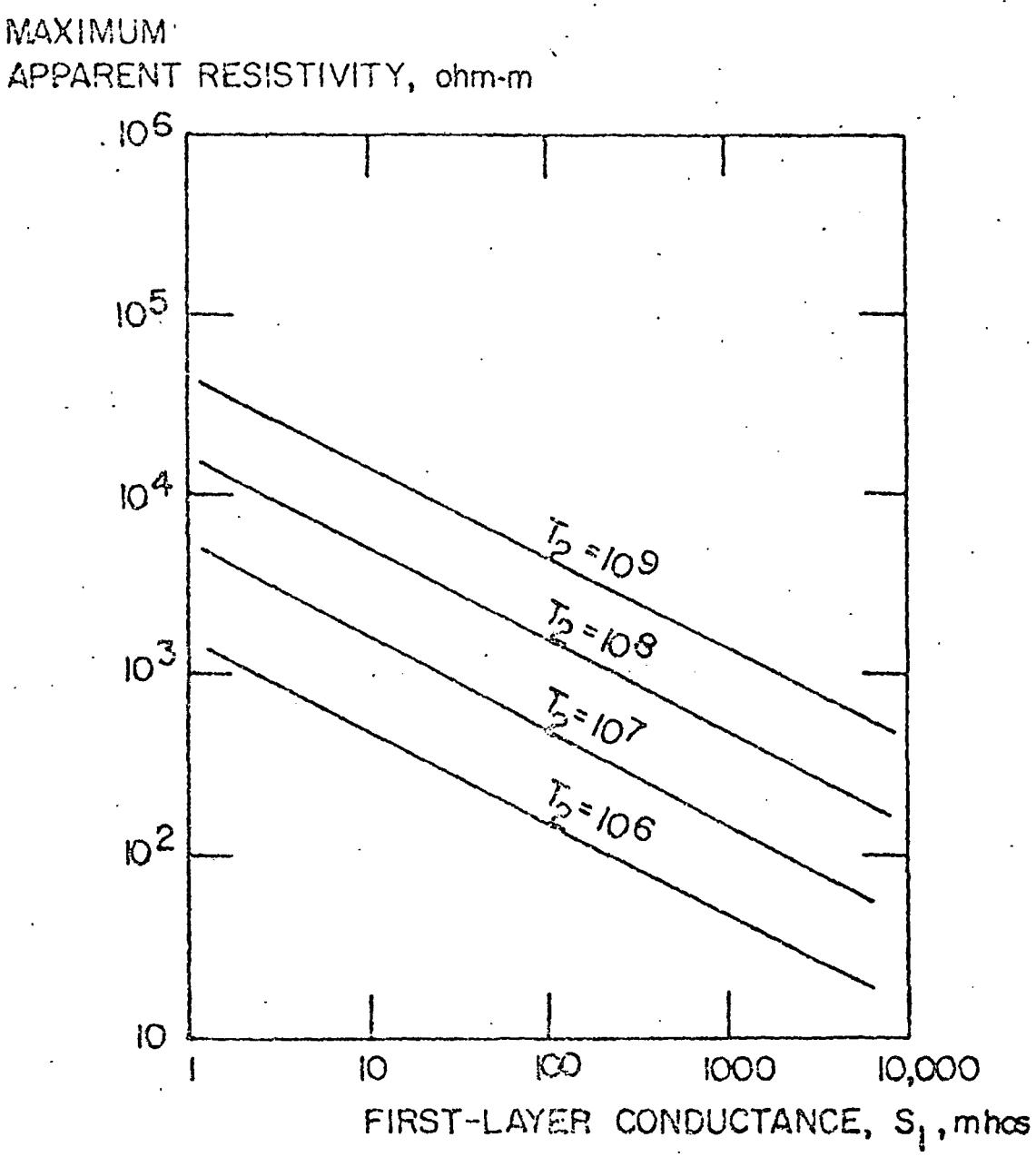
MAXIMUM
APPARENT RESISTIVITY, ohm-m
10^6
10^5
10^4
10^3
10^2
10
$T_2 = 10^9$
$T_2 = 10^8$
$T_2 = 10^7$
$T_2 = 10^6$
1
10
100
1000
10,000
FIRST-LAYER CONDUCTANCE, S_1, mhos

FIGURE 4

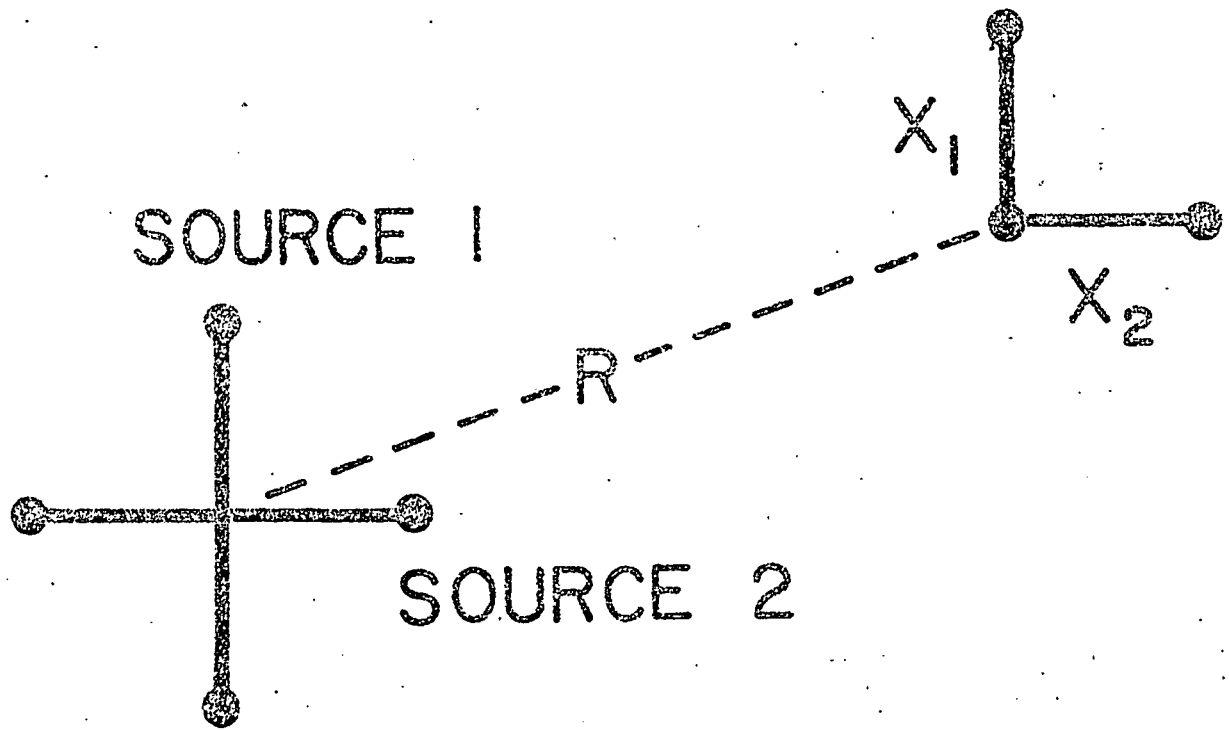

Fig 5
Figure 5

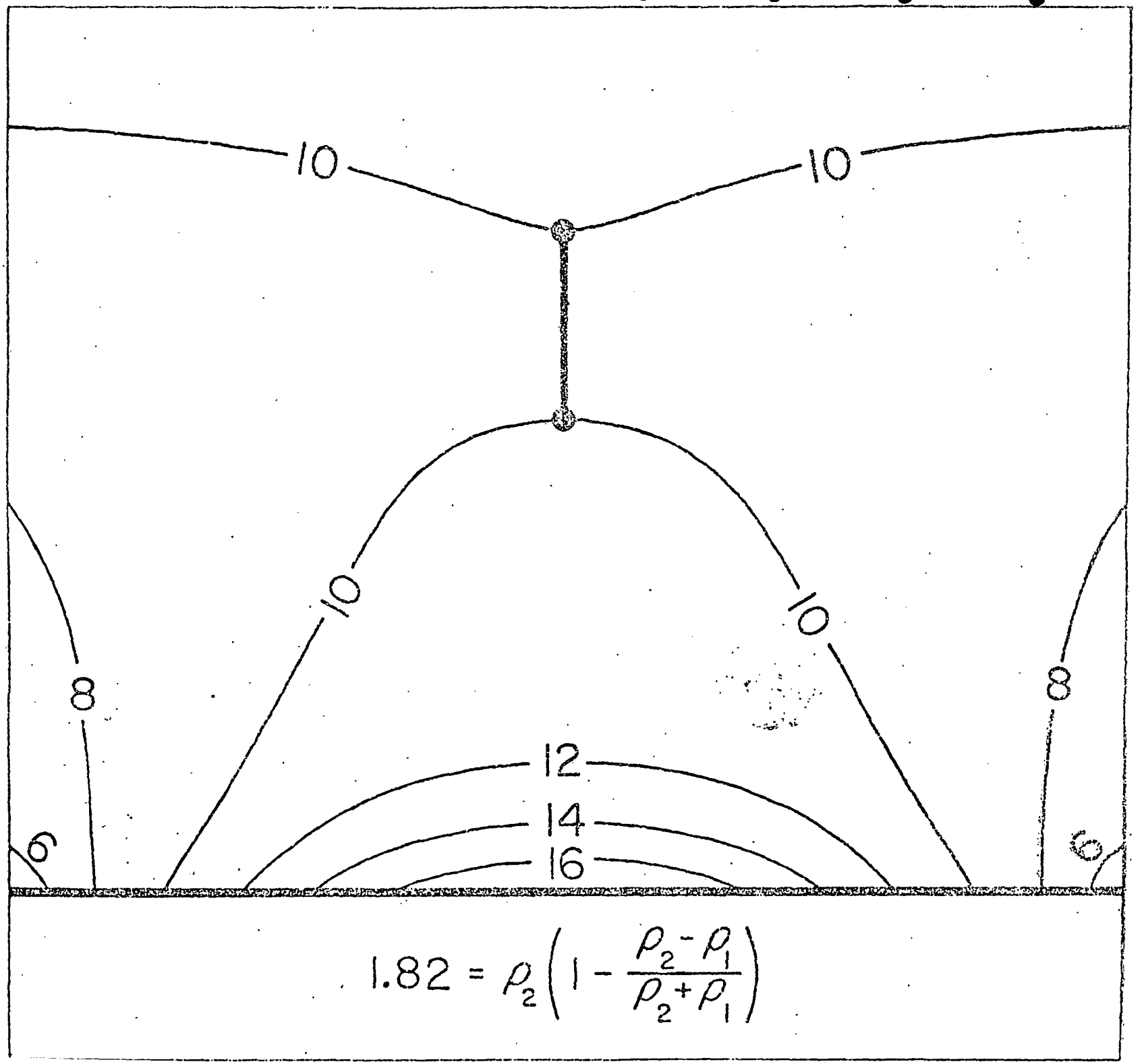
10
10
10
10
8
8
12
14
16
6
6
$\rho_1 = 10$
$\rho_2 = 1$
$1.82 = \rho_2\left(1 - \frac{\rho_2 - \rho_1}{\rho_2 + \rho_1}\right)$

FIG 6

FIG 7

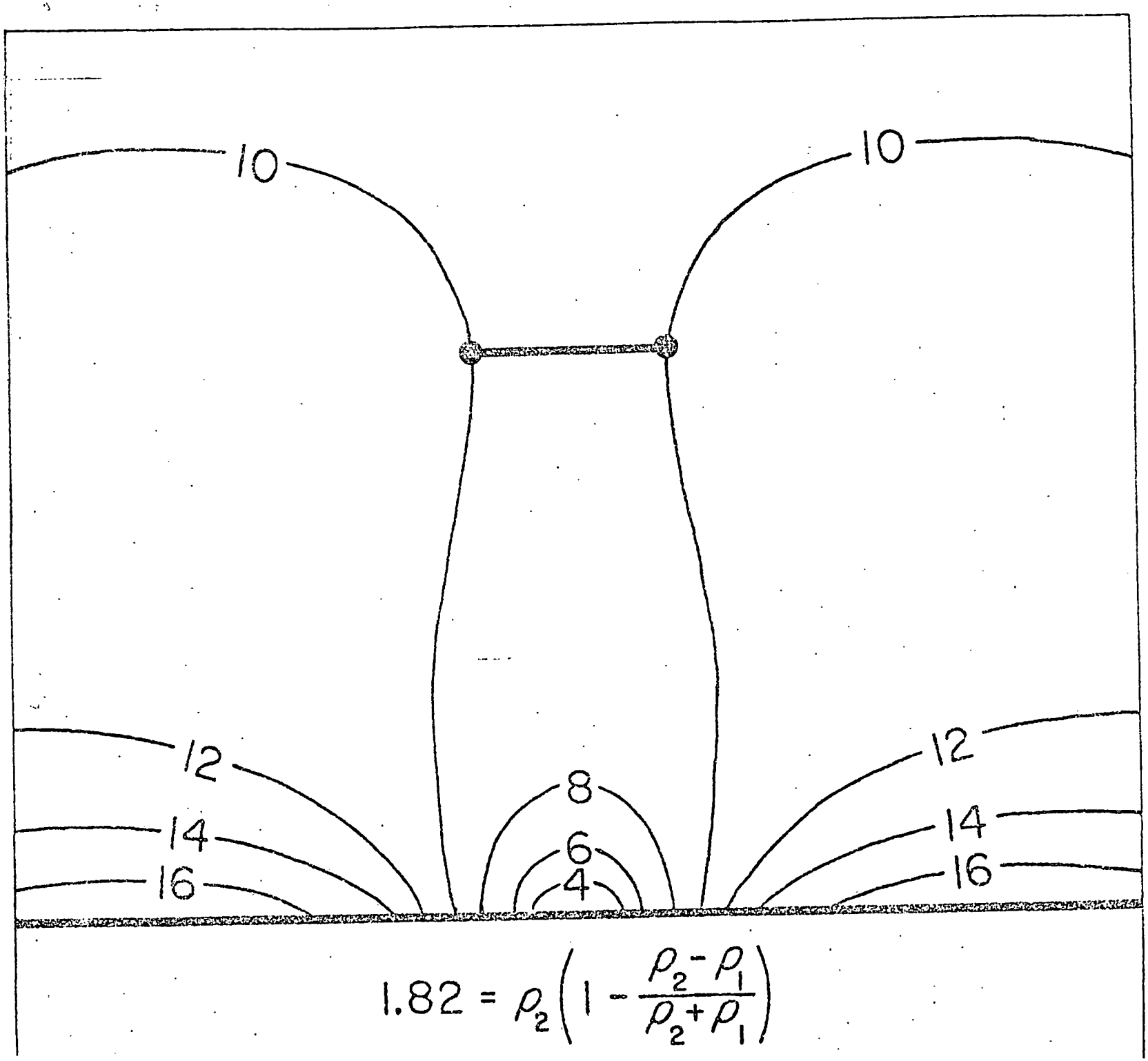

$\rho_1 = 10$

$$1.82 = \rho_2\left(1 - \frac{\rho_2 - \rho_1}{\rho_2 + \rho_1}\right)$$

$\rho_2 = 1$

Fig 2-D

$$\frac{1}{2}\left(\rho_{R,MAX} + \rho_{R,MIN}\right)$$

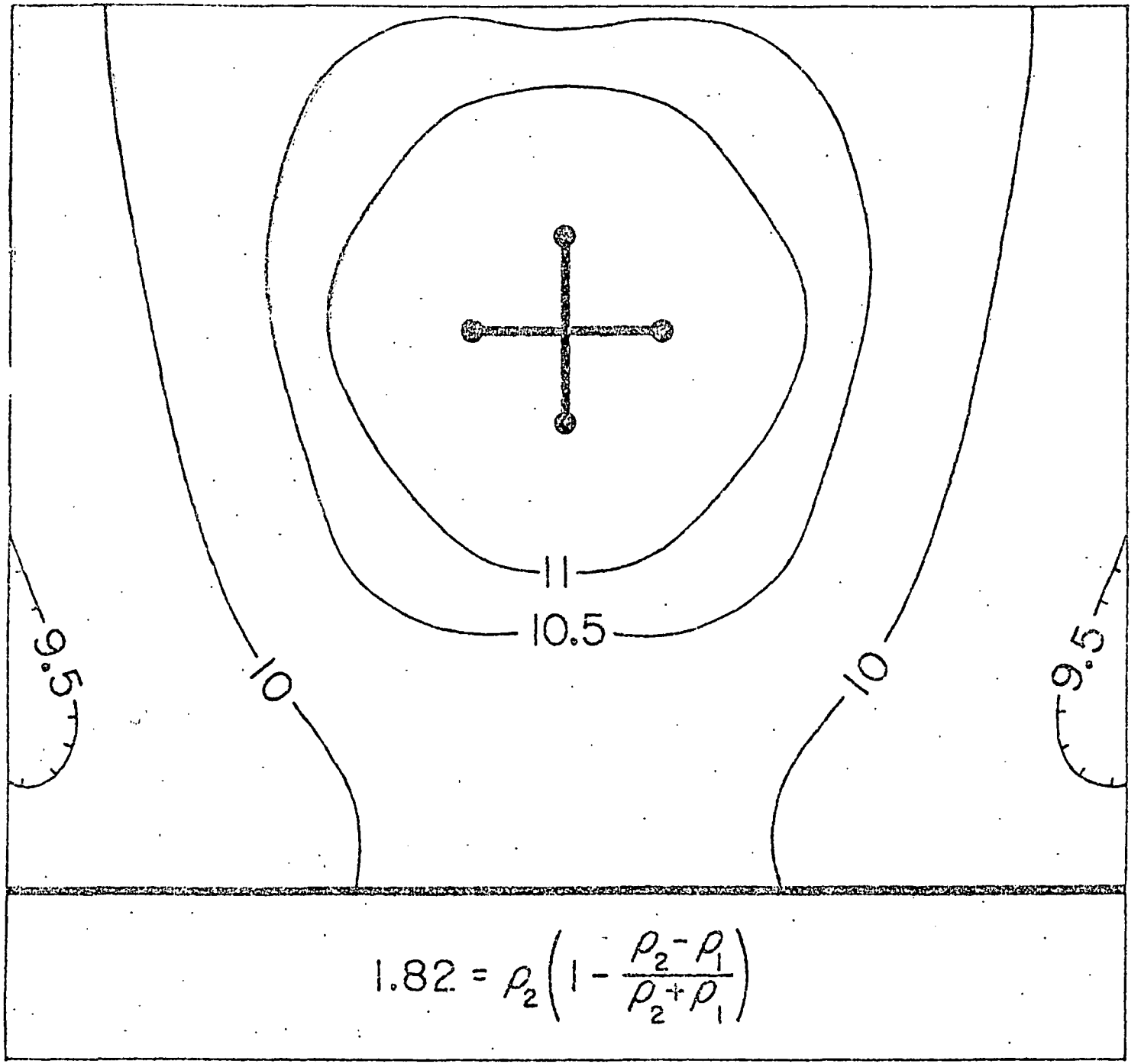

$\rho_1 = 10$

$$1.82 = \rho_2\left(1 - \frac{\rho_2 - \rho_1}{\rho_2 + \rho_1}\right)$$

$\rho_2 = 1$

FIG 7

$(\rho_{R,MAX}/\rho_{R,MIN})^2$

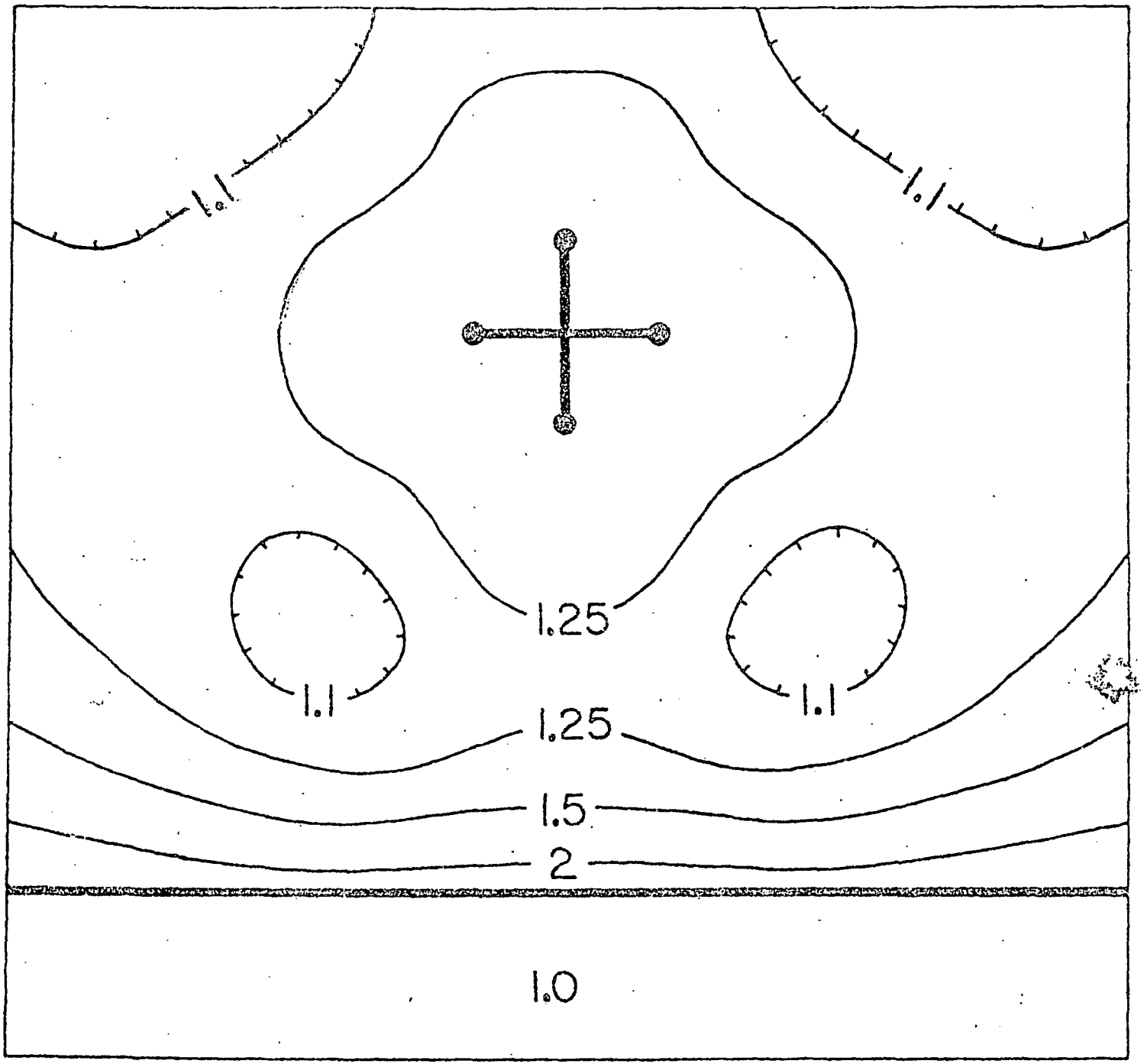

$\rho_1 = 10$

$\rho_2 = 1$

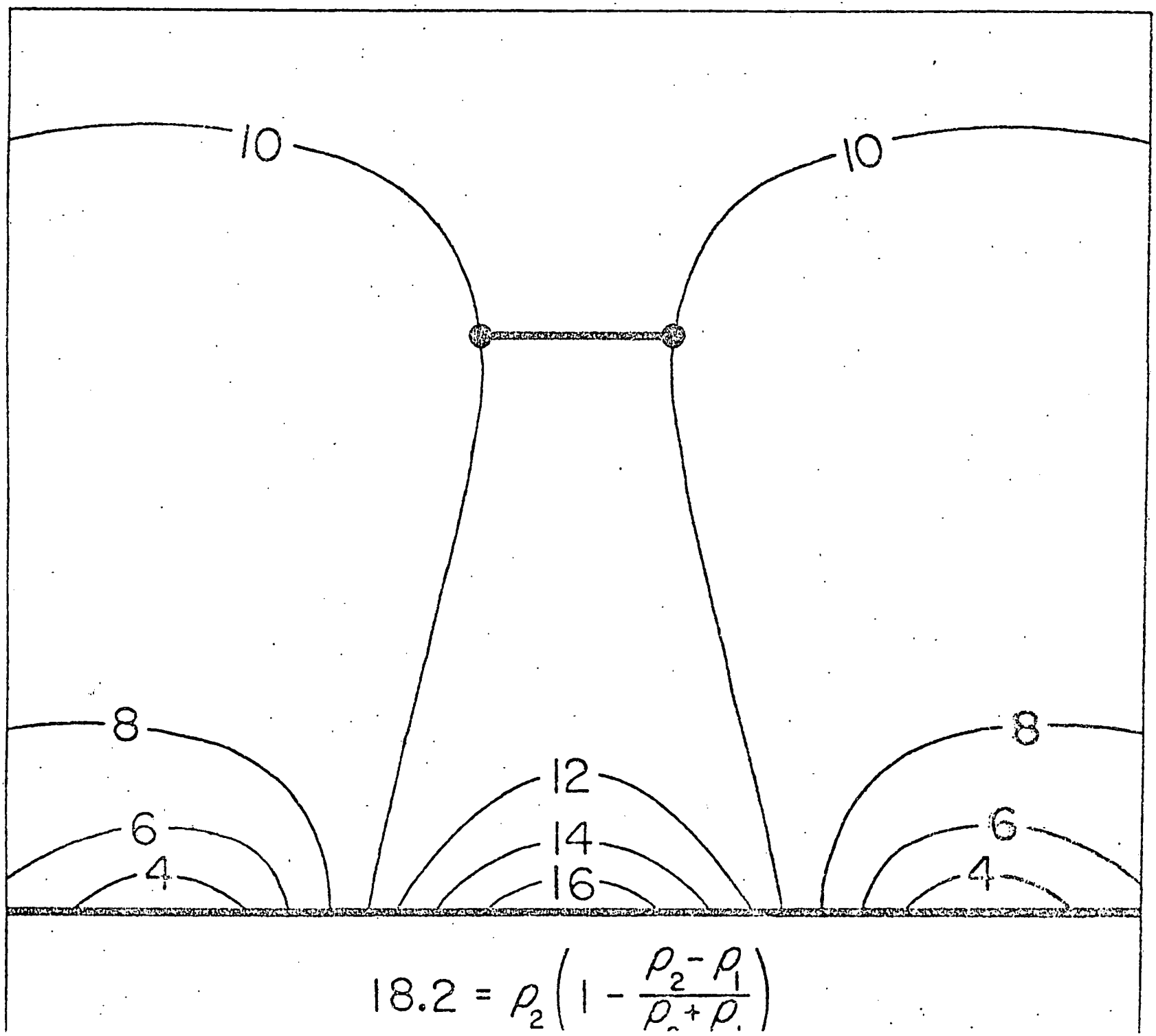

$\rho_1 = 10$

$\rho_2 = 100$

$$18.2 = \rho_2\left(1 - \frac{\rho_2 - \rho_1}{\rho_2 + \rho_1}\right)$$

FIG 3

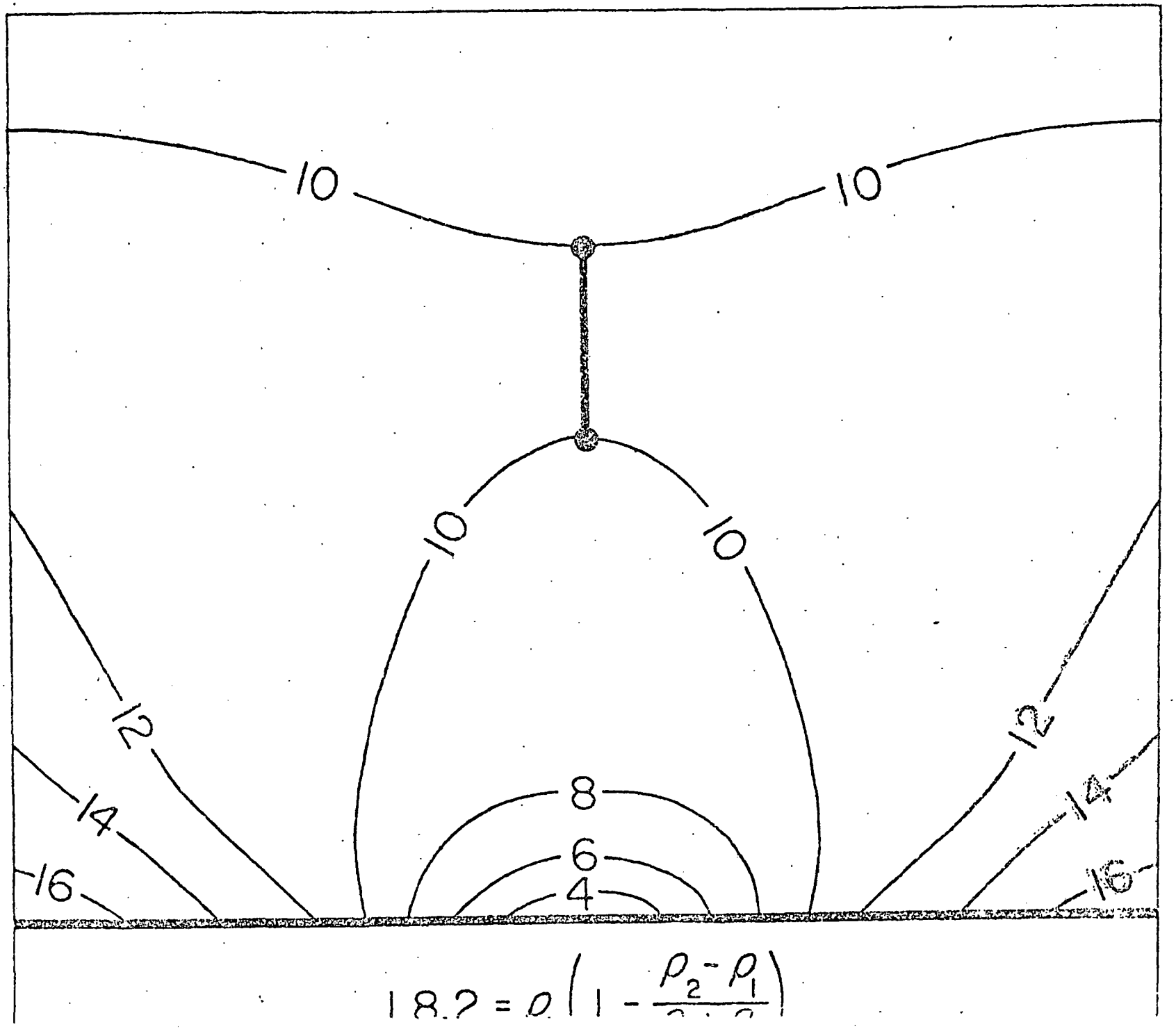

$\rho_1 = 10$

$$18.2 = \rho\left(1 - \frac{\rho_2 - \rho_1}{\quad}\right)$$

$\rho_2 = 100$

$$\frac{1}{2}\left(\rho_{R,MAX} + \rho_{R,MIN}\right)$$

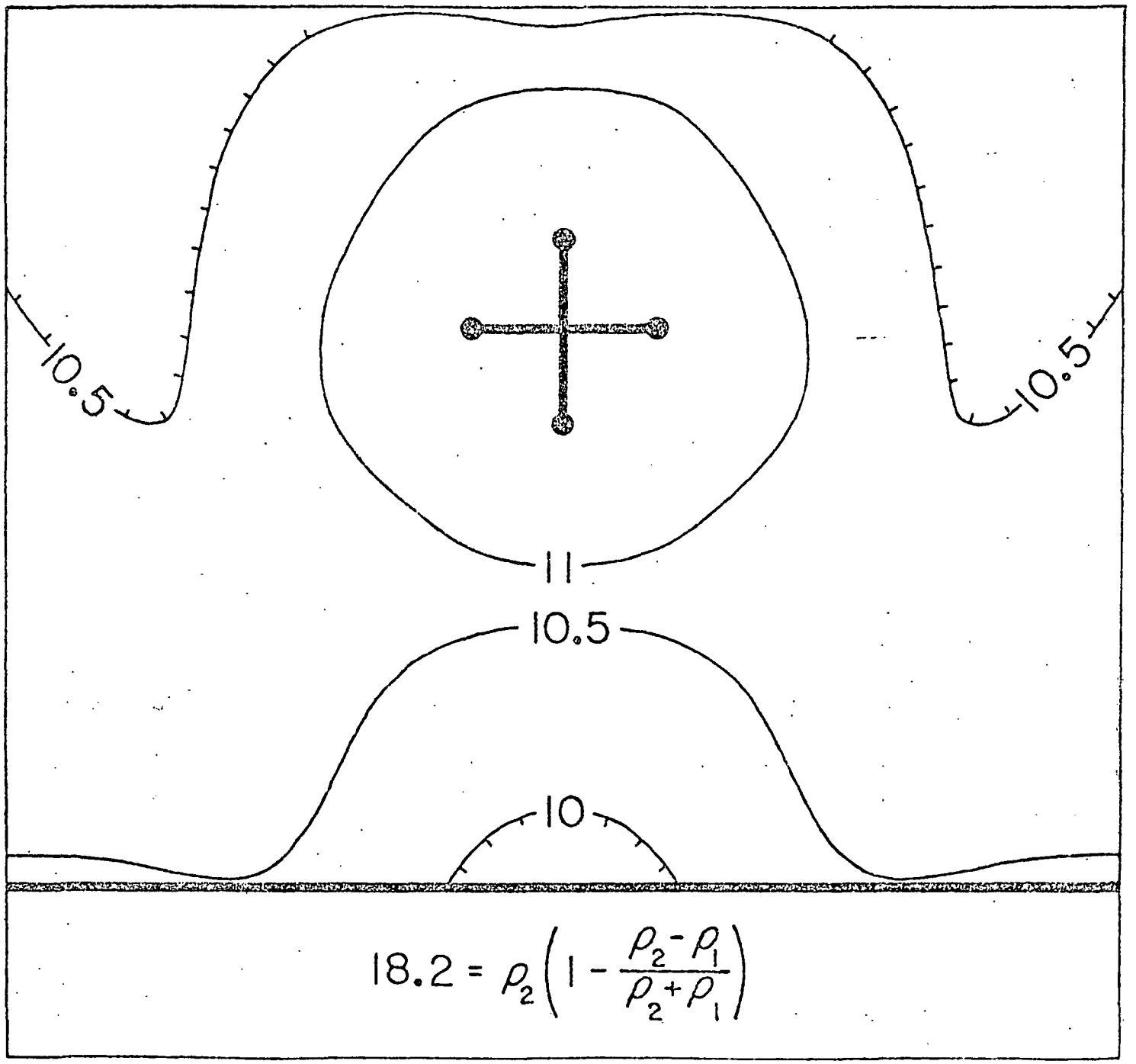

$\rho_1 = 10$

$\rho_2 = 100$

FIG 12

$\left(\rho_{R,MAX}/\rho_{R,MIN}\right)^{\frac{1}{2}}$

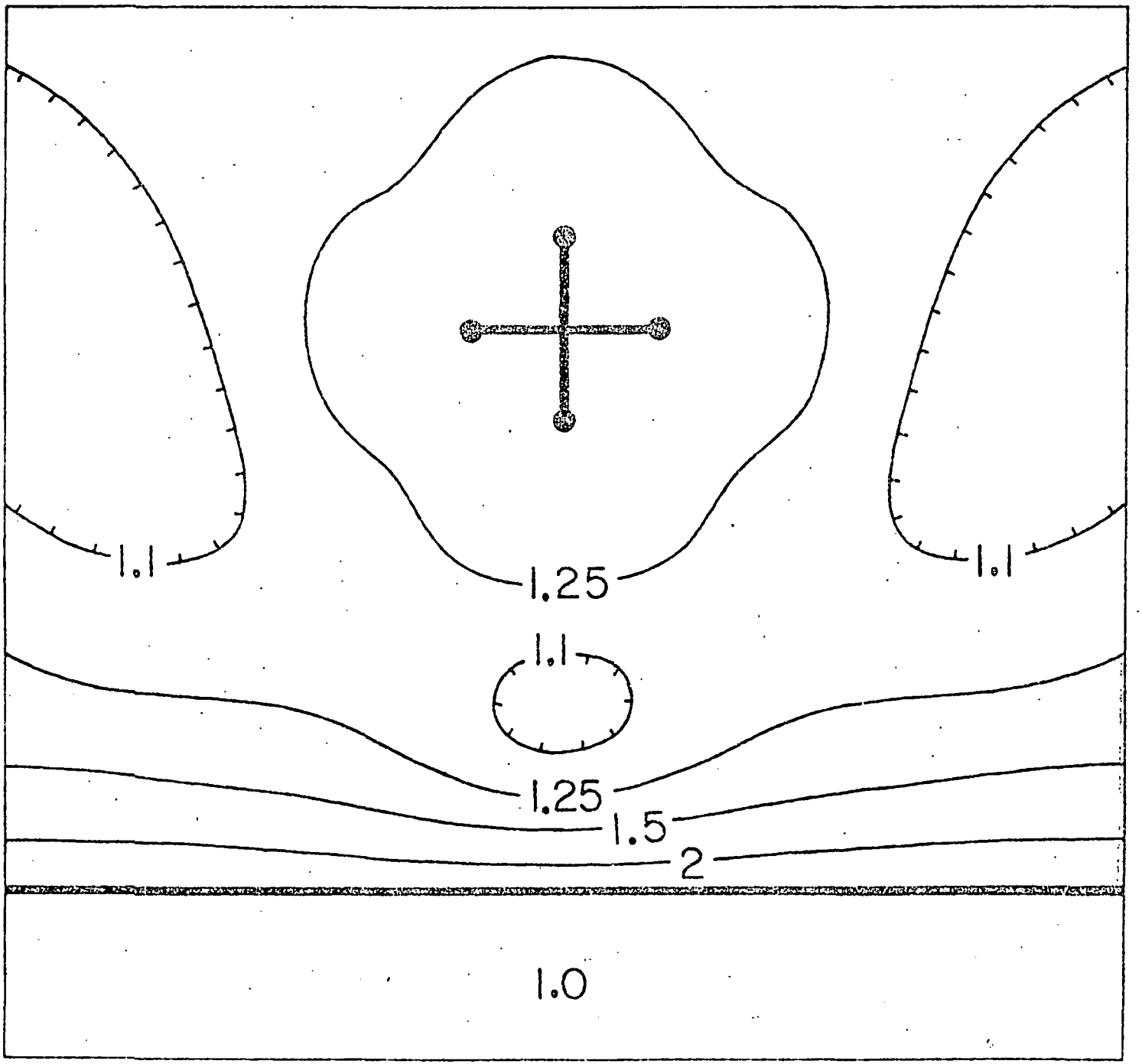

$\rho_1 = 10$

$\rho_2 = 100$

FIG-13

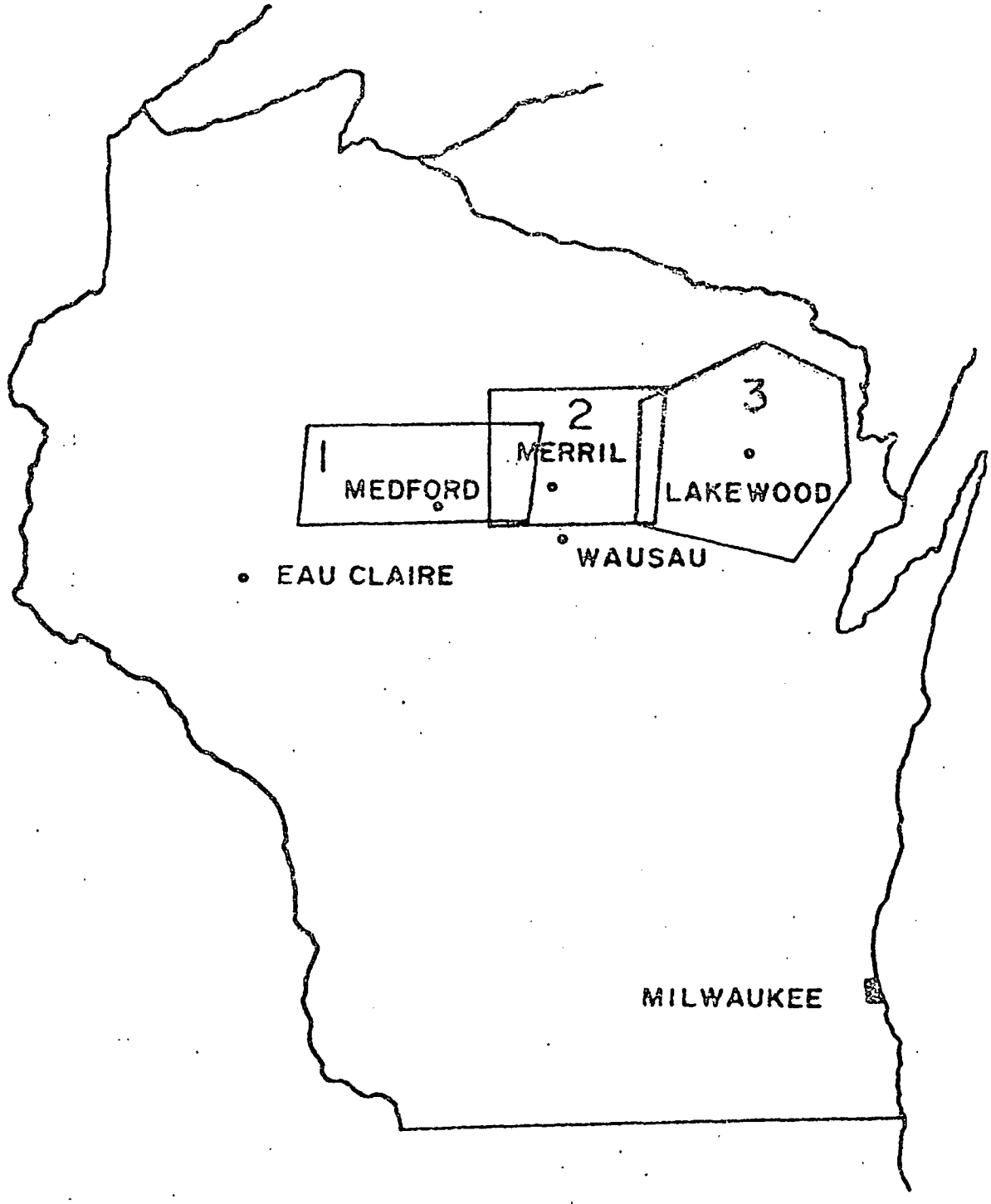

FIGURE 14

LOCATION MAP OF 3 SETS OF BIPOLE SOURCES SHOWING GENERAL EXTENT OF THE AREA MAPPED WITH EACH PAIR

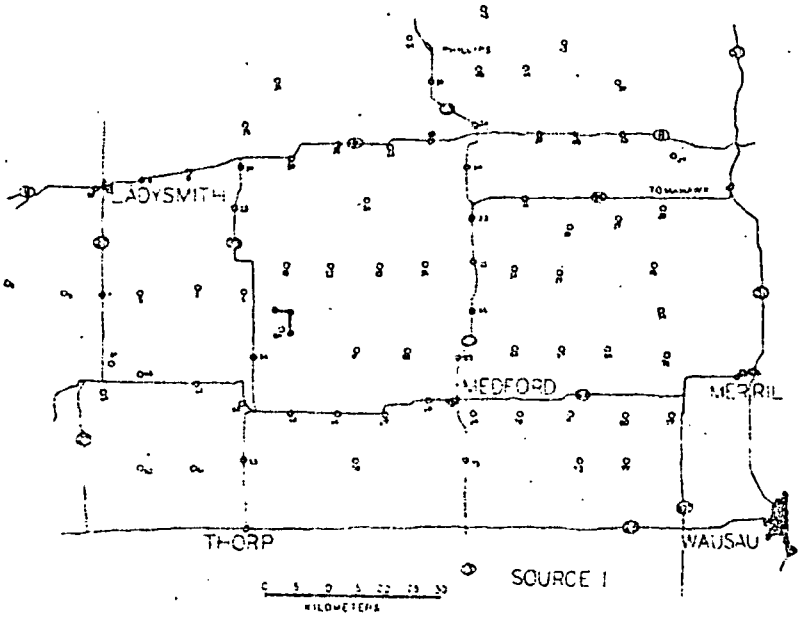
LADYSMITH
MEDFORD
MERRIL
THORP
WAUSAU
SOURCE 1
KILOMETERS

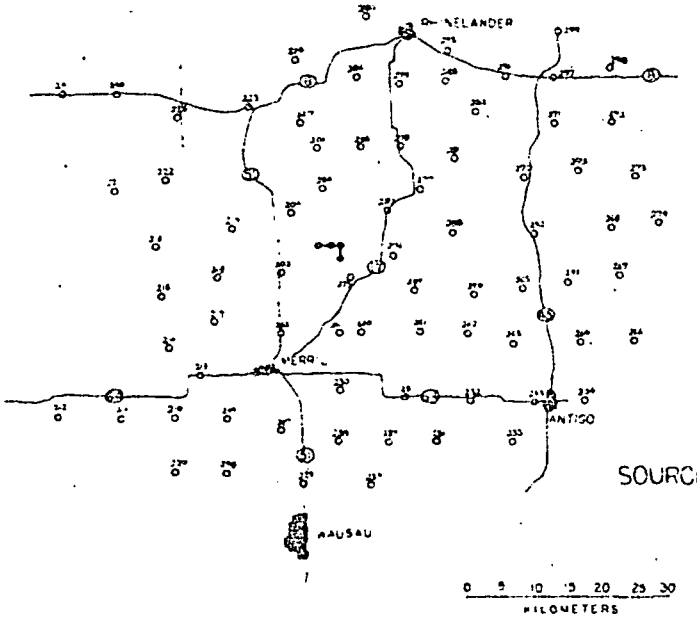
RHINELANDER
MERRILL
ANTIGO
WAUSAU
SOURCE 2
0 5 10 15 20 25 30
KILOMETERS

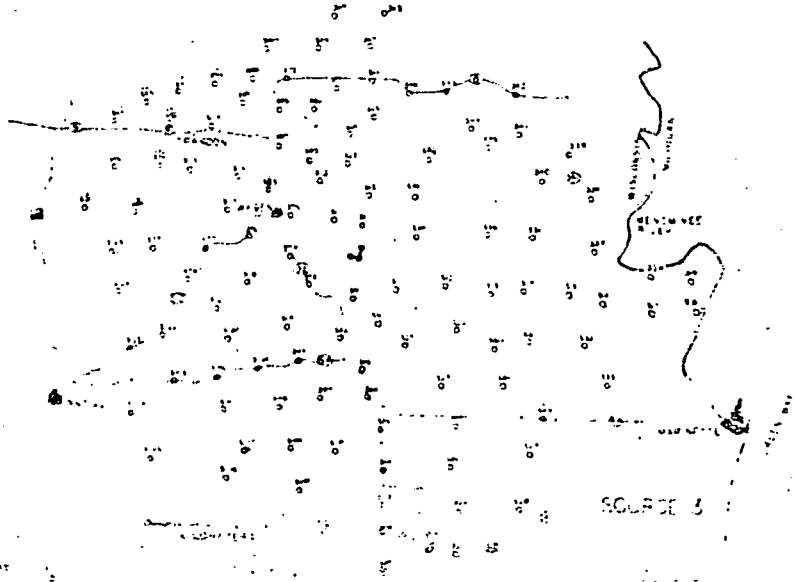
SOURCE 3

FIG 16

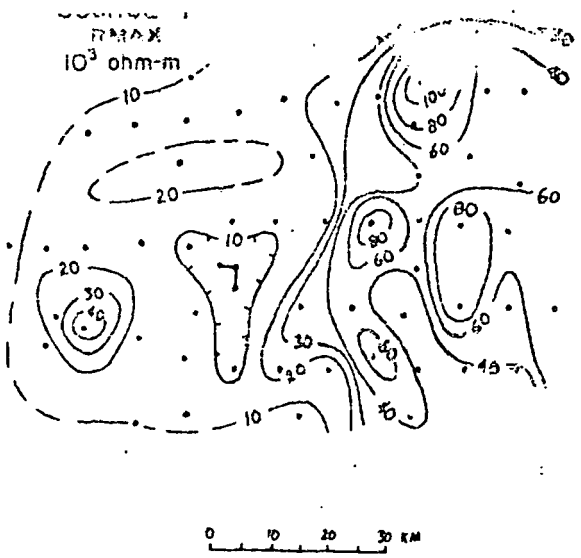
RMAX
10^3 ohm-m
0 10 20 30 KM

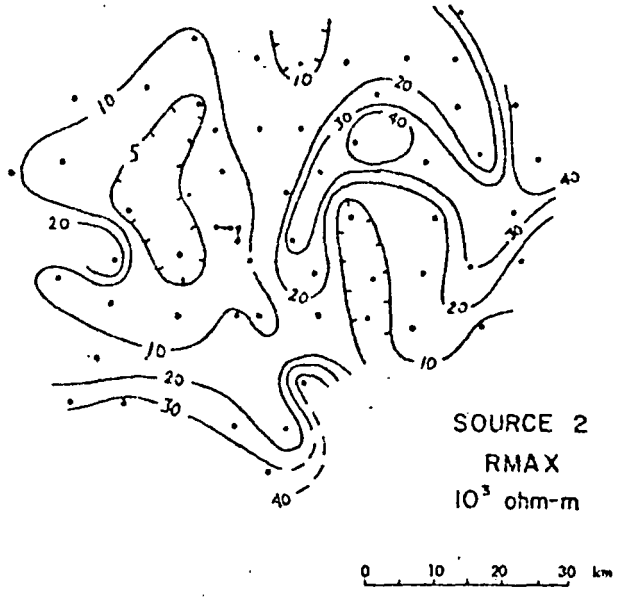
SOURCE 2
RMAX
10^3 ohm-m
0 10 20 30 km

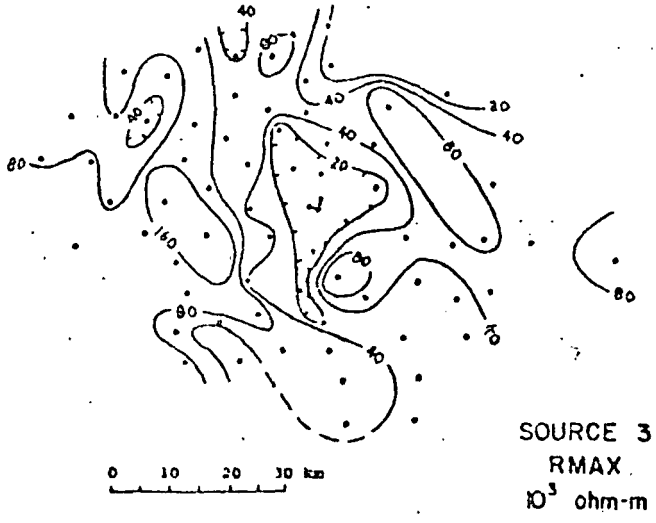
SOURCE 3
RMAX
10^3 ohm-m
0 10 20 30 km

FIG 17

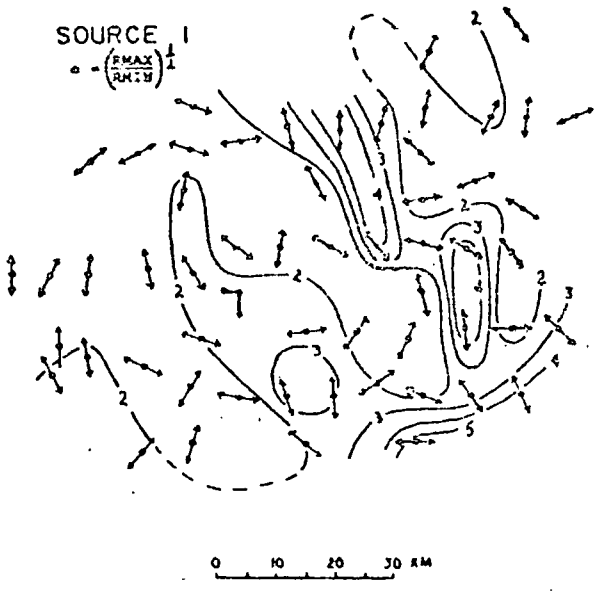
SOURCE 1
$\alpha = \left(\frac{RMAX}{RMIN}\right)^{\frac{1}{2}}$
0 10 20 30 KM

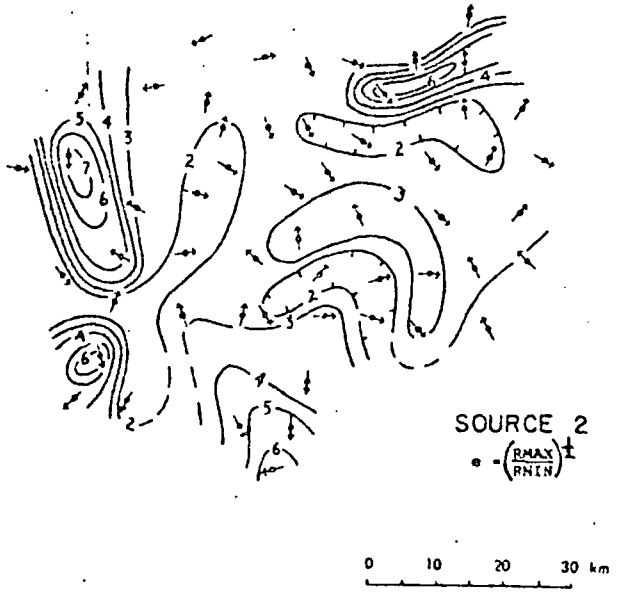
SOURCE 2
$\alpha = \left(\frac{RMAX}{RMIN}\right)^{\frac{1}{2}}$
0 10 20 30 km

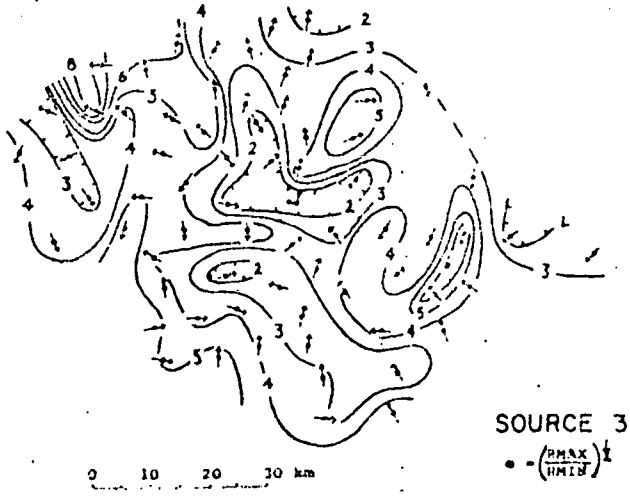
SOURCE 3
$\alpha = \left(\frac{RMAX}{RMIN}\right)^{\frac{1}{2}}$
0 10 20 30 km

FIG 15

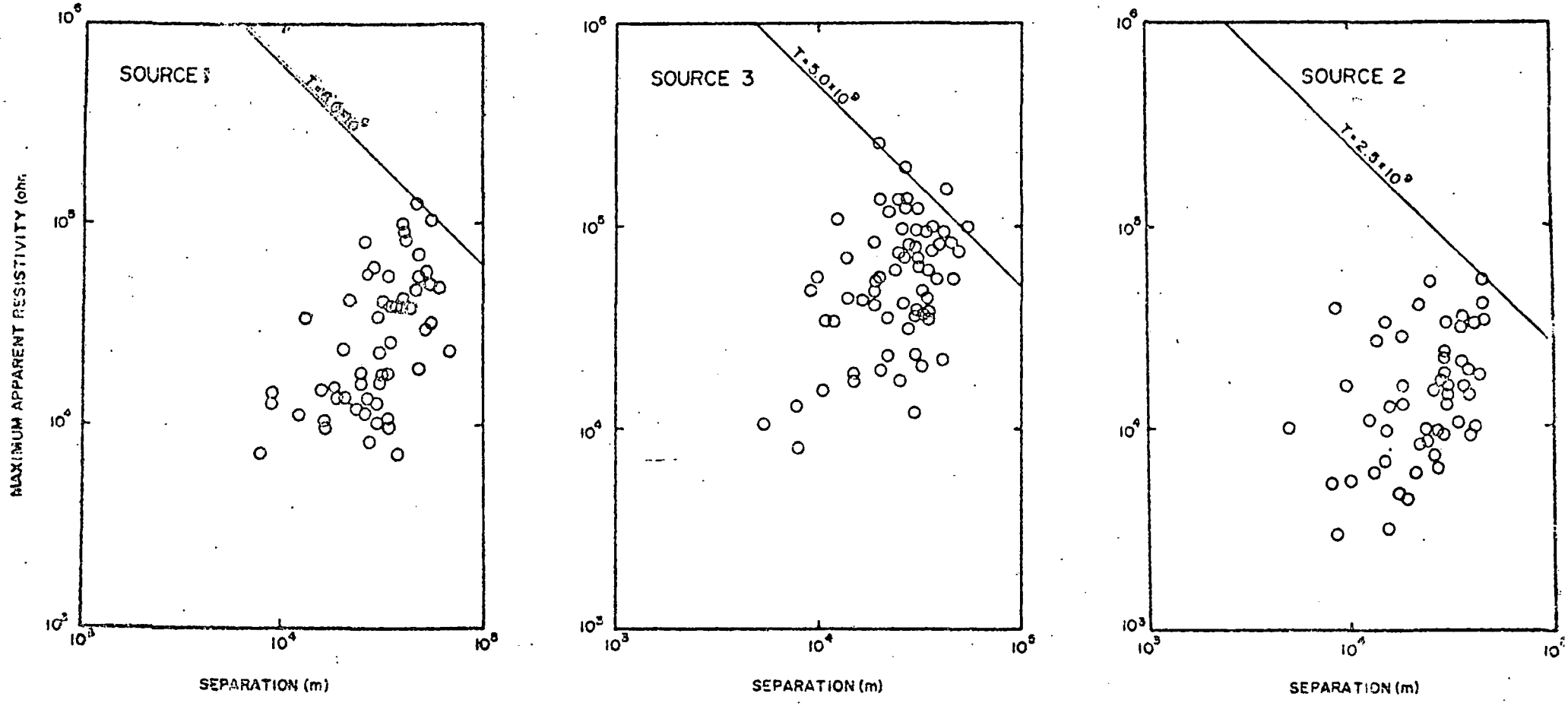
SOURCE 1
T=6.0×10⁸
SOURCE 3
T=5.0×10⁸
SOURCE 2
T=2.5×10⁸
MAXIMUM APPARENT RESISTIVITY (ohm
SEPARATION (m)
SEPARATION (m)
SEPARATION (m)

FIG-19

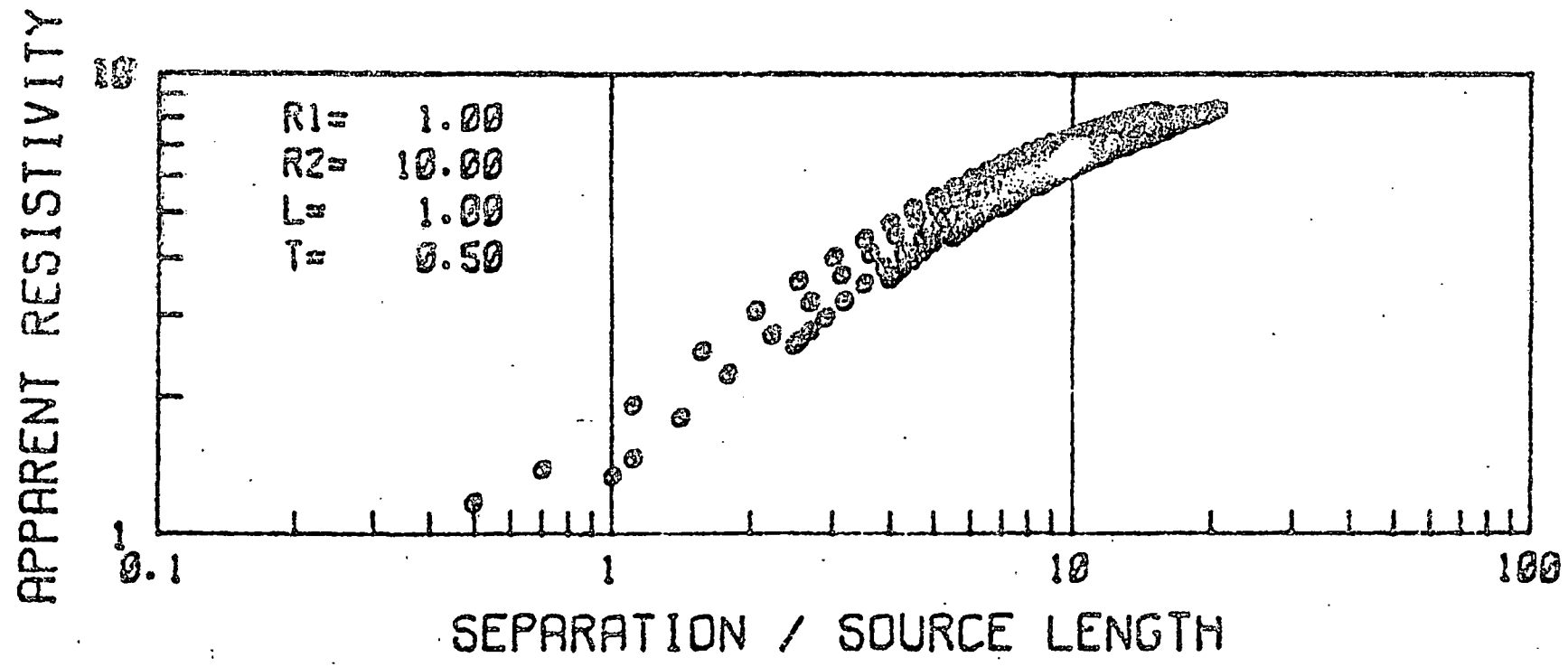

TWO HORIZONTAL LAYERS

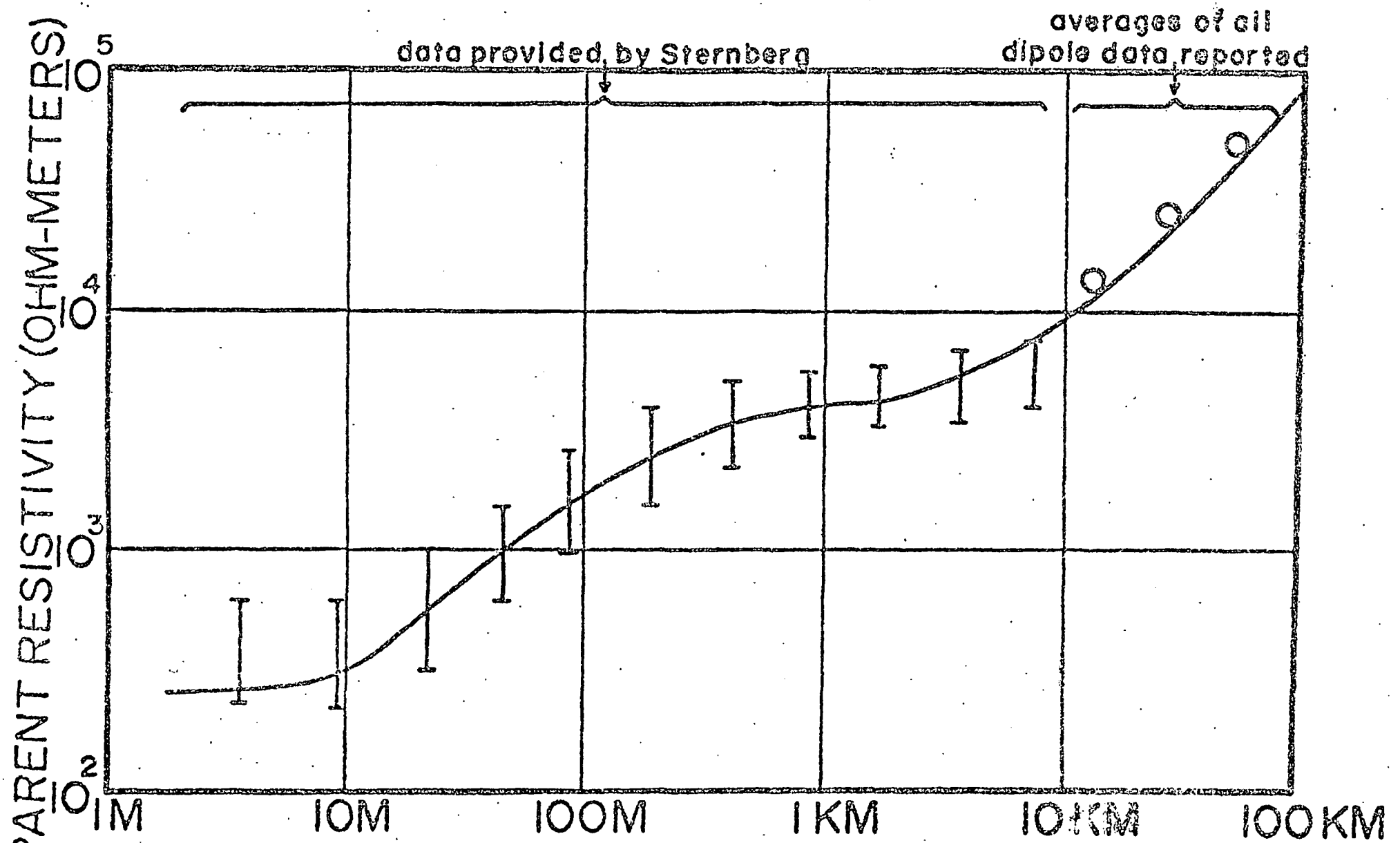
averages of all
dipole data reported
data provided by Sternberg
APPARENT RESISTIVITY (OHM-METERS)
10^5
10^4
10^3
10^2
1M
10M
100M
1KM
10KM
100KM
SPACING

FIGURE 7

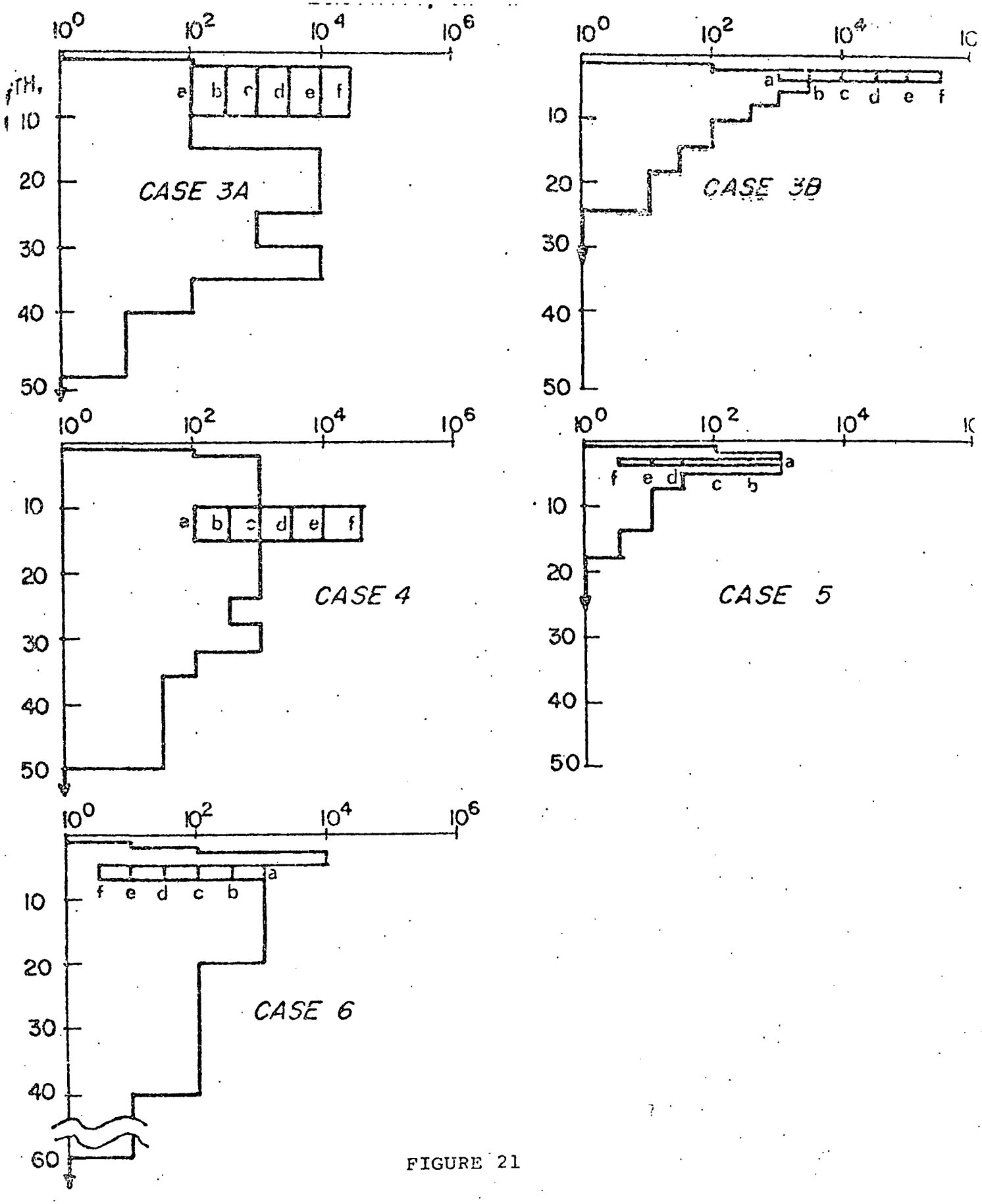
10^0
10^2
10^4
10^6
TH,
10
20
30
40
50
a b c d e f
CASE 3A
CASE 3B
CASE 4
CASE 5
CASE 6
f e d c b a

FIGURE 21

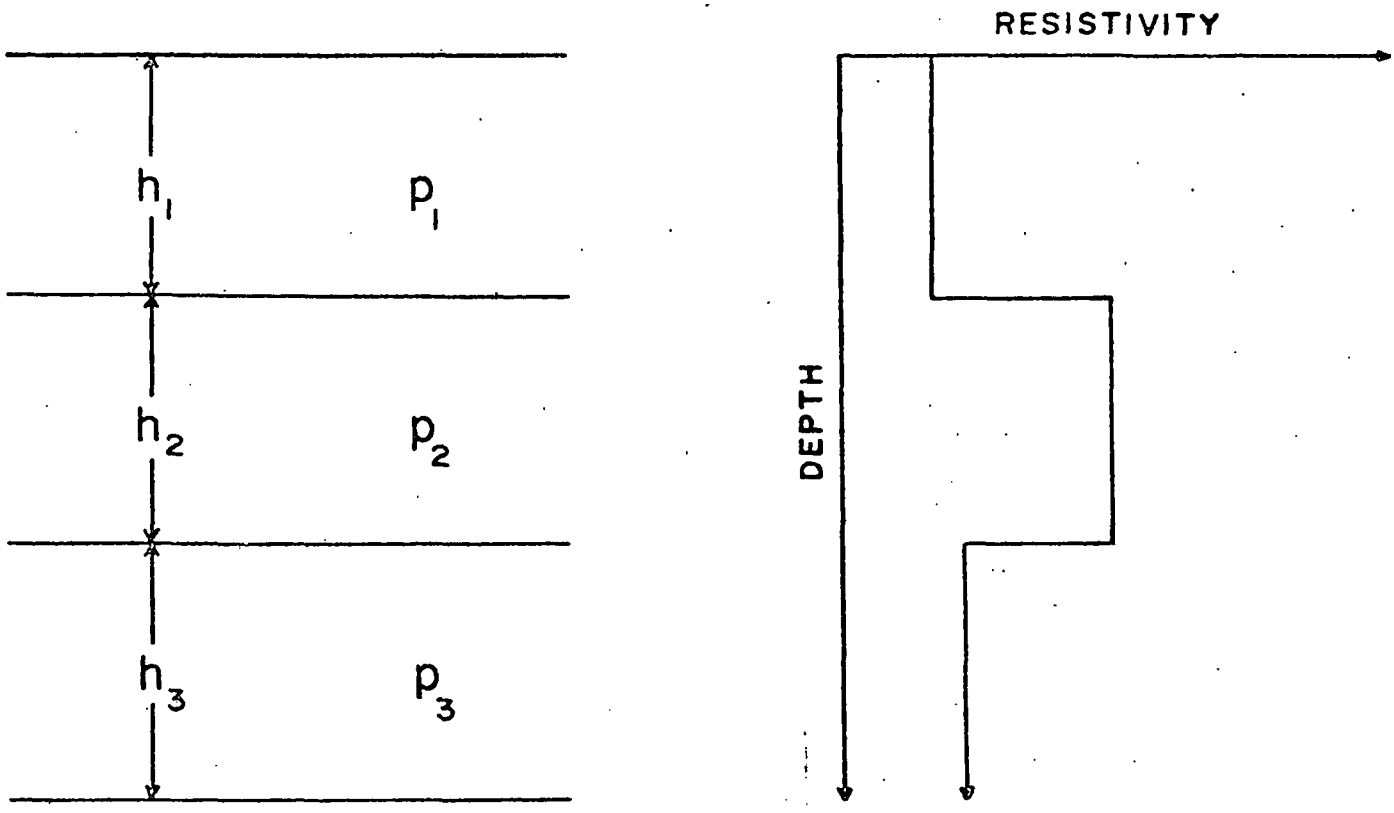

FIGURE 1

SIMPLIFIED CRUSTAL RESISTIVITY PROFILE

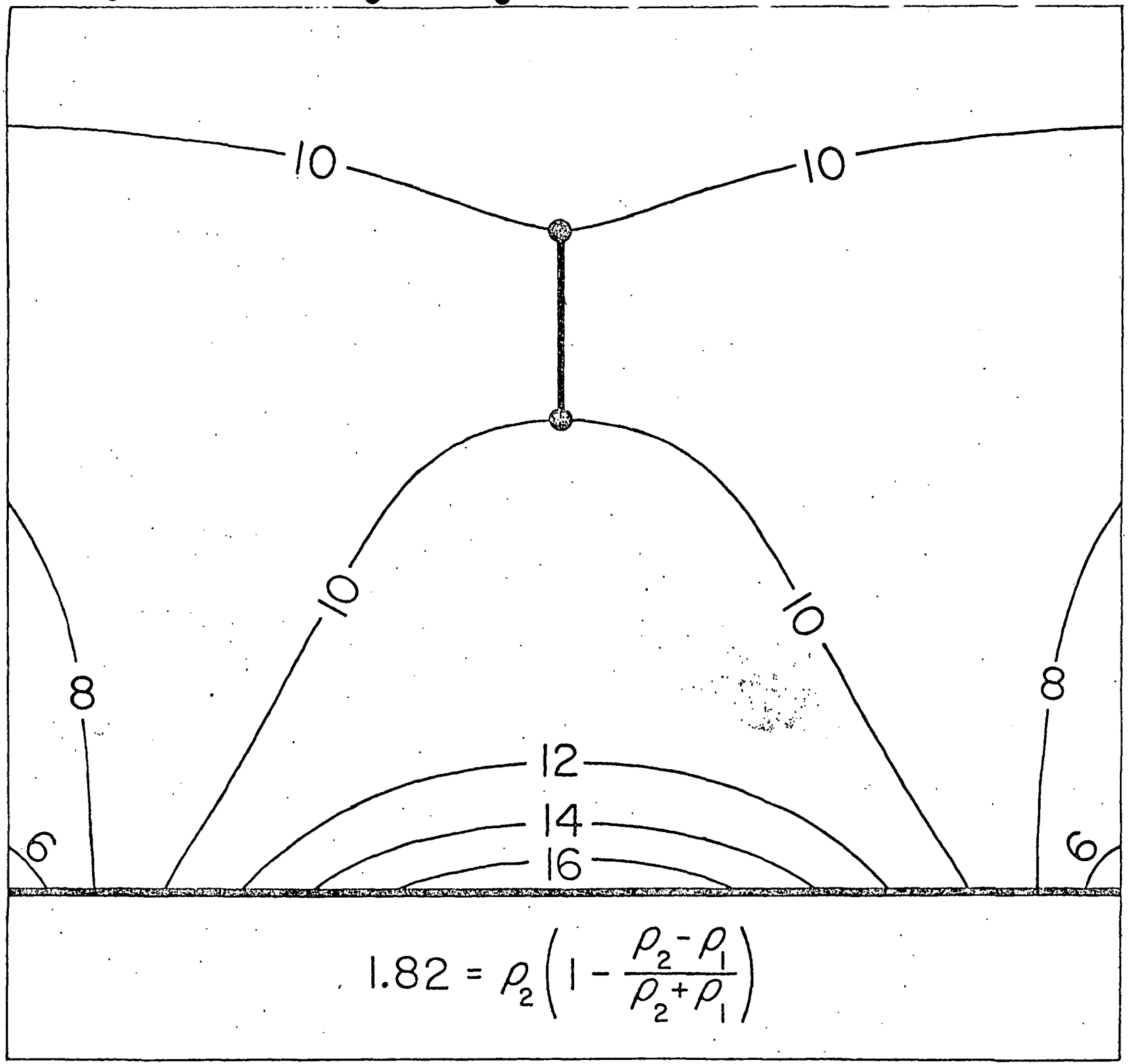
10
10
10
10
8
8
12
14
16
6
6
$\rho_1 = 10$
$\rho_2 = 1$
$1.82 = \rho_2\left(1 - \frac{\rho_2 - \rho_1}{\rho_2 + \rho_1}\right)$

FIG 6

7/E

APPENDIX III

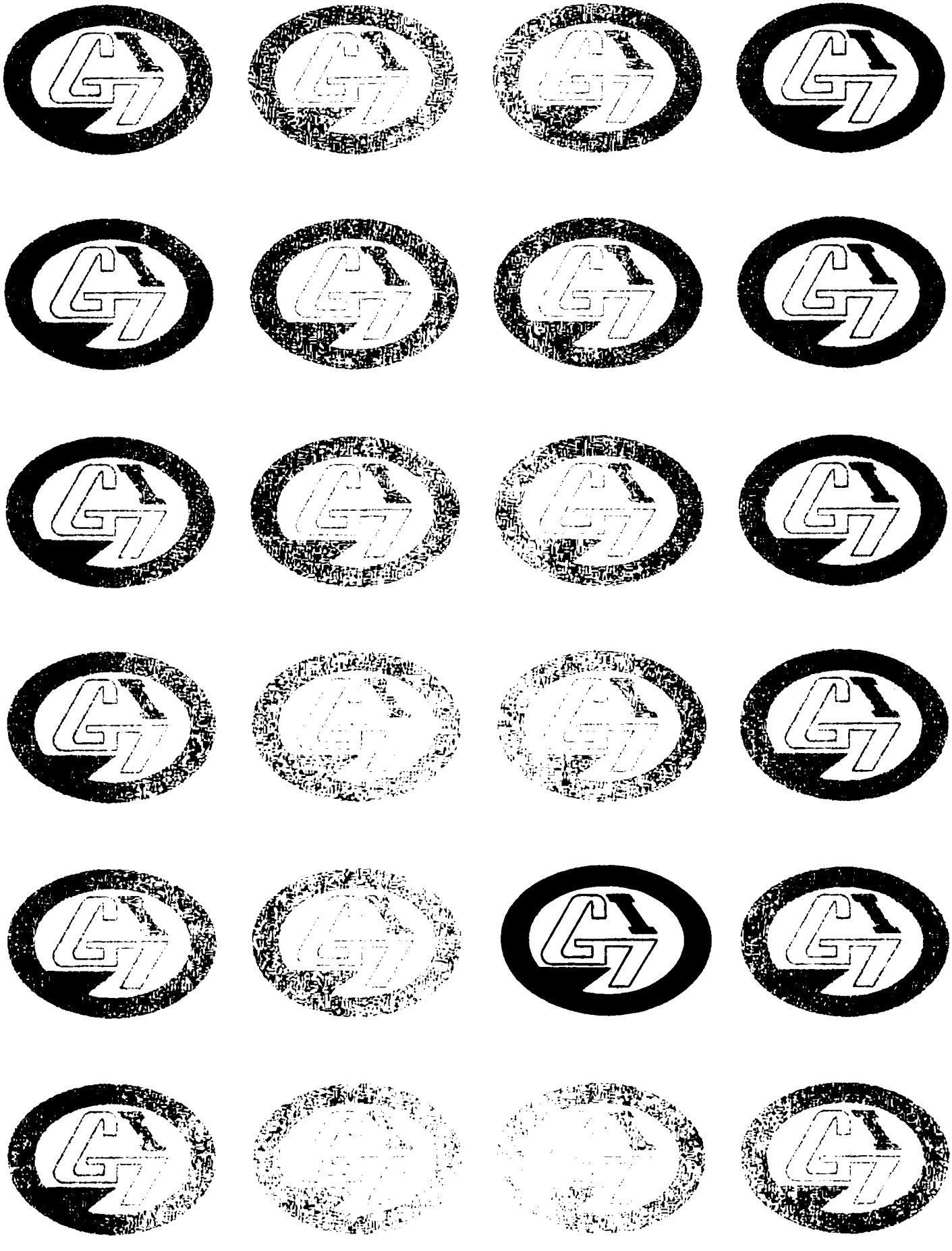

APPENDIX III

PROPOSAL EY-R-08-007

to

ENERGY RESEARCH AND DEVELOPMENT ADMINISTRATION

from

GROUP SEVEN, INC.

1301 Arapahoe Street

Golden, Colorado 80401

TIME DOMAIN ELECTROMAGNETIC SOUNDING

BY

George V. Keller, Catherine K. Skokan,
Robert A. Crewdson, and Jeffrey J. Daniels

Abstract

Time domain electromagnetic sounding is one of a group of electrical prospecting methods which are capable of producing information about the electrical properties of rocks at depths of several kilometers or more in the earth. In the method, an electromagnetic field is generated by passing current steps through a short grounded wire source. The transient magnetic field accompanying this step is recorded at a receiver station. The way in which the transient field changes with time can be interpreted in terms of the electrical structure of the earth. The method is being applied extensively in exploration for geothermal reservoirs, because the elevated temperatures in such systems often reduce resistivity by significant amounts. This experience has shown that time-domain electromagnetic sounding has at least one important advantage over other electrical sounding methods. The time-domain electromagnetic method provides different responses for currents induced beneath the receiver and those induced laterally away from the receiver. As a consequence, in interpretation, there is little risk in confusing a lateral change in resistivity for a layer at depth.

TIME DOMAIN ELECTROMAGNETIC SOUNDING

by

George V. Keller, Catherine K. Skokan, Robert A. Crewdson, and Jeffrey J. Daniels

Introduction

Time-domain electromagnetic sounding is one of a group of electrical prospecting methods which are capable of producing information about the electrical properties of rocks at depths of several kilometers or more in the earth. Other, perhaps better known, methods for deep electrical sounding include the expanding-array direct-current method and the magneto-telluric method. In the method to be discussed in this paper, a pulse-like magnetic field is generated, and the transient decay of induction currents in the earth is observed; hence, the name TDEM (Time-Domain Electromagnetic method).

Initially, interest in developing a deep penetration electromagnetic method stemmed from the possibility that such a technique would be valuable in exploration for oil and gas (Vanyan, 1967). It is well known that porous rocks saturated with oil and gas are considerably more resistive than similar rocks which carry only water in their pores. If an electrical sounding method were sensitive enough to detect this contrast in resistivity, electrical surveys could provide a direct means for locating oil and gas (Keller, 1967). Unfortunately, neither the direct-current

sounding method nor the magnetotelluric method provide enough accuracy to permit detection of oil or gas zones at reasonable depths. Early work by Russian geophysicists (Vanyan, 1967) indicated that electromagnetic soundings can be carried out with better accuracy than other electrical soundings, offering the hope that direct detection of hydrocarbons might be possible.

An application of deep electrical sounding which has developed in recent years and which accounts for much of the use of the TDEM method today is the search for and evaluation of geothermal reservoirs. Heating of the rocks in a geothermal reservoir reduces their resistivity markedly, by factors of 5 to 10. As a result, geothermal reservoirs have unusually low resistivities; most geothermal systems have resistivities below 10 ohm-meters, and many have resistivities of only 1 to 3 ohm-meters (Meidav and Tonani, 1976). Because of the low resistivity and great depth extent of geothermal reservoirs, it is often difficult to use direct-current sounding methods successfully, and electromagnetic methods can be more effective in obtaining information from great depth (Keller, 1969; 1970).

The TDEM technique is reasonably well developed at the present time, both with respect to theory and practice. The following sections of this paper will first describe the theoretical basis for TDEM sounding, followed by a discussion of field practice and the interpretation of TDEM surveys.

Theory of TDEM Soundings

The geometry fo the transmitter and receiver used in TDEM sounding is shown in Figure 1. An electromagnetic field is generated by passing current steps through a short grounded wire. At some distance R from the center of this source wire, the time-rate of change of the vertical component of the magnetic field is detected and measured. Other source-receiver combinations might be used in electromagnetic sounding, but experience to date suggests that the use of a grounded wire source and a vertical component magnetic receiver is preferred. Keller and Rapolla (1976) describe experiments in which a vertical axis loop is compared with a grounded wire as a source for the electromagnetic field. Results indicated that greater depth of penetration can be obtained using the grounded wire source than the loop source, except in rare cases. Ofrey (1975) described experiments in which three components of magnetic induction from a grounded wire source were recorded. Only the vertical component could be readily interpreted in terms of earth resistivity. Because of these and similar experiences, I will only consider the use of a short grounded wire as a source and a vertical-component magnetic detector as a receiver in this paper.

The theory for electromagnetic field behavior over a horizontally stratified earth is well developed in the literature (Vanyan, 1967; Wait, 1962). For the geophysical case, in the solution of Maxwell's equations, displacement currents are neglected, and the solution which is obtained is termed a

quasi-static solution. For a short grounded wire source which can be approximated as a current dipole (its effect can be expressed in tarms of the product of current flowing in the wire and the length of the wire), and using Wait's approach (1966) as modified by Daniels (1974), the vertical component of the magnetic field is

$$H_z = \frac{I ds}{4\pi} \sin\theta \int_0^\infty \lambda \left(1 + R_1(\lambda)\right) J_1(\lambda r)\, d\lambda \qquad \ldots 1$$

The symbols used in eq (1) are defined as follows:

I ds is the current moment of the dipole source,

θ is the angle between the axis of the dipole source and the radius from the center of the source to the point where the magnetic field is being observed (see the sketch in figure 1),

λ is the separation constant introduced in the solution of Maxwell's equations by the method of separation of variables (it enters only as a dummy variable and no special values need be assigned), and

J_1 is Bessel's function of the first kind of order 1.

$R_1(\lambda)$ is a correction factor which takes the effect of layering in the earth on the electromagnetic field behavior into account. This quantity is obtained by evaluating a recursive expression:

$$R_1(\lambda) = \frac{N_0 - Y_1}{N_0 + Y_1} \qquad \ldots 2$$

where

$$N_0 = \frac{\lambda}{i\mu_0\omega}$$

and

$$Y_n = N_n \frac{Y_{n+1} + N_n \tanh(u_n h_n)}{N_n + Y_{n+1} \tanh(u_n h_n)}$$

where

$$N_n = \frac{u_n}{i\mu_0\omega} \; ; \quad Y_N = \frac{u_N}{i\mu_0\omega} \; ; \quad n = 1, 2, \cdots N$$

Each of the layers is characterized by a conductivity, σ_n, and a thickness, h_n. The wave number for each layer, γ_n, is given by

$$\gamma_n = (i\mu_0 \omega \sigma_n)^{1/2}$$

and the modified wave number, u_n, by

$$u_n^2 = \lambda^2 + \gamma_n^2$$

where ω is the radian frequency.

The Hankel transform integral in eq (1) can be evaluated readily only in the case of a uniform earth (Wait, 1966; Vanyan, 1967; Keller and Frischknecht, 1966; Keller, 1967). This solution, in the frequency domain, is:

$$H_z = \frac{Ids}{2\pi\omega\mu_0\sigma r^4}\left[3 - (3 + 3\gamma r + \gamma^2 r^2)e^{-\gamma r}\right] \quad \ldots 3$$

Equation (3) can be evaluated numerically in the frequency domain and then transformed numerically to the time domain. A set of time-domain curves for a completely uniform earth is shown in Figure 2; the spacing between source and receiver is 7.5 kilometers in each case, but the resistivity of the earth was taken to be 0.5 to 50 ohm-meters to generate the various curves. These calculations show some of the more important features of the behavior of TDEM sounding curves. It is clearly seen tat as the earth becomes more conductive, the transient magnetic field is lower in amplitude and persists for a longer period of time. With an earth resistivity of 50 ohm-meters, the magnetic field at a distance of 7.5 kilometers begins to decay rapidly after only 200 milliseconds, but with an earth resistivity of 0.5 ohm-meters, the magnetic field persists for 10 seconds before it begins to decay rapidly.

The duration of the transient magnetic field also depends on the separation between the source dipole and the receiver. A set of curves is shown in Figure 3 for measurements made over a uniform earth with a resistivity of 3 ohm-meters, but with the separation between source and receiver ranging from 2 to 10 kilometers. As may be seen from these curves, at a separation of 2 kilometers, the transient magnetic field begins to decay after only 100 milliseconds, but at 10 kilometers distance, the field persists for about 3 seconds.

It is not particularly convenient to discuss electromagnetic coupling in terms of units of magnetic field intensity per source moment strength. To avoid this, a method for defining apparent resistivity is necessary. Apparent resistivity is defined as being the resistivity of a uniform earth which yields the same field strengths as are actually measured in a real, usually heterogeneous earth. With direct-current measurements, there always is some fictitious uniform earth which will give the field strengths observed in field measurements. However, with electromagnetic coupling measurements, it is possible to observe field strengths over a heterogeneous earth which cannot be measured over any uniform earth. Because of this, there is no general definition for apparent resistivity for electromagnetic sounding methods; instead, definitions valid over some restricted range of variables must be selected.

One definition of apparent resistivity for electromagnetic coupling measurements proposed originally by Vanyan (1967) is based on the early behavior of the transient magnetic field.

This definition is based on the detection of the vertical component of magnetic field strength by using a vertical-axis induction coil with an effective area, A. The voltage generated in the coil by the time-varying magnetic field described by equation 3 is:

$$V(\omega) = \frac{-AIds}{2\pi\sigma r^4}\left[3-(3+3\gamma r+\gamma^2 r^2)e^{-\gamma r}\right] \quad \ldots 4$$

Initial and final values of Fourier transform pairs are uniquely related, so that by finding the limit to the expression in (4) for high frequencies, the limit for small times in the time domain is also determined. Letting frequency tend to be infinite in equation (4) leads to the result:

$$\lim_{\omega\to\infty} V(\omega) = \frac{-3AIds}{2\pi\sigma r^4}$$

Apparent resistivity can be defined by inverting this last equation:

$$\rho_a = \frac{2\pi r^4}{3Ads}\,\frac{V}{I} = K_g\frac{V}{I} \quad \ldots 5$$

The geometric factor, $K_g = 2\pi r^4/3A\,ds$ is applicable both in the time-domain and in the frequency domain. Because of the way in which the voltage scales on Figures 2 and 3 were normalized, these scales are numerically equal to the apparent resistivity as defined by eq. (5).

It may be seen that the use of the geometric factor defined above leads to apparent resistivity values which are correct for the earth only during the early part of the transient coupling. It can be shown that the condition which must be satisfied in order that the apparent resistivity computed

using equation (5) be an accurate characterization of the earth is:

$$\frac{t}{\mu\sigma r^2} \lesssim \frac{1}{3} \qquad \ldots 6$$

An expression for the magnetic coupling in the time domain, valid at large times, can be found by expanding the frequency-domain expression in eq (1) in its low frequency limit and applying the Fourier transform. Replacing the exponential function in eq (6) by the first eight terms of its series expansion, we have:

$$V(\omega) = \frac{-AIds}{2\pi\sigma r^4}\left(\frac{1}{2}\gamma^2 r^2 - \frac{1}{8}\gamma^4 r^4 + \frac{1}{15}\gamma^5 r^5 - \frac{1}{48}\gamma^6 r^6 + \frac{1}{210}\gamma^7 r^7\right) \qquad \ldots 7$$

The inverse Fourier transform of this equation would give the time-domain response for impulse excitation. The response for step-like excitation is found by dividing this function by $-i\omega$:

$$\frac{V(\omega)}{-i\omega} = \frac{-iAIds}{2\pi\omega\sigma r^4}\left(\frac{1}{2}\gamma^2 r^2 - \frac{1}{8}\gamma^4 r^4 + \frac{1}{15}\gamma^5 r^5 - \frac{1}{48}\gamma^6 r^6 + \frac{1}{210}\gamma^7 r^7\right) \qquad \ldots 8$$

Of these terms, only those containing odd powers in γ provide a time function which is non-zero at positive times. So, for our purposes, we can write the spectrum of the voltage in the receiving coil as:

$$\frac{V(\omega)}{-i\omega} = \frac{-iAIds}{2\pi\omega\sigma r^4}\left(\frac{1}{15}\gamma^5 r^5 + \frac{1}{210}\gamma^7 r^7 + Q\right) \qquad \ldots 9$$

where Q is a remainder term which does not contribute anything of interest in the time domain.

In defining an expression for apparent resistivity valid at large times (late time), it can be assumed that the second term in eq (9) is negligible compared to the first:

$$\frac{V(\omega)}{-i\omega} \cong \frac{-iAIds\,\mu_o^{5/2}\sigma^{3/2}r}{30\pi\sqrt{2}}\left(\omega^{3/2}+i\omega^{3/2}\right) \qquad \ldots 10$$

From the physical reality of the problem, we can state that the transient voltage prior to the instant of the step excitation is identically zero. Therefore, in carrying out the inverse transform of the spectrum, the unilateral cosine transform of the real part of the spectrum can be used instead of the bilateral exponential transform:

$$V(t) = \frac{2}{\pi}\int_0^{\infty} \text{Real}\left\{\frac{V(\omega)}{-i\omega}\right\}\cos\omega t\, d\omega = \frac{AIds\,\mu_o^{5/2}\sigma^{3/2}}{40\pi^{3/2}t^{5/2}} \qquad \ldots 11$$

The definition of late-time apparent resistivity is obtained by inverting this last expression:

$$\rho_{a,late} = \left[\frac{AIdsr}{V\,t^{5/2}} \cdot \frac{4}{5}\pi\times 10^{-17\frac{1}{2}}\right]^{2/3} \qquad \ldots 12$$

The coupling curves for a uniform earth show in Fig. 2 are shown again in Figure 4. As may be seen, the apparent resistivity computed from the late part of the transient coupling is correct for the earth.

It must still be established how late "late" is; that is, the range of times over which this expression gives proper results must be determined. This may be done by comparing the size of the second term in eq. (9) with the size of the first. In order for the first term to be a good approximation

to the series, we will require that the second term be no more than 5% of the first term. The second term is:

$$-\frac{i A I ds\, r^3 \mu_o^{7/2} \sigma^{5/2}}{420\pi\sqrt{2}} (\omega^{5/2} + i\omega^{5/2}) \qquad \ldots 13$$

which transforms in the time domain to an error voltage of:

$$\delta V(t) = \frac{A I ds\, \mu_o^{7/2} \sigma^{5/2} r^3}{224\, \pi^{3/2} t^{7/2}} \qquad \ldots 14$$

The requirement that the voltage contributed by the second term be less than 5% of the voltage caused by the first term leads to the condition:

$$\frac{\mu\sigma r^2}{t} \leq \frac{1}{3} \qquad \ldots 15$$

Figure 6 is a nomogram showing the times which would be considered early, late, and intermediate as a function of source receiver separation and earth conductivity.

A third appoach to defining apparent resistivity is to normalize the entire transient coupling curve by the response for a uniform earth. To see the effect this method has on presentation of results, it is necessary to consider an earth model with at least two layers. Curves for two or more layers must be obtained by numerical integration of the Hankel transform integral in eq. (1). This integration may be done using one of several numerical techniques; spline fitting of the integrand has been desribed by Vanyan (1966), Gaussian quadrature has been used by Meinardus (1970) and

by Anderson (1973), and condolution has been used by Strakhov (1969), Ghosh (1971) and Anderson (1973). The convolution approach is the most rapid of the three, and thus, the least costly.

The Hankel transform integral in eq. (1) can be converted to a convolution integral by a simple transformation of variables. First, it is convenient to reexpress eq. (1) in terms of dimensionless groups of variables, as Frischknecht (1967) has done. These dimensionless groups are:

$$g = \delta\lambda$$

$$K_n = \rho_1/\rho_n$$

$$D_n = \frac{2h_n}{\delta}$$

$$B = \frac{r}{\delta}$$

where $\delta^2 \triangleq \frac{2\rho_1}{\mu_o\omega}$ $\qquad U_n = \frac{V_n}{\delta}$

and $$V_n^2 = g^2 + 2jK_n \qquad \ldots 16$$

To insure convergence of the integrals during numerical evaluation, it is desirable to subtract the uniform earth response from the integrand in eq. (1) and add back the closed-form expression for a uniform earth outside the integral. Doing this, and using the dimensionless groups of variables defined above, we have:

$$H_z = \frac{Ids}{2\pi\delta^2}\sin\theta\int_0^\infty \frac{g^2V_1(1-F_1)}{(g+V_1)(g+V_1F_1)}J_1(gB)dg - \frac{iIds\delta^2\sin\theta}{4\pi r^4}\{3-(3+3(1+i)B+ \qquad \ldots 17$$

$$+ 2iB^2)e^{-(1+i)B}\}$$

The function F_1 in this expression is found by evaluating the recursive expression:

$$F_n = \frac{V_{n+1}F_{n+1} + V_n\left(\frac{1-e^{-V_nD_n}}{1+e^{-V_nD_n}}\right)}{V_n + V_{n+1}F_{n+1}\left(\frac{1-e^{-V_nD_n}}{1+e^{-V_nD_n}}\right)} \qquad \text{where } F_N=1.$$

In evaluation, the counter n is taken to run down from its last value, N (the number of layers), to 1.

To form a convolution, we make the following transformation of variables:

$$x = \ln(B)$$

$$y = \ln\left(\frac{1}{q}\right)$$

...18

Substituting these into eq. (17) leads to an integral of the convolution form:

$$H_z = \frac{I\,ds\sin\theta\, e^{-x}}{2\pi\delta^2}\int_0^\infty \frac{e^{-2y}V_1(1-F_1)}{(e^{-y}+V_1F_1)(e^{-y}+V_1)}e^{x-y}J_1(e^{x-y})dy$$

$$-i\frac{Ids\,\delta^2\sin\theta}{4\pi r^4}\left\{3-(3+3(1+i)B+2iB^2)e^{-(1+i)B}\right\} \qquad ...19$$

or

$$H_z = \frac{Ids\sin\theta e^{-x}}{2\pi\delta^2}\int f(y)\cdot g(x-y)dy + Q$$

where

$$F(y) = \frac{e^{-2y}V_1(1-F_1)}{(e^{-y}+V_1F_1)(e^{-y}+V_1)} \qquad ...20$$

and

$$g(x-y) = e^{x-y}J_1(e^{x-y}) \qquad ...21$$

with Q representing the uniform earth response.

If the two expressions in (19) and (20) are discretized by evaluating them only at a set of equally spaced points in the variable y, the convolution integral becomes a convolution

sum:

$$H_z = \frac{I\,ds\,\sin\theta\,e^{-x}}{2\pi\delta^2} \sum_{i=1}^{n} H(a_j)\,c_i(y_i) \qquad \ldots 22$$

The set of weights, c_i, used in the convolution are obtained by performing the Hankel transform on a function whose transform can be derived analytically. This has been done by Strakhov (1969), Ghosh (1971) and Anderson (1973). The set of coefficients given by Anderson (1973) is given in Table 1.

Eq. (22) was used to compute the two sets of curves shown in Figures 5 and 6. In one case (Fig. 5), the surface layer in a two-layer sequence is more conductive than the substratum, while in the other case (Figure 6), the surface layer is more resistive than the substratum. In the case of a resistant basement, the TDEM curves show a characteristic behavior in that a bump grows on the curve over the mid-ranges in time. The larger the separation is in comparison with the depth to the resistant substratum, the greater will be the relative height of this bump.

The effect of a conductive substratum, as shown by the curves in Fig. 6, is to cause the apparent resistivity curve to "roll over", or begin a rapid decrease at earlier times than would be the case for a uniform earth at the same separation. The shallower a conductive substratum is, the greater will be the reduction in roll-over time..

TDEM curves can be computed for any number of layers with about equal ease using eq. (22), but earth models represented by 3 or 4 layers are usually the most complicated

that can be used in practice. When more than two layers are present, the problem of one layer masking another may become quite serious for certain combinations of resistivities between successive layers.. The three-layer case which is most easily recognizable is that of the resistor-conductor-resistor (type H) sequence. A group of curves for such a case is shown in Figure 7; these curves were computed for a layer with a resistivity of 1 ohm-meter embedded between two layers with a resistivity of 30 ohm-meters. The depth to the top of the conductive layer is 1 kilometer, while the separation from source to receiver is taken to be 10 kilometers. The thickness of the conductive layer ranges from 10 meters to 1 kilometer for the various curves. As may be seen, even a relatively thin conductive layer can exert a measurable influence on the TDEM curve.

The inverse of the case in Figure 7 is shown by the curves in Figure 8. Here, TDEM curves were computed for a sequence of three layers, with the middle layer having a resistivity of 1000 ohm-meters and the outer layers having a resistivity of 3 ohm-meters. Again, the separation is 10 kilometers, and the depth to the top of the middle layer is 1 kilometer. The middle layer was assigned thicknesses ranging from 500 meters to 2 kilometers. As may be seen, the resistive layer has considerably less effect on the TDEM curve than did the conductive layer.

Similar calculations can be made for three-layer cases in which the resistivity in the layers increases or decreases monotonically with depth. No such curves are presented here,

but as one might expect, the curves which have been calculated look very much like two-layer curves. In interpretation of field data, it would probably be necessary to have independent information available to recognize the presence of a monotonic increase or decrease of resistivity with depth.

Although the layered-earth model is widely used in interpreting electrical geophysical surveys, it is not adequate for many of the exploration problems met in practice. The general problem of electromagnetic response caused by three-dimensional bodies buried in an earth with differesnt electrical properties is one that is particularly difficult to solve in a satisfactory manner. By in large, with the exception of the work of Hohmann (1973) and Parra (1974), the theory for the excitation of an inhomogeneity in electrical structure using a fixed source has been restricted to two-dimensional models in the frequency domain. Excitation of conductive masses in a half-space has been computed for a line source or for plane waves by Parry (1971), Hohmann (1971), Swift (1971), Coggon (1971), Dey and Morrison (1973) and others.

The problem of secondary fields around three-dimensional conductive bodies buried in the earth was first examined in detail by Hohmann (1973), and his work has been extended by Parra (1974). According to Parra, the total electric field E generated by a current dipole can be broken into two parts, one which is due to the impressed electric currents from the dipole source, E^i, and the other is the scattered electric field, E^s, due to polarization or scattering current which

exists only in the inhomogeneity. The scattered electric field can be obtained as the product of a Green's function K and the scattered current density, J_s, integrated over the volume of the inhomogeneity:

$$E_s = \int_{v'} K(x,y,z,x',y',z') \cdot J_s(x',y',z')\, dv' \qquad \ldots 23$$

where x,y,z are the coordinates of a point where the scattered electric field is being computed, and x',y',z' are the coordinates of points in the inhomogeneity over which the integration is being carried out. The incident electric field is computed, using expressions such as those developed by Wait (1961). A point-matching method is then use to solve the resulting integral equation (Harrington, 1968).

Parra (1974) modelled a buried dike with infinite strike extent but neither outcropping nor extending to infinite depth. The model is shown in Fig. 9. The source is a 100 meter length of grounded cable carrying 10 amperes of current at the frequency of 1000 Hz. The source cable is parallel to the strike of the dike, and located 250 meters away from it. The depth to the top of the dike is 25 meters, the thickness is 15 meters, and the depth extent is 150 meters. The resistivity of the host rock is 1000 ohm-meters; that of the dike, one ohm-meter.

Parra computed both the electric field components and the magnetic field components for the model. He concluded that only the magnetic field responses were worthy of study; because the electric field components did not express the presence of the dike well. The strength of the magnetic field vertical component with the dike present is shown in

Fig. 10A while the same component is shown for a uniform earth in Fig. 10B. The corresponding patterns of phase response are shown in Fig. 11A and 11B.

The coupling strengths shown in these two sets of maps has been computed in the frequency domain, for a single frequency. To be applicable for the time domain, a spectrum of frequencies would need to be used, followed by an apprpp-riate Fourier transform process to obtain the transient coupling for step excitation. This has not yet been done, but still, the maps shown in Figures 10 and 11 are useful in understanding the nature of coupling around inhomogeneities in an otherwise layered or homogeneous earth. Of particular interest, as will be shown later in one of the field examples, is the change in sign of phase seen over part of Fig. 11. For a uniform earth, the phase is all of the same sign. A reversal in phase can shown to lead to a reversal in polarity of the time-domain equivalent.

Field Examples

The ability to handle the calculation of electromagnetic coupling for a wide variety of earth models represents one aspect of the modern development of deep-probing electro-magnetic sounding methods, while the ability to carry out such surveys successfully in the field is another. As noted before, early application of the TDEM method in exploration for oil and gas has been noted by Vanyan (1966); more recently, the method has been applied in exploration for geothermal reservoirs (Harthill, 1976). All of the examples to be given

in this paper were taken from research studies on the application of the TDEM method to geothermal exploration carried on by the Colorado School of Mines. The first example will be a survey carried on at Kilauea Volcano, Hawaii, by C. K. Skokan (1975); the second will be a study carried out in a potentially geothermal area of Nevada, in the Basin and Range province of the western United States, by R. A. Crewdson (1976).

Kilauea Volcano rises to an altitude of about 1300 meters above sea level on the southeast flank of the Island of Hawaii. It is composed almost entirely of basaltic flows, intrusions, and minor amounts of basaltic ash. The volcano has been active frequently over the past two decades.

TDEM sounding has been used by Jackson and Keller (1973) and by Keller and Rapolla (1976) to locate and define areas of low electrical resistivity near the summit of Kilauea. It is believed that these areas of low resistivity are caused by heating of ground water by a shallow magma chamber. Skokan attempted to locate other areas of anomalously low resistivity along a rift zone extending eastward from the summit of Kilauea Volcano (Skokan, 1974).

Hawaiian Volcanoes, including Kilauea, are often characterized by having rift systems which extend outwards from the central caldera. These rifts are centers of spreading, and lava flows from the lower reaches of these rift faults as often as it flows from the central caldera. The northeast rift of Kilauea extends about 30 kilometers from the central crater until it reaches the coastline in the District of Puna;

it then extends another 70 kilometers beneath the ocean before it disappears completely. The submarine portion of the rift is a prominent ridge which contains a composite plug or dike complex. On land, the rift is believed to be intruded by a dike complex also, probably at a depth of one or two kilometers. Extensive flows were extruded from the rift zone in the Puna District at altitudes ranging from sea level to 400 meters in the late 1950s and early 1960s. Even today, there is considerable steaming from the trace of the rift near these eruption sites.

The survey carried out by Skokan was done over a small area (about 50 square kilometers) along the northeast rift zone, south of the village of Pahoa, as indicated on the map in Figure 12. The location was selected because of extensive steaming from rift fractures in this area, and because earlier drilling to shallow depths had revealed the presence of boiling water at a depth equivalent to sea level.

A map of the area surveyed is shown in Figure 1 . A single source was used to provide signals over the entire area to be surveyed; this source consisted of a grounded wire 2.5 kilometers in length. This source cable was grounded by burying lengths of iron pipe in shallow trenches, and saturating the ground around the pipes with salt water. Power for excitation of the source was provided from a mobile gasoline-engine motor generator set with a capacity of 15 KVA. The 60 Hz 220 V output of the generator was stepped up to 1300 volts with a transformer, rectified with silicon

diodes, and switched periodically to reverse the direction of current flow in the source cable. Cam-actuated mechanical switches were used, with the switching interval being 10 seconds. On switching, a current step with peak to peak amplitude of approximately 25 amperes was obtained.

The magnetic field associated with the step current in the source was detected and recorded at numerous sites around the source, at distances ranging from $2\frac{1}{2}$ to 10 kilometers, as indicated on Figure 13. The time-rate of change of the magnetic field was measured using a vertical-axis induction loop. This induction loop was formed by laying a length of 26-conductor cable on the ground in the form of a square, and connecting the turns in series. The perimeter of the loop was 320 meters, providing an effective area for the loop of 0.24 square kilometers. The voltage generated in the loop by the changing magnetic field when the source current reversed direction was amplified and recorded on a direct-writing oscillographic recorder. An example of a record of a single transient is shown in Figure 14.

Signals such as that shown in Figure 14 were processed as follows. Synchronous addition, or "stacking", of 10 or more transient signatures was done in order to improve the signal to noise ratio. Distortion introduced by shortcomings in the response of the recording system was removed by deconvolution. The voltages were then smoothed with an exponentially time varying filter to reduce uncorrelated noise, and, finally, the voltages were converted to values of apparent resistivity using eq (5).

In stacking, a group of signals recorded at a single receiver station were digitized at a 40 millisecond interval, and added together. Prior to addition, a statistical test was applied to each data point to see if it fell within a reasonable distance (two standard deviations) from the average for that point. If not, the data point would not be included in the stacking. Using 10 signals, the relative noise reduction was two-fold to three-fold.

After stacking, the response of the recording system was removed by deconvolution. The logic of this deconvolution is shown in Figure 15. The recorded signal, which ideally would be the response of the earth to a step excitation, is actually somewat different because it has been convolved with the step response of the recording equipment during recording. The time-domain response of the recording equipment was obtained by recording its response to a step input of voltage. Then, both the signal and the response of the equipment were transformed to the frequency domain to provide spectrums. The spectrum of the recorded signal was divided by the spectrum of the transfer function of the recording equipment, thus removed it from the record. The compensated signal spectrum is transformed back to the time domain for interpretation.

Both the digitizing process and deconvolution increase the relative amount of high frequency noise in the signal. To reduce this uncorrelated noise, smoothing was applied to the aignal after deconvolution. The filtering method

selected was based on the shape invariant property of TDEM curves when they are plotted on logarithmic coordinates. The field data were digitized at equal time intervals along a linear time base. When these digitized data are plotted on logarithmic coordinates, the early part of the signal appears to be sparsely sampled while the later part appears to be densely sampled. Noise superimposed on the signal appears to increase in frequency for progressively later parts of the signal, when data are plotted on logarithmic coordinates. Moreover, the signal to noise ratio is higher in the early part of the signal than in the late part. This change in the signal to noise ratio as the apparent frequency of the noise component changes can be used to design a filter that discriminates against the noise in the late part of the signal without undoing the effect of deconvolution in the early part. Filtering was accomplished by applying a linear smoothing filter in the logarithmic domain, which is equivalent to applying a logarithmically time-compressed filter in the original linear time domain.

Once the field data have been processed to provide curves as close as possible to the actual response of the earth to step-current excitation, there are several ways in which the data can be managed for further interpretation. The first step is usually some simple approach to comparing the character of response over the area surveyed. One way of doing this is to contour the maximum values of apparent resistivity recorded at each receiver station; this has been done in Figure 13. For the area surveyed, the most prominent feature is an area of high resistivity along the rift zone,

centered on Puulena Crater. Considering the fact that this resistivity high is centered on the rift zone in the area of eruptive activity of the 1950s and 1960s, it is reasonable to conclude that the high resistivity is associated with the intrusion of hot dikes, which reduce the water content in the subsurface. A hole drilled recently by the University of Hawaii to a depth of 2 kilometers in this area of high resistivity (Shupe, personal communication, 1976) did indeed show the subsurface temperatures to be high, in the vicinity of the boiling-point versus depth curve.

One problem with the maximum apparent resistivity presentation is that there is no clear indication as to the depth to which the resistivity has been sampled. In the Puna area, for example, resistivity soundings made with the direct-current method indicate the presence of a surface layer with a resistivity of several hundred to several thousand ohm-meters extended to a depth roughly equivalent to sea level. The TDEM curves give no indication of any surface layer with such a high resistivity, because the recording equipment was incapable of detecting the very early part of the signal prior to 40 milliseconds. This loss of the early part of the signal means that a high resistivity layer can remain hidden at the surface, undetected by the TDEM sounding. The thickness that such a hidden layer might have can be estimated roughly by computing a skin depth in the time domain. If the thickness of a layer is less than

a tenth of a skin depth, then the effect on the TDEM curve will be to change the apparent resistivity by no more than 10 percent of the value for the second layer. A curve showing the time-domain skin-depth as a function of resistivity is shown in Figure 16; for the known surficial resistivities of 200 to 2000 ohm-meters, a surface layer with a thickness ranging from a few hundred meters to more than a kilometer could be present and not be detected on the TDEM sounding.

A more complete interpretation of TDEM curves may be made by comparing them with theoretically derived curves for a layered earth, such as those shown earlier in this paper. This may be done using conventional graphical curve matching techniques, such as those that have been highly developed for use in interpreting direct-current sounding data (Keller and Frischknecht, 1966), or the modern methods, in which a computer is used to determine a series of successively better theoretical curves to simulate the field data.

Graphical curve matching of TDEM curves has several significant limitations. Few catalogs of theoretical curves are available; sets of curves provided by Silva (1969) and King (1971) are sparse, and in addition, TDEM curves tend to lack the characteristic shapes that are so useful in matching direct-current sounding curves.

In graphical curve matching, both the field curve and the theoretical curves must be plotted to a common scale on logarithmic coordinates. The theoretical curves are made dimensionless by dividing the vertical scale, ρ_a, by the

resistivity of the first layer, ρ_1, and the horizontal scale, t, by the factor $\mu\sigma_1 r^2$. Then, the field plot is overlaid on the theoretical curves, and shifted about until a match is found between the field data and one of the theoretical curves. In seeking a match, it is important to note that only one degree of freedom is available in shifting the field curve with respect to the theoretical curves. This comes about because both axes on the dimensionless plot of theoretical curves depends on the resistivity of the surface layer. The field curve can only be shifted in such a way that the value of ρ_1 derived from the vertical scale agress with the value of σ_1 derived from the horizontal scale. The one degree of freedom is characterized by a line of slope -1 on the field plot, on which the origin of the set of theoretical curves must lie when a match is obtained. An example of a match between one of the sets of field data obtained in the Puna area of Hawaii and a set of tehoretical curves is shown in Figure 17.

Computer assisted interpretation is more convenient and can provide better results than graphical curve matching, if a computer of moderate capacity is available. Two types of computer-assisted interpretations are widely used, generalized linear inversion and optimal simulation.

In linear inversion or in optimal simulation, the first requirement in developing an interpretation scheme is to define a measure of the goodness or poorness of an interpretation. Almost universally, the least-squares measure of misfit between a model curve and the field data is used. This measure is illustrated in Figure 18 ; here, a theoretically

generated curve is shown superimposed on a discrete set of measured app rent resistivity values, representing a field-defined TDEM curve. The points do not lie exactly on the theoretical curve, but are displaced at varying distances from it. The misfit can be characterized by the average of the squares of the distances from the theoretical curve:

$$E = \frac{1}{N} \sum_{n=1}^{N} (\ln \rho_{f,n} - \ln \rho_{m,n})^2 \qquad \ldots 24$$

where E is the error, or misfit, N is the number of points matched, ρ_f are resistivity values taken from the field data, and ρ_m are the computed resistivity values at the same times.

The error, E, will become larger or smaller as the resistivities and thicknesses used in the model to compute the theoretical curve become larger or smaller. There should be some set of values for layer thicknesses and resistivities which provides a minimum value for the error, E_o, but it is unlikely that there is any set of parameters which will reduce the error to zero. Inversion consists of finding the set of parameters which will yield the minimum error. The relationship between the error of fit and the values for the various parameters used in the theoretical model can be expressed as a Taylor's series expanded about the minimum error, E_o:

$$E = E_o + \sum_{i=1}^{n} (\rho_{m,i} - \rho_{f,i}) \frac{\partial E}{\partial \rho_{m,i}} + \sum_{i=1}^{n-1} (h_{m,i} - h_{f,i}) \frac{\partial E}{\partial h_{m,i}} + \text{higher derivat's} \qquad \ldots 25$$

where ρ_i and h_i are the resistivities and thicknesses for each of the n layers in the model. The differences in each

term are the differences between an arbitrarily select4d model and the model which will give the minimum error. The problem is linearized by ignoring all the terms in the series expansion except those that contain derivatives of first order, and in which the differences in parameters enters linearly:

$$E = E_o + \delta_{\rho_i} \frac{\partial E}{\partial \rho_i} \qquad \ldots 26$$

where ρ_i is used to indicate a parameter, either the thickness or resistivity of a layer. The set of equations in (26) can be "inverted" or solved for the differences in parametric values, thus yielding optimum values for the parameters, providing the assumption of linearity is reasonably correct. In other words, the initial estimate of the model must be close enough to the ideal model that the higher order terms in eq (25) are not significant.

The field curves obtained from the Puna district were interpreted using Marquardt's (1963) scheme in a program witten by Daniels (1974) and modified by Skokan (1974). A cross section taken from these interpretations along line A-A' on Figure 13 is shown in Figure 19. Over the fift, relatively high resistivities (23-24 ohm-meters) were found to extend from the near surface to depth. A zone of low apparent resistivity was found adjacent to the rift on the seaward side, which may be water-saturated volcanic flows heated on contact with the rocks in the dike.

The second example of a TDEM survey carried out in the search for geothermal energy is one reported by Crewdson

(1976) in the Basin and Range province of the western United States. Many thermal springs occur in the area, and geophysical evidence indicates that the heat flow is higher than normal over much of the area. As opposed to the generation of a geothermal system in Hawaii by contact between water-laden porous rocks and molten rock, thermal systems may arise in the Basin and Range province only because of regionally high thermal gradients; no immediate heat source such as an intrusion is necessary. The exploration problem remains the same -- to locate a reservoir of water heated to a high enough temperature to be useful in producing electricity. Measurement of electrical resistivity are often useful in detecting the effect of anomalous heating underground.

The survey to be described here was carried out north of the town of Gerlach, in northern Nevada (see Figure 20 for a location map). The study area consisted mainly of the Black Rock Desert and Hualapai Flat, which are alluvial-filled intermontane basins. Hot springs occur along the margins of the valleys, giving evidence for high heat flow. Details of the area are shown in Figure 21.

In the survey of the Gerlach area, two source bipoles were used, as indicated on Figure 21. They were at approximately the same location, but oriented at right angles to each other. This permitted measurements to be made in any direction from the source, which is not possible if a single source is used (the signal is very weak along the longitudinal axis of the source). Each source cable was approximately 1.5

kilometers in length. The source equipment was the same as that used in Hawaii. Well casings extending to a depth of several tens of meters wereused as electrodes. Peak to peak current amplitudes of 100 amperes were obtained. Measurements were made at 170 receiver sites at distances ranging from 3 to 20 kilometers. Signals from both sources were recorded at each receiver site, provideding a total of 340 TDEM soundings for the survey. These data were processed in the same manner as described earlier.

Contours of the maximum value of apparent resistivity observed at each receiver location are shown on F$_i$gure 21. These maximum values clearly delineate major areas of high and low resistivity. The areas of low resistivity are areas underlain by alluivial sediments, while the areas of high resistivity are areas underlain by granite, or other rocks known to have high resistivity. The importance of these data in so far as we are concerned here is not in knowing that the resistivity map can be used to identify the underlying rock, but that the TDEM method can be used in an area where strong lateral changes in resistivity are present. Other electrical sounding methods are difficult to interpret when such changes are present.

The change in character of the TDEM transient curves in these areas with differing resistivity is shown clearly by the examples in Figure 22. The first two examples (stations 944W and 96W) were obtained at locations where a moderate thickness of conductive alluvium covers resistant basement. Each curve rises abruptly at the time of switching of the source, after which, the signal rises slowly to a maxiaum

and then decays. The more conductive the overburden is, the longer is the duration of the traansient. The next two examples (stations 11W and 12E) are examples of transients recorded in an area where resistivity decreases with depth. Here, the voltage rises abruptly to its maximum value, then decreases slowly with time for a while before beginning to decay more rapidly.

Not all recorded transients were as simple as those shown in Fig. 22. Several examples of transients recorded near boundaries between zones with radically different resistvities are shown in Figure 23. The effect of a strong lateral change in resistivity is to cause the transient coupling to change sign, as was noted at stations 947E, 924W and 927E. Transient coupling recorded over a layered earth has always the same polarity. Negative coupling can occur when the earth is not horizontally uniform because coupling between a receiver loop and eddy currents displaced to one side of the loop is opposite in sign to the coupling between a receiver loop and eddy currents directly beneath the loop (see Figure 24).

Sign reversals in recorded transients have been found to be an excellent way to locate the boundary between regions with different resistivities. They occur only within a short distance of the boundary, rarely at distances greater than 500 meters. The relatively short distance from a boundary at which the coupling curve returns to a behavior characteristic of a layered earth is also an advantage. With other

electrical sounding methods, it is often difficult to distinguish between the effect of layering at depth and lateral changes in resistivity, with the TDEM method, later changes cause a diagnostic behavior in the TDEM curve (a sign reversal) which cannot be confused with response from a layer at depth. At the same time, because of the preferential coupling of a loop receiver to eddy currents immediately beneath the receiver site, the method provides higher lateral resolution and the capacity to make layered earth interpretations even in areas where the layers are not laterally extensive.

Conclusions

The TDEM sounding method is an effective way of studying the electrical structure of the earth to depths of several kilometers. It has advantages and disadvantages with respect to other electrical sounding methods. For example, while installation of a source cable capable of supporting the high current intensities required for effected TDEM measurements, the amount of effort involved in making soundings is not nearly so great as that required in direct-current sounding methods. The effort is more than that required in magneto-telluric soundings to the same depth, but in TDEM soundings, measurements can be completed at a receiver location in a matter of 5 or 10 minutes, as opposed to a requirement for a recording interval of 50 to 100 minutes with the magnetotelluric method. In routine exploration, much of the cost is related to the time required for the measurements, rather than to the cost of equipment.

The TDEM method has the advantage of high lateral

resolution in comparison with both direct-current sounding and magneto-telluric sounding. Moreover, the effects caused by lateral changes in resistivity differ dramatically from those caused by layering, so that lateral effects cannot be confused with layering.

A significant limitation to TDEM sounding is a relatively narrow window for recognizing the presence of layers at depth. Shallow layers of high resistivity are difficult to recognize because their effect on coupling is not long enough to be recorded faithfully.

Time-domain electromagnetic sounding is a useful tool for studying resistivities in the range from 1 to 50 ohm-meters at depths ranging from a few hundred meters to a few kilometers. Improvements in equipment and technique may extend these ranges in the future.

References

Anderson, W. L., 1973, Fortran IV programs for the determination of the transient tangential electric field and vertical magnetic dipole for an M-layered stratified earth by numerical integration and digital linear filtering: USGS Publ. P8-226 240/5, Denver, Co.

Coggon, J. H., 1971, Ph.D. Dissertation, University of California, Berkeley, California, 381 pp.

Crewdson, R. A., 1976, Geophysical studies in the Black Rock Desert geothermal prospect, Nevada: Ph.D. Thesis T-1866, Colorado School of Mines, Golden, Co., 180 pp.

Daniels, J. J., 1974, Interpretation of electromagnetic soundings using a layered earth model: Ph.D. Thesis T-1627, Colorado School of Mines, Golden, Co., 86 pp.

Dey, A., and Morrison, F. H., 1973, Electromagnetic response of two dimensional inhomogeneities in a dissipative half-space for Turam interpretations: Geophys. Prosp., vol. 21, pp. 340-365.

Frischknecht, F. C., 1967, Fields about an oscillating magnetic dipole over a two-layer earth: Colorado School of Mines Quarterly, vol. 62, no. 1, 370 pp.

Ghosh, D. P., 1971, The application of linear filter theory to the direct interpretation of geoelectrical resistivity sounding measurements: Geophys. Prosp., vol. 19, no. 2, pp. 192-217.

Harthill, N., 1976, Time-domain electromagnetic sounding: IEEE Trans. on Geoscience Electronics, vol. GE-14, no. 4, pp. 256-260.

Harrington, R. F., 1968, Field computation by moment methods: New York, MacMillan, 229 pp.

Hohmann, G. W., 1971, Electromagnetic scattering by conductors in the earth near a line source of current: Geophysics, vol. 36, pp. 101-131.

Jackson, D. B., and Keller, G. V., 1973, An electromagnetic sounding survey of the summit of Kilauea Volcano, Hawaii: Jour. Geophys. Research, vol. 77, no. 26, pp. 4957-65.

Keller, G. V., 1968, Electrical prospecting for oil: Quarterly, Colorado School of Mines, vol. 63, no. 2, 268 pp.

Keller, G. V., 1970, Induction methods in prospecting for hot water: Geothermics (Special Issue 2), vol. 2, pt. 1, pp. 318-332.

Keller, G. V., and Rapolla, A., 1975, Electrical prospecting methods in volcanic and geothermal environments: in Physical Volcanology, Amsterdam, Elsevier, pp. 133-166.

Keller, G. V., and Rapolla, A., 1976, A comparison of two electrical probing techniques: IEEE Trans. on Geoscience Electronics, vol. GE-14, no. 4, pp. 250-256.

Keller, G. V., and Frischknecht, F. C., 1966, Electrical methods in Geophysical Prospecting: Oxford, Pergamon Press, 527 pp.

King, C. A., 1971, Time-domain electromagnetic coupling: M.Sc. Thesis T-1427, Colorado School of Mines, Golden, Co.

Marquardt, D. W., 1963, An algorithm for least-squares estimation of nonlinear parameters: Journ. Soc. Indus. Appl. Math., vol. 11, no. 2, pp. 431-441.

Meidav, T., and Tonani, F., 1976, A critique of geothermal exploration techniques: Proc. Second United Nations Symposium om the Development and Use of Geothermal Resources: pp 1143-1154.

Meinardus, H. A., 1967, The kernal function in direct-current resistivity interpretation: D.Sc. Thesis T-1103, Colorado School of Mines, Golden, Co.

Ofrey, Ofiafate, 1975, Detection and interpretation of various magnetic field components in time-domain electromagnetic sounding: M.Sc. Thesis T-1749, Colorado School of Mines, Golden, Co.

Parry, J. R., and Ward, S. H., 1971, Electromagnetic scattering from cylinders of arbitrary cross-section in a conductive half-space: Geophysics, vol. 36, pp. 67-100.

Silva, L. R., 1969, Two-layer master curves for electromagnetic sounding: M.Sc. Thesis T-1250, Colorado School of Mines, Golden, Co.

Skokan, C. K., 1974, A time-domain electromagnetic survey of the East Rift zone, Kilauea Volcano, Hawaii: Ph.D. Thesis T-1700, Colorado School of Mines, Golden, Co.

Swift, C. M., Jr., 1971, Theoretical magneto-telluric and Turam response from two-dimensional inhomogeneities: Geophysics, vol. 36, pp. 38-52.

Vanyan, L. L., 1967, Electromagnetic depth soundings: New York, Consultants Bureau

Wait, J. R., 1961, The electromagnetic fields of a horizontal dipole in the presence of a conducting half-space: Can. Journ. Phys., vol. 39, pp. 1017-1028.

Wait, J. R., 1962, Electromagnetic waves in stratified media: New York, The MacMillan Co., 372 pp.

Wait, J. R., 1966, Fields of a horizontal dipole over a stratified anisotropic half-space: IEEE Trans. Ant. and Prop., vol. AP-14, no. 6, pp. 790-792.

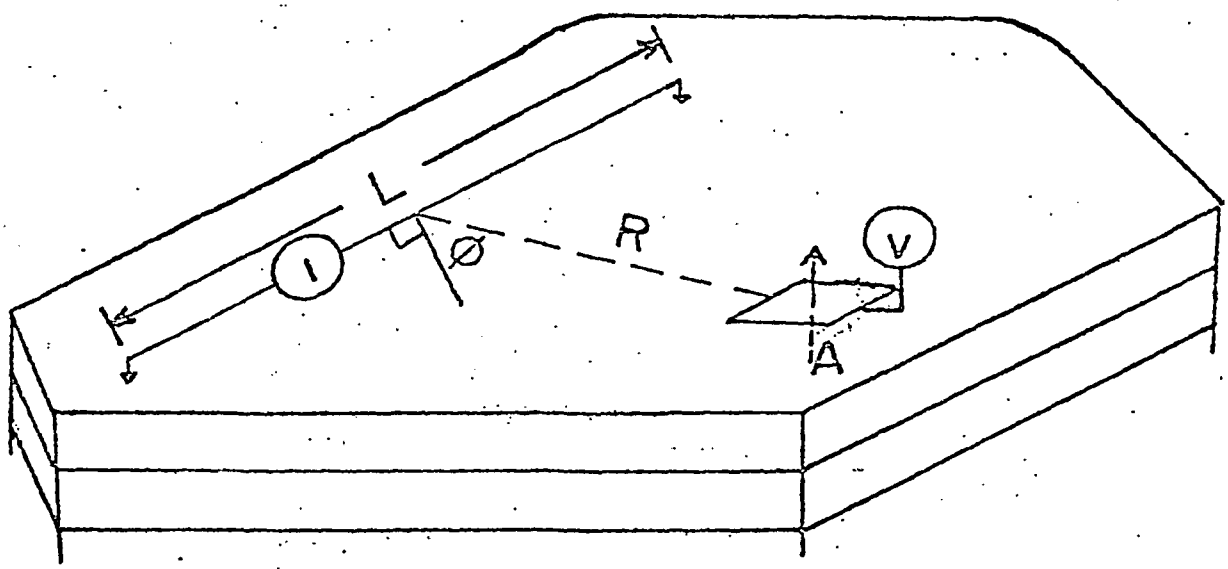

Figure 1. Source-receiver arrangement for time-domain electromagnetic soundings.

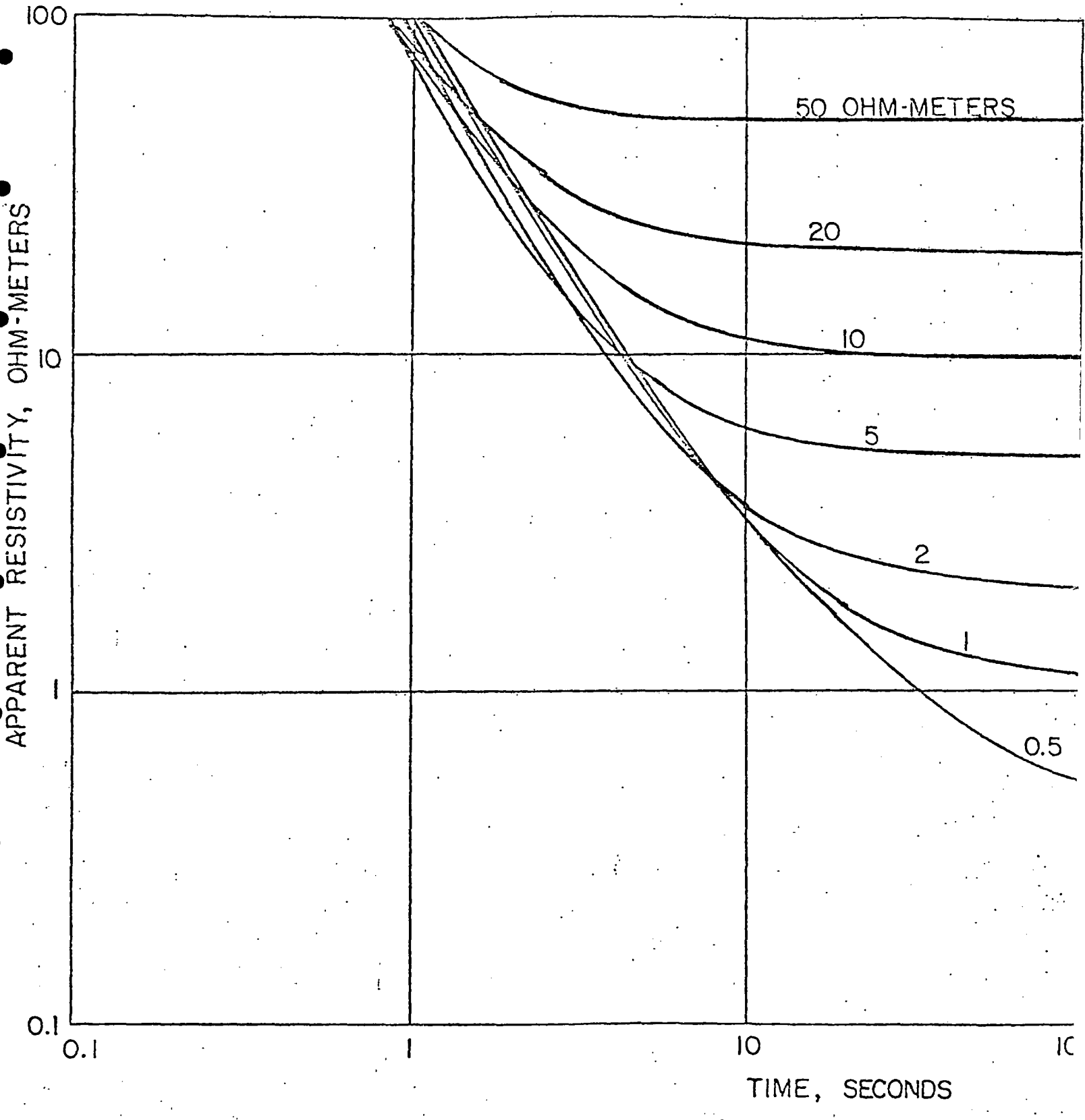

Figure 4. Computed voltage transient curves from Figure 2 presented as apparent resistivity curves using the late-time formula for apparent resistivity.

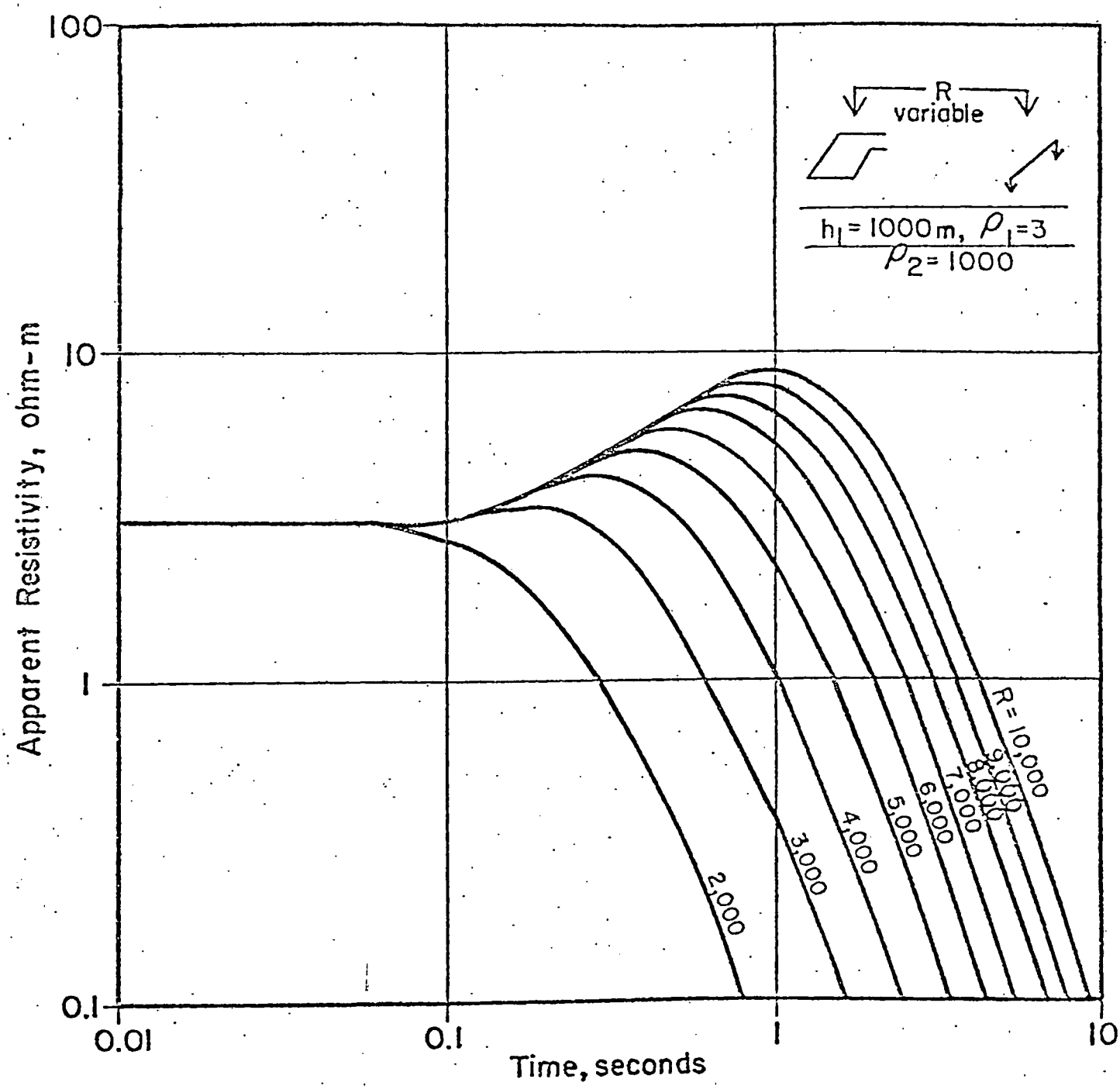

Figure 5. Calculated time-domain electromagnetic sounding curves for a sequence of two layers in which the second layer is more resistive. The parameter on each curve is the separation between source and receiver, in meters.

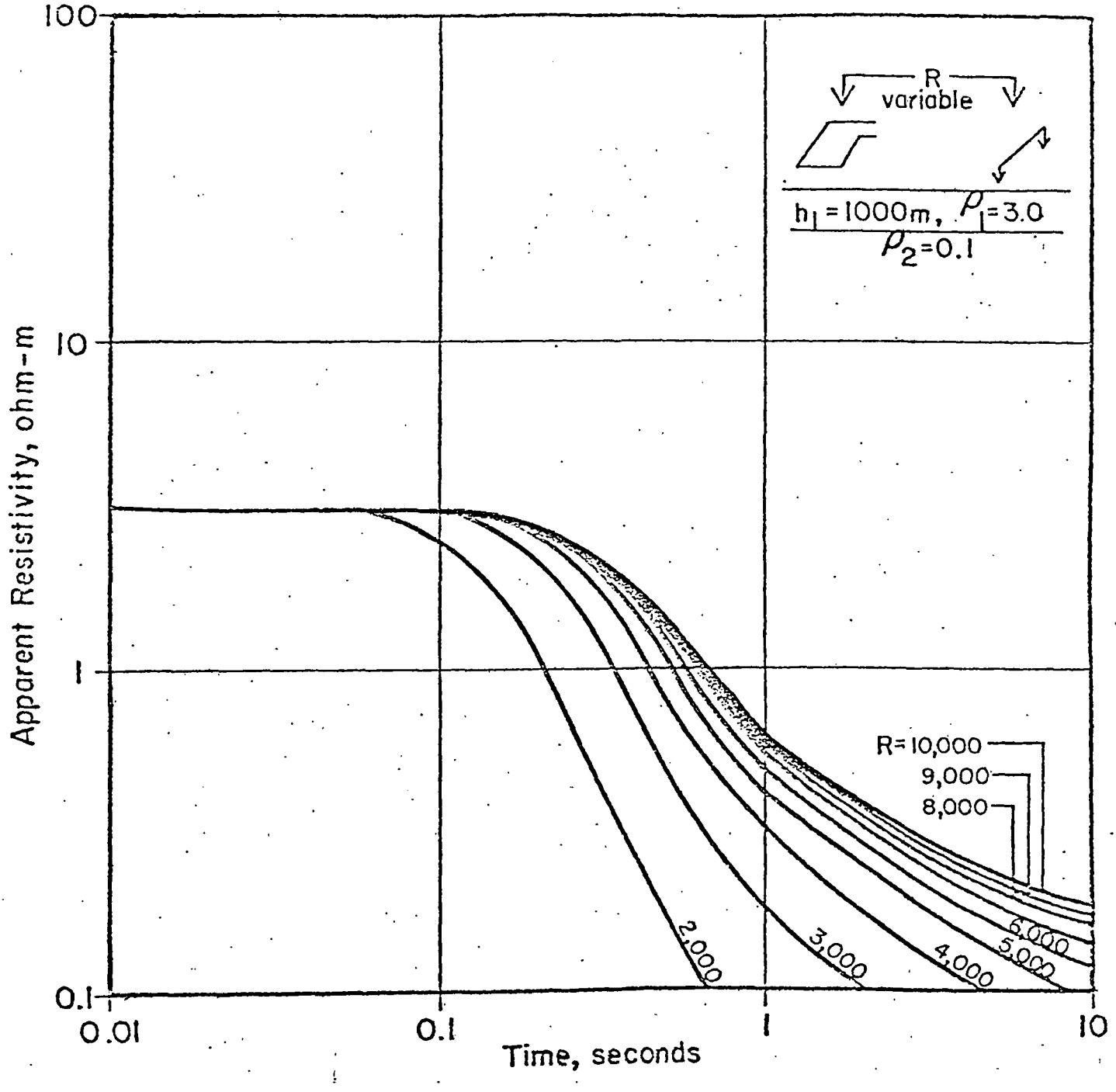

Figure 6. Time-domain electromagnetic sounding curves for a sequence of two layers in which the second layer is more conductive than the first. The parameter on each curve is the separation between source and receiver, in meters.

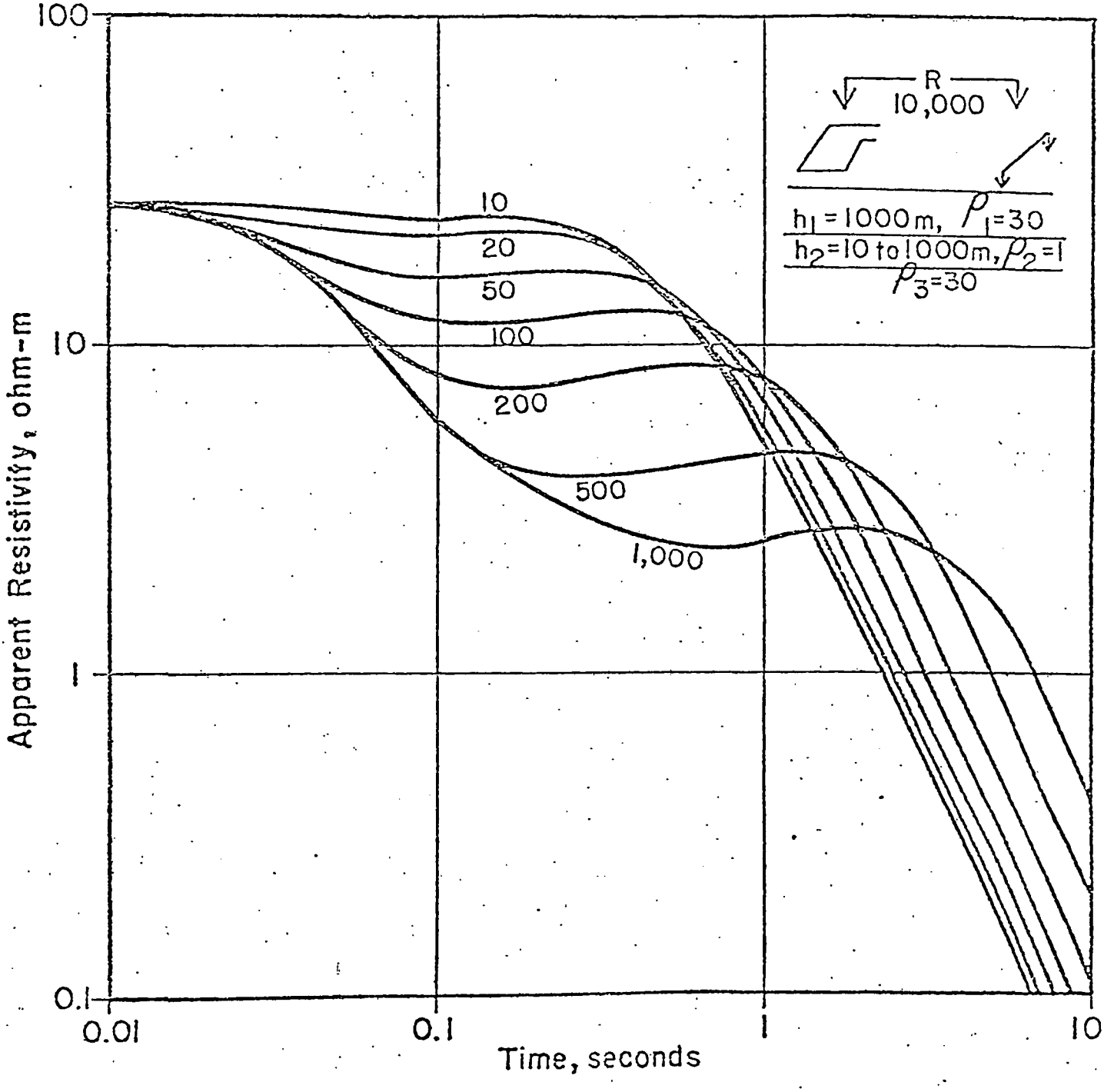

Figure 7. Computed time-domain electromagnetic sounding curves for a sequence of three layers in which the middle layer is the most conductive. The parameter on each curve is the thickness of the conductive layer, in meters.

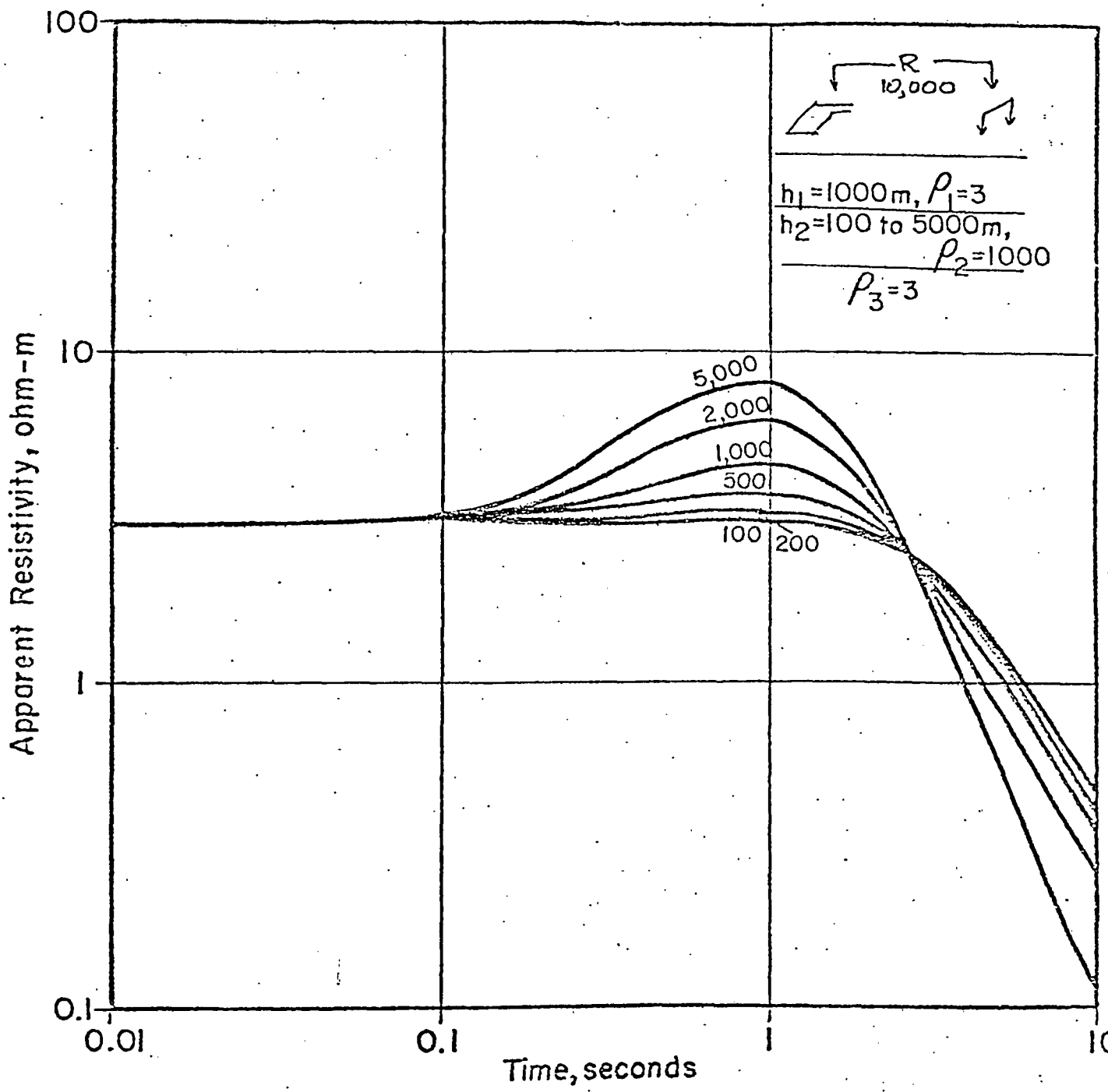

Figure 8. Computed time-domain electromagnetic sounding curves for a sequence of three layers in which the middle layer is most resistive. The parameter on each curve is the thickness of the middle layer, in

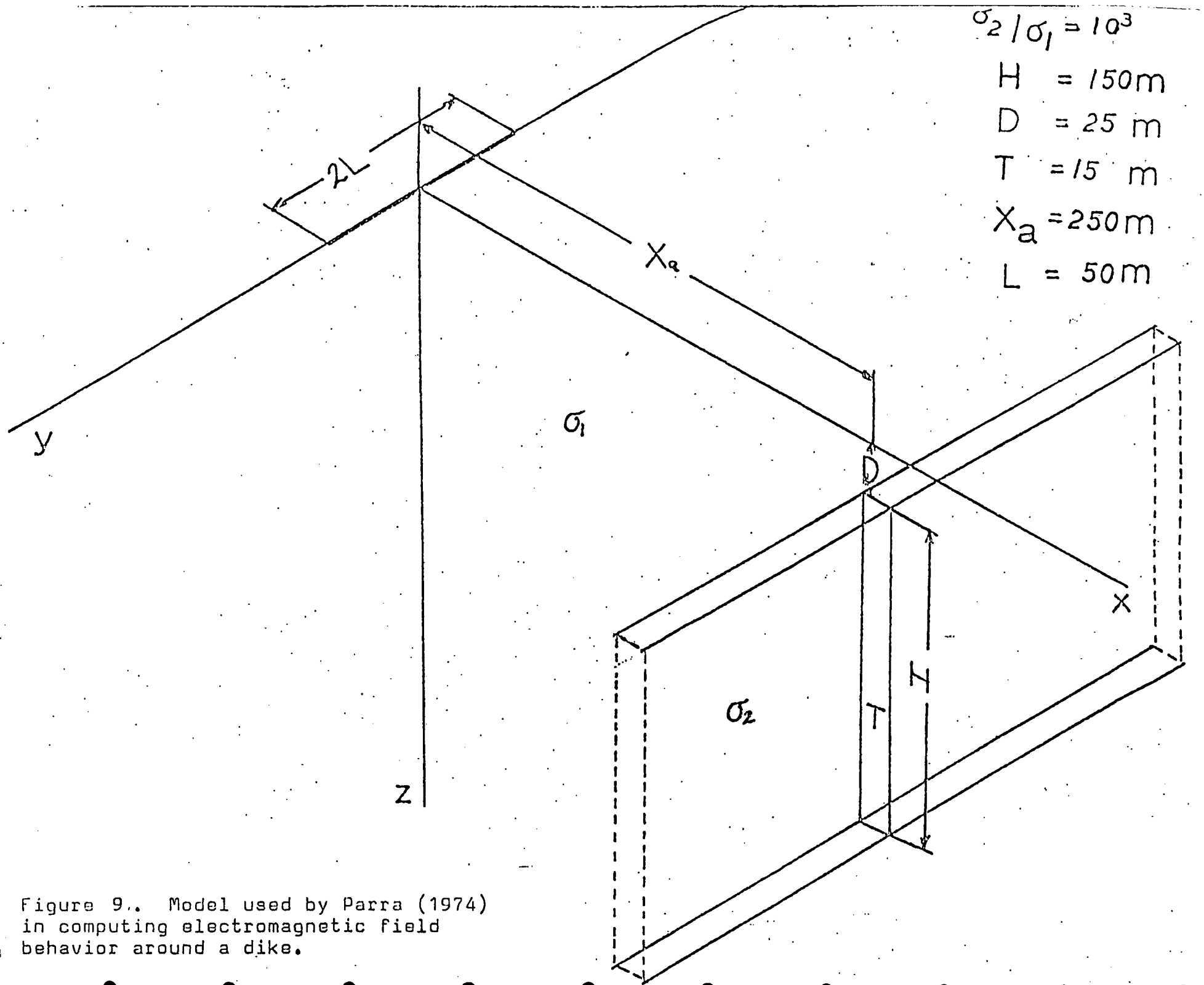

Figure 9. Model used by Parra (1974) in computing electromagnetic field behavior around a dike.

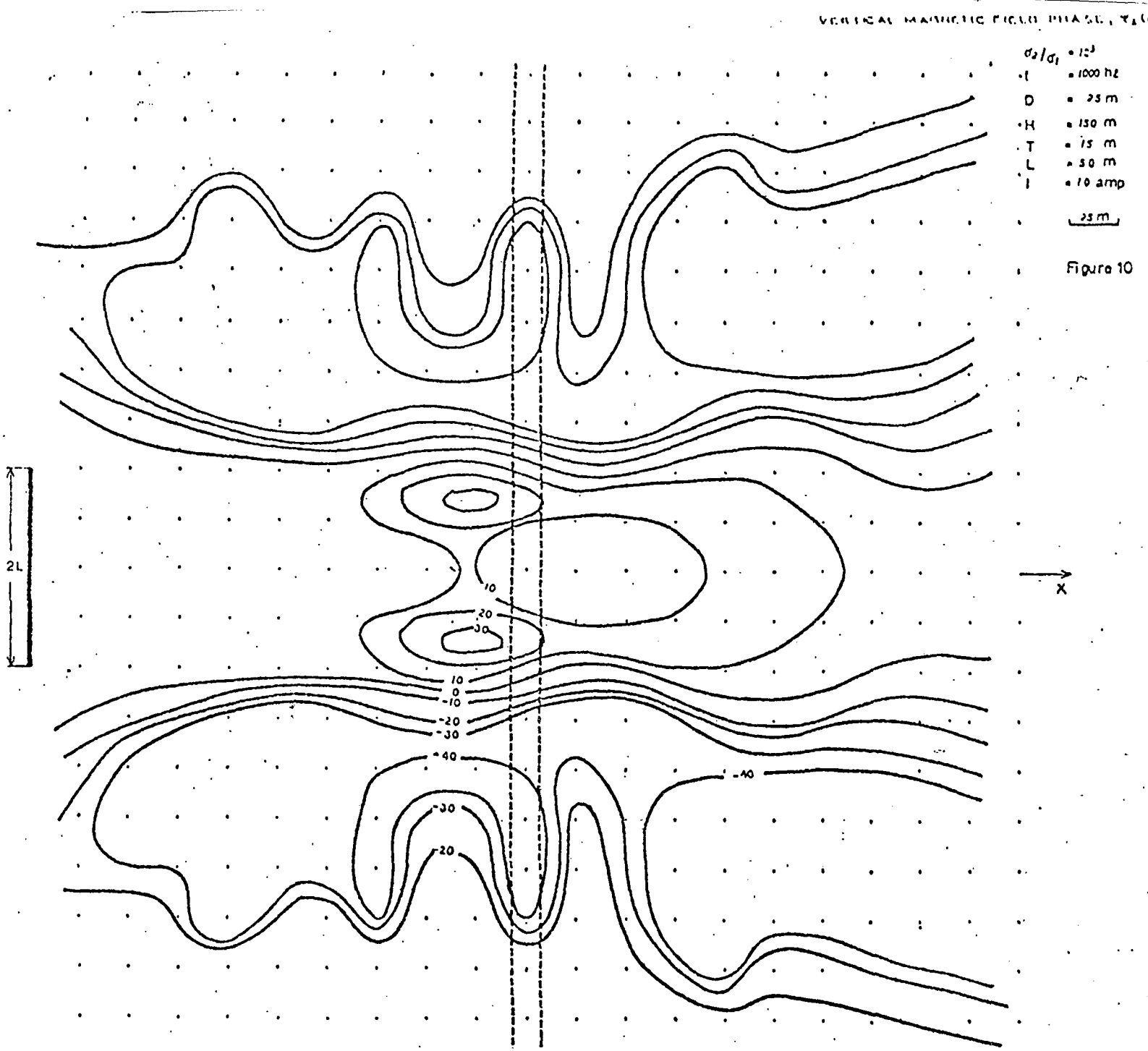

Figure 11A. Phase differente between the magnetic vertical induction and current in the source for measurements made in the vicinity of a dike.

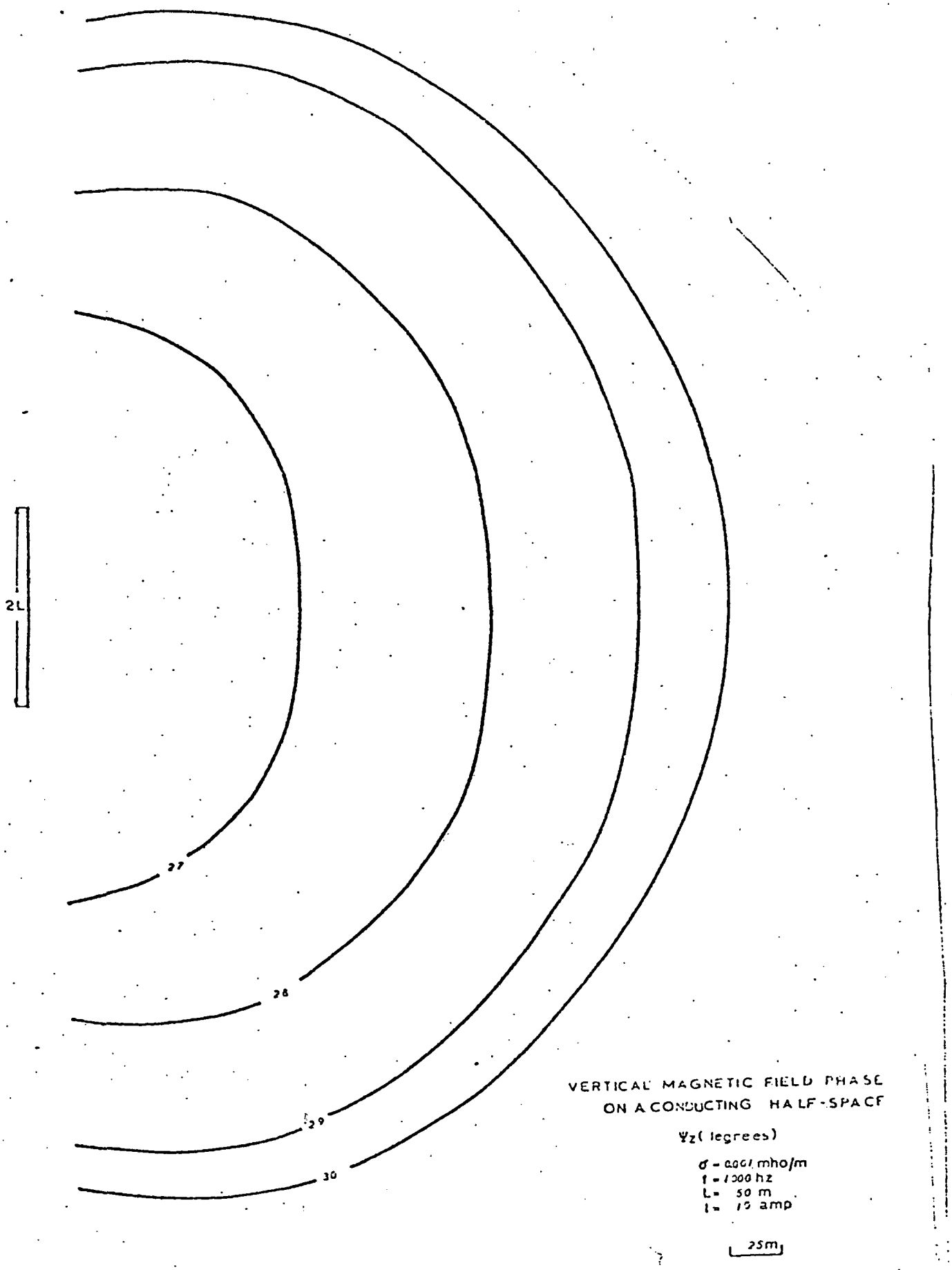

Figure 118. Map of the phase shift between vertical magnetic field strength and source current for a dipole source over a uniform earth.

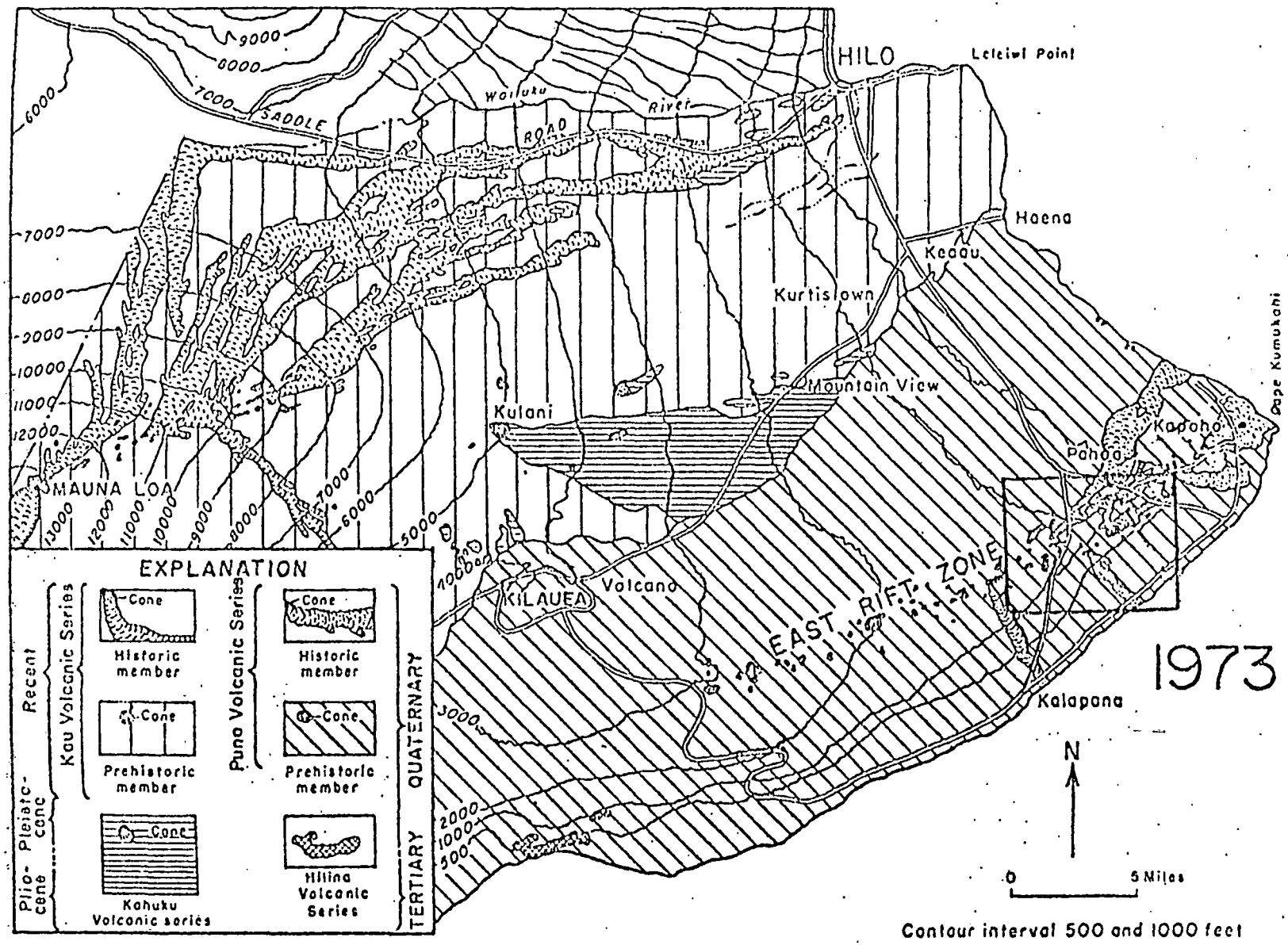

Figure 10. Geological map of the Puna District, Island of Hawaii. Area of TDEM survey is indicated.

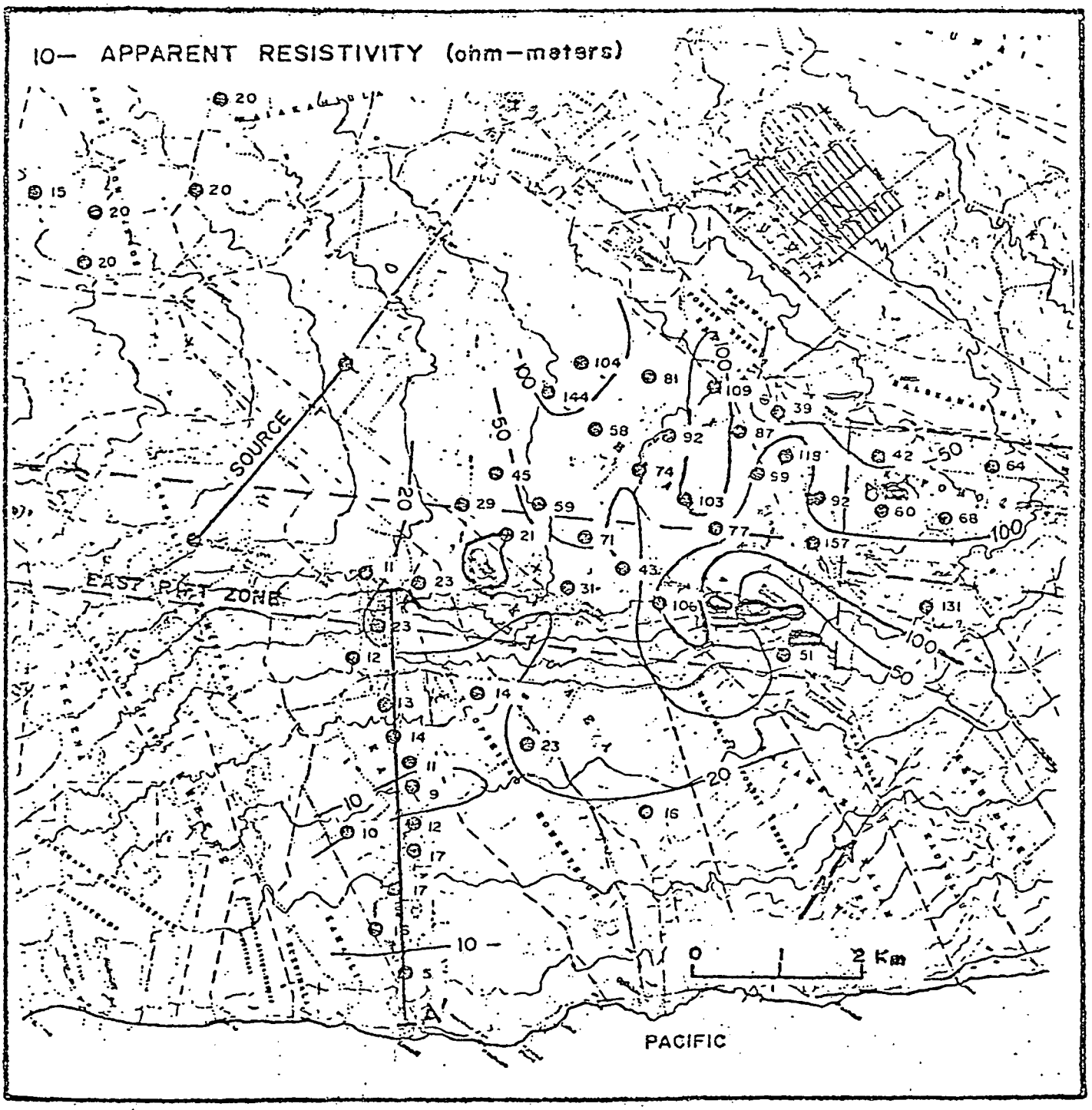

Figure 13. Map of an area in the Puna District, Island of Hawaii, where a TDEM survey was carried out. Maximum values of apparent resistivity from the TDEM soundings are contoured (in ohm-meters).

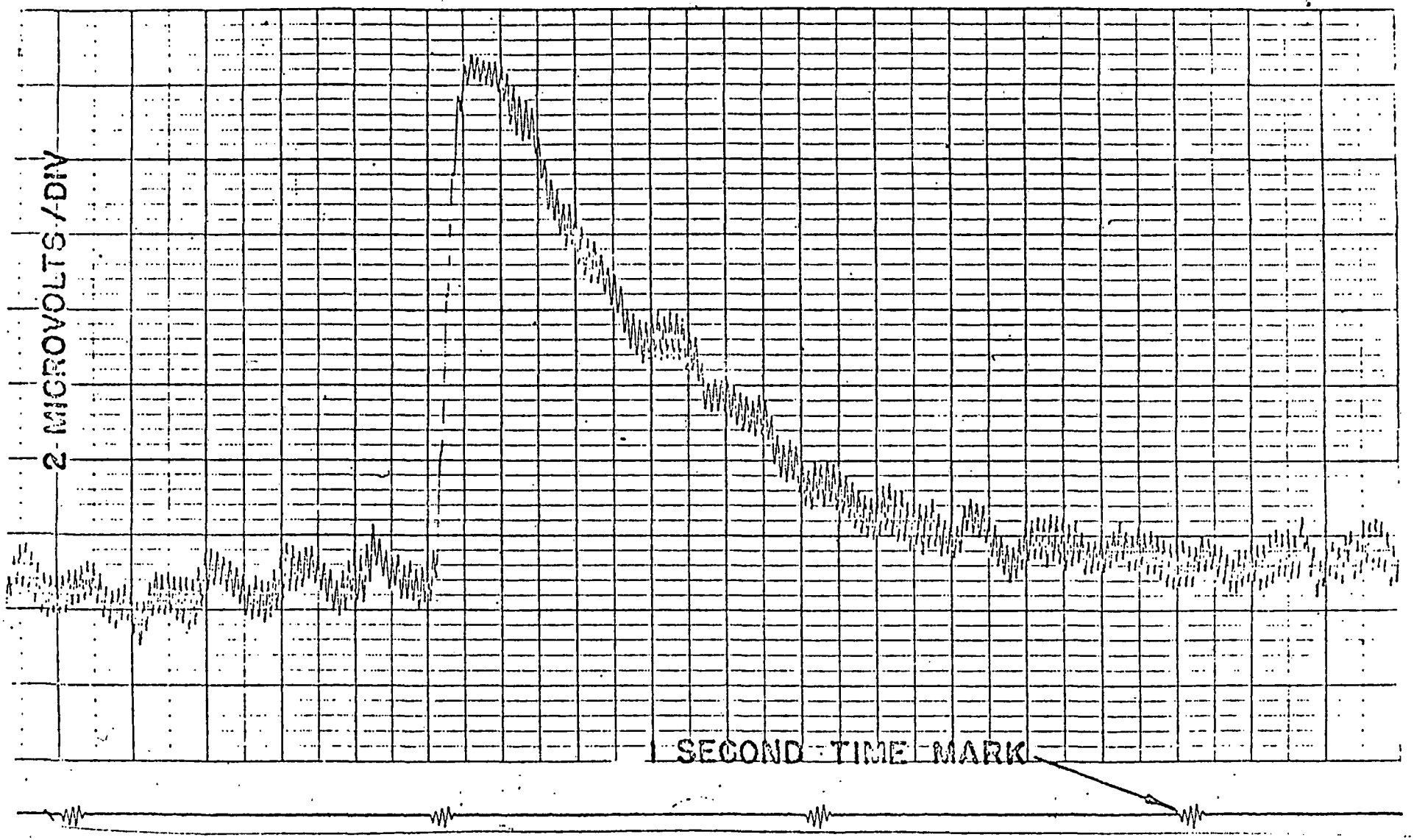

Figure 14. Example of a field recording obtained in TDEM sounding in Hawaii. The high frequency noise superimposed on the signal is at a frequency of 60 Hz.

STEP 1:

STEP 2:

STEP 3: FOURIER TRANSFORM EACH OUTPUT

$$OUT1(\omega) = E(\omega) \cdot R(\omega) \cdot D^{-1}(\omega)$$

$$OUT2(\omega) = R(\omega) \cdot D^{-1}(\omega)$$

$$E(\omega) = \frac{OUT1}{OUT2} \quad \frac{\text{(recorded transient)}}{\text{(recorded instrument step response)}}$$

STEP 4:

$$E(\omega) \cdot j\omega \Longrightarrow e(t) * \delta^{-1}(t)$$

This is the step response of the earth alone.

TIME DOMAIN

$\delta^{-1}(t)$ - step

$e(t)$ - earth function

$r(t)$ - recorder function

FREQUENCY DOMAIN

$D^{-1}(\omega)$ - step

$E(\omega)$ - earth function

$R(\omega)$ - recorder function

Figure 15. Schematic logic of process used to compensate a transient curve recorded in the time domain for limited response of the recording system.

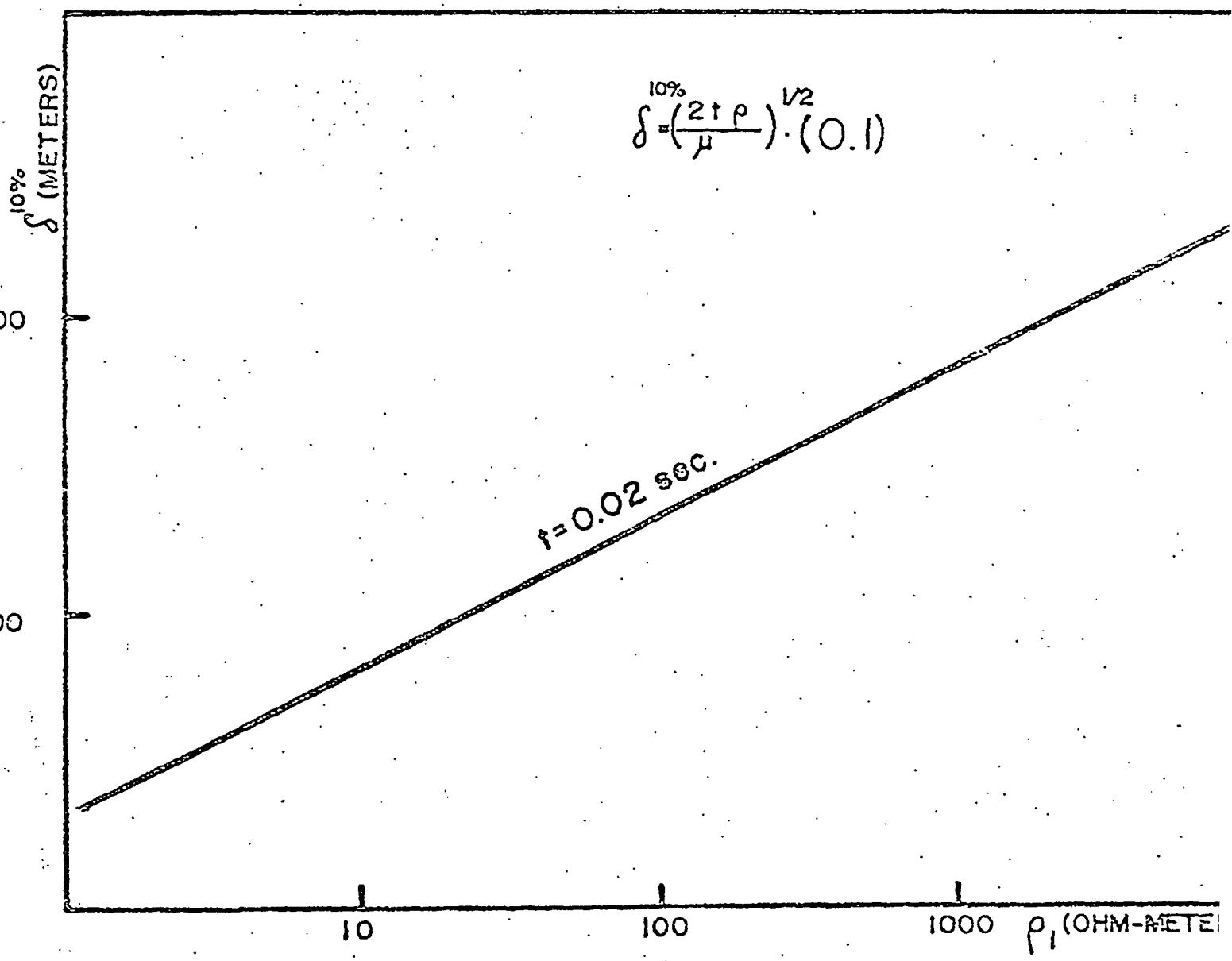

Figure 16. Thickness of a layer which contributes 10% of a skin depth in the time domain after 20 milliseconds. Such a layer would not be apparent on a TDEM curve that starts at 20 milliseconds.

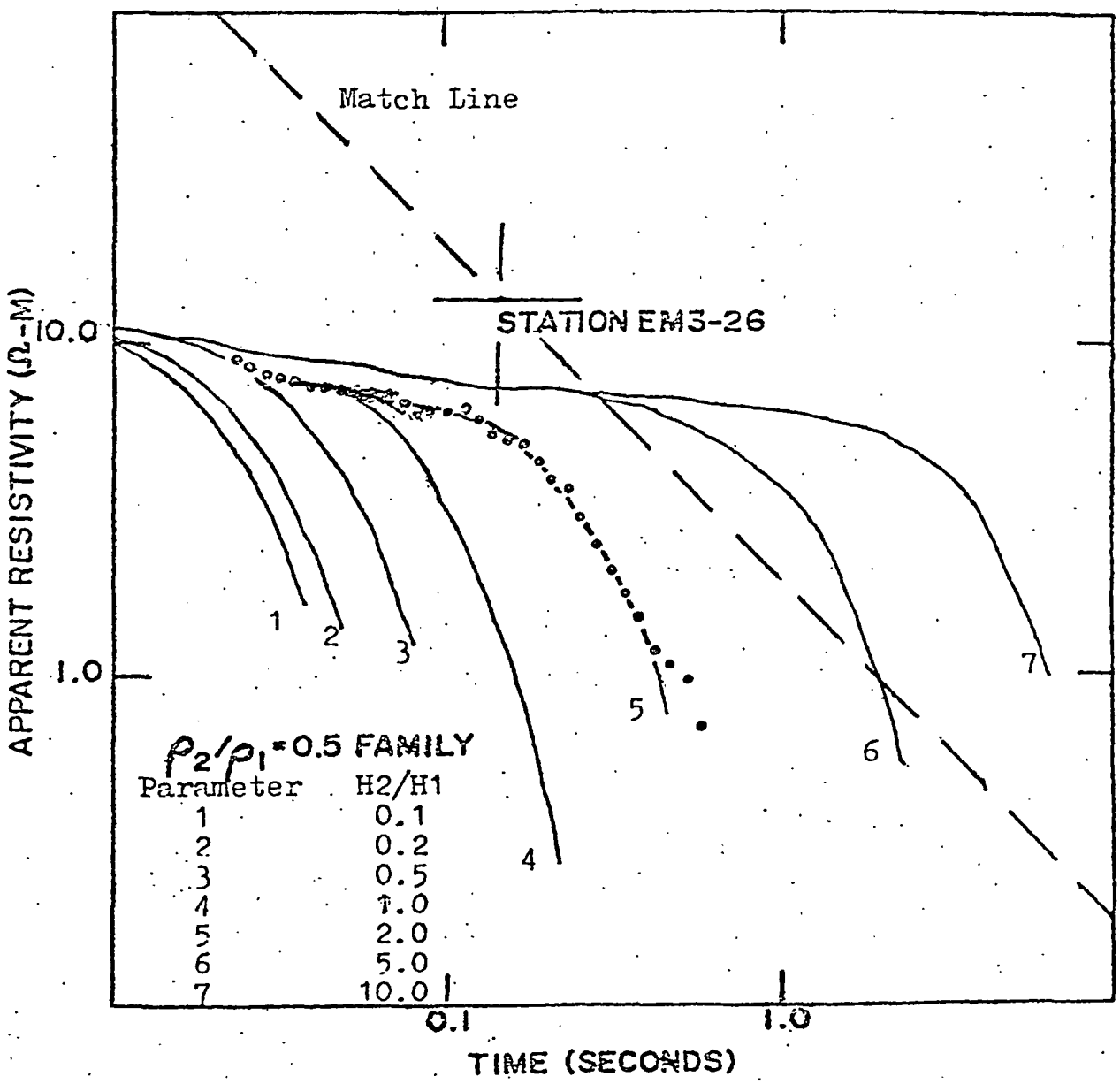

Figure 17. Example of graphical curve matching of TDEM data. The scales on the graph and the locus of the match line pertain to the field data. The theoretical curves are plotted to dimensionless scales, with the origin located at the solid cross.

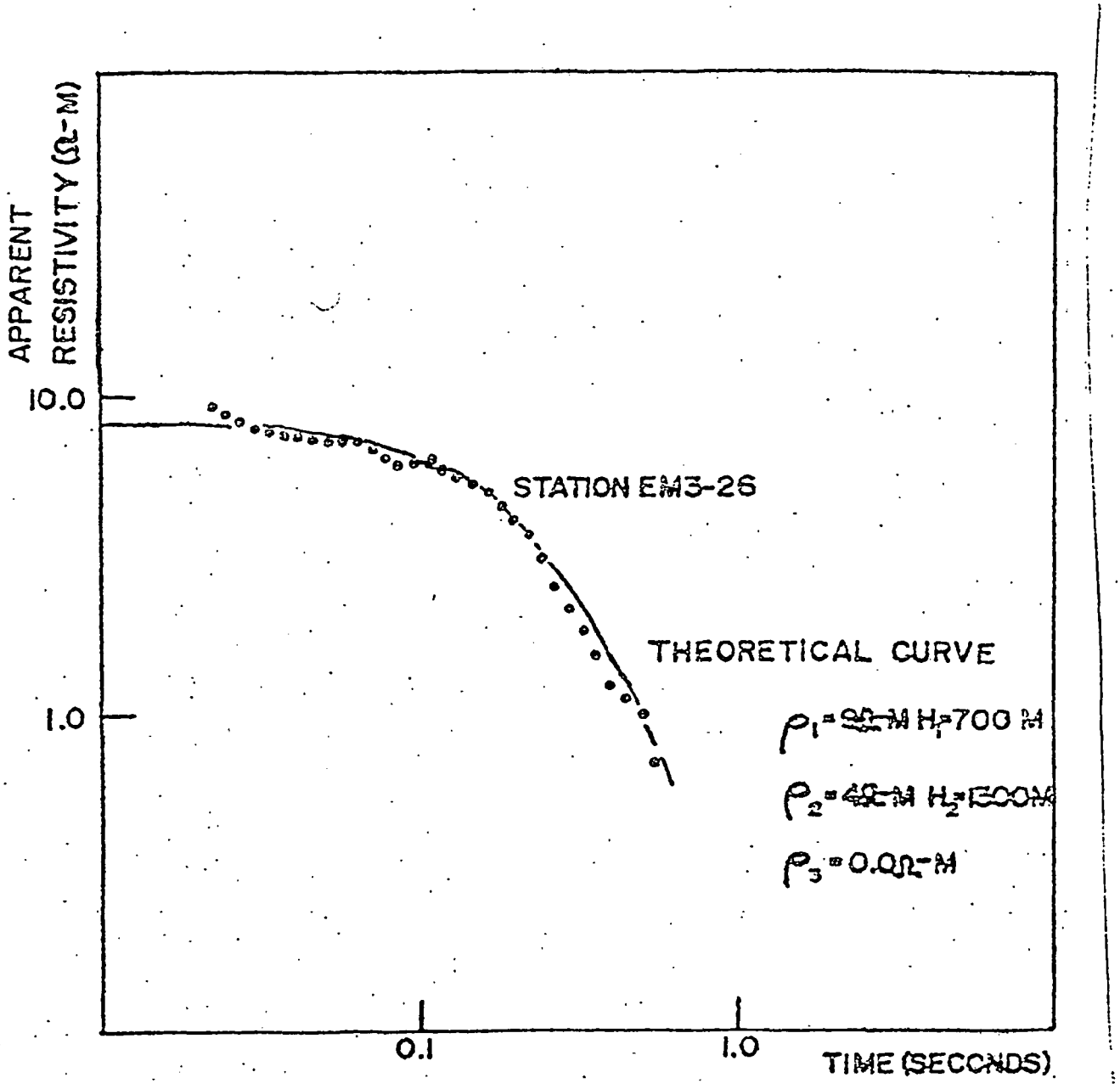

Figure 18. Example of the fit between a computed TDEM curve and a set of field measurements.

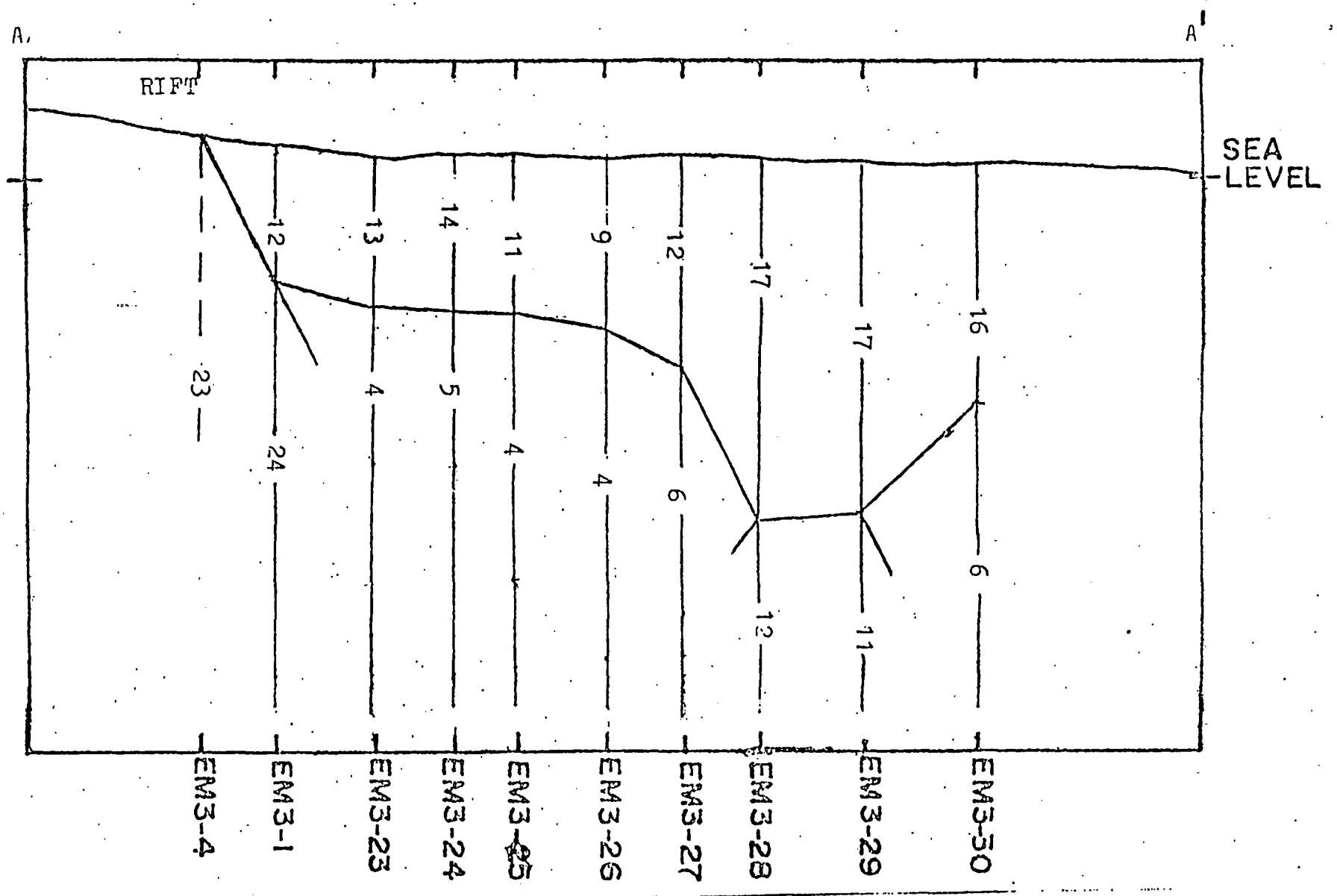

Figure 19. Cross section of the electrical structure along a traverse extending from the East Rift to the coast in the Puna District, Hawaii. Location of the traverse A-A' is shown on the map in Figure 14.

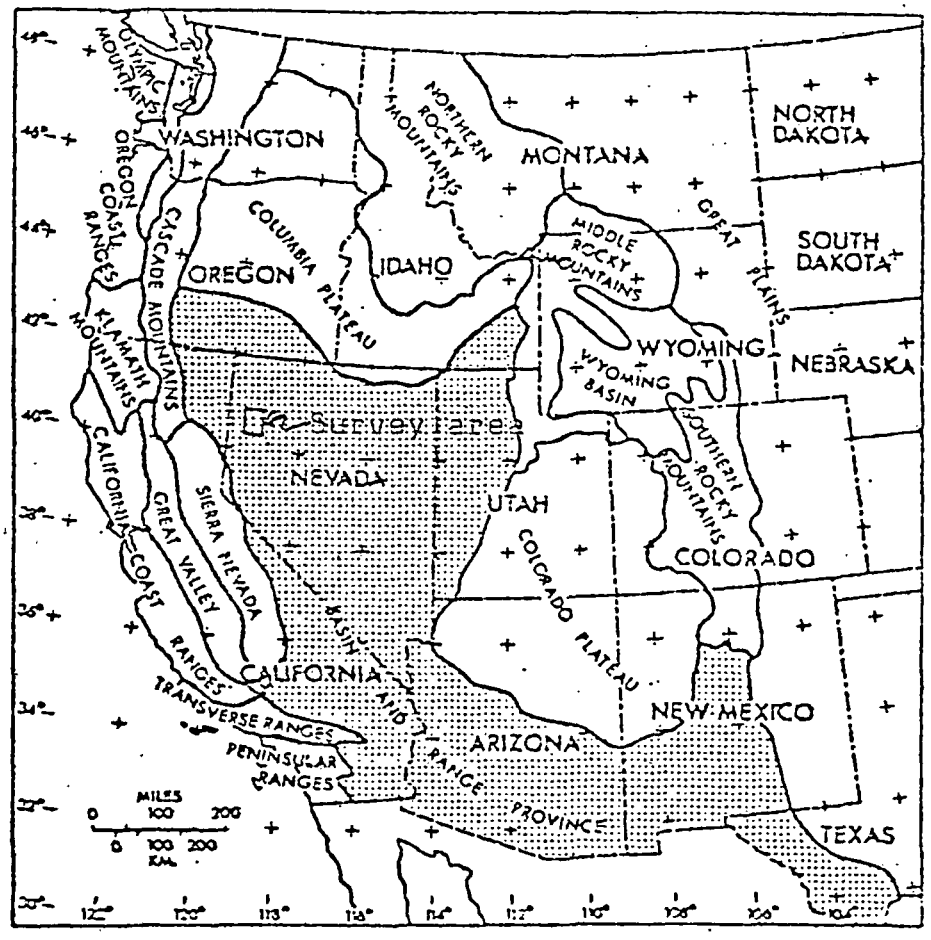

Figure 20. Physiographic provinces of the western United States. The Basin and Range province is shown as stippled.

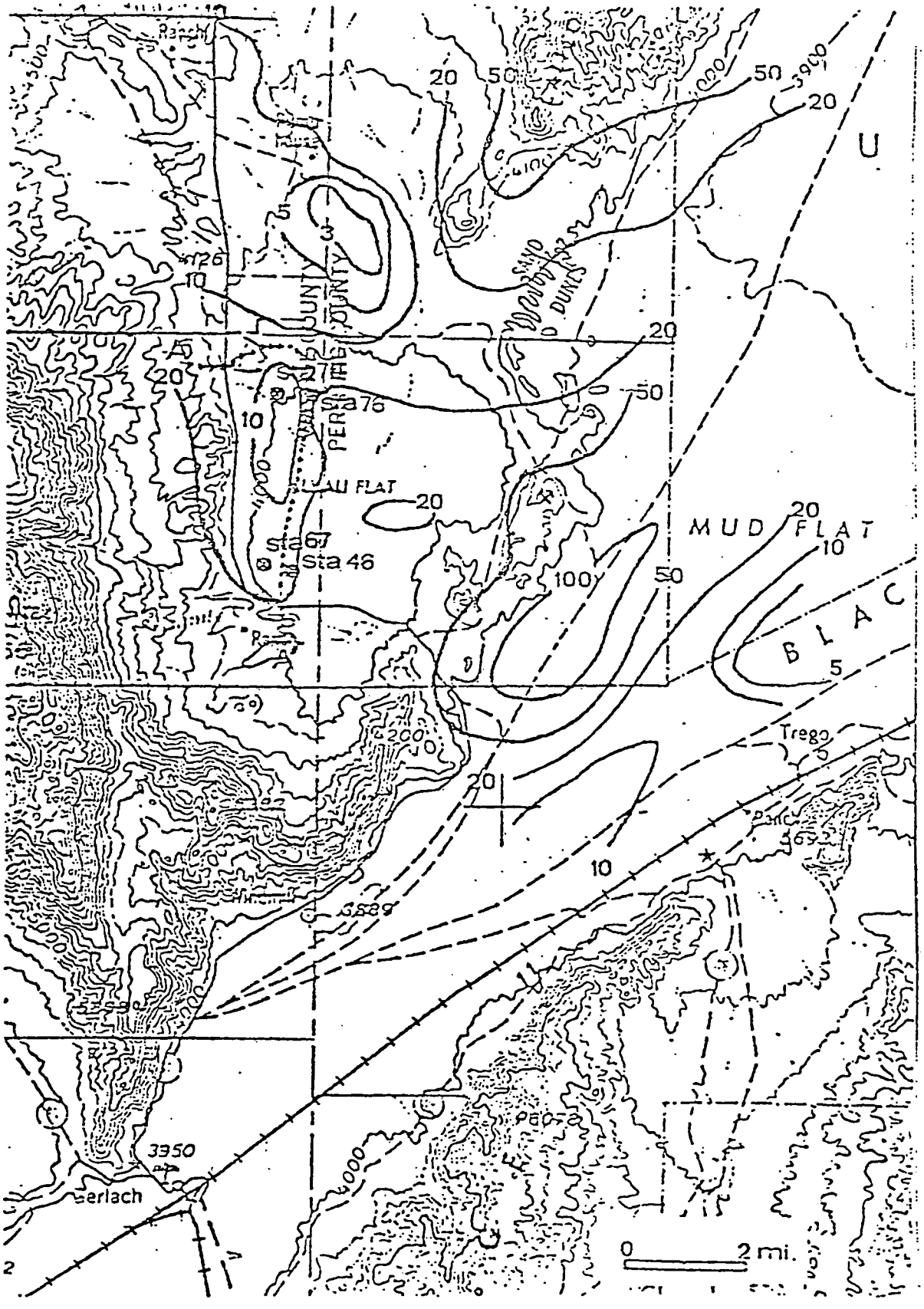

Figure 21. Map of the southern Black Rock Desert and Hualapai Flat, Nevada. The maximum apparent resistivity recorded on TDEM soundings is contoured. Units are ohm-meters.

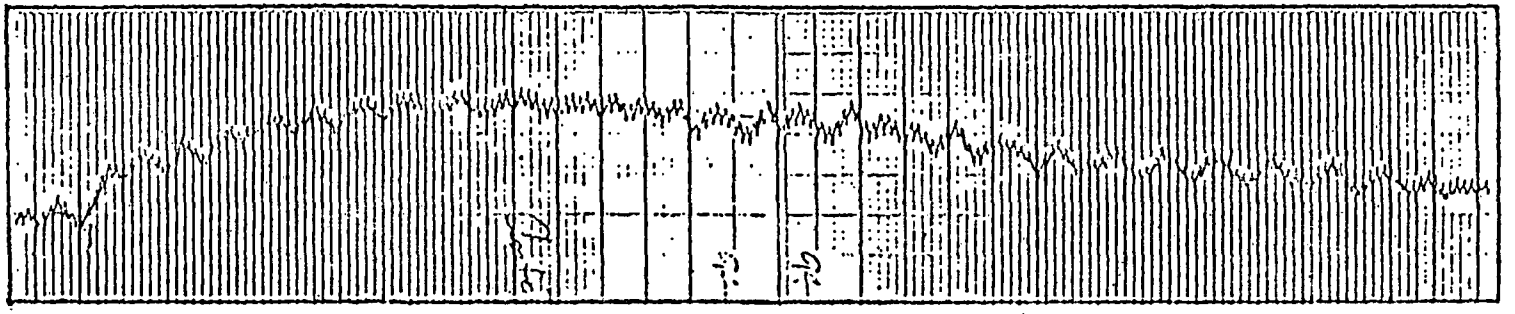

044W CONDUCTOR

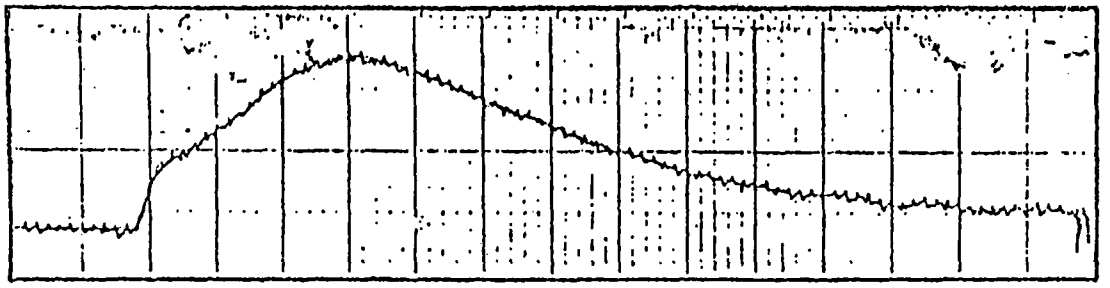

06W RESISTOR OVER CONDUCTOR

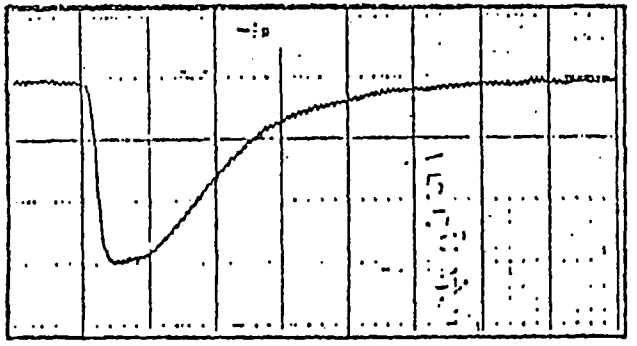

11W RESISTOR OVER CONDUCTOR

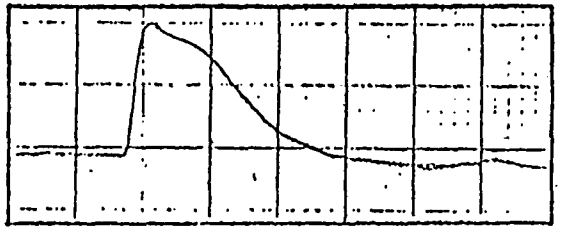

12 E RESISTOR OVER CONDUCTOR

Figure 22. Examples of transient magnetic coupling signals recorded in a geothermal survey in Nevada. The shapes are characteristic ofa layered earth. Horizontal scale is 0.2 seconds between heavy lines; vertical scale varies.

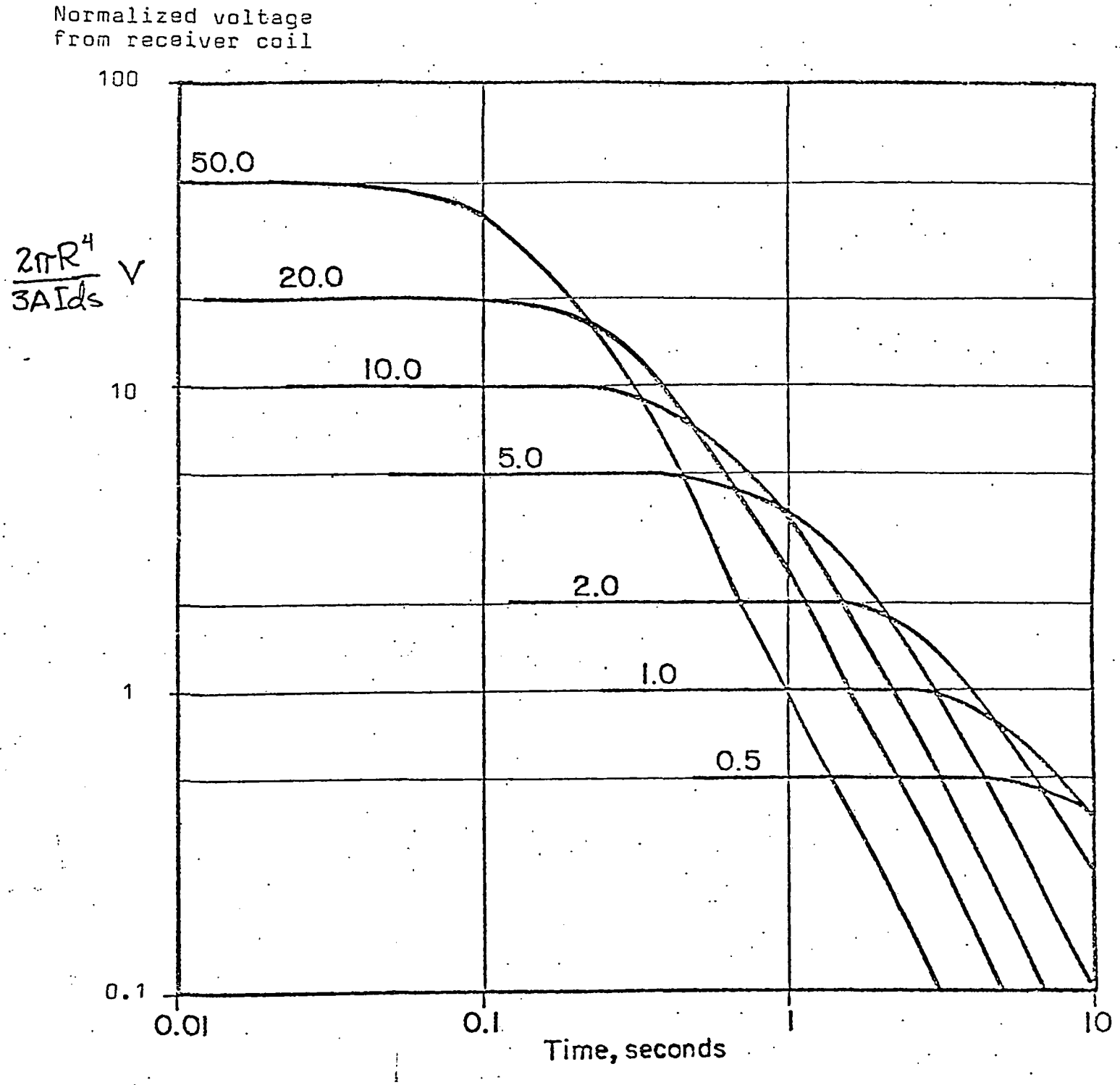

Figure 2. Computed voltage transient curves for coupling between a grounded wire source and a vertical axis loop receiver separated by a distance of 7.5 kilometers over a uniform earth with a resistivity as indicated by the parameter on each curve.

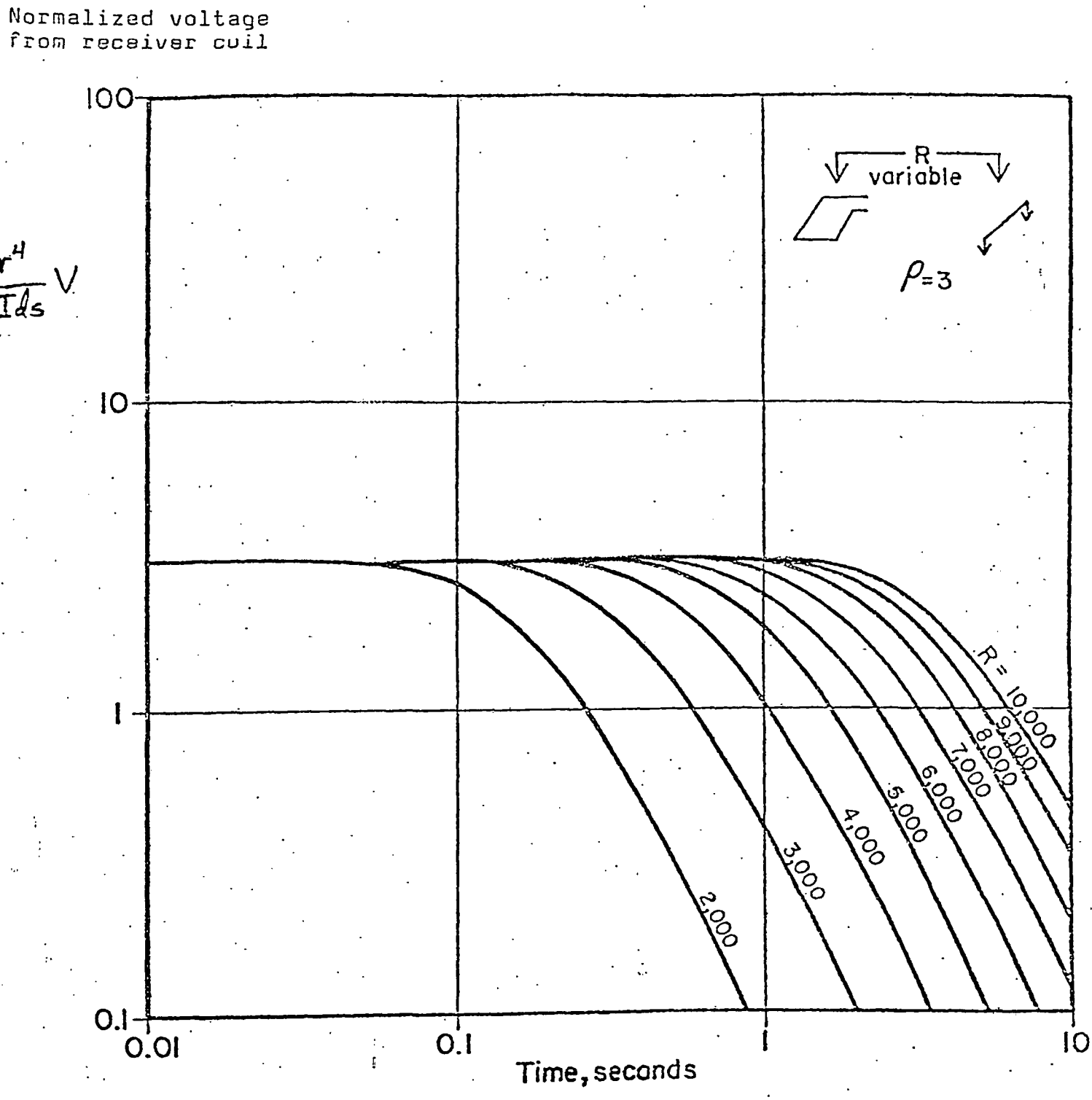

Figure 3. Computed voltage transient curves for coupling between a grounded wire source and a vertical axis loop receiver separated by distances as indicated on each curve. The earth is uniform and has a resistivity of 3 ohm-meters.

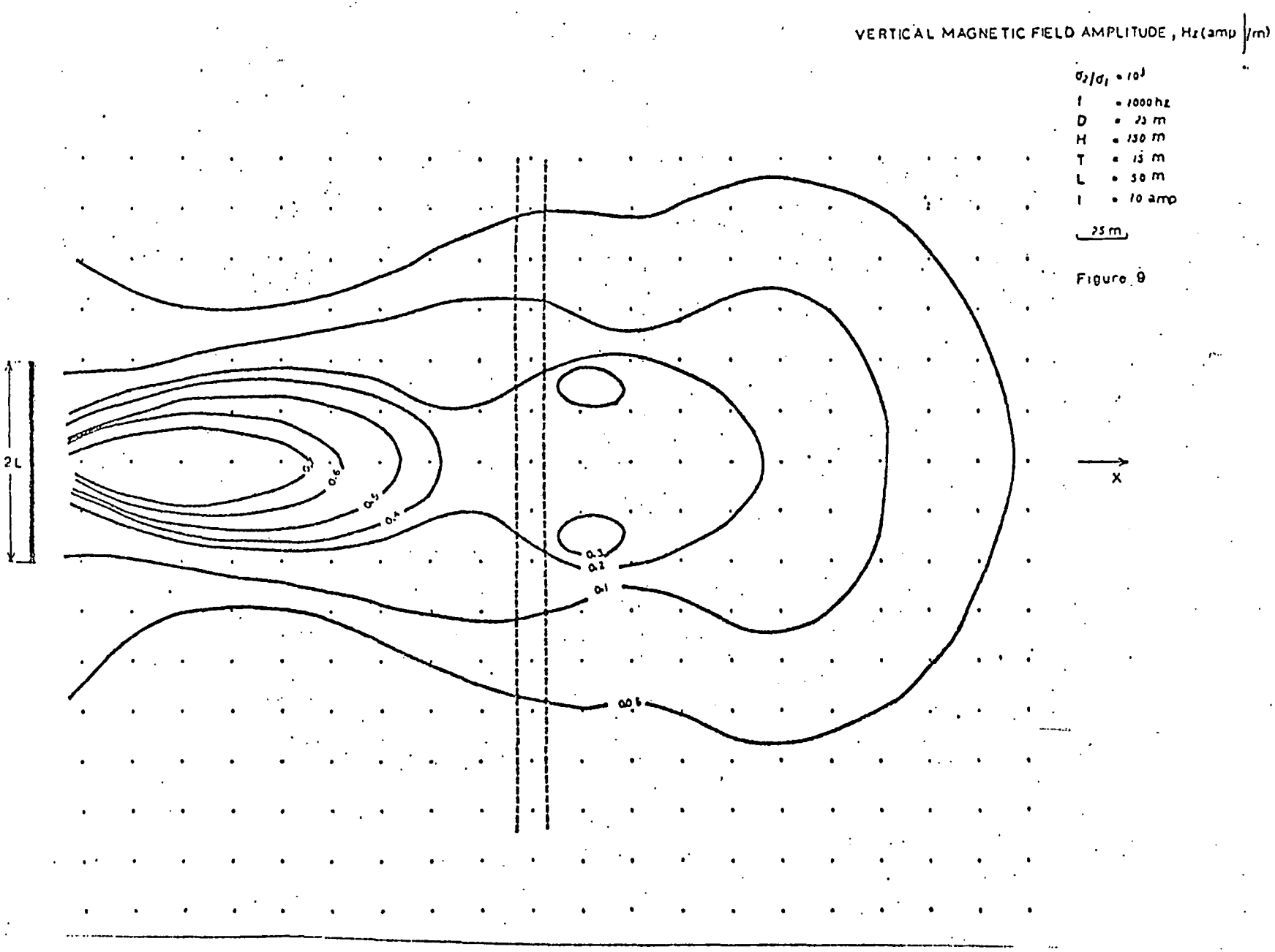

Figure 12A. The amplitude of the vertical component of magnetic induction around the dike defined in Figure 10.

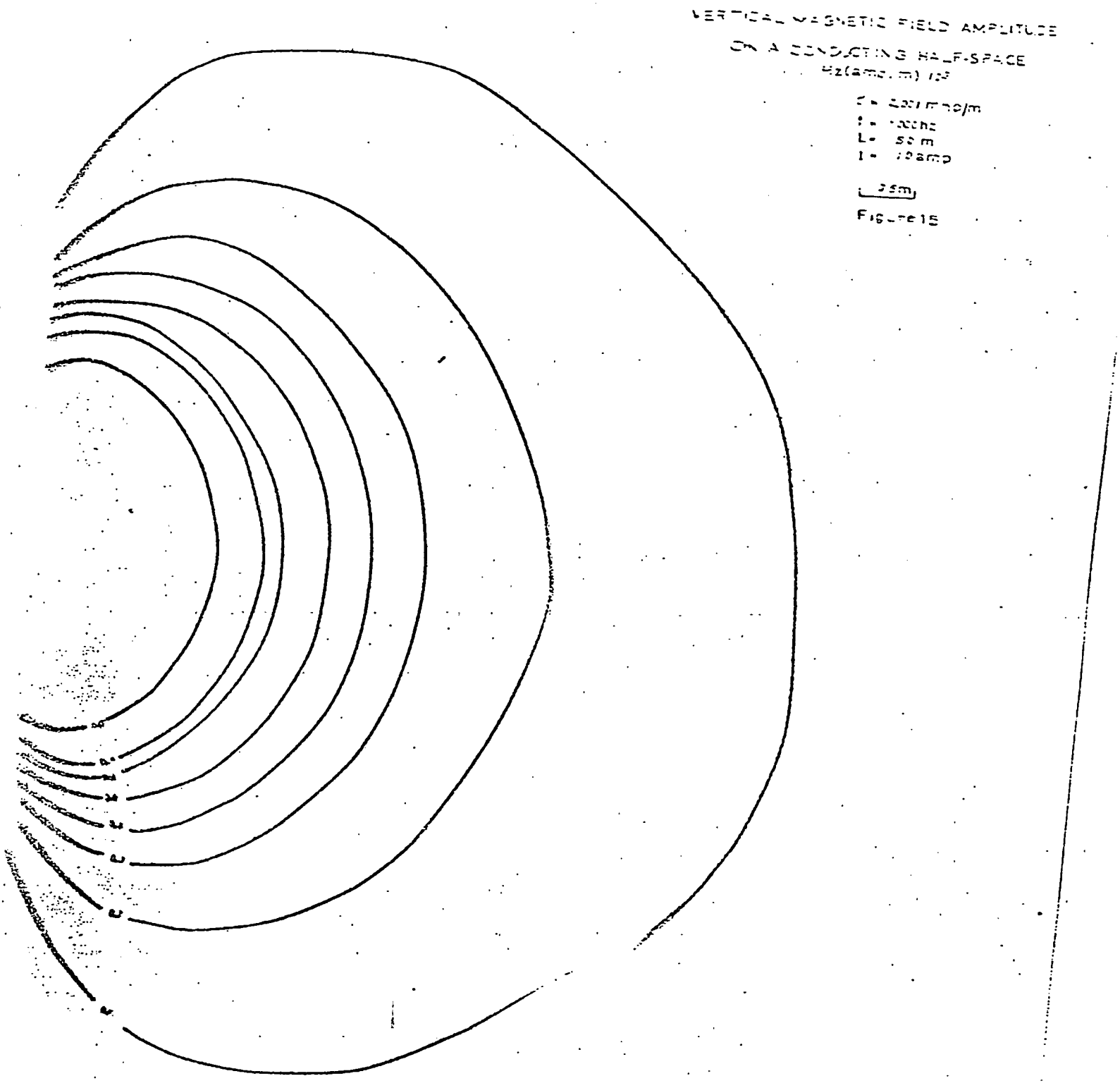

Figure 108. Amplitude of the vertical magnetic induction from a dipole source over a uniform earth.

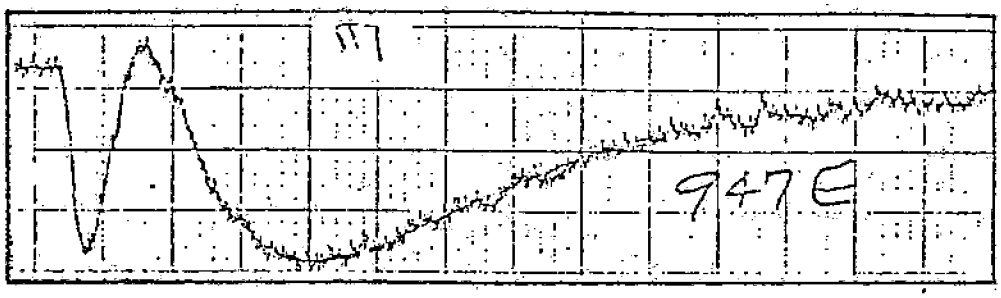

947E LATERAL BOUNDARY

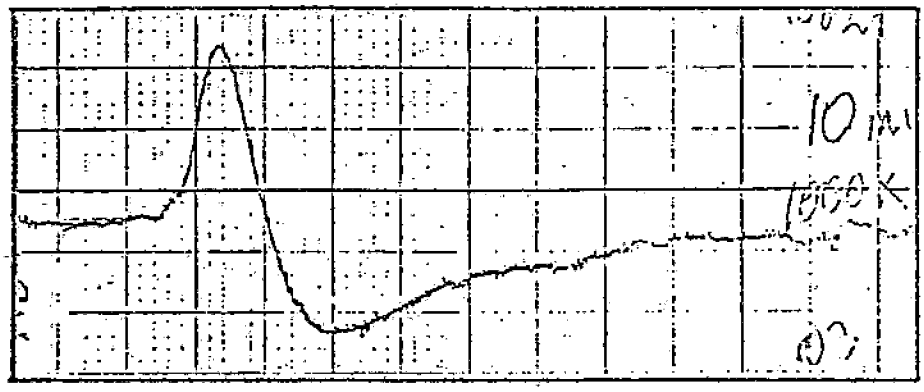

924W LATERAL BOUNDARY

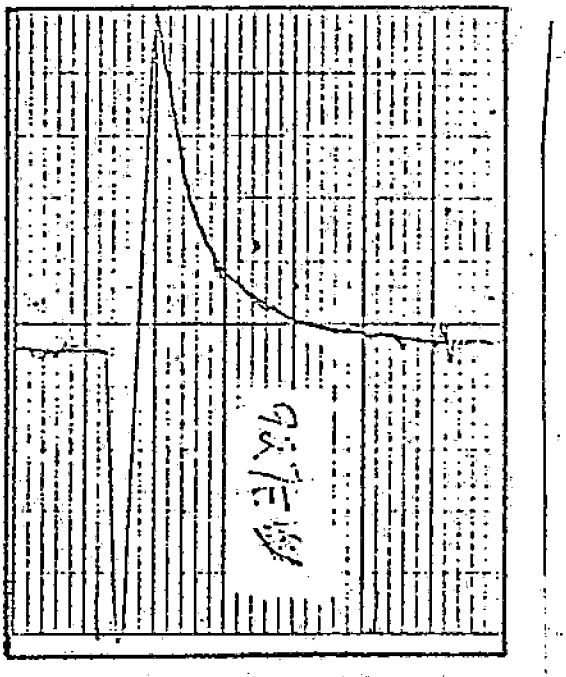

927 E LATERAL BOUNDARY

Figure 23. TDEM transient signals recorded during a survey of an area in Nevada. The reversals in sign of the transients indicate lateral changes in resistivity. The horizontal scale is 0.2 seconds between heavy lines.

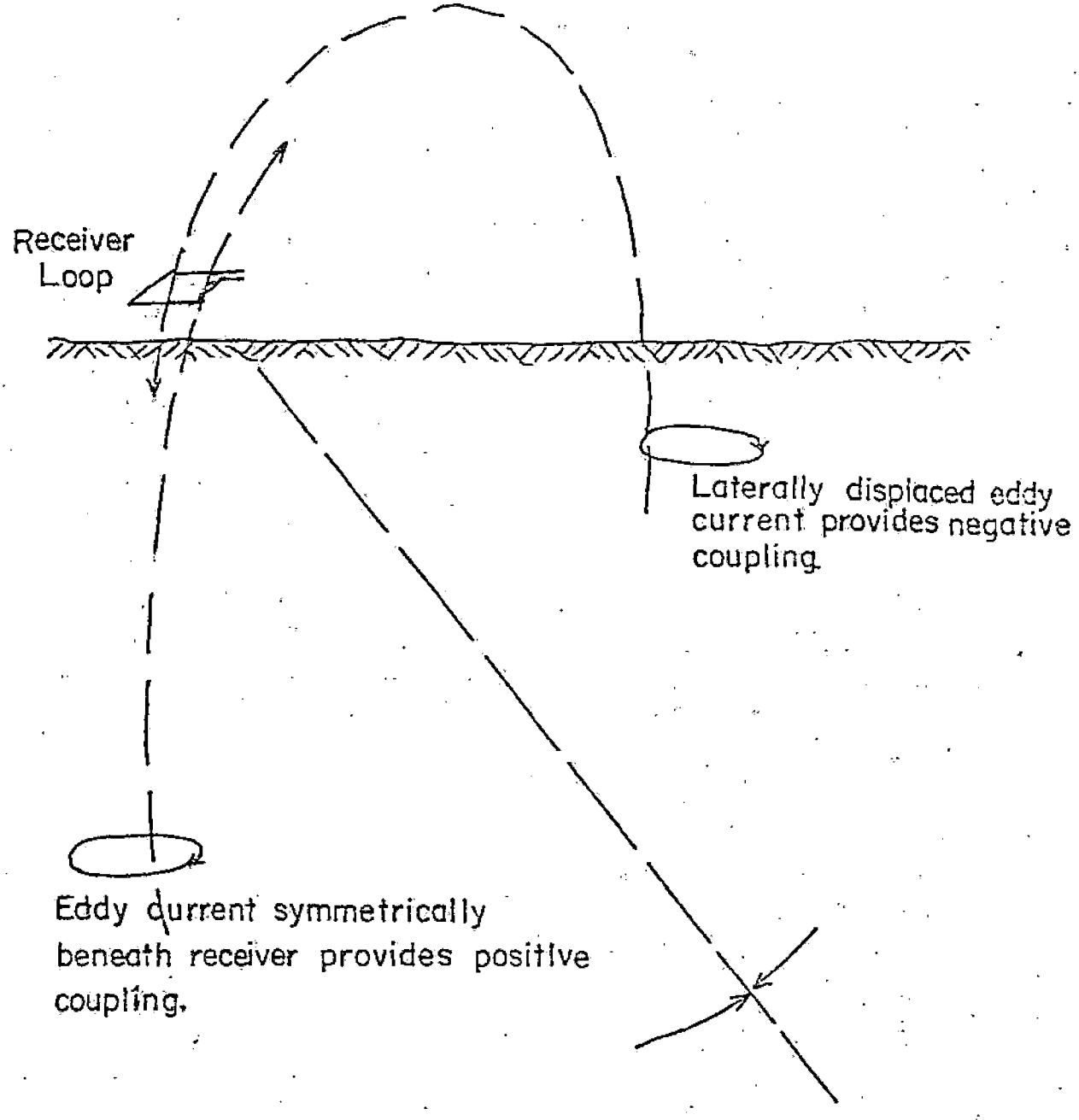

Figure 24. Sketch showing how lateral changes in resistivity can cause assymetry in development of eddy currents and the reversal in sign of a time-domain electromagnetic signal.